

**Characterisation of Androgen Receptor Variants in Breast Cancer and  
the Development of Thieno[2,3-*b*] Pyridines as Novel Anti-Cancer  
Compounds**

Mohammad A. Alkheilewi

**A thesis submitted for the degree of Doctor of Philosophy in  
Molecular Medicine**

School of Biological Sciences

University of Essex

Date of submission February 2019

## Abstract

In Breast Cancer (BCa), steroid receptors play a key role in the progression of the majority tumours. Oestrogen Receptor- $\alpha$  (ER $\alpha$ ), for example, drives the growth of approximately 70% of tumours and is therefore a useful therapeutic target for this disease. Interestingly, the Androgen Receptor (AR) is the most commonly expressed steroid receptor in normal breast tissue and appears to also play an important role in BCa. In ER $\alpha$ -positive disease the crosstalk between ER $\alpha$  and AR is inhibitory to tumour growth. Sequencing studies have identified the presence of AR mutations in BCa, however little is known about the role of these in disease progression. This study aimed to further characterise AR-ER $\alpha$  cross-talk and to analyse the effect of AR mutations upon receptor activity. Several mutations were found to affect receptor activity, but these did not affect AR-ER $\alpha$  cross-talk.

AR signalling is also important in Prostate Cancer (PCa) and hence therapies often target this signalling axis. Although successful initially, these treatments invariably fail and the tumours progress to the aggressive castrate resistant stage of the disease. Thieno[2,3-*b*]pyridine derivatives have been previously demonstrated to be effective inhibitors in BCa. Here we expanded the research by investigating the efficacy of these compounds upon PCa. Using growth assays, flow-cytometry analysis, florescent imaging and cell tracking assays it was demonstrated that the compounds are potent inhibitors of PCa proliferation and motility. Importantly, the drugs were found to induce multi-nucleation, G<sub>2</sub>/M arrest and promote apoptosis. Further, a drug pull-down assay suggested that the compounds bind to multiple targets involved in, for example, cytoskeleton dynamics and p53 signaling. In conclusion, these compounds represent a novel therapeutic approach for PCa and further work to assess their efficacy is warranted.

## **Statement of Originality**

Unless otherwise stated in the text, this thesis is the result of my own work.

## Acknowledgements

Firstly, I would like to express my sincere gratitude to my supervisor Dr. Greg N. Brooke for the continuous support throughout my Ph.D. studies and related research, for his patience, motivation, and immense knowledge. His guidance helped me throughout my research and the writing of this thesis. I could not have imagined having a better supervisor and mentor for my Ph.D. studies. Next, my sincere thanks goes to Prof. Elena Klenova, Dr. Philip J. Reeves Dr. Ralf Zwacka, and Dr. Andrea Mohr for guidance and advice throughout my Ph.D. Also I would like to thank my fellow lab mates, members of the Molecular Oncology Lab, who I have worked with during my project: Dr. Rosie Bryan, Ms. Angela Pine, Ms. Laura Beliokaite, Dr. Amna Allafi and Dr. Mila Pavlova. Next, special thanks goes to Mrs. Emma Revill, department graduate administrator, and Mrs. Adele Angel for their continuous support during all years of my Ph.D.

I would like to acknowledge my collaborators Dr. Jóhannes Reynisson, Dr Euphemia Leung, Dr Michelle Van Rensburg and Prof David Barker (Auckland Cancer Society Research Centre, The University of Auckland, New Zealand) for providing the inhibitors and discussions throughout the thesis. Appreciation goes to Dr David Guttery (University of Leicester) for his guidance with the DNA extraction from Breast Cancer samples, Dr Metodi Metodiev (University of Essex) for his assistance with the mass spectrometry analysis, Prof Simak Ali (Imperial College London) for providing the ER $\alpha$  mutant constructs and Dr Pradeep Madapura (Queen Mary College) for his guidance on CRISPR. I am also grateful to Dr Damien Leach and Prof Charlotte Bevan for their assistance with the tumour explant studies.

I am also grateful to King Faisal Specialist Hospital & Research Centre and Saudi Arabian Cultural Bureau for funding my PhD scholarship. Also, many thanks to the University of Essex for being such a great study environment. Last but not the least, I would like to thank my wife, my parents and all my family members for supporting me spiritually throughout the writing of this thesis and in my life in general.



## Abbreviations

1<sup>o</sup>: Primary

2<sup>o</sup>: Secondary

Ab: Antibody

AF1: Activation Function 1

AF2: Activation Function 2

AI: Aromatase Inhibitor

Akt: AKT Serine/Threonine Kinase (PKB)

APS: Ammonium persulphate

AR: Androgen Receptor

ARA70: Androgen Receptor Co-activator 70 kDa Protein

ARE: Androgen Response Element

BBS: (BES)-buffered saline

BCa: Breast Cancer

BIC: Bicalutamide

BPH: Benign Prostatic Hyperplasia

BRCA1: Breast Cancer 1, Early Onset

BRCA2: Breast Cancer 2, Early Onset

BSA: Bovine serum albumin

C-Terminal: Carboxyl-Terminal

CaCl<sub>2</sub>: Calcium chloride

CARM1: Coactivator-Associated Arginine Methyltransferase 1 CDK3:

Cyclin-Dependent Kinase 3

cDNA: Complementary DNA

ChIP-Seq: Chromatin Immunoprecipitation sequencing

ChIP: Chromatin Immunoprecipitation

CK14: Cytokeratin 14

Co-IP: Co-Immunoprecipitation

CO<sub>2</sub>: Carbon dioxide

CRPC: Casteration resistant prostate cancer

DAG: Diglyceride

DBD: DNA Binding Domain  
DCIS: Ductal Carcinomas *in situ*  
DDC: Dopa Decarboxylase  
ddH<sub>2</sub>O: Double distilled water  
DHEA: Dehydroepiandrosterone  
DHT: Dihydrotestosterone  
DMEM: Dulbecco's Modified Eagle's Medium  
DMSO: Dimethyl sulphoxide  
DNA: Deoxyribonucleic acid  
dNTPs: Deoxyribonucleotides  
*E. coli*: *Escherichia coli*  
E2: 17- $\beta$ -Oestradiol  
EDTA: Ethylenediaminetetraacetic acid  
EGF: Epidermal Growth Factor  
EGFR: Epidermal Growth Factor Receptor  
EMT: Epithelial-to-Mesenchymal Transition  
ERE: Oestrogen Response Element  
ER $\alpha$ : Oestrogen Receptor alpha  
ER $\beta$ : Oestrogen Receptor beta  
*ESR1*: Oestrogen Receptor 1  
*ESR2*: Oestrogen Receptor 2  
EtOH: Ethanol EV: Empty Vector  
FBS: Foetal bovine serum  
FGF: Fibroblast Growth Factor  
FGFR: Fibroblast Growth Factor Receptor  
FOXA1: Forkhead Box A1  
FULV: Fulvestrant  
GFP: Green Fluorescent Protein  
GH: Growth Hormone  
GnRH: Gonadotropin Releasing Hormone  
GnRH $\alpha$ : Gonadotropin-Releasing Hormone agonist

GREB1: Gene Regulated in Breast Cancer 1  
HCl: Hydrochloric acid  
HER-2: Human Epidermal Growth Factor Receptor 2  
HRE: Hormone Response Element  
HSP: Heat Shock Protein  
IGF1: Insulin-Like Growth Factor-1  
IHC: Immunohistochemistry (IHC)  
IL6: Interleukin 6  
IPTG: Isopropyl  $\beta$ -D-1-thiogalactopyranoside  
ISH: *in situ* Hybridisation  
KCl: Potassium chloride  
kDa: Kilodaltons  
L-Glutamine-PenStrep: L- Glutamine-Penicillin-Streptomycin  
L19: RPL19 ribosomal protein  
LB: Luria Broth  
LBD: Ligand Binding Domain  
LHRH: Luteinizing Hormone Releasing Hormone  
MABC: Molecular Apocrine Breast Cancer  
MAPK: Mitogen-Activated Protein Kinase  
MeOH: Methanol  
MgCL2: Magnesium chloride  
MgSO4: Magnesium sulphate  
MIB: Mibolerone  
MRI: Magnetic Resonance Imaging  
mRNA: Messenger RNA  
mTOR: Mammalian Target Of Rapamycin  
MYC: Myelocytomatosis Oncogene Cellular Homolog  
N-Terminal: Amino-Terminal  
NaCl: Sodium chloride  
NaOH: Sodium hydroxide

NCI: National Cancer Institute  
NDRG1: N-myc Downstream-Regulated Gene 1  
NGS: Next Generation Sequencing  
NLS: Nuclear localization signal  
  
NR: Nuclear Receptor  
O/N: Overnight  
  
OHF: Hydroxyflutamide  
  
OS: Overall Survival  
  
PBS: Phosphate-buffered saline  
  
PCa: Prostate Cancer  
  
PCR: Polymerase Chain Reaction  
  
PFA: Paraformaldehyde  
  
PH: Pleckstrin homology  
  
PI: Propodeum Iodide  
  
PI: Protease Inhibitor  
  
PI3K: Phosphatidylinositol-4,5-Bisphosphate 3-Kinase  
  
PIN: Premalignant Prostatic Intraepithelial Neoplasia  
  
PIP2: Phosphatidylinositol 4,5-bisphosphate  
  
PKB: Protein Kinase B (Akt)  
  
PMSF: Phenylmethylsulphonyl fluoride  
  
PR: Progesterone Receptor  
  
PSA: Prostate Specific Antigen  
  
PTEN: Phosphatase and Tensin Homolog  
  
PTEN: Phosphate and Tensin homologue  
  
qPCR: Real-Time quantitative PCR  
  
RIPA: Radioimmunoprecipitation assay buffer  
  
RNA-Seq: RNA-Sequencing  
  
RNA: Ribonucleic acid  
  
RPMI: Roswell Park Memorial Institute  
  
RPMI: Roswell Park Memorial Institute  
  
rRNA: ribosomal RNA

RT: Radiation Therapy  
RT: Room Temperature  
SARM: Selective Androgen Receptor Modulator  
SDS-PAGE: Sodium dodecyl sulphate polyacrylamide gel electrophoresis  
SDS: Sodium dodecyl sulphate  
SFCS: charcoal Stripped Foetal Calf Serum  
SHBG: Sex Hormone-Binding Globulin  
SHBG: Steroid Hormone Binding Globulin  
siRNA: small interfering RNA  
SMAC/Diablo: Second Mitochondria-derived Activator of Caspases/Direct  
SOB: Super Optimal broth with Catabolite repression  
T: Testosterone  
TAM: Tamoxifen  
TE: Tris/EDTA  
TEB: Terminal End Bud  
TEMED: Tetramethylethylenediamine  
TF: Transcription Factor  
TFF1: Trefoil Factor 1  
TKI: Tyrosine Kinase Inhibitor  
Tm: Melting temperature  
TNBC: Triple Negative Breast Cancer  
UV: Ultra Violet  
WW: Watchful Waiting  
ZF: Zinc Finger

<b>Abstract</b>	<b>2</b>
<b>Acknowledgements</b>	<b>4</b>
<b>Abbreviations</b>	<b>5</b>
<b>List of Tables</b>	<b>14</b>
<b>List of Figures</b>	<b>15</b>

## **CHAPTER 1**

### **INTRODUCTION**

<b>1.1 Normal Breast</b>	<b>17</b>
1.1.1 Mammary Gland Structure & Development	17
1.1.2 Mammary Gland Function	19
<b>1.2 Breast Cancer</b>	<b>19</b>
1.2.1 Epidemiology	19
1.2.2 Symptoms, Management & Risk Factors	20
1.2.3 Treatment	21
1.2.4 Molecular Subtypes	22
<b>1.3 Nuclear Receptors</b>	<b>23</b>
1.3.1 Nuclear Receptors Structure and Function	24
1.3.2 Steroid Hormone Receptors	25
1.3.3 Oestrogen Receptor and Hormone Therapies	26
1.3.4 Endocrine Resistance	28
1.3.5 Androgen Receptor	29
1.3.6 Receptors in Breast Cancer	30
<b>1.4 Androgen Receptor Signalling in Breast Cancer</b>	<b>32</b>
1.4.1 AR expression in Breast Cancer	32
1.4.2 AR/ER Cross Talks in BCa	33
1.4.3 AR as Prognostic and Therapeutic Factor in Breast Cancer	34
1.4.4 Molecular Apocrine Breast Cancer (MA)	34
1.4.5 AR Mutations in Breast Cancer	36
<b>1.5 The Prostate Gland</b>	<b>36</b>
1.5.1 Location and description	36
1.5.2 Prostate development	38
1.5.3 Prostate Diseases	40
1.5.3.1 Prostatitis	40
1.5.3.2 Benign prostatic hyperplasia (BPH)	40
1.5.3.3 Prostatic intraepithelial neoplasia (PIN)	41
1.5.4 Prostate cancer (PCa)	42
1.5.4.1 Prostate cancer epidemiology	42
1.5.4.2 Risk factors	43

1.5.4.3 Grading and staging	43
1.5.4.4 Detection and monitoring of Prostate cancer	47
1.5.4.5 Prostate cancer treatment	48
1.5.4.6 Development of castration-resistant prostate cancer (CRPC)	50
1.6 Phospholipase C (PLC)	51
1.6.1 Structure & function	51
1.6.2 The role of PLCs in cancer	54
1.6.3 Apoptosis and tumour cell death	55
1.6.4 Signalling pathways in PCa	58
1.6.5 New anticancer derivatives (thieno[2,3-b]pyridine)	60
1.7 Project objectives	61

## **CHAPTER 2**

### **MATERIALS AND METHODS**

2.1 Reagents, solutions and buffers	62
2.2 Mammalian cell culture	68
2.3 Freezing and defrosting cells	71
2.4 Transient transfection of mammalian cells	72
2.4.1 Calcium phosphate	72
2.4.2 jetPRIME	72
2.4.3 FuGENE HD	73
2.4.4 siRNA knockdown	73
2.5 Bacterial cultures, transformation and DNA preparation	73
2.5.1 Bacterial strains and culture	73
2.5.2 Transformation	74
2.5.3 DNA preparation	74
2.6 Site-directed mutagenesis	75
2.7 Cloning of AR mutant Q739* using CRISPR/ CAS9	76
2.8 Reporter assays	78
2.9 Gene expression analysis	79
2.9.1 RNA extraction	80
2.9.2 cDNA synthesis	80
2.9.3 Real-Time quantitative PCR (qPCR)	80
2.10 Genomic DNA extraction from breast cancer tumours	82
2.11 Protein analysis	83
2.11.1 Cell collection	83
2.11.2 DC protein assay	83
2.11.3 SDS-PAGE	84
2.11.4 Immunoblotting	84

2.12 Cell staining and confocal imaging	85
2.13 Single cell tracking by widefield microscopy	86
2.14 WST-1 proliferation assays	87
2.15 Crystal Violet proliferation assays	87
2.16 Immunoprecipitation	88
2.17 Biotin drug pull-down	88
2.18 Flow Cytometric Measurement of Apoptotic and Necrotic Cells	90
2.19 Flow cytometric analysis of cell cycle	90
2.20 Assessment of caspase 3/7 activity and viability	91
2.21 Ex vivo culture of human prostate tumours	91
2.22 Statistical analysis	92
2.23 Image and software analysis	92

## **CHAPTER 3**

### **Results I: The Role of the Androgen Receptor in Breast Cancer and its Cross-Talk with Oestrogen Receptor alpha**

3.1 Introduction	93
3.1.1 Chapter Aims	94
3.2 Characterisation of AR-ER $\alpha$ Cross-talk	95
3.2.1 Androgen signalling inhibits oestrogen induced growth	95
3.2.2 The interaction between AR and ER $\alpha$ is ligand-independent	97
3.2.3 AR and ER $\alpha$ inhibit each others activity in reporter assays	98
3.2.4 Characterisation of AR-ER $\alpha$ cross-talk using ER $\alpha$ mutants	103
3.2.5 Investigation of AR-ER $\alpha$ target genes	112
3.2.6 Investigation of target gene expression following siRNA depletion of AR and ER $\alpha$ .	114
3.3 Androgen Receptor (AR) Variants in Breast Cancer	117
3.3.1 Identification of AR mutations in BCa	117
3.3.2 Some of the mutant ARs are constitutively active	123
3.3.3 Investigation of the cellular localisation of AR mutants identified in BCa	125
3.3.4 AR mutants are not activated by alternative hormones or anti-oestrogens	133
3.3.5 AR/ ER $\alpha$ cross-talk with AR mutants	135
3.3.6 AR editing in MCF-7 cells using CRISPR/ CAS9	136
3.3.7 Genomic DNA was successfully extracted from BCa tissue	138
3.4 Discussion	139
3.4.1 AR and ER $\alpha$ cross-talk in Breast Cancer	139
3.4.2 Characterisation of the mechanisms of cross-talk between the AR and	140



ER $\alpha$	
3.4.3 Regulation of the AR and ER $\alpha$ expressions	141
3.4.4 The potential role of AR mutations in BCa	143
3.4.5 Investigation of AR mutations in endogenous protein	146

## **CHAPTER 4**

### **Results II: The Effect of thieno[2,3-b]pyridine Derivatives on Prostate Cancer Cell Lines**

4.1 Introduction	148
4.1.1 Chapter aims	150
4.2 Investigation if the PLC isoforms expression in PCa cell lines	151
4.3 Thieno[2,3-b]pyridine inhibit PCa cell lines proliferation and viability	153
4.4 Thieno[2,3-b]pyridine inhibitors induce G2/M arrest in PC3	158
4.5 Thieno[2,3-b]pyridine inhibitors promote apoptosis in PC3	160
4.6 The thieno[2,3-b]pyridine inhibitors promote caspase dependant cell death	163
4.7 Thieno[2,3-b]pyridine inhibitors increase PC3 cell size and promote multi-nucleation	166
4.8 Thieno[2,3-b]pyridine inhibitors reduce PC3 motility	171
4.9 The thieno[2,3-b]pyridine 160 inhibits human prostate tumours	173
4.10 Investigation if the thieno[2,3-b]pyridine inhibitors bind to PLC- $\delta$	175
4.11 Discussion	177
4.11.1 Thieno[2,3-b]pyridine derivatives potently inhibit PCa cell line proliferation	177
4.11.2 Thieno[2,3-b]pyridine derivatives promote caspase-dependant apoptosis in PC3	179
4.11.3 Anti-cancer drugs affect on cell morphology impact PC3 cell motility	180

## **CHAPTER 5**

### **CONCLUSION**

5.1 The role of the Androgen Receptor in Breast Cancer	183
5.2 The development of novel targeted therapies for the treatment of prostate cancer	187
5.3 Future work	189
<b>References</b>	<b>190</b>

## List of Tables

<b>Table 1.1: The five main classifications of Breast Cancer.</b>	<b>23</b>
<b>Table 2.1: Preparation of reagents, solutions and buffers.</b>	<b>62</b>
<b>Table 2.2: Mammalian cells used in this thesis.</b>	<b>69</b>
<b>Table 2.3: Cell culture media used.</b>	<b>70</b>
<b>Table 2.4: Reagents for cell treatment.</b>	<b>71</b>
<b>Table 2.5: List of mutagenesis primers.</b>	<b>76</b>
<b>Table 2.6: List of guide strand primers and their oligos used for CRISPR to construct the Q739* mutation in MCF-7 cell line.</b>	<b>77</b>
<b>Table 2.7: List of repair strand primers used for CRISPR to construct the Q739* mutation in MCF-7 cell line.</b>	<b>78</b>
<b>Table 2.8: List of plasmids used in this thesis.</b>	<b>79</b>
<b>Table 2.9: Sequences of gene expression primers for use with qPCR.</b>	<b>81</b>
<b>Table 2.10: List of genomic DNA primers used for the BCa tumours DNA extraction.</b>	<b>82</b>
<b>Table 2.11: Description of the antibodies and concentrations used for immunoblotting.</b>	<b>85</b>
<b>Table 2.12: Description of the compounds used for biotin pull-down.</b>	<b>89</b>
<b>Table 3.1: ER<math>\alpha</math> variants cellular localisation upon oestradiol treatment.</b>	<b>107</b>
<b>Table 3.2: AR and ER<math>\alpha</math> variants cellular localisation upon androgen and oestradiol treatment.</b>	<b>111</b>
<b>Table 3.3: AR mutants found in BCa and their expressed receptors.</b>	<b>120</b>
<b>Table 3.4: AR variants cellular localisation upon androgen treatment.</b>	<b>132</b>
<b>Table 3.5: The concentration of genomic DNA extracted from BCa patient tissues.</b>	<b>138</b>
<b>Table 4.1: Description of the thieno[2,3-<i>b</i>]pyridine inhibitors used with PCa cell lines.</b>	<b>153</b>
<b>Table 4.2: The IC<sub>50</sub> values (nM) of the thieno[2,3-<i>b</i>]pyridine compounds demonstrate that 160 is the most effective inhibitor.</b>	<b>156</b>
<b>Table 4.3: Biotin pull-down analysis of the thieno[2,3-<i>b</i>]pyridine compounds.</b>	<b>176</b>

## List of Figures

<b>Figure 1.1: Structure of the human mammary gland.</b>	<b>18</b>
<b>Figure 1.2. General structure and functional domains of nuclear receptors.</b>	<b>25</b>
<b>Figure 1.3. Genomic and non-genomic signalling of the Oestrogen Receptor (ER).</b>	<b>26</b>
<b>Figure 1.4: <i>AR</i> gene location on the X chromosome and its modular structure.</b>	<b>30</b>
<b>Figure 1.5: Anatomy of the prostate.</b>	<b>37</b>
<b>Figure 1.6: Cell Types in the prostate.</b>	<b>39</b>
<b>Figure 1.7: Projection of cancers in the UK.</b>	<b>43</b>
<b>Figure 1.8: The Gleason Grading system.</b>	<b>46</b>
<b>Figure 1.9: Prostate cancer TNM staging system.</b>	<b>47</b>
<b>Figure 1.10: Structure of the different Phospholipase C isoforms.</b>	<b>52</b>
<b>Figure 1.11: Phospholipase C signalling pathways involving PIP2.</b>	<b>53</b>
<b>Figure 1.12: Apoptosis signalling pathways.</b>	<b>57</b>
<b>Figure 1.13: PLC and PI3K signalling pathways.</b>	<b>59</b>
<b>Figure 3.1: AR signalling inhibits E2-induced proliferation of MCF-7 cells.</b>	<b>96</b>
<b>Figure 3.2: AR-ER<math>\alpha</math> interaction.</b>	<b>97</b>
<b>Figure 3.3: AR and ER<math>\alpha</math> cross-talk inhibits receptor activity.</b>	<b>99</b>
<b>Figure 3.4: Bicalutamide dose not affect AR and ER<math>\alpha</math> cross-talk.</b>	<b>101</b>
<b>Figure 3.5: Enzalutamide does not affect AR and ER<math>\alpha</math> cross-talk.</b>	<b>102</b>
<b>Figure 3.6: Mutation of the ER<math>\alpha</math> NLS and DBD inhibits receptor activity.</b>	<b>104</b>
<b>Figure 3.7: Deletion of the ER<math>\alpha</math> NLS results in cytoplasmic accumulation of the receptor.</b>	<b>106</b>
<b>Figure 3.8: AR/ ER<math>\alpha</math> variants crosstalk measuring AR activity upon ligand binding.</b>	<b>108</b>
<b>Figure 3.9: ER<math>\alpha</math> reduces AR nuclear translocation.</b>	<b>110</b>
<b>Figure 3.10: Investigation of the effects of AR-ER<math>\alpha</math> cross-talk on endogenous target genes.</b>	<b>113</b>
<b>Figure 3.11: AR and ER<math>\alpha</math> knock-down in MCF-7 cell line.</b>	<b>115</b>
<b>Figure 3.12: Relative expressions of AR and ER<math>\alpha</math> target genes upon receptors knock-down in MCF-7 cell line.</b>	<b>116</b>
<b>Figure 3.13: Locations of AR mutations identified in Breast Cancer.</b>	<b>119</b>
<b>Figure 3.14: Chromatographs of the wild-type and mutant ARsa.</b>	<b>121</b>
<b>Figure 3.15: The mutant ARs are successfully expressed in COS-1 cell line.</b>	<b>122</b>
<b>Figure 3.16: Transcriptional activity of the mutant ARs.</b>	<b>124</b>
<b>Figure 3.17: The cellular localisation of wild-type and mutant AR in response to androgen.</b>	<b>131</b>
<b>Figure 3.18: AR variant activity in response to different ligands.</b>	<b>134</b>
<b>Figure 3.19: AR mutations in BCa do not affect AR/ ER<math>\alpha</math> cross-talk.</b>	<b>135</b>
<b>Figure 3.20: CRISPR/ CAS9 in MCF-7 resulted in AR silencing.</b>	<b>137</b>
<b>Figure 3.21: Possible mechanisms of repression present in AR- ER<math>\alpha</math> cross talk.</b>	<b>142</b>
<b>Figure 3.22: Locations of AR mutations in Breast Cancer.</b>	<b>145</b>
<b>Figure 4.1: Heat map of PLC isoforms expression levels in PCa cell lines.</b>	<b>152</b>

<b>Figure 4.2: The thieno[2,3-<i>b</i>]pyridine compounds inhibit prostate cancer cell lines.</b>	<b>155</b>
<b>Figure 4.3: The thieno[2,3-<i>b</i>]pyridine compounds IC50 and cellular viability.</b>	<b>157</b>
<b>Figure 4.4: The thieno[2,3-<i>b</i>]pyridine compounds promote cell cycle arrest in PC3 cells.</b>	<b>159</b>
<b>Figure 4.5: The thieno[2,3-<i>b</i>]pyridine compounds promote apoptosis in PC3 cells.</b>	<b>161</b>
<b>Figure 4.6: Necrosis analysis of PC3 cells upon the treatment with the thieno[2,3-<i>b</i>]pyridine compounds.</b>	<b>162</b>
<b>Figure 4.7: The thieno[2,3-<i>b</i>]pyridine compounds promote caspase dependant cell death in PC3.</b>	<b>164</b>
<b>Figure 4.8: The capsase inhibitor Z-VAD reduces thieno[2,3-<i>b</i>]pyridine-induced apoptosis.</b>	<b>165</b>
<b>Figure 4.9: Confocal microscopy analysis for PC3 cell line investigating thieno[2,3-<i>b</i>]pyridine inhibitors.</b>	<b>169</b>
<b>Figure 4.10: Thieno[2,3-<i>b</i>]pyridine inhibitors increase cell size and promote multi-nucleation.</b>	<b>170</b>
<b>Figure 4.11: The thieno[2,3-<i>b</i>]pyridine inhibitors reduce cell motility.</b>	<b>172</b>
<b>Figure 4.12: The thieno[2,3-<i>b</i>]pyridine 160 anti-cancer inhibit activity in cultured human prostate tumours.</b>	<b>174</b>

# CHAPTER 1

## INTRODUCTION

### 1.1 Normal Breast

#### 1.1.1 Mammary Gland Structure & Development

The mammary gland is an exocrine gland that in human it develops from the embryological tissue where epithelium invades the stroma during the fifth week of pregnancy. The glandular tissue within the breast is present in both genders and after puberty sex hormones (e.g. oestrogen) promote breast maturation in females (Geddes, 2007; Lombardi *et al.*, 2014). Tubule and branching formation occur during puberty where the basic arboreal ducts network is spread out from the nipple (Lemaine and Simmons, 2013). Oestrogen action is dependant on growth hormone (GH), which is released from the pituitary gland. GH has been shown to act via stimulation of insulin-like growth factor-1 (IGF-1), which also modulates mammary gland development (Javed, 2013). The breast is composed of multiple lobes (15-20) and each consists of up to 40 clusters of alveoli where milk is secreted and stored. Surrounding each lobe is a network of myoepithelial cells which are responsible of the contraction of the mammary glands to eject milk. These clusters are connected to mammary tubules which gather to form multiple ducts who are also capable of temporary milk storing ready to drain to the nipple upon hormonal signals (Figure 1.1) (Lemaine and Simmons, 2013). All lobes are supported by connective tissue, mainly collagen and elastin, which come together into suspensory ligaments called cooper's ligaments that anchor the breast to the chest wall on the pectoral muscles. This structure has spaces in between which are filled by an adipose tissue containing blood vessels and surrounded by lymph nodes (Javed, 2013). During pregnancy, the ovarian follicles initially produce

oestrogen and progesterone, but these hormones are subsequently produced by the placenta, promoting breast growth and milk production (Lombardi *et al.*, 2014). Moreover, oestrogens promote elongation of the ducts and stimulate branching morphogenesis while, progesterone increases the lobules number and size in order to facilitate the breast to perform its function (Geddes, 2007). Normally, the breast reaches its highest maturation levels during pregnancy in preparation for lactation, and then after this stage it is able to regress into an arrested state (Hassiotou and Geddes, 2013; Lemaine and Simmons, 2013).

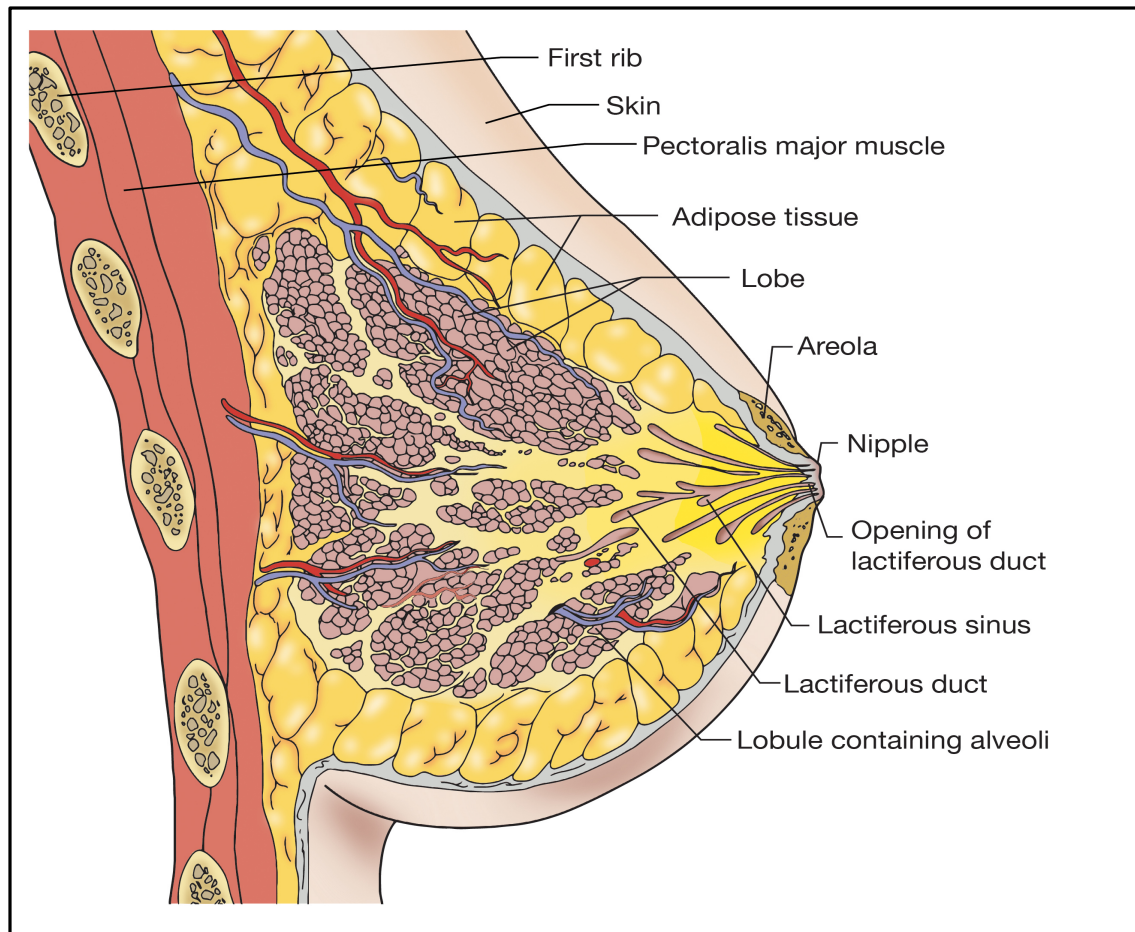


**Figure 1.1: Structure of the human mammary gland.** The breast anatomy, ducts spreading out of the nipple to form 15- 20 lobes lining on a fat pad within the adipose tissue. [obtained from Medscape 2016].

### **1.1.2 Mammary Gland Function**

The primary function of the mammary glands is lactation in which the produced milk provides nourishment and immunity to the new born baby. Prior to childbirth and in the few days following, the breast produces a yellowish substance known as colostrum that is rich in protein and lactose but low in lipids (Yang, 2017). Also during this period, the anterior pituitary gland releases prolactin which stimulates gland cells in the breast to produce milk enriched with fat, carbohydrate, proteins, vitamins and minerals (Hassiotou and Geddes, 2013). Furthermore, when the female starts nursing, the mechanoreceptors in the nipple are stimulated, generating an electrical signal that is carried to the hypothalamus in the brain (Rezaei, 2016; Yang, 2017). In response to this signal, the hypothalamus sends a signal to the posterior pituitary gland to initiate the production of oxytocin, which stimulates the myoepithelial cells to squeeze the milk out to the nipple. At the same time, the hypothalamus sends an off signal to specific neurons in the anterior pituitary gland, which releases prolactin inhibiting hormone, resulting in less inhibition to the neurons responsible for prolactin production (Macias, 2012). Oxytocin not only promotes milk release, but also stimulates the mother's uterus to return to its normal size and shape (Lombardi *et al.*, 2014).

## **1.2 Breast Cancer**

### **1.2.1 Epidemiology**

Generally, cancer occurs due to mutations in the DNA resulting in the proliferation and homeostasis process of the normal cell (Tomasetti *et al.*, 2017). The manipulation of the cell physiology causes deactivation in the anticancer defence mechanism of the affected tissues (Hanahan and Weinberg, 2000; Tomasetti and Vogelstein, 2015). Moreover, cancer cell

genotyping indicated six alterations, known as the hallmarks of cancer, and are believed to drive the malignant growth of the tumour. These changes include: self-sufficiency in growth signals, insensitivity to growth-inhibitory signals, tissue invasion and metastasis, limitless replicative potential, sustained angiogenesis and evading apoptosis. Further, the genome instability of the tumour cells leads to the reprogramming of energy metabolism and evading of immune destruction (Hanahan and Weinberg, 2000; Hanahan and Weinberg, 2011).

Breast Cancer (BCa) is a heterogeneous disease and is the most common cancer in women worldwide. 54,800 females and 370 males were diagnosed with Breast Cancer in 2015 in the UK and approximately 1:5 will die from the disease (Cancer Research UK, 2015). BCa is the 2<sup>nd</sup> most common cause of cancer death in women in the UK's and incidence rates are projected to rise by 2% within the next 20 years (Cancer Research UK, 2015).

### **1.2.2 Symptoms, Management & Risk Factors**

The main symptom of breast cancer is a lump felt by the patient, however, some cases are detected at an early stage through mammographic screening. Lumps within the lymph nodes in the armpit can also indicate the presence of breast cancer. Some other symptoms may include changes in breast tissue thickness, disproportionate breast size, dimpling and inflammation, changes in the nipple shape or position and unusual secretions from the nipples (Cancer Research UK, 2015).

Physical examination and mammography are commonly used as early detection procedures where micro classifications are observed. In the latter, x-rays are applied to the patient's breast for the detection of abnormal masses. For suspicious cases, fine needle aspiration



(FNA) is performed and the sample is examined using microscopy to evaluate the sample. This usually provides an accurate diagnosis, otherwise patients may undergo additional testing such as Magnetic Resonance Imaging (MRI) and core biopsy where larger parts of the affected tissue are examined (Cancer Research UK, 2015). Breast Cancer cases have variable management guidelines based on the sub-type and other clinical criteria e.g. age, stage and tumour size. Treatment protocols include a combination of adjuvant hormonal therapy, chemotherapy, radiotherapy and surgery (Fioretti *et al.*, 2014; Cancer Research UK, 2015). A number of risk factors have been associated with breast cancer and these include gender, lack of physical exercise, obesity, alcohol consumption, smoking, genetics and hormonal therapies at certain periods such as menopause (Cancer Research UK, 2015). Like other types of cancer, breast cancers develop as a result of a combination of external (environmental) and/or internal (genetic) factors.

### **1.2.3 Treatment**

Due to the heterogeneity of BCa, there are multiple treatment options dependant on the stage and sub-type of the disease. Surgical removal of the breast, (lumpectomy, quadrantectomy or mastectomy), combined with radiotherapy and chemotherapy is commonly used with localised tumours (Tilstra and McNeil, 2017). Radiation is delivered after surgery via brachytherapy or external beam radiotherapy, where it is applied to the tumour area and the surrounding lymph nodes to destroy any cancer cells that might have escaped the surgery. The decision to administer adjuvant or neoadjuvant chemotherapy is dependent upon the presence of metastases (Ali and Coombes, 2002). Oncotyping of the ductal carcinoma *in situ* (DCIS) aids a more appropriate treatment strategy for this non-invasive BCa subtype (Tilstra and McNeil, 2017). Endocrine therapies, which aim to block ER $\alpha$  activity, are often preferred for patients with metastatic ER $\alpha$ -

positive Luminal disease. These therapies include anti-oestrogens, Aromatase Inhibitors (AIs) and Gonadotropin- Releasing Hormone agonists (GnRHAs), which can be used either separately or together (Vorobiof, 2016). Docetaxel, methotrexate and fluorouracil are the most chemotherapy regimes used in BCa and aim to target the fast growing/replicating cancer cells. In HER-2 positive disease, monoclonal antibodies (e. g. Pertuzumab) are commonly used in combination with other treatments to block HER-2 receptor dimerization (Vorobiof, 2016). In advanced BCa, where the tumour has metastasised from the the primary site, endocrine therapies (e. g. anti-oestrogens and aromatase inhibitors) are an effective treatment option for patients with ER  $\alpha$  -positive disease (Ben-Baruch *et al.*, 2015; Vorobiof, 2016).

#### **1.2.4 Molecular Subtypes**

Based on molecular profiling, BCa can be classified into at least five distinct malignant subtypes (Luminal A, Luminal B, HER2-enriched, normal-like and basal-like BCa) based on the expression of the Oestrogen Receptor  $\alpha$  (ER $\alpha$ ), Progesterone Receptor (PR) and Human Epidermal growth factor Receptor 2 (HER2) (Table 1.1) (Lehmann-Che *et al.*, 2013; Prat *et al.*, 2015).

Luminal subtypes are both ER $\alpha$  and PR positive but differ in the presence of the HER2 oncogene where type A is negative and type B is positive for this receptor. The HER2-enriched subtype is negative for the hormone receptors ER $\alpha$  and PR, with amplification of the oncogene HER2. The normal-like subtype is ER $\alpha$  positive while the basal-like subtype, also known as

Triple Negative BCa, is negative for all of the receptors (ER $\alpha$ , PR and HER2) (Lehmann-Che *et al.*, 2013; Héquet *et al.*, 2011). BCa can also be divided into two types based on the site of development within the breast tissue. Non-invasive *in situ* carcinoma is known to develop in the breast ducts and are unable to metastasize to other parts of the body. This type is commonly referred to as ductal carcinoma *in situ* (DCIS) (Prat *et al.*, 2015; Sinn and Kreipe, 2013). In contrast, invasive breast cancer develops in the cells surrounding the breast ducts (invasive ductal breast) and this sub-type is associated with a higher risk of tumour spread outside of the breast (Souzaki *et al.*, 2011).

**Table 1.1: The five main classifications of Breast Cancer.** BCa molecular classification according to the presence or absent of Oestrogen Receptor Alpha (ER $\alpha$ ), Progesterone Receptor (PR) and Human Epidermal Growth Factor Receptor 2 (HER-2).

Subtype	ER $\alpha$	PR	HER-2
<b>Luminal A</b>	+	+	-
<b>Luminal B</b>	+	+/-	+
<b>HER-2 enriched</b>	-	-	+
<b>Normal-like</b>	+	N/A	N/A
<b>Basal-like</b>	-	-	-

## 1.3 Nuclear Receptors

### 1.3.1 Nuclear Receptors Structure and Function

Nuclear receptors (NR) are transcription factors that regulate the expression of specific genes. Members of this super family are essential in development, reproduction, differentiation and metabolism in eukaryotes (Tocchini-Valentini *et al.*, 2003). Typically, nuclear receptor activation requires interaction with ligands that circulate within the body. Those ligands dissociate from their carrier plasma protein to enter the cell via passive diffusion or specific transport processes to bind to their specific receptor. In humans, there are 48 nuclear receptors which all share a common well-characterized structure (Figure 1.2); the variable N-terminal region contains Activation Function-1 (AF-1). Central to the receptor is highly conserved DNA binding domain (DBD), consisting of two alpha-helical structures (zinc-fingers), responsible for DNA specificity and receptor dimerization (Bain *et al.*, 2007; Robinson-Rechavi *et al.*, 2003). Next to this is the less conserved hinge region; a flexible region containing the nuclear localization signal (NLS). The C-terminus of the receptor contains the ligand-binding domain (LBD), which is moderately conserved between receptors. This region is often responsible for receptor binding to specific hormonal or non-hormonal ligands (Brooke and Bevan 2009). The LBD contains Activation Functions-2 (AF-2) that in some receptors synergizes with AF-1 to reduce ligand-off rate and subsequently increase gene expression. The C-terminal region varies in length amongst the different nuclear receptors (Tocchini-Valentini *et al.*, 2003; Brooke and Bevan 2009).

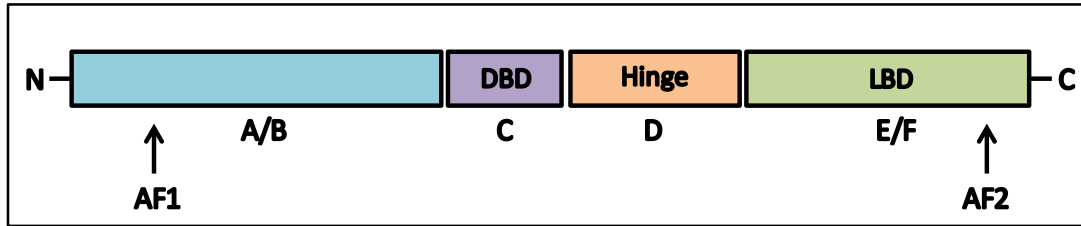


**Figure 1.2. General structure and functional domains of nuclear receptors.** Nuclear receptors (NRs) are comprised of four functional domains: N-terminal domain, DBD= DNA binding domain, Hinge and LBD= ligand binding domain. AF1, 2= activation function 1,2. [Adapted from Bain *et al.*, 2007].

### 1.3.2 Steroid Hormone Receptors

Nuclear receptors are classified into 6 subfamilies (NR1-6) based on their sequence similarity. One family that has been demonstrated to be particularly important in BCa is the steroid hormone receptors subfamily (Oestrogen Receptor-like) (Brooke and Bevan 2009). This group contains the oestrogen receptors (ER $\alpha$  and ER $\beta$ , activated by oestrogens), glucocorticoid receptor (GR, activated by cortisol), mineralocorticoid receptor (MR, activated by aldosterone) and the 3-ketosteroid receptors (PR and AR, activated by progesterone and androgen hormones respectively). Since steroid hormones are lipid-soluble, they can cross the cell membrane via simple diffusion and therefore bind to their specific intracellular receptors. Upon ligand binding, the steroid receptors become activated and modulate gene expression (Hickey *et al.*, 2012).

In general, steroid receptors have two mechanisms in controlling cell behaviour; genomic and non-genomic (Figure 1.3). In classical genomic signalling, the receptor is held in an inactive state through a heat-shock protein (HSP) complex (Heemers *et al.*, 2007). Ligand activation of the receptor promotes the dissociation of this complex, resulting in nuclear translocation and dimerization of the receptor. The dimer is then able to bind to hormone response elements, a

specific target sequence found in the regulatory regions of target genes (Carroll *et al.*, 2006). Receptors recruit accessory proteins and the basal transcriptional machinery to subsequently regulate transcription (Heemers *et al.*, 2007). The second mechanism of cell signalling is non-genomic, where steroid receptors can regulate target expression/ activity in the absence of DNA binding. This activation pathway is dependent on receptor regulation of signal transduction pathways (Hickey *et al.*, 2012; Heemers *et al.*, 2007). An example of non-genomic signalling is the activated ER $\alpha$  interaction with the IGF-IR (insulin-like growth factor 1 receptor) and MAPK pathways resulting in regulation of gene transcription (Lipovka and Konhilas 2016).

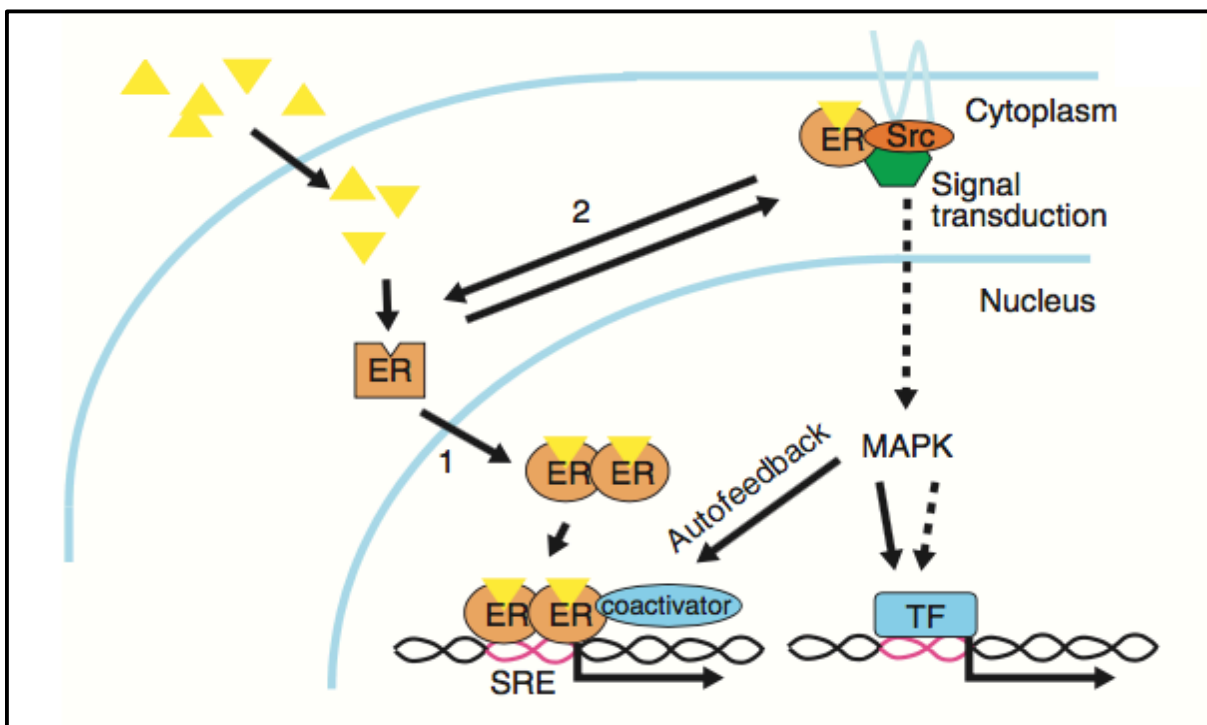


**Figure 1.3. Genomic and non-genomic signalling of the Oestrogen Receptor (ER).** 1- Genomic signalling, ER activated by ligand binding (E2) leading to gene transcription. 2- Non-genomic, E2 binding to ER result in receptor activation then interaction with other molecules/ pathways (e. g. MAPK) to initiate transcription of target genes. [obtained from Edwards and Boonyaratanakornkit 2003].

### 1.3.3 Oestrogen Receptor and Hormone Therapies

In mammals, there are two Oestrogen Receptor (ER) variants: ER $\alpha$  and ER $\beta$  encoded by the genes *ESR1* and *ESR2* respectively. Both receptors have similarities in DNA-ligand binding characteristics but they are distinct in their functions and tissue distribution. Oestrogen signalling influences the growth and function of many body tissues and has been implicated in the development of multiple diseases (Alluri *et al.*, 2014; Fioretti *et al.*, 2014). For example, oestrogen signalling has been demonstrated to play an essential role in various types of cancer such as breast, ovarian, prostate and colorectal. In breast cancer, it has been found that ER is expressed in 60-70% of tumours (McNamara *et al.*, 2014).

In the majority of ER positive BCa, modulation of oestrogen signalling is an effective strategy to treat the disease. Oestrogen signalling can be targeted in a number of different ways: i, tissue specific antagonists, e.g. Tamoxifen and Raloxifen, act as selective modulators of ER in breast cancer. ii, oestrogen receptor down-regulators, e.g. Fulvestant which promotes ER degradation. iii, inhibitors of oestrogen synthesis e.g. the aromatase inhibitors Exemestane, Anastazole and Letrazole (Ben-Baruch *et al.*, 2015; Vorobiof, 2016). The latter are predominantly used for postmenopausal women due to the importance of the aromatase enzyme in oestrogen synthesis in this group of women (Alluri *et al.*, 2014). Importantly, endocrine therapies have significantly contributed to a reduction in BCa development, recurrence and morbidity (McNamara *et al.*, 2014; Viedma-Rodríguez *et al.*, 2014).

### 1.3.4 Endocrine Resistance

Disease recurrence, following treatment with the anti-oestrogen Tamoxifen, has been shown to occur within 15 years of treatment in one-third of patients (Alluri *et al.*, 2014). Multiple molecular mechanisms have been proposed to explain endocrine resistance in breast cancer e.g. ER $\alpha$  signalling pathway crosstalk with up/down-regulated growth factors such as the human epidermal growth factor 2, phosphoinositide-3-kinase, mitogen-activated protein kinase and insulin-like growth factor 1 (Alluri *et al.*, 2014; McNamara *et al.*, 2014). Recently it has also been demonstrated that mutations in ER $\alpha$  can also drive therapy resistance. These studies have demonstrated that through mutation, the ER $\alpha$  becomes ligand independent and can therefore bind to DNA and regulate gene expression in the absence of ligand (Fioretti *et al.*, 2014).

ER $\alpha$  mutations are detectable in up to 54% of metastatic BCa cases. Alluri *et al.*, (2014) reported that there is a significant up-regulation in the expression of ER $\alpha$  responsive genes, such as *GREB1* in tumours expressing a mutant ER $\alpha$ . This suggests an essential role of the active ER $\alpha$  pathway in converting the endocrine-sensitive tumour to a resistant phase. More understanding about the mutant genes involved in resistant tumours could contribute to treatment regime selection. For example, reliable clinical approaches to detect *ESR1* mutants could help clinicians to change from an aromatase inhibitor treatment protocol to an anti-oestrogen. This switch in therapeutic regimes is known to be effective for patients with BCa resistant to aromatic inhibitors (Fioretti *et al.*, 2014; Alluri *et al.*, 2014).



### 1.3.5 Androgen Receptor

The androgen receptor (AR) is another member of the steroid hormone receptor family. It is encoded by the *AR* gene located on the Q arm of the X chromosome (q11-q12) and consists of 8 exons encoding a protein of 919 amino acids. The AR has a similar structure (Figure 1.4) and mechanism of action to ER $\alpha$  and other nuclear receptors (Lehmann-Che *et al.*, 2013). Generally, androgens are the key regulators of male sex organ development and function. In addition to this, they also play a key role in maintaining male skeletal integrity, while in the female they tend to be less essential regardless of their high presence in different body tissues (Fioretti *et al.*, 2014). The AR is widely characterized to be critical in prostate gland physiology and pathology and the oncogenic driver of prostate cancer at all stages (Brooke and Bevan, 2009). Also, it has been recently demonstrated that ARs are involved in different types of tumours such as lung, liver and breast cancer. For example, it has recently been demonstrated that the AR has an oncogenic role in certain molecular subtypes of breast cancer, such as Molecular Apocrine BCa (Lehmann-Che *et al.* 2013).

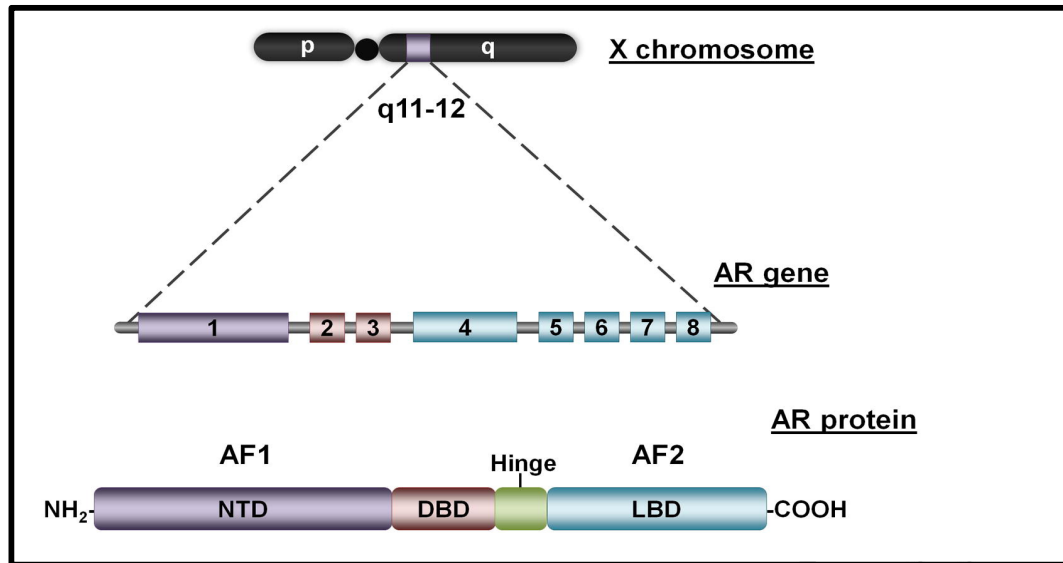


**Figure 1.4: AR gene location on the X chromosome and its modular structure.** Image shows four functional domains of the AR and the gene structure consisting of 8 exons. NTD = N-terminal domain, DBD = DNA binding domain. LBD = ligand binding domain. AF = activation function. [obtained from Anestis *et al.*, 2015].

### 1.3.6 Receptors in Breast Cancer

Approximately 60% of BCa tumours are classed as ER $\alpha$  positive. ER $\alpha$  is known to play an important role in breast cells and overexpression of the receptor has been shown to increase DNA replication and cell replication (Gross and Yee 2002; Fioretti *et al.*, 2014). The steroid hormone oestradiol binds to Oestrogen Receptor  $\alpha$  (ER $\alpha$ ) and plays an important role in BCa progression. When oestrogen binds to ER $\alpha$ , the receptor is activated and translocates into the nucleus. The receptor stimulates genes transcription through binding to responsive elements located in the regulatory regions of target gene.

Deregulation of the HER family of receptors has also been demonstrated to play a role in the growth of BCa (Serra *et al.*, 2011). In particular, the HER-2 receptor has been found to be highly overexpressed in 20% of BCAs. The HER-2 receptor is activated by ligand induced

dimerization or pairing with other HER family receptors (Serra *et al.*, 2011). The dimers phosphorylate specific tyrosine residues through activation of the intrinsic tyrosine kinase domain and subsequently activate downstream signalling pathways. HER-2 overexpression leads to inappropriate activation of signalling pathways that promote tumour cell proliferation and disease progression (Ménard *et al.*, 2000; Serra *et al.*, 2011).

Combination of the anti-HER2 monoclonal Trastuzumab and other tyrosine kinase inhibitors are used for managing HER2 positive BCa whereas hormonal therapies, such as the anti-oestrogen Tamoxifen, are widely used to manage ER $\alpha$  positive disease (Kelly *et al.*, 2010; Serra *et al.*, 2011). Although the AR is highly expressed in the mammary tissue, the normal biological role of this receptor is still unclear (Robinson *et al.*, 2011). However, a new subgroup of basal-like BCa has been recently identified as Molecular Apocrine Breast Cancer (MA). This subgroup is characterized as ER $\alpha$  and PR negative, AR positive and HER2 positive/negative. In ER $\alpha$  positive disease the AR is associated with good prognosis and this appears to be via inhibition of ER $\alpha$  activity. In molecular apocrine disease, the AR appears to be able to drive growth (Robinson *et al.*, 2011). It has therefore been proposed that MA BC could be treated with anti-androgens (AR antagonist) such as Bicalutamide. It is important to better characterise the role of the AR in BCa to investigate how the receptor could be utilised as a therapeutic target for the different subtypes of the disease (Lehmann-Che *et al.*, 2013)

## 1.4 Androgen Receptor Signalling in Breast Cancer

### 1.4.1 AR expression in Breast Cancer

Androgen hormones are known to be relevant to the male gender, but various androgens have also been identified in serum from women, such as Dehydroepiandrosterone (DHEA), testosterone, 5 $\alpha$ -dihydro-testosterone (DHT) and androstenedione (A4) (McNamara *et al.*, 2014). These androgens are predominantly secreted from the ovaries and adrenal glands, but also to a lesser extent from peripheral tissues including breast and bone. Steroid Hormone Binding Globulin (SHBG) binds to, and controls the bioavailability of, androgens as well as oestrogens. During the menstrual period, testosterone has fluctuating concentrations which decline by the age of menopause. In contrast, adrenal androgens continue to be produced even after menopause (Labrie *et al.*, 2003). It has been suggested that excessive levels of androgens could be considered as a sign of BCa development, since elevated levels of testosterone has been associated with breast cancer in postmenopausal women (McNamara *et al.*, 2014).

The enzyme aromatase is able to metabolize testosterone into oestradiol (E2) and 5 $\alpha$ -reductase converts testosterone into the more potent androgen dihydrotestosterone (DHT) (Fioretti *et al.*, 2014). The relative expression of aromatase and 5 $\alpha$ -reductase within the breast epithelium therefore plays a key role in AR activation in this tissue. Aromatase activity is the main source of E2 in post-menopausal women where androgens are primarily synthesized locally within the breast tissue (McNamara *et al.*, 2014).

AR activity in breast cancer cell lines has been found to be modulated by different signalling pathways such as PI3K/AKT/MAPK, FOXA1 and p53 which impacts upon the outcome of the AR action (Claessens and Tilley, 2014; Alluri *et al.*, 2014). The main member of the forkhead family, FOXA1, is considered to be an essential factor in breast cancer growth

because it regulates AR and ER $\alpha$  DNA binding capacity. Chromatin Immunoprecipitation-Sequencing (ChIP-seq) studies performed on the molecular apocrine BCa cell line MDA-MB-453, demonstrated a high correlation between FOXA1 and AR binding sites, which suggests that FOXA1 mediates AR DNA-binding in this subtype of BCa (Ni *et al.*, 2013, Robinson *et al.* 2011). The factor FOXA1 has been found to be essential in directing AR DNA binding and siRNA knock-down of FOXA1 reduced androgen induction of MYC and reduced cell growth (Ni *et al.*, 2013).

#### **1.4.2 AR/ER Cross Talks in BCa**

The AR appears to have different roles in breast cancer development, oncogenic in ER $\alpha$ -negative disease and acting as a tumour suppressor in ER $\alpha$ -positive disease. In the latter, it appears that AR inhibits ER $\alpha$  activity to inhibit breast cancer progression and various crosstalk mechanisms have been described (Hickey *et al.*, 2012). For example, direct interaction between the N-terminus of the AR and the LBD of ER $\alpha$  blocks the activity of both receptors (Heemers *et al.*, 2007). Also, AR is able of bind to oestrogen response elements (EREs) and therefore block ER $\alpha$  binding to DNA. This was demonstrated through the transfection of the AR DBD into BC cell lines, which was shown to significantly reduce ER $\alpha$  activity (McNamara *et al.*, 2014). Also, competition for histone modifying cofactors is also likely to have a bearing on receptor activity. For example, Androgen Receptor Associated co-regulator 70 (ARA70) can enhance the activity of both the AR and ER $\alpha$  and the AR may sequester this factor, resulting in a decrease in ER $\alpha$  activity. Lastly, competition for accessory proteins important in non-genomic activity for AR and ER $\alpha$  may also be important in receptor cross-talk. For example, M-BAR which is responsible of

regulating signalling pathways at the cell membrane, is shared between these receptors (McNamara *et al.*, 2014; Heemers *et al.*, 2007).

### **1.4.3 AR as Prognostic and Therapeutic Factor in Breast Cancer**

Anti-androgens have been used in various medical conditions in women, such as ovarian cancer. In breast cancer AR has been found in 85% of primary BCs and 75% of metastatic lesions. A number of studies have suggested AR as a prognostic indicator in ER $\alpha$ -positive BC, based on correlations between AR levels, clinical characteristics and disease outcome (McNamara *et al.*, 2014). Further, AR positivity is associated with longer survival, smaller tumour size, metastasis free and lower histological grade (Lehmann *et al.*, 2011). The synthetic steroidal androgen, Flouxymesterone, has been used clinically for the treatment of BCa (ER $\alpha$ -positive) via activating the AR to promote cross-talk with ER $\alpha$  and found to effectively inhibit proliferation when combined with the anti-oestrogen Tamoxifen (Tam) (Africander *et al.*, 2014). Current clinical trials for the anti-androgen Enzalutamide (Enz) have shown promising results and has been demonstrated to be effective in disease multiple subtypes, including the molecular apocrine disease (Schwartzberg *et al.*, 2017). However, further investigation of this drug is still ongoing with the aim of optimising the effective dosage and the best combinations with other therapies.

The selective androgen receptor modulator (Enobosarm) is another promising drug which has been investigated as a treatment option for multiple BCa subtypes (Vontela *et al.*, 2017). This treatment was found to reduce tumour size and proliferation in a xenograft model (MDA-

MB-453-AR) and reduced the expression of Interleukin 6 (IL6), which has been shown to be important in tumour metastasis (Narayanan *et al.*, 2014; Vontela *et al.*, 2017).

#### **1.4.4 Molecular Apocrine Breast Cancer (MA)**

Molecular Apocrine (MA) BCa is characterized as having high expression of the AR and is similar to the Luminal BCa subtype, but the absence of ER $\alpha$ . MA represents 12% of total diagnosed breast cancer cases and it is often enriched with the *HER2* oncogene (Robinson *et al.*, 2011). MA tends to be more aggressive than other BCa subtypes and shows poor prognosis and much evidence exists to suggest that AR signalling drives proliferation of these tumours. Currently, the MDA-MB-453 cell line is the most common cell line used for MA research (Moore *et al.*, 2012). Androgens can enhance the proliferation of MDA-MB-453 cells and AR antagonists have been shown to inhibit proliferation. Chromatin immunoprecipitation sequencing (ChIP-Seq), performed to examine AR binding sites in MDA-MB-453, demonstrated that 50.9% of AR sites overlap with ER $\alpha$  sites, suggesting that the AR regulates similar factors to ER $\alpha$  in MA breast cancer (Lehmann *et al.*, 2011; Robinson *et al.*, 2011).

The AR antagonists Bicalutamide is currently in clinical trials to investigate its efficacy in advanced AR-positive BCa (McGhn *et al.*, 2014). This drug is currently approved for clinical use for the treatment of advanced PCa as a monotherapy or in combination with LHRH agonists. Also, the newer AR antagonist, Enzalutamide, is under investigation in MA disease and clinical trails testing this drug in the TNBC subtype revealed promising tumour responses (McGhan *et al.*, 2014; Traina *et al.*, 2018).

### **1.4.5 AR Mutations in Breast Cancer**

It appears that AR signalling plays an important role in the development and progression of the BCa (Lehmann *et al.*, 2011). The investigation of AR targeting in BCa clinical trials has increased the importance of further characterisation of androgen signalling in this disease. It is well known that AR mutations promote resistance to antiandrogens therapies in prostate cancer (Alluri *et al.*, 2014). Little is known about the prevalence and role of AR mutations in BCa. The expansion of NGS sequencing of patients samples have demonstrated that mutations in the AR are associated with BCa, but the role of these mutations in disease development and progression is unclear. Therefore, this study aims to identify AR mutants in BCa and to evaluate the effect of these substitutions upon androgen signalling and cross-talk with other signalling pathways.

## **1.5 The Prostate Gland**

### **1.5.1 Location and description**

The prostate is an exocrine gland within the male reproductive system, located at the base of the bladder, surrounding the exiting urethra and in front of the rectum. The gland is described as being the shape of a walnut or like a rounded cone, with approximate size of 3x4x2 cm and weight of 20-30 grams in adults (Chan *et al.*, 2012). Approximately two thirds of the prostate is composed of glandular tissue with many ejaculatory ducts responsible for the secretion of the seminal fluid. A fibromuscular stroma forms the remaining third, which consists of smooth muscle, elastin and dense connective tissue containing collagen fibers (Aaron *et al.*, 2016). Upon ejaculation, the stroma contracts in order to push out seminal fluid into the urethra and it forms the outmost layer of the prostate. The prostatic secretions are essential for male fertility as they



have a role in semen coagulation and liquefaction, nourish and protect the spermatozoa and lubricating urethral surface (Toivanen & Shen 2017). The prostatic fluid is composed of fructose, proteolytic enzymes, zinc, citric acid, acid phosphate and lipids (Verze *et al.*, 2016).

The prostate gland is clinically divided into two lateral lobes separated by a central sulcus and middle lobe that may project into the bladder in old men (Timms & Hofkamp 2011). However, more important is the anatomical and histological division of the prostate into different zones (Figure 1.5). The central zone, represent 25% of the gland and surrounds the ejaculatory ducts. The transitional zone, comprises approximately 5-10% of the prostate and is located centrally surrounding the urethra. The peripheral zone makes up the glandular bulk (approximately 65%) and is the main area felt during the digital rectal examination (DRE). Lastly, a non-glandular anterior fibromuscular zone of stroma accounts for about half of the volume of the prostate (Toivanen & Shen 2017; Verze *et al.*, 2016).

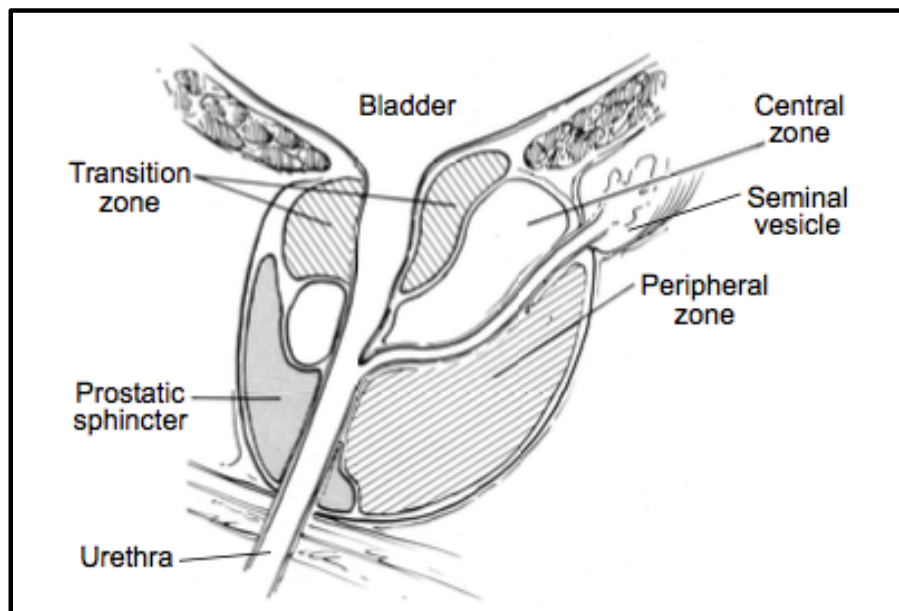


**Figure 1.5: Anatomy of the prostate.** The human prostate gland is divided into three zones: the central zone, the transition zone and the peripheral zone. [obtained from Abate-Shen & Shen 2000].

### 1.5.2 Prostate development

The molecular development of the prostate has been mainly established in transgenic and gene knock-out animal models (mouse and rat) (Aaron *et al.*, 2016). During embryogenesis, the structure of the prostate rises from the primitive urogenital sinus resulting in the formation of the caudal extension of the hindgut (Schaeffer *et al.*, 2008). This structure stays as one joint excretory tract in the embryonic cloaca until approximately the 8<sup>th</sup> week post conception, where it divides into the urogenital and anorectal tracts. The primitive urogenital sinus can be subdivided to the rostral of the bladder, the urogenital sinus (UGS) and the penile urethra at the 10<sup>th</sup> week of gestation when the epithelial budding of the prostate is initiated from the UGS (Kellokumpu-Lenhtinen *et al.*, 1980; Marker *et al.*, 2003).

Prior to the epithelial budding, circulating androgens mediate the induction of the prostate in males and influence its organogenesis prenatally until it reaches its mature size during puberty (Schaeffer *et al.*, 2008). After prostatic fate is determined, the urogenital sinus epithelium buds into the surrounding urogenital sinus mesenchyme via paracrine signalling; this initiates tissue outgrowth and branching morphogenesis resulting in a system of ducts composed of epithelial cords. The androgen receptor (AR) has an essential role in controlling the distal branching to the mature ductal network and the solid epithelial cords (Toivanen & Shen 2017). These cords undergo canalisation creating the ductal lumen and cyto-differentiation to form a functional glandular epithelium with fully differentiated cell types. Prostate growth is minimal between birth and puberty, at which point androgen levels increase, resulting in the gland's full maturation (Aaron *et al.*, 2016; Donjacour *et al.*, 1988).

The epithelium of the mature prostate consists of several distinct cell types based on cell morphology (Figure 1.6). The luminal cells are tall columnar epithelial cells that express

cytokeratins 8 and 18, the androgen receptor and secrete proteins such as prostatic specific antigen (PSA) (Wang *et al.*, 2001). The non-secretory basal cells, under the luminal layer, express cytokeratins 5 and 14 and p63 with low levels of the AR. Within the basal layer, occasional intermediate cells express the same markers as luminal and basal cells, with the addition of cytokeratin 19 (Toivanen & Shen 2017; Wang *et al.*, 2001). Lastly, neuroendocrine cells, which represent the minority of epithelial cells, express secreted neuropeptides and other hormones and are androgen-independent. These cells are believed to produce paracrine signals that control luminal cell development (Abrahamsson 1999).

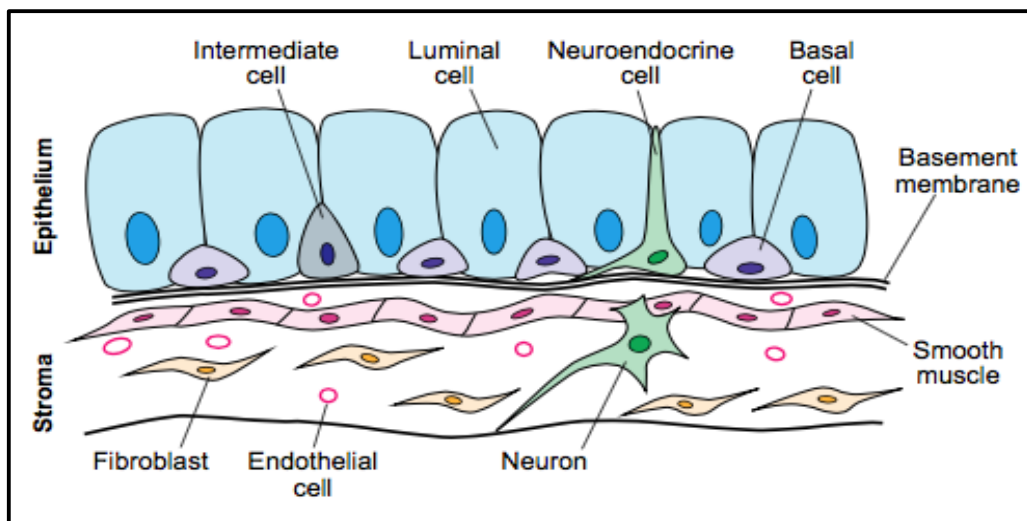


**Figure 1.6: Cell Types in the prostate.** The epithelial compartment is composed of basal cells that line the basement membrane, secretory luminal cells, and rare intermediate and neuroendocrine cell populations. These epithelial ducts are adjacent to a stromal compartment that includes smooth muscle cells, fibroblasts, and vascular and neural components [obtained from Toivanen & Shen 2017].

### **1.5.3 Prostate Diseases**

#### **1.5.3.1 Prostatitis**

Prostatitis is the inflammation of the prostate gland and can be subtyped into two types with both types treated with Fluoroquinolone, anti-inflammatory drugs or alpha blockers (Domes *et al.*, 2012). Acute prostatitis occurs in young men and is commonly caused by bacteria similar to strains that cause urinary tract infections (Touma & Nickel 2011). This acute inflammation is rare and causes pain in the perineum, rectal and/or lower back. As the prostate is enlarged and tender as a result of the infection, patients may experience dysuria.

Chronic prostatitis is more common in older men and it may not necessary follow acute prostatitis. This disease has been linked to obstructive urinary tract abnormalities. 95% of patients complain from intermittent urinary frequency, dysuria, pelvic pain and/or lower back pain (Touma & Nickel 2011; Weidner *et al.*, 2008). Microscopic analysis has identified lymphocyte, plasma cell and macrophage infiltration (Weidner *et al.*, 2008). In prostatitis, bacteria damages the secretory gland and is linked to a a noticeable elevation of the PSA (not more than double normal levels) (Domes *et al.*, 2012). Microbicide oxidants are released by the inflammatory cells in response to the infection, which is believed to induce tissue and genomic damage followed by cell growth and potentially cancer in the prostate (Eiserich *et al.*, 1983).

#### **1.5.3.2 Benign prostatic hyperplasia (BPH)**

Benign prostatic hyperplasia is a non-malignant enlargement of the prostate that refers to hyperplasia of the fibromuscular and glandular epithelial in the transition zone of the gland. By the age of 50, one in four men have some degree of hyperplasia, however, about 10% of these

cases are symptomatic and severe enough to require surgical or medical therapy (Bushman 2009). This enlargement extends to the lateral lobes and affects the prostatic urethra causing bladder outflow obstruction with slight elevation in PSA levels. Microscopic findings of BPH illustrate nodules in the glands and stroma, variable in size with prominent papillary infoldings in the larger glands (Auffenberg *et al.*, 2009; Bushman 2009). This growth is believed to be driven by altered androgen levels, specifically dihydrotestosterone (DHT), therefore treatment with 5- $\alpha$ -reductase inhibitors can reduce the size of the enlarged prostate. Alpha blockers, e.g.  $\alpha$ -1-adrenergic receptor blocker, can also be administered as these relax the bladder's smooth muscle and ease the pressure caused by prostate enlargement (Andriole *et al* 2004).

### **1.5.3.3 Prostatic intraepithelial neoplasia (PIN)**

Prostatic intraepithelial neoplasia (PIN) is a non-cancerous proliferation of the epithelial lining of the gland and is divided into low and high grade PIN. Histologically, it is characterised as having progressive basal cell layer disruption, nuclear and nucleolar abnormalities, increasing proliferative potential and microvessel density, variation in DNA content and allelic loss (Ayala & Ro 2007). The glands and basal layer in PIN remain intact unlike in adenocarcinoma of the prostate. High grade PIN is differentiated with more hyperchromatism and pleomorphism and cells might have more prominent nucleoli (Ayala and Ro 2007; Lipski *et al.*, 1996). PIN commonly develops in the peripheral zone of the gland, the same location where the majority of malignant tumours occurs. Patients with PIN are put under increased surveillance due to the risk of prostate adenocarcinoma development (Lipski *et al.*, 1996).

## **1.5.4 Prostate cancer (PCa)**

### **1.5.4.1 Prostate cancer epidemiology**

In the UK, prostate cancer is the most common cancer in males with around 47,700 new cases yearly and 25% mortality rate, making it 2<sup>nd</sup> most cause of cancer deaths after lung cancer. A projection of 12% increase in incidence rate is expected between 2014 and 2035 as well as a 2.38% increase in mortality for the same period (Figure 1.7) (Cancer Research UK, 2014). Incidence rates differ between countries, in part due to coverage of PSA screening (Schröder *et al.*, 2014). Population-based screening of men aged between 55 and 69 years, using PSA testing, has been evaluated in randomised trials and these show a significant reduction in PCa mortality when the screening and control groups are compared (Schröder *et al.*, 2014). Currently, there is no national screening programme in the UK for PCa. However, the Prostate Cancer Risk Management programme was introduced in 2002 to test PSA levels among men over the age of 50 who are concerned about the disease (NHS Cancer Screening Programmes, 2012).

In Europe, PCa incidence has been increasing, but mortality rates have decreased significantly and this has been attributed to improved prognosis as a result of PSA screening and the availability of imaging techniques in these countries (Smittenaar *et al.*, 2016). In the UK, the five-year survival rate for PCa has increased from 37% during 1971- 1972 to 85% during 2010-2011 and this is strongly associated to PSA testing in the population and improvements in treatment options (Cancer Research UK, 2014). Despite these results, screening for PCa is controversial because of adverse effects, such as over-diagnosis and overtreatment, which is estimated to include 40–50% of screen-detected cases and results in unnecessary therapy associated side-effects. It is estimated that the global number of PCa incidence and deaths will

increase to 1.7 million cases and 477,000 deaths by 2030 respectively, as a result of population growth and aging (Ferlay *et al.*, 2010; Smittenaar *et al.*, 2016).

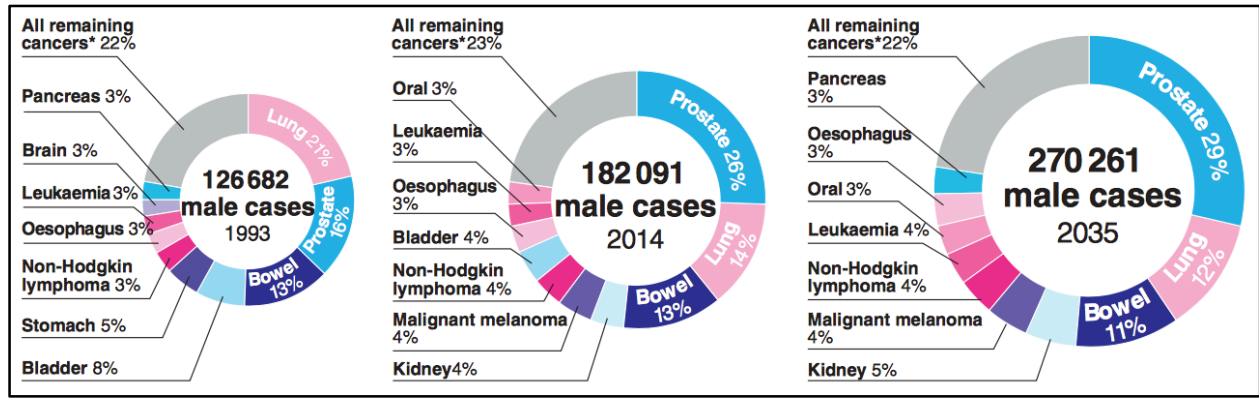


**Figure 1.7: Projection of cancers in the UK.** Proportion of total cancer cases by cancer site in 1993 (observed), 2014 (observed) and 2035 (projected). The size of each segment is scaled to reflect the total number of cases. [obtained from Smittenaar *et al.*, 2016].

#### 1.5.4.2 Risk factors

Studies have not shown any specific life style choices linked to PCa morbidity, however, there are multiple endogenous and exogenous risk factors that affect the probability of a man developing the disease. For example, PCa is rare in males under the age of 50 and incidence rates exponentially increase with age (Bostwick *et al.*, 2004). Another example is family history; the risk for men, with a first-degree relative affected by PCa, is twice higher than of the general population and even higher if the relative was younger than 60 years at diagnosis. Therefore, family history has resulted in much research to identify genetic linkage and Ewing *et al.*, (2012) discovered a rare but recurrent mutation in the *HOXB13* gene. Also, the rare BRCA2 mutation, associated with breast and ovarian cancers, correlates with higher risk of PCa. Ethnicity is also a notable endogenous factor and clinical studies have demonstrated that PCa incidence is 60%

higher in Black Americans than white men in the USA (Ferlay *et al.*, 2015).

Studies analysing migrant populations (from countries with low to high PCa morbidity) have shown that a Western lifestyle is linked to increased incidence rate (Bostwick *et al.*, 2004). A diet with high intake of red meat and saturated fat with low antioxidants, micronutrients and vitamins is suggested to have a link with disease occurrence. Obesity and lack of physical activity are also believed to increase PCa mortality, however, there is still not enough evidence to support this data (Markozannes *et al.*, 2016). Additionally, exposure to environmental factors such as radiation or hormonal agents correlate to PCa occurrence. The UK Atomic Energy Authority analysed data from dead employees and found that the only malignancy related to radiation exposure was PCa. Lastly, endocrine disrupting chemicals (EDCs) can alter hormone activity affecting reproduction, development and carcinogenesis (Bostwick *et al.*, 2004).

#### **1.5.4.3 Grading and staging**

The dominant method for scoring PCa is the Gleason Grading System (Figure 1.8), which is based on the histological diagnosis of the primary tumours (Gardner 1982). This grading is performed microscopically at low-power magnification (10x- 40x) to define the pattern into five different grades (1 to 5). The score is generated from the addition of the largest two examined patterns and therefore range from 2 to 10. Grades 2-4 are well-differentiated and provide the best prognosis, while 8-10 are poorly-differentiated cancer and carry a poor prognosis (Gardner 1982; Humphrey 2004).

Pathological staging of PCa is determined following the TNM classification after prostatectomy (Ukimura *et al.*, 1998). Stage A (T1, N0, M0) represents a tumour that cannot be palpated during DRE and these can be further divided into T1a (involves <5% of the gland) and



T1b (involves >5% of the gland). Both are well-differentiated and evaluated for surgical procedures following the same criteria of the for BPH (Figure 1.9). T1c is refers to cases were the prostate was biopsied in response to elevated PSA levels. Stage B (T2, N0, M0) is where the tumour is contained within the gland and a nodule or hard region was identified by DRE (Strief 2007). This stage is divided into: T2a - up to one-half of one lobe, T2b - more than one-half of one lobe, and T2c - where a palpable node is found in both lobes. Stage C (T3, N0, M0) is divided into: T3a - unilateral capsular penetration, T3b - bilateral extra-capsular extension, and T3c - the tumour has invaded the seminal vesicles. Lastly, stage D (T4, M+) is where the cancer has reached adjacent structures e. g. the bladder neck, sphincter, rectum and pelvis. Inclusion of N and M in the staging indicates if the tumour has reached lymph nodes and distant metastases respectively (Ukimura *et al.*, 1998; Strief 2007).

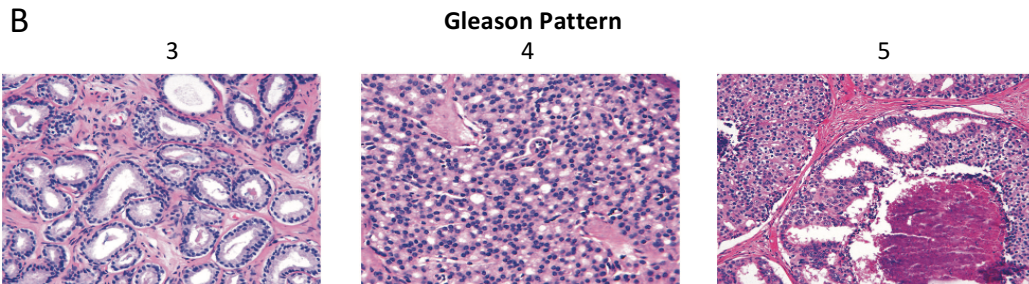
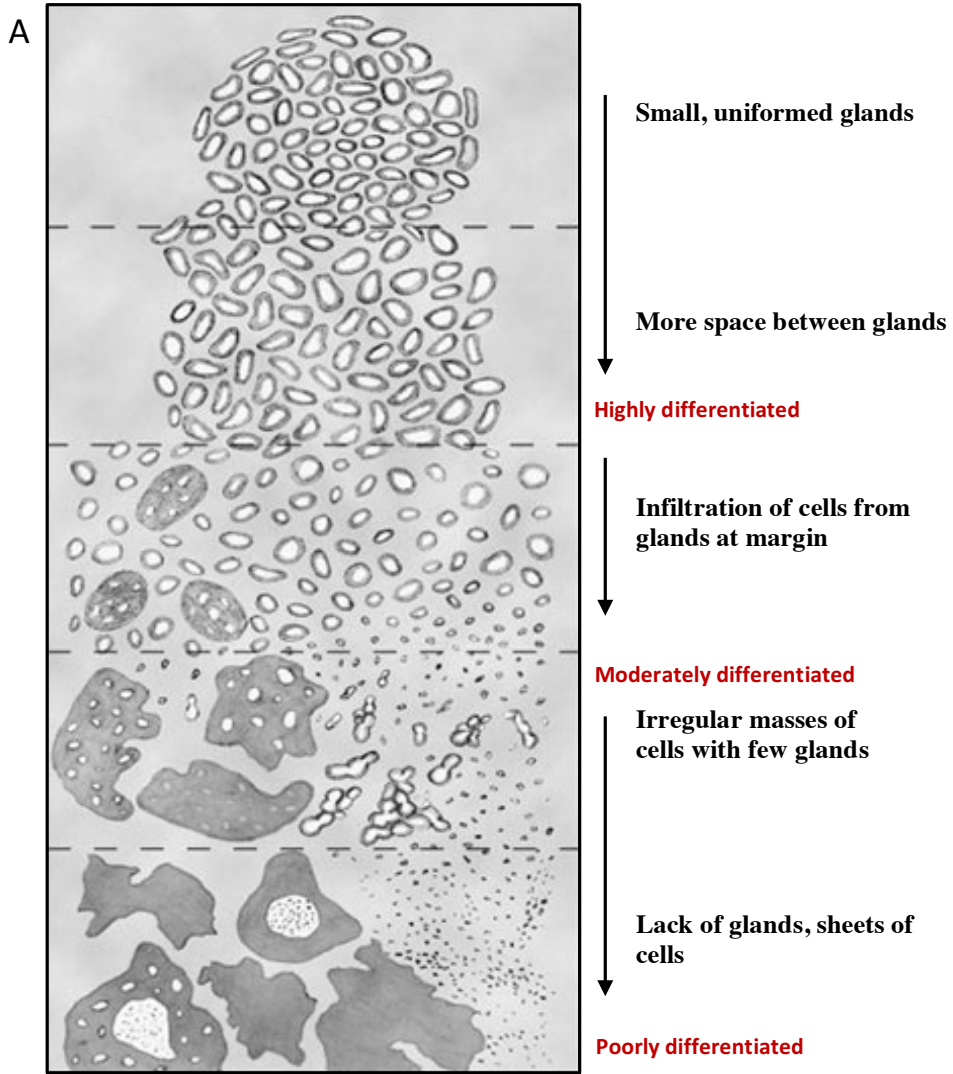


**Figure 1.8: The Gleason Grading system.** A) Gleason scoring according to glandular architecture and patterns. B) Gleason histological features of the grades 3, 4 and 5. [obtained from Humphrey 2004].

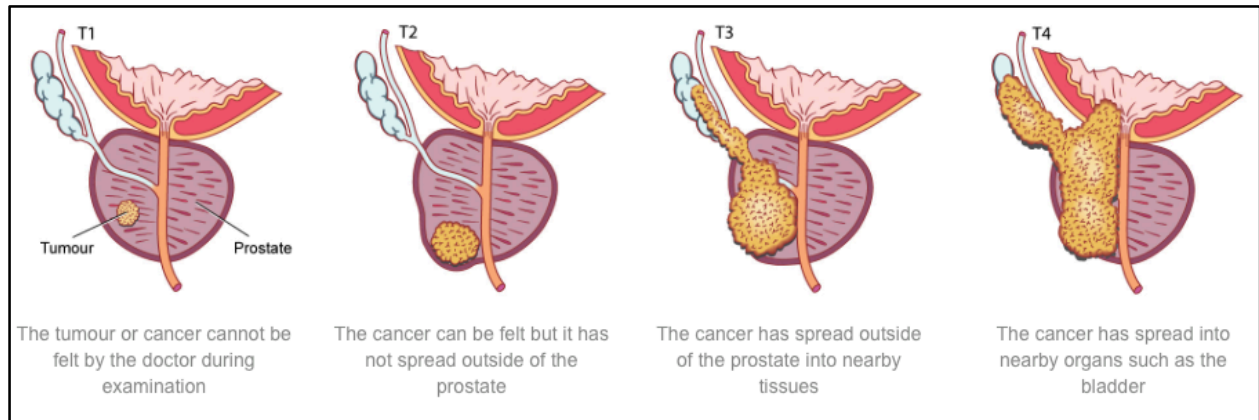


**Figure 1.9: Prostate cancer TNM staging system.** Schematic of the different stages of prostate cancer, with illustration of each stage based on the TNM system. [obtained from Cancer Research UK 2014].

#### 1.5.4.4 Detection and monitoring of Prostate cancer

Initial investigations for prostate cancer are often done by DRE and the evaluation of Prostate Specific Antigen (PSA) levels in the blood (Berger *et al.*, 2007). If one or both of these examinations raise concern, further investigation should follow as intervention at this stage may cure or control the tumour. In the DRE, the examiner assesses the gland texture, asymmetric nodules and consistency using the index finger against the posterior surface of the prostate through the anterior rectal wall. However, recent studies indicated a low specificity and sensitivity in DRE calling (Djulgovic *et al.*, 2010; Naji *et al.*, 2018). PSA is an enzyme specifically created by prostate cells and is a component of the seminal fluid. PSA levels are elevated in response to disruption of the prostate capsule, but this is not specific for PCa. This test has been met with some controversy as increasing levels of PSA are also seen in the presence of prostatitis, BPH, prostate abscess, manipulation of the prostate, prostatic infarction, and ejaculation within the previous 48 hours (Strief 2007). However, patients with PSA higher than 10ng/ml are usually diagnosed with PCa and 95% of patients with metastasised PCa have a significant increase in their PSA levels (Berger *et al.*, 2007). Since all the screening methods

have their limitation, a combination of methods are used to increase detection efficiency. Imaging of the prostate gland is also used in tumour detection, specially magnetic resonance imaging (MRI) and ultrasound (US). Further, positron emission tomography (PET) combined with MRI has been introduced in recent years for more sensitive detection (Mapelli & Picchio 2015). The application of MRI imaging is widely used in the PCa, not only the disease detection, but to perform proper diagnosis, staging and surgical planning of the disease (Bonekamp *et al.*, 2017).

#### **1.5.4.5 Prostate cancer treatment**

The therapeutic management of PCa has become more complex due to the various stage-specific therapeutic options available nowadays. Unfortunately, it is difficult to recommend that one therapy is superior over another, as this field lacks randomized controlled clinical trials (Heidenreich *et al.*, 2010). Therefore, and to avoid overtreatment, patients with low-risk PCa are follow more conservative management plans. Generally, this could be divided into two strategies: watchful waiting (WW) and active surveillance (AS) (Bott *et al.*, 2003). WW monitors the tumour and delays treatment until symptoms appear. This option is commonly used for patients with other health problems and/or elderly men with localized disease aiming to improve their quality of life without aggressive interventions. The AS approach delays active treatment whilst the tumour is at an unthreatening stage (Lund *et al.*, 2014). Patients under AS are continuously assessed for disease progression indicators, including PSA levels, Gleason grade, tumour size and the development of metastases. This approach has shown greater improvement in survival rates than WW, but AS should be followed by active curative

treatments if cancer progression is reported (Bott *et al.*, 2003; Lund *et al.*, 2014).

Another PCa management option is radical prostatectomy (RP) and this is commonly chosen for patients with localised tumour who are expected to live at least another 10 years (Heidenreich *et al.*, 2010). Surgery options can be either open surgery (retropubic or perineal) or laparoscopic (e. g. Da Vinci) (Damber 2005). The majority of patients prefer the longer laparoscopic procedure over open surgery and a recent study demonstrated that the robotic-assisted RP is linked with less surgical margins, reduced need for intraoperative blood transfusions, shorter catheter duration, improved post-operative complications and overall shorter hospitalisation duration. Although pelvic lymphadenectomy in RP is controversial, this is still routinely performed for men with intermediate to high risk of PCa (Niklas 2016).

Besides RP, radiation therapy (RT) is one of the current first line treatment options for PCa. This approach is performed through the application of a radiation beam to the tumour tissue either with an external source of radiation (external beam radiotherapy, EBRT) or internally using brachytherapy (Strief 2007). EBRT has similar efficacy to surgical options and is usually performed for a duration of 4 to 6 weeks, while brachytherapy involves the insertion of radioactive sources (seeds and rods) directly into the prostate gland. Physicians usually choose this procedure based on the detailed anatomy of the gland, tumour size and area, to prevent any unwanted tissue damage to the surrounding organs such as the rectum and bladder (Sadeghi *et al.*, 2010). According to the required doses, injected seeds emit radiation for short-term high dose-rate brachytherapy (HDRB) or long-term low dose-rate brachytherapy (LDRB) (Cesaretti *et al.*, 2007; Skowronek 2013). Since RT affects normal tissues, temporary side-effects include urinary incontinence and erectile dysfunction. There is also an increased risk of developing secondary malignancies due to genetic alteration after radiation exposure (Skowronek 2013).

Androgen Deprivation Therapy (ADT) is often used in the management of the localised and metastasised form of the cancer. As androgens play an essential role in PCa development and progression, inhibition of AR signalling is performed either by medical or surgical approaches (Isbarn *et al.*, 2009). This type of treatment can be used as the primary option in disease management and can be used in combination with RT or RP for better prognosis (Scher *et al.*, 2012). Reduction of testosterone levels upon surgical castration (e. g. bilateral orchiectomy) is one of the best approaches in ADT, however, this procedure is the least popular due to its permanent side-effects (Karantanos *et al.*, 2013). Instead, non-surgical methods such as oestrogen agonists and gonadotrophin-releasing hormone (GnRH) agonists and antagonists are often used to reduce testosterone production (Karantanos *et al.*, 2013; Isbarn *et al.*, 2009). In addition to ADT, the AR can be directly targeted through the use of anti-androgens (e. g. Bicalutamide and Flutamide), which bind to and inhibit the AR, inhibiting its transcriptional activity (Goa and Spencer. 1998; Scher *et al.*, 2012).

#### **1.5.4.6 Development of castration-resistant prostate cancer (CRPC)**

Current hormonal therapies for PCa are highly effective in the early stages of the disease. However, in most patients, the tumour relapses within 2 to 3 years and the disease progresses to a stage known as CRPC, which is associated with poor prognosis and lower survival rates (Brooke *et al.*, 2008; Cookson *et al.*, 2013). A number of mechanisms have been proposed to explain CRPC and these include AR mutations, overexpression or hyper-activation of the AR, independent production of steroids within the tumour or alterations in co-activators and co-repressors (Mostaghel *et al.*, 2009). Moreover, it is proposed that constitutively active AR splice variant (AR-Vs), that lack the ligand binding domain, are up-regulated in CRPC and this also promotes tumour growth in the presence of hormone depletion and anti-androgens. Androgen

ablation therapy appears to provide the selective pressure necessary for clonal amplification of cells with mutated AR that can be activated by AR antagonists (Coutinho *et al.*, 2016; Gaddipati *et al.*, 1994). Furthermore, in CRPC the genomic instability caused by the tumour provides higher mutations occurrence in the AR. Few treatment options exist for CRPC. Chemotherapies, such as docetaxel, have been the classical option to treat this stage of the disease (Hotte and Saad 2010), however, since AR drives CRPC, a number of newer therapies, such as enzalutamide, have been developed to target this signalling axis (Coutinho *et al.*, 2016).

## **1.6 Phospholipase C (PLC)**

### **1.6.1 Structure & function**

The Phospholipase C (PLC) family is comprised of 13 different isoforms that are classified into 6 subfamilies (PLC- $\beta$  (1-4),  $\gamma$  (1-2),  $\delta$  (1,3,4),  $\epsilon$ ,  $\zeta$  and  $\eta$  (1-2)) based on their biochemical properties (Béziau *et al.*, 2015). PLCs are membrane bound proteins which regulate multiple cellular functions. All isoforms share a conserved structure in addition to other domains specific for each subfamily that reflect their particular regulatory roles in cells (Figure 1.10). The core protein is composed of a pleckstrin homology (PH) domain, four tandem EF hand domains, a TIM barrel domain and a C2 domain (Cai *et al.*, 2017). The PH domain, which is absent in PLC- $\zeta$ , is important for binding various lipids and proteins where in each phospholipase subfamily it can bind to different molecules, such as PIP<sub>2</sub>, Ca<sup>2+</sup>, G $\beta$  $\gamma$  or the small GTPase. The EF tandem hands are Ca<sup>2+</sup> binding domains as well as the C2 domain, which besides calcium binding, targets PLC for membrane surface binding (Cai *et al.*, 2017; Kadamur and Ross 2013).

The TIM barrel harbours the protein's active site and contains the catalytic residues and Ca<sup>2+</sup> binding site. This domain is interrupted by an auto-inhibitory region that differs among the

different subfamilies in sequence and size. This inhibition is due to the presence of the negatively charged X-Y linker and, upon PLC binding to the negatively charged plasma membrane, the linker is removed from auto-inhibitory confirmation resulting in activation of the protein (Kadamur and Ross 2013; Rebecchi and Pentyla 2000). In the PLC- $\gamma$  sub-family, the TIM barrel contains an SRC homology domains (nSH2, cSH2 and SH3) located in between the X-Y linker, which facilitates interaction of the protein with numerous regulatory proteins. Lastly, PLC- $\epsilon$  contains two RA domains (RA1 and RA2) and a GEF domain, linking this family of PLCs to the RAS signalling pathway (Cai *et al.*, 2017; Park *et al.*, 2012).

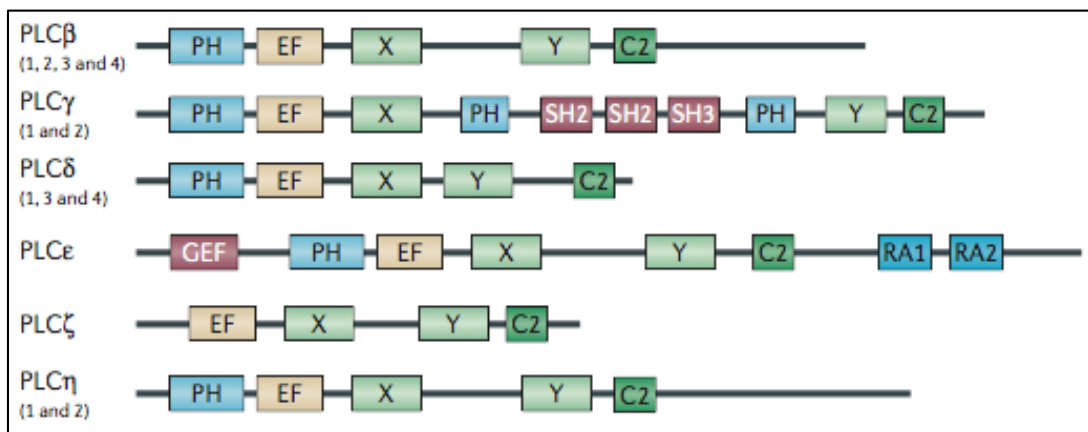


**Figure 1.10: Structure of the different Phospholipase C isoforms.** Thirteen mammalian PLC isoforms are subdivided into six subfamilies. X and Y domains contain catalytic activity. Several isoforms have pleckstrin homology (PH) or SRC homology (SH) domains. The calcium-binding (C2) domain can regulate PLC activity. The EF-hand domain responsible for forming a flexible tether to the PH domain. PLC- $\epsilon$  has a RAS guanine nucleotide exchange factor (GEF) domain, and the RA2 domain mediates the interaction with GTP-bound RAS [obtained from Park *et al.*, 2012].

PLCs hydrolyse phosphatidylinositol 4,5-diphosphate (PIP<sub>2</sub>) into diacylglycerol (DAG) and inositol 1,4,5-triphosphate (IP<sub>3</sub>) (Figure 1.11). DAG activates the phospholipid-dependent serine/threonine kinase and protein kinase C (PKC), while IP<sub>3</sub> mediates cell motility and



proliferation through the activation of  $IP_3$  receptors ( $IP_3R$ ), located on the endoplasmic reticulum (ER) membrane, releasing calcium into the cytoplasm (Park *et al.*, 2012; Nakamura *et al.*, 2017). Signalling molecules such as heterotrimeric G protein subunits, tyrosine kinase, calcium and phospholipids work as activators of the PLCs resulting in the regulation of many cellular functions e. g. cytoskeletal reorganization, cytokinesis, membrane dynamics, nuclear events and channel activity (Nakamura *et al.*, 2017). It has been suggested that each isoform regulates specific cellular responses, which has been supported by several studies using knockout animal models. For example, PLC- $\epsilon$  absence is related to abnormal development in the aortic and pulmonary valves, while manipulation of PLC- $\beta 2$  expression affects calcium and superoxide production in neutrophils (Nakamura and Fukami 2009). More importantly, PLC- $\delta$  activation in cancer cells has been found to regulate tumourigenesis, metastasis, invasion and angiogenesis. For this reason, PLC- $\delta$  has been proposed as a novel therapeutic target for cancer (Park *et al.*, 2012).

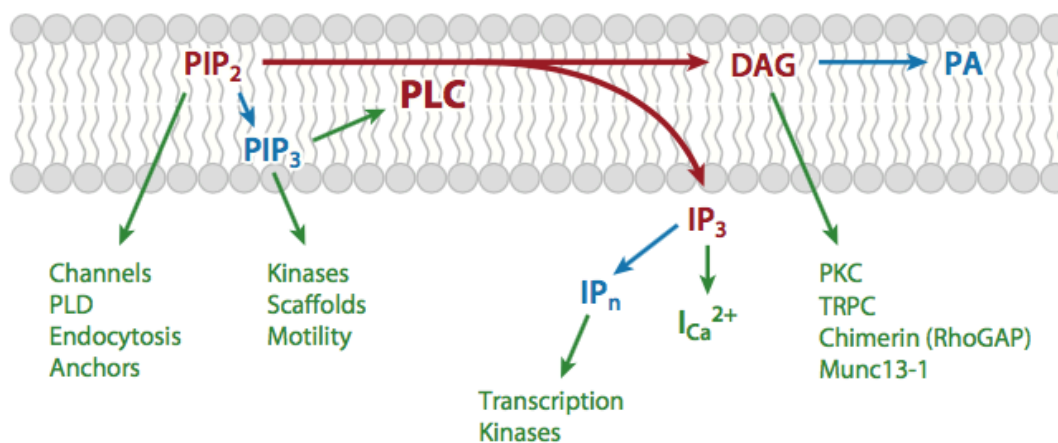


**Figure 1.11: Phospholipase C signalling pathways involving PIP<sub>2</sub>.** PLC hydrolyzes PIP<sub>2</sub>, which is both a signalling molecule in its own right and the precursor of another signalling molecule, PIP<sub>3</sub>. The PLC reaction creates two new signalling molecules, phosphatidic acid and inositol polyphosphates. The PLC reaction is shown in red, other signalling metabolites are blue, and regulatory targets are green [obtained from Kadamur and Ross 2013].

## 1.6.2 The role of PLCs in cancer

PLCs are essential for the metabolism of inositol lipids and therefore play a crucial role in multiple transmembrane signal transduction pathways, regulating numerous cell processes including proliferation and motility (Cai *et al.*, 2017). Although their exact role in tumorigenesis is unclear, the enzymes have been shown to modify proliferation, migration and invasion (Lattanzio *et al.*, 2013). In many cancers, an increase in PLC activity and/or expression has been associated with increased metastasis and proliferation in these tumours. For example, PLC- $\gamma$  and PLC- $\epsilon$  act as oncogenes due to their involvement in Ras signalling which regulates proliferation (Cai *et al.*, 2017). In contrast, the absence or down-regulation of PLC- $\beta$  and PLC- $\delta$  have been demonstrated in human leukaemia suggesting that these have tumour suppressor activity (Cai *et al.*, 2017). In BCa, poor clinical outcome has been linked to increased expression levels of PLC- $\beta$ 2 making it a molecular marker which is indicative of disease severity (Lattanzio *et al.*, 2013). This isoform drives the transition from G<sub>0</sub>/G<sub>1</sub> to S/G<sub>2</sub>/M phase of the cell cycle, which is important in cancer progression and inositol lipid-related modifications of the cytoskeleton architecture that occur during tumour cell division, motility and invasion (Bertagnolo *et al.*, 2007). In recent studies, PLC- $\delta$ 4 has been shown to be up-regulated in BCa cells where its overexpression enhances proliferation (Wang *et al.*, 2015).

Little is known about the expression and role of PLCs in PCa. However, it has been found that PLC- $\gamma$  is essential in tumour invasion as it has a role in regulating cell motility upon the activation by growth factors where the hydrolysis of P<sub>2</sub> polymerizes actin (Lattanzio *et al.*, 2013). Wang *et al.* (2015) investigated 37 PCa patient samples and found increased PLC- $\epsilon$  expression. Further, the group demonstrated that silencing of this isoform, in PC3 and LNCaP cells, significantly reduced proliferation.

### 1.6.3 Apoptosis and tumour cell death

Investigation of the molecular pathways that regulate cell growth and death have greatly contributed to the discovery of targeted therapies for the treatment of many types of cancer. In humans, there are multiple mechanisms of cell death, which include programmed cell death (PCD, for example apoptosis and autophagy), non-physiological necrosis and mitotic catastrophe (Ricci and Zong 2006). The decision as to which of these cell death pathways will occur is dependent upon the type of tissue, physiological nature, developmental stage and the type of death signal. Treatment of cancers, through promotion of cell death, can be achieved by any of these mechanisms (Fulda and Debatin 2006; Ouyang *et al.*, 2012). However, apoptosis is commonly targeted in cancer therapy as many tumours inhibit this signalling pathway to promote survival and drug resistance. The process of apoptosis is well characterised, where a series of events leads to phenotypical changes including cell membrane blebbing, cell shrinkage, chromatin condensation, DNA fragmentation and loss of adhesion to other cells followed by the formation of apoptotic bodies which are engulfed by macrophages or neighbouring cells (Ouyang *et al.*, 2012).

There are two activation mechanisms for apoptosis: firstly, the intrinsic pathway (also known as the mitochondrial pathway) is initiated by intracellular signals generated from the mitochondria in response to e.g. DNA damage or oxidative stress (Figure 1.12). The pro-apoptotic bcl2 factors (Bax, Bak, and Bid) initiate the permeabilisation of mitochondrial membranes to release apoptotic proteins such as cytochrome c, Smac/DIABLO, Omi/HtrA2, apoptosis-inducing factor (AIF) and endonuclease G (Degterev *et al.*, 2003; Fulda and Debatin 2006). Secondly, the extrinsic pathway (also known as the death receptor pathway) is activated via extracellular ligands such as tumour necrotic factor- $\alpha$  (TNF $\alpha$ ), first-apoptotic signal receptors

(FasR) ligands (e. g. CD95/APO1) or TRAIL (TNF related apoptosis inducing ligand). Both pathways lead to the activation of caspases, a family of cysteine proteases that act as common death effector molecules (Ouyang *et al.*, 2012).

Caspases, initiators (2, 8, 9 and 10) and executioners (3, 6 and 7), activate each other by the cleavage of different substrates in the cytoplasm or nucleus, resulting in amplification of caspase activity through a protease cascade causing apoptotic cell death (Degterev *et al.*, 2003). The intrinsic pathway triggers caspase-3 activation via the cytochrome *c*/Apaf-1/caspase-9-containing apoptosome complex, whereas Smac/DIABLO and Omi/HtrA2 promote caspase activation through neutralisation of the inhibitory effects to the inhibitor of apoptosis protein (IAP) (Degterev *et al.*, 2003; Hengartner 2000). In contrast, the extrinsic pathway recruits procaspase-8/10 to form the death inducing signalling complex (DISC), leading to caspase-8 activation which then cleaves caspase-3 and the rest of the apoptotic pathway that binds to the cell-surface death receptors. Links between the two apoptotic pathways does exist. For example, cleavage of caspase-6, part of the intrinsic pathway, can feedback to the death receptor pathway through cleavage of caspase-8 (Fulda and Debatin 2006).

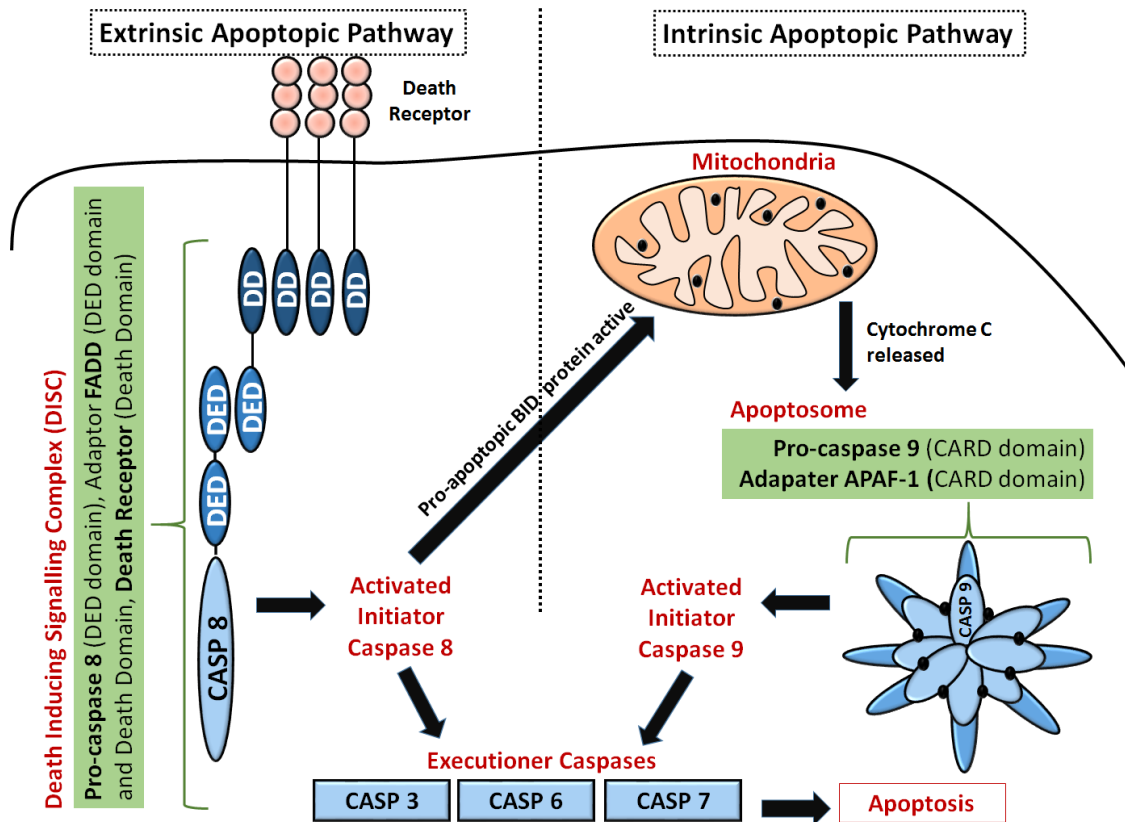


**Figure 1.12: Apoptosis signalling pathways.** The intrinsic pathway is triggered by intracellular signals leading to activation of the caspase cascade. The extrinsic cascade is stimulated by death receptors followed by caspase 8 then caspase 3 cleavage and activation of apoptosis [obtained from Elmore 2007].

#### 1.6.4 Signalling pathways in PCa

In addition to AR signalling, multiple other pathways have been demonstrated to drive PCa progression, proliferation and migration. In CRPC it is well established that tumour proliferation is still under the regulation of AR or via cross-talk with other signalling pathways (Bitting & Armstrong 2013). Activation of the AR could occur by other molecules including growth factors such as Insulin-like Growth-Factor-1 (IGF-1), Keratinocyte Growth Factor (KGF) and Epidermal Growth Factor (EGF), which are found to be overexpressed in PCa (Culig *et al.*, 1994). These growth factors are ligands for receptor tyrosine kinases, which initiate signalling cascades, leading to transactivation of the AR in the absence of androgen (Culig *et al.*, 1994; Wu *et al.*, 2006). Another important pathway in PCa is the PI3K-Akt-mTOR, which is often found to be constitutively active in the disease due to the loss of the tumour suppressor PTEN, hence targeting this pathway leads to increased clinical activity in CRPC (Phin *et al.*, 2013).

PI3K phosphorylates PIP<sub>2</sub> to PIP<sub>3</sub> activating Akt and mTOR, which is involved in regulating cell growth. PI3K activation of the protein kinase c (PKC) is also associated with cell proliferation and survival (Bitting & Armstrong 2013). PTEN removes phosphate groups from 3-phosphorylated inositol lipids, such as PIP<sub>3</sub>. It has been demonstrated that 60% of localised PCa have monoallelic loss of PTEN and complete loss in all cases of CRPC (Phin *et al.*, 2013). Furthermore, due to the overlap between PI3K and PLC signalling pathways, mostly in the activation of PKC, inhibition of PKC could aid as an effective treatment for advanced forms of the disease (Figure 1.13) (Zhang *et al.*, 2012). However, the biggest challenges in targeting signalling pathways in cancer therapy is the redundancy and rewiring of these axis due to the alteration of the cellular genomics. Developed anticancer could encounter number of limitations

as a result of the tumour microenvironment maintain cell variability through altering pathways despite drug inhibition (Lito *et al.*, 2013; Sever and Brugge, 2015). Therefore, due to the heterogeneity of the molecular alterations in PCa, it appears that targeting common factors downstream of altered signalling pathways could be a more effective strategy in the treatment of CRPC.

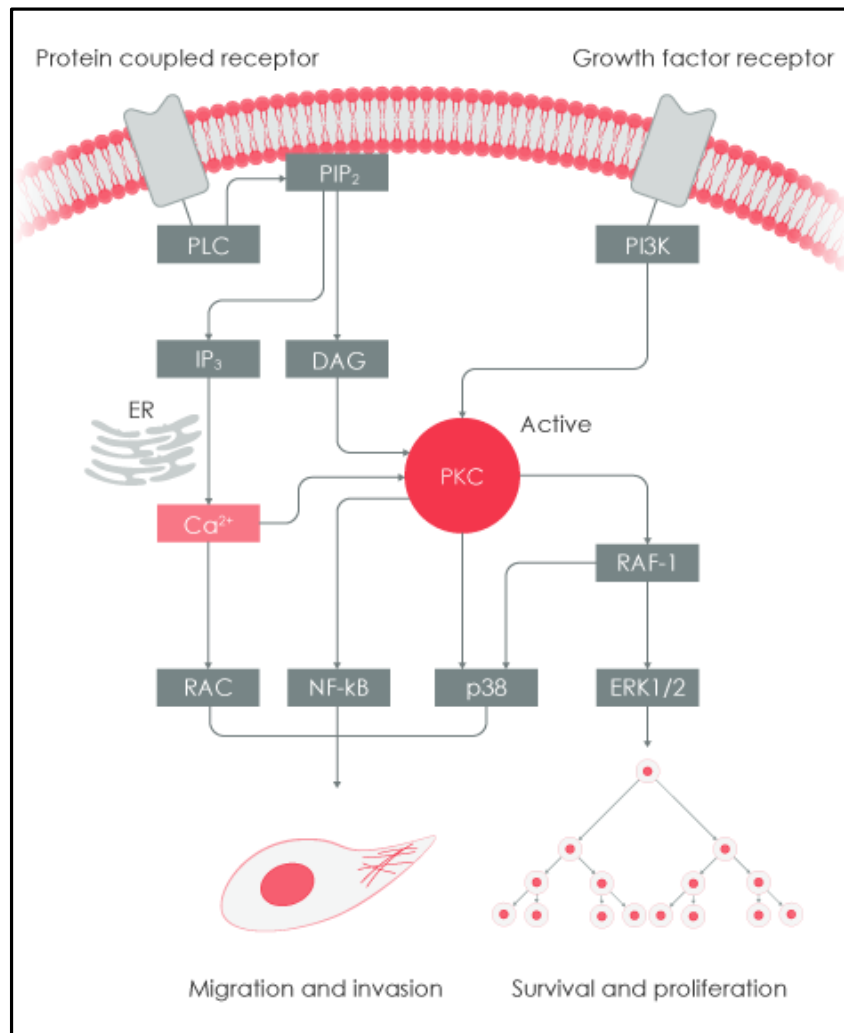


**Figure 1.13: PLC and PI3K signalling pathways.** Phospholipase C and PI3K signalling pathways, where PKC activation overlaps between the two pathways. Upon activation, signals promote cellular proliferation, migration, invasion and survival [obtained from Grang 2014].

### 1.6.5 New anticancer derivatives (thieno[2,3-*b*]pyridine)

Due to its role in cancer, PLC- $\delta$  has been proposed to be a valid target for the treatment of cancer. To identify novel inhibitors of PLC-  $\delta$ , virtual high throughput screening (vHTS) was performed using GOLD (Genetic Optimisation for Ligand Docking) docking algorithm and a crystal structure for the binding site of the PLC-  $\delta$  (Reynisson *et al.*, 2009). Thieno[2,3-*b*]pyridine compounds identified to be potential hits and were subsequently demonstrated to have potent anticancer activity against a variety of tumour cell lines (Reynisson *et al.*, 2009). For example, in the breast cancer cell line MDA-MB-231, these compounds were shown to reduce proliferation, to induce blebbing of the plasma membrane, increase cell cycle arrest in the G<sub>2</sub>/M phase and to decrease cell motility (Leung *et al.*, 2016). Similar effects were noticed when the anticancer agents were investigated with stem/progenitor-like cell populations from breast and prostate cancers (Mastelić *et al.*, 2017). Furthermore, the thieno[2,3-*b*]pyridine compounds induced apoptosis. *In-vitro* testing of the thieno[2,3-*b*]pyridine compounds has therefore demonstrated that these compounds are promising anti-cancer therapeutic agents and hence the efficacy and mechanism of action of these inhibitors requires further investigation.



## 1.7 Project objectives

Investigation of AR signalling in BCa has increased significantly over recent years and several clinical trials are assessing the efficacy of anti-androgens as therapeutics for this disease. There is therefore a need to better characterise the role of AR signalling in BCa,

Aim 1- To characterise the mechanisms of cross-talk between the AR and ER $\alpha$ .

Aim 2 – To identify AR mutations associated with BCa and to investigate if these substitutions affect receptor activity and ligand specificity.

Aim 3 – To investigate if mutations in the AR affect receptor cross-talk with the ER $\alpha$  pathway.

Few therapeutic options exist for CRPC and there is therefore a great need to identify novel treatment options for this stage of the disease. The second part of this thesis investigates the efficacy of thieno[2,3-b]pyridine inhibitors as a treatment option for CRPC.

Aim 1 – To investigate the effect of thieno[2,3-b]pyridine inhibitors upon the proliferation of a panel of prostate cell lines.

Aim 2 – To characterise the effect of thieno[2,3-b]pyridine inhibitors upon the cell cycle and mechanism of cell death and to assess the effect of the inhibitors upon cell motility.

Aim 3 – To investigate the mechanism of action of the inhibitors and identify which proteins that these inhibitors target.

## CHAPTER 2

### MATERIALS AND METHODS

#### 2.1 Reagents, solutions and buffers

Reagents, solutions and buffers used in this thesis are listed below. Final concentrations of reagents are given and all solutions were made in distilled deionised water (ddH<sub>2</sub>O), unless otherwise specified (table 2.1).

**Table 2.1: Preparation of reagents, solutions and buffers.**

<b>General stock solutions</b>			
<i>SOLUTION</i>	<i>RECIPE</i>	<i>STORAGE</i>	<i>STERILISATION</i>
<b>1 % Bovine serum albumin (BSA) in PBS-T (1 % BSA-PBS-T)</b>	0.1 g BSA lyophilised powder (Sigma- Aldrich) in a total volume of 10 mL PBS- T.	4 °C, used within 24 hrs of making	0.22 µm filter sterilise
<b>0.08 % Crystal violet</b>	32 mg crystal violet (Sigma- Aldrich) in a final volume of 40 mL double distilled water (ddH <sub>2</sub> O).	RT	0.22 µm filter sterilise
<b>0.5 M Ethylenediaminetetraacetic acid (EDTA)</b>	186.12 g EDTA disodium salt (Fisher Scientific) to a final volume of 1 L using ddH <sub>2</sub> O, adjusted to pH 8.0 using 5 M NaOH stock solution.	RT	Autoclave
<b>4 M Hydrochloric acid (HCl)</b>	19.6 mL of 32 % HCl (Fisher Sceintific) with 30.4 mL of ddH <sub>2</sub> O.	RT	N/A
<b>4% Paraformaldehyde</b>	4 g of PFA (Sigma-Aldrich) dissolved in PBS to a final volume of 100 mL. Heated on a stirring	-20 °C, in 5- 10 mL	N/A

<b>(PFA)</b>	plate within a fume cupboard until fully dissolved.	aliquots	
<b>1 x Phosphate buffered saline (PBS)</b>	10 (Dulbecco A) tablets (Oxoid Limited) dissolved in ddH <sub>2</sub> O to a final volume of 1 L.	RT	Autoclave
<b>PBS-0.1 %-Tween (PBS-T)</b>	0.5 mL of Tween®-20 (Sigma-Aldrich) in a total of 500 mL PBS.	4 °C	N/A
<b>0.2 M Phenylmethanesulphonylfluoride (PMSF)</b>	0.35 g of PMSF (Sigma-Aldrich) to a total of 10 mL using ddH <sub>2</sub> O.	-20 °C	N/A
<b>5 M Sodium hydroxide (NaOH)</b>	20 g of NaOH pellets (Fisher Scientific) to a final volume of 100 mL with ddH <sub>2</sub> O.	RT	N/A

### Flow cytometry (FACS) buffers

<i>SOLUTION</i>	<i>RECIPE</i>	<i>STORAGE</i>	<i>STERILISATION</i>
<b>Nicoletti buffer</b>	10 g of Sodium citrate, 10 ml Triton X-100 (Sigma-Aldrich), to 1000 ml with ddH <sub>2</sub> O.	4 °C	N/A
<b>Propidium Iodide (PI) staining solution for apoptosis measurements</b>	200 µl PI (1 mg/ml, Sigma-Aldrich), 5 ml Nicoletti buffer.	4 °C	N/A
<b>PI staining solution for cell cycle measurements</b>	1 ml PBS, 20 µl RNase (10 mg/ml) (Fisher Scientific), 10 µl PI (1 mg/ml in).	Freshly prepared	N/A

### Agarose gel electrophoresis

<i>SOLUTION</i>	<i>RECIPE</i>	<i>STORAGE</i>	<i>STERILISATION</i>
-----------------	---------------	----------------	----------------------

<b>1 % and 1.4 % Agarose gels</b>	1 g (1 %) or 1.4 g (1.4 %) of agarose (Fisher Scientific) dissolved in 100 mL of 1 X TAE via boiling. This is briefly allowed to cool prior to the addition of 5 µL of ethidium bromide (10 mg/mL, Sigma-Aldrich) and casting.	RT, or gels can be wrapped and stored at 4 °C O/N if necessary	N/A
<b>1 X Tris-acetate-EDTA (TAE)</b>	40 mM Tris base (4.846 g, Fisher Scientific), 1.114 mL glacial acetic acid (Fisher Scientific) and 1 mM EDTA (2 mL of 0.5 M stock), in a total of 1 L ddH <sub>2</sub> O.	RT	N/A

### Bacterial Culture

<i>SOLUTION</i>	<i>RECIPE</i>	<i>STORAGE</i>	<i>STERILISATION</i>
<b>100 mg / mL Ampicillin stock</b>	1 g ampicillin sodium salt (Sigma-Aldrich) to a final volume of 10 mL ddH <sub>2</sub> O. Added to LB broth/agar to a final concentration of 100 µg/mL.	-20 in 1 mL aliquots	0.22 µm filter sterilise
<b>1 M Glucose stock</b>	90.08 g of Glucose (Fisher Scientific) in a final volume of 500 mL ddH <sub>2</sub> O.	RT	0.22 µm filter sterilise
<b>20 mg / mL Isopropyl β-D-1-thiogalactopyranoside (IPTG) stock</b>	0.2 mg of IPTG powder (Sigma-Aldrich) dissolved to a final volume of 1 mL in ddH <sub>2</sub> O.	-20 in 50 µL aliquots	N/A
<b>50 mg / mL Kanamycin stock</b>	0.5 g kanamycin (Sigma-Aldrich) in 10 mL of ddH <sub>2</sub> O.	-20 in 1 mL aliquots	0.22 µm filter sterilise
<b>Luria Broth (LB)</b>	20 g LB (Lennox, larger granules, Fisher Scientific) dissolved in a	4 °C	Autoclave

	total of 1 L of ddH <sub>2</sub> O, with the pH adjusted to 7.2 where necessary. Supplemented, if required, with antibiotics.		
<b>LB Agar plates</b>	8.75 g of LB Agar (Sigma-Aldrich) to a final volume of 250 mL ddH <sub>2</sub> O, supplemented if required with antibiotics. Melted prior to use and poured to make agar plates whilst still molten.	4 °C	Autoclave
<b>LB/ampicillin/IPTG/X-gal plates</b>	40 µL Xgal stock solution was mixed with 4 µL of IPTG stock solution per plate. To a prepared LB Agar plate, supplemented with antibiotics (equilibrated to RT after 4 °C storage), 44 µL of Xgal-IPTG solution was spread over the plate surface, and left to dry agar side up at 37 °C for approximately 2 hrs prior to use.	Prepared immediately before use	N/A
<b>1 M Magnesium chloride (MgCl<sub>2</sub>) stock</b>	101.655 g of MgCl <sub>2</sub> (Fisher Scientific) in a final volume of 500 mL ddH <sub>2</sub> O.	RT	Autoclave
<b>1 M Magnesium sulphate (MgSO<sub>4</sub>) stock</b>	120.366 g of MgSO <sub>4</sub> (Fisher Scientific) in a final volume of 500 mL ddH <sub>2</sub> O.	RT	Autoclave
<b>Super Optimal Broth (SOB) media</b>	20 g of Tryptone (Oxoid), 5 g of Yeast Extract (Oxoid), 0.58 g of Sodium chloride (10 mM, NaCl, Sigma- Aldrich), 0.18 g Potassium chloride (2.5 mM, KCl, Sigma-Aldrich), 10 mL of 1 M MgCl <sub>2</sub> stock (10 mM) and 10 mL of 1M MgSO <sub>4</sub> stock (10 mM), dissolved in ddH <sub>2</sub> O up to 1 L.	4 °C	Autoclave
<b>Super Optimal broth</b>	20 g of Tryptone (Oxoid), 5 g of	4 °C	Autoclave (prior

<b>with Catabolite repression (SOC) media</b>	yeast extract (Oxoid), 0.58 g of NaCl (10 mM, Sigma-Aldrich), 0.18 g KCl (2.5 mM, Sigma-Aldrich), 10 mL of 1 M MgCl <sub>2</sub> stock (10 mM), 10 mL of 1M MgSO <sub>4</sub> stock (10 mM), and 20 mL of 1 M Glucose stock, dissolved in ddH <sub>2</sub> O up to 1 L.			to adding sterile glucose)
<b>20 mg/mL 5-Bromo-4-chloro-3-indolyl β-D-galactopyranoside (X-gal) stocks</b>	100 mg of X-gal powder (Sigma-Aldrich) dissolved to a final volume of 5 mL in DMSO (Sigma-Aldrich).	-20 °C in 120 µL aliquots, kept in the dark		N/A

### Transfections

<i>SOLUTION</i>	<i>RECIPE</i>	<i>STORAGE</i>	<i>STERILISATION</i>
<b>N,N-Bis(2-hydroxyethyl)-2-aminoethanesulphonic acid (BES)-buffered saline (BBS) 2 x solution</b>	50 mM BES (10.66 g, Sigma-Aldrich), 280 mM NaCl (16.36 g, Sigma-Aldrich), 1.5 mM Sodium phosphate dibasic (Na <sub>2</sub> HPO <sub>4</sub> , 0.21 g, Sigma-Aldrich), to a final volume of 1 L using ddH <sub>2</sub> O, adjusted to pH 6.95 using 5 M NaOH stock solution.	-20 °C, in 50 mL aliquots	0.22 µm filter sterilise
<b>2.5 M Calcium Chloride (CaCl<sub>2</sub>)</b>	138.73 g of anhydrous granular CaCl <sub>2</sub> (Sigma-Aldrich) to a total of 500 mL in ddH <sub>2</sub> O.	-20 °C, in 50 mL aliquots	0.22 µm filter sterilise

### Western blotting

<i>SOLUTION</i>	<i>RECIPE</i>	<i>STORAGE</i>	<i>STERILISATION</i>
<b>10 % Ammonium persulphate (APS)</b>	1 g of APS (Sigma-Aldrich) dissolved in a total volume of 10	-20 °C, in 160 µL	N/A

	mL ddH <sub>2</sub> O.	aliquots	
<b>Blocking solution</b>	2.5 g (5 %) dried skimmed milk powder (Marvel) to a total of 50 mL in PBS-T.	4 °C, used within 24 hrs	N/A
<b>10 % Polyacrylamide Gel</b>	Per gel, a 10 % resolving gel was made, consisting of 1.65 mL Acrylamide/Bis-acrylamide 30 % solution (Sigma-Aldrich), 1.9 mL of 1 M Tris/HCl at pH 8.9, 1.4 mL of ddH <sub>2</sub> O and 50 µL of 10 % SDS. Immediately prior to pouring, 10 µL of 10 % APS stock and 2.5 µL N,N,N',N'-Tetramethylethylenediamine (TEMED, Sigma-Aldrich) were added. Additionally a stacking gel was made, consisting of 425 µL of Acrylamide/Bis-acrylamide 30 % solution (Sigma-Aldrich), 937.5 µL of 1 M Tris/HCl at pH 6.8, 1.0875 mL of ddH <sub>2</sub> O and 25 µL of 10 % SDS. Immediately prior to pouring, 10 µL of 10 % APS and 2.5 µL TEMED were added.	4 °C, kept moist and used within a week	N/A
<b>Radioimmunoprecipitation assay (RIPA) buffer</b>	0.5 mL of 1 M Tris-Cl (pH 8.0) stock (10 mM), 20 mg of EDTA (1 mM, Fisher Scientific), 0.5 mL of Triton X- 100 (1 %, Sigma-Aldrich), 50 mg of Sodium deoxycholate (0.1 %, Sigma-Aldrich), 0.5 mL of 10 % SDS stock solution (0.1 %) and 0.41 g of NaCl (Sigma-Aldrich). Supplemented with 5 µL of 0.2 M PMFS stock and 10 uL of Halt Protease Inhibitor (PI) Cocktail (ThermoScientific) per 1 mL of RIPA just prior to use.	4 °C	0.22 µm filter sterilise

<b>1 x Running Buffer</b>	3 g of Tris base (25 mM, Fisher Scientific), 14.45 g of Glycine (0.2 M, Fisher Scientific) and 0.5 g of SDS (0.05 %, Fisher Scientific) were dissolved in a total volume of 1 L ddH <sub>2</sub> O.	RT	N/A
<b>10 % Sodium dodecyl sulphate (SDS)</b>	50 g of SDS (Fisher Scientific) dissolved in a total volume of 500 mL ddH <sub>2</sub> O.	RT	N/A
<b>Semi-Dry Transfer Buffer</b>	5.63 g Glycine (150 mM, Fisher Scientific), 1.22 g Tris base (20 mM) and 100 ml of Methanol (20 %, MeOH, Fisher Scientific), dissolved in a total volume of 500 mL ddH <sub>2</sub> O.	4 °C, used within 1 month	N/A
<b>IP buffer</b>	150 mM NaCl, 1% NP-40, 50mM Tris pH8.0, 1 mM DTT	4 °C	N/A
<b>1 M Tris</b>	12.114 g of Tris base (Fisher Scientific) dissolved to a final volume of 100 mL, adjusted to pH 6.8/8.0/8.9 using 4 M HCl stock solution.	RT	Autoclave

## 2.2 Mammalian cell culture

The mammalian cell lines (ATCC) used in this project were cultured under incubation conditions of 37 °C and 5 % Carbon dioxide (CO<sub>2</sub>), with regular microscopy observations to monitor cell confluence and health. Once the cell confluence reached approximately 70–80 %, cell passaging was completed. Cell lines together with their associated description and growth conditions are listed in Table 2.2. Details on media, additives and ligand used for *in vitro* work



are described in Tables 2.3 and 2.4.

**Table 2.2: Mammalian cells used in this thesis.**

<i>CELL LINE</i>	<i>DESCRIPTION</i>	<i>MEDIA</i>
<i>COS-1</i>	African Rhesus Monkey (kidney) immortalised with SV40 large T.	DMEM
<i>MCF-7</i>	Breast cancer cell line isolated from human (pleural effusion), primary tumour with invasive breast ductal carcinoma.	DMEM
<i>HEK 293</i>	Human embryo kidney.	DMEM
<i>PC3</i>	Androgen-independent cell line model that was established from a human PCa bone metastasis.	RPMI-1640
<i>PC3-GFP</i>	PC3 cell that were stably transfected with GFP.	RPMI-1640
<i>LNCaP</i>	Human lymph node PCa metastasis from Caucasian male.	RPMI-1640
<i>DUI145</i>	A model of castration resistant prostate cancer derived from a central nervous system metastasis.	RPMI-1640
<i>C42</i>	A metastatic cell line derived from LNCaP following co-injection with fibroblasts into castrated mice.	RPMI-1640
<i>C42B</i>	Metastatic subline derived from C42B after re-inoculation into castrated mice.	RPMI-1640
<i>22RV1</i>	Androgen-dependent PCa xenograft line derived from CWR22R.	RPMI-1640

<i><b>BPH1</b></i>	A benign hyperplastic prostatic epithelial cell line.	RPMI-1640
<i><b>PNTA1</b></i>	Normal prostatic epithelial cells that were immortalised RPMI-1640 with SV40.	RPMI-1640

**Table 2.3: Cell culture media used.**

<i><b>MEDIA</b></i>	<i><b>DESCRIPTION</b></i>	<i><b>ADDITIVES</b></i>
<b>DMEM</b>	Dulbecco's Modified Eagle Medium	5% FCS, 1% PSG (100units/mL penicillin, 0.1 mg/ml streptomycin, 2 mM glutamine)
<b>PHENOL RED FREE DMEM</b>	Dulbecco's Modified Eagle Medium	5% sFCS (charcoal stripped FCS), 1% PSG (100units/mL penicillin, 0.1 mg/ml streptomycin, 2 mM glutamine)
<b>RPMI-1640</b>	Roswell Park Memorial Institute	5% FCS, 1% PSG (100units/mL penicillin, 0.1 mg/ml streptomycin, 2 mM glutamine)
<b>PHENOL RED FREE RPMI-1640</b>	Roswell Park Memorial Institute	5% sFCS (charcoal stripped FCS), 1% PSG (100units/mL penicillin, 0.1 mg/ml streptomycin, 2 mM glutamine)
<b>Wash Media</b>	Phenol Red Free DMEM	2% sFCS. 1% PSG (100units/mL penicillin, 0.1 mg/ml streptomycin, 2 mM glutamine)
<b>Freezing Media</b>	90% FCS 10 % DMSO	N/A

**Table 2.4: Reagents for cell treatment.**

<i>LIGAND</i>	<i>STOCK PREPARATION</i>	<i>STORAGE</i>
<i>17β-OESTRADIOL (E<sub>2</sub>)</i>	10 mM stock in 100% Ethanol (EtOH)	-20 °C
<i>MIBOLERONE (MIB)</i>	10 mM stock in 100% Ethanol (EtOH)	-20 °C
<i>PROGESTERONE (PR)</i>	10 mM stock in 100% Ethanol (EtOH)	-20 °C
<i>FULVESTRANT (FULV)</i>	10 mM stock in 100% Ethanol (EtOH)	-20 °C
<i>TAMOXIFEN (TAM)</i>	10 mM stock in 100% Ethanol (EtOH)	-20 °C
<i>BICALUTAMIDE (BIC)</i>	10 mM stock in 100% DMSO	-20 °C
<i>ENZALUTAMIDE (ENZA)</i>	10 mM stock in 100% DMSO	-20 °C
<i>Docetaxel (Doc)</i>	10 mM stock in 100% DMSO	-20 °C
<i>thieno[2,3-<i>b</i>]pyridine inhibitors (97, 144, 145, 154 and 160)</i>	10 mM stock in 100% DMSO	-20 °C

### 2.3 Freezing and defrosting cells

To freeze cell, after passaging, cells were pelleted for 3 mins at 1,500 rpm then re-suspended in pre-warmed freezing mixture (Table 2.3). 1 mL of cells mixture was transferred to cryovials tubes then wrapped in insulating material and stored in liquid nitrogen. For defrosting, frozen cells were defrosted at 37 °C then transferred into a 10 mL tube with pre-warmed media. Cell suspension was then centrifuged for 3 mins 1,500 rpm then the supernatant was transferred

and the cells re-suspended in the adequate amount of relevant media (Table 2.1) and returned to culture conditions.

## **2.4 Transient transfection of mammalian cells**

### **2.4.1 Calcium phosphate**

The Calcium phosphate method was performed as previously described in Chen and Okayama (1987). In a 24 well plate, the desired DNA was mixed and diluted to 45  $\mu$ L using ddH<sub>2</sub>O (Refer: Section 2.8). After that, 5  $\mu$ L of 2.5 M CaCl<sub>2</sub> and 50  $\mu$ L of 2 x BBS were added then gently mixed by bubbling using a Gilson pipette. The transfection mixture was then mixed and incubated at RT for 15 mins then were added in a drop-wise manner to the wells.

### **2.4.2 jetPRIME**

Transfections were performed using the JetPrime® Polyplus Transfection Reagent following the manufacturer instructions. Cells were seeded in either 96-, 24- or 6-well plates with full media for 24 hrs before transfection. Transfections were performed with the amount of DNA recommended by the manufactory guidelines relevant to the plate size. Each  $\mu$ g of DNA was mixed with the transfection reagent in a ratio of 1:3. The mixture was then incubated for 10 min at RT following the transferring onto the cells. Then DNA mixture was added in a drop-wise manner to each well after that cells were incubated for 4 hours then media was replaced and incubated for further 24 hours until hormone treatment and processing according to the experiment to be performed.

### **2.4.3 FuGENE HD**

COS1 cells were plated at 30% confluence on cover slips in 24 well plates. Then cells were transfected with desired plasmids using FuGENE HD (Promega) and incubated for 24 hrs before treatment with hormones for 2 hrs. Wells were washed 3x with PBS and incubated in 1% paraformaldehyde for 10 min, washed 3x in PBS and incubated for a further 10 min in 0.1% Triton X-100 in PBS. Wells were again washed 3x with PBS, incubated in blocking solution (5% BSA in PBS) for 30 min and a further 1 hr with the desired antibodies. Wells were washed 3x with PBS, re-blocked and incubated for 1 hr with the desired secondary antibody. A final 3x PBS washes was performed before the coverslips were mounted onto glass slides containing DAPI. Images were obtained using a Zeiss Confocal Microscope.

### **2.4.4 siRNA knockdown**

Cells were seeded in 6 well or 12 well plates with the relevant hormone-depleted media for 24 hrs prior to transfection. On-target small interfering RNA (siRNA) targeting AR/ER $\alpha$  or control non-target (NT) siRNA (Dharmacon) were transfected using Lipofectamine RNAiMAX Reagent, following the manufacturer's protocol (Invitrogen), to a final concentration of 30 nM (12 well) or 50 nM (6 well). Immunoblotting analysis and qPCR were used to confirm successful Knockdown.

## **2.5 Bacterial cultures, transformation and DNA preparation**

### **2.5.1 Bacterial strains and culture**

For transformation procedures the max efficiency DH5 $\alpha$  (Invitrogen) the *Escherichia coli*

(*E. coli*) strain of competent cells was conducted. All preparations for the bacterial work were performed in sterile conditions then the bacterial suspensions were incubated with shaking, this was conducted at 225 rpm, 37 °C.

### **2.5.2 Transformation**

The DH5 $\alpha$  cells were transformed following the manufacturer protocol outlined by Invitrogen with a few adjustments. Briefly, 50  $\mu$ L of DH5 $\alpha$  cells were thawed on ice then gently mixed with 50 ng of plasmid DNA. The mixture was then incubated on ice for 30 mins following heat shock for 45 secs using a 42 °C water bath. After that, cells were then incubated on ice for a further 2 mins and then incubated in 950  $\mu$ L of pre-warmed SOC media for 1 hr at 37 °C while shaking as a recovery period. The desired amount of cell suspension was spread onto LB Agar plates with the required antibiotic selection (ampicillin/kanamycin) (Table 2.1) and then incubated overnight (O/N) at 37 °C.

### **2.5.3 DNA preparation**

A single bacterial colony was selected and transformed from each bacterial plate using a sterile pipette tip. This was performed to inoculate 5 mL of LB supplemented with the desired antibiotic for 12 hrs at 37 °C while shaking. Initially, a small-scale isolation of plasmid DNA was purified using the Plasmid Miniprep Kit (Qiagen), using the outlined protocol. Sequencing (Source Bioscience) was conducted to verify harvested DNA plasmids if cloning was performed, or via fast digestion restriction enzymes for confirmation (Thermo Scientific) following the manufacturer's protocol. Digested products were assessed via 1 % agarose gel electrophoresis (Table 2.1). Plasmid were stored using glycerol stocks made by mixing 200  $\mu$ L of glycerol

(Fisher Scientific) with 800  $\mu$ L of cell suspension from a bacterial culture and kept at -80  $^{\circ}$ C.

DNA plasmids were subsequently isolated on a larger scale. First, glycerol stocks were spread onto LB Agar plates (with the correct antibiotic selection) and grown O/N. Then a single bacterial colony was used to inoculate 5 mL of LB broth supplemented with the required antibiotic for 16 hrs at 37  $^{\circ}$ C with shaking. The suspension was then transferred to 200 mL of LB and kept O/N at 37  $^{\circ}$ C shaking. DNA Plasmids were harvested using the Plasmid Midiprep Kit (Qiagen) following the manufacturer's protocol. After mini and midi DNA preparation, DNA concentrations were quantified using the NanoDrop<sup>®</sup> ND- 1000 UV/VIS Spectrophotometer (Nanodrop, LabTech) and assess purity, following to the stander guidelines.

## **2.6 Site-directed mutagenesis**

Site directed mutagenesis (QuickChange II, Agilent DE, USA) was performed to introduce AR mutations into the ER $\alpha$  expression plasmid (pSG5-ER $\alpha$ ) following the manufacturer's instructions. Mutagenesis primer sequences are listed in Table 2.5. Amplified products were transformed into DH5 $\alpha$  bacterial transformation and colonies cultured overnight prior to plasmid isolation using a mini-prep kit (QIAGEN<sup>®</sup>). Mutations were confirmed by sequencing (Source Biosciences) and chromatograms analysed in 4Peaks (V1.7.1) and EnzymeX (V3.1) to confirm successful mutagenesis.

**Table 2.5: List of mutagenesis primers.** Bases in red are the ones being mutated. All sequences were provided by G. Brooke.

<i>PRIMER</i>	<i>SEQUENCE</i>
<b>C290Y-F</b>	CATTGGCCGAAT <b>A</b> CAAAGGTTCTCTG
<b>E355K-F</b>	GGAGCACTGGAC <b>A</b> AGGCAGCTGGCTA
<b>S568F-F</b>	GAGATGAAGCTT <b>T</b> TGGGTGTCACTAT
<b>L638M-F</b>	AAACTTGGTAAT <b>A</b> TGAAACTACAGG
<b>S663*-F</b>	AGCTGACAGTGT <b>G</b> ACACATTGAAGGC
<b>Q739*-F</b>	ATGGCTGTCATT <b>T</b> AGTACTCCTGGAT
<b>D840N-F</b>	ATCAAGGAACTC <b>A</b> ATCGTATCATTGC
<b>D865E-F</b>	AAGCTCCTGGA <b>A</b> TCCGTGCAGCC
<b>Q868H-F</b>	GACTCCGTGCAT <b>C</b> CTATTGCG
<b>L881Q-F</b>	TCACTTTTGACC <b>A</b> GCTAATCAAGTCA

## 2.7 Cloning of AR mutant Q739\* using CRISPR/ CAS9

The ZangLab tools were used to identify PAM sites near the targeted mutation (Q739) and the relevant guide strands (Table 2.6). The guide strands were subsequently cloned into the PX459 V2 plasmid (provided by Dr Pradeepa M Madapura) and confirmed using sequencing. The corresponding repair strands were designed using Benchling online tool (<https://benchling.com>) (Table 2.7). Briefly, guide strands were annealed and phosphorylated using T4PNK (37 °C for 30 min; 95 °C for 5 min; ramp down to 25 °C at 5 °C min<sup>-1</sup>). The guide



strands were subsequently ligated into the vector with T7 ligase and incubated for 1 hr using the manufacturer's reagents and protocol (BioLabs, NEW ENGLAND). The mixture was digested with PlasmidSafe exonuclease (37 °C for 30 min) followed by 70 °C for a further 30 min. The product was and transformed into DH5α cells following the protocol in Section 2.5.2.

MCF-7 cells were seeded at 70% confluence, incubated for 24 hrs and transfected with PX459 Q739\* and the repair strands using the FuGENE® transfection reagent, following the manufactory guidelines. Cells were separated into 4 treatment groups: mock transfected, empty plasmid only, PX459 V2\_Q739\*\_1 plus repair strand, PX459 V2\_Q739\*\_2 plus repair strand. After 24 hours, transfected cells were treated with puromycin (2 µg/ ml) for 48 hrs and cultures were monitored during the following weeks for colony collection. Individual colonies were expanded and screened using immunoblotting and sequencing (Source Bioscience).

**Table 2.6: List of guide strand primers and their oligos used for CRISPR to construct the Q739\* mutation in MCF-7 cell line.**

<i>PRIMER</i>	<i>TOP OLIGO</i>	<i>BOTTOM OLIGO</i>
PX459 V2_Q739*_1	CACCGGGCCCACTTACTCAGTTTCC	AAACGGAAACTGAGTAAGTGGGC CC
PX459 V2_Q739*_2	CACCGGCACTCCCTCCCGCTTTGTAC	AAACGTACAAAGCGGGAGGGAGT GCC

**Table 2.7: List of repair strand primers used for CRISPR to construct the Q739\* mutation in MCF-7 cell line.**

<i>PRIMER</i>	<i>SEQUENCE</i>
<b>PX459 V2_Q739*_1</b>	GACTTAGCTCAACCCGTCAGTACCCAGACTGACCACTGCCTCTGCCTCTTCT TCTCCAGGCTTCCGCAATCTACACGTGGACGACCAGATGGCTGTCATTtAGT ACTCCTGGATGGGGCTCATGGTGTGGCCATGGGCTGGCGATCCTTCACCA ATGTCAACTCCAGGATGCTCTACTTCGCCCTGATCTGGTTTTCA
<b>PX459 V2_Q739*_2</b>	GACTTAGCTCAACCCGTCAGTACCCAGACTGACCACTGCCTCTGCCTCTTCT TCTCCAGGCTTCCGCAACTTACACGTGGACGACCAGATGGCTGTCATTtAGT ACAGCTGGATGGGGCTCATGGTGTGGCCATGGGCTGGCGATCCTTCACCA ATGTCAACTCCAGGATGCTCTACTTCGCCCTGATCTGGTTTTCA

## 2.8 Reporter assays

COS-1 and MCF-7 cells were grown in the relevant hormone-depleted media (Table 2.3) at approximately 60 % confluence in 24 well plates and incubated for 24 hrs prior to transfection. Cells were transfected with 50 ng pSV-AR, pSG5-ER $\alpha$  or Empty Vector (EV); 10 ng  $\beta$ -galactosidase or Renilla; and 1  $\mu$ g ARE-/ERE-luciferase reporter (Table 2.8) using either the Calcium Phosphate (Section 2.4.1) or jetPRIME (Section 2.2.2). 24 hrs post transfection, then cells were washed twice using pre-warmed hormone-depleted media. After that, medium was replaced with a fresh hormone-depleted media containing the required concentration of hormone/ drug/ vehicle and incubated for 24 hrs. Then cells were washed twice using pre-chilled PBS and lysed by adding 60  $\mu$ L of 1 x Reporter Lysis Buffer (Promega), kept at -80  $^{\circ}$ C until frozen. Luciferase assays (Promega) were performed on 20  $\mu$ L of defrosted lysate alongside the  $\beta$ -galactosidase assay Galacto-Light (Life Technologies) on 5  $\mu$ L for normalisation, following the

manufacturer's guidelines. Luminescence was measured using the FLUOstar Omega plate reader (BMG Labtech).

**Table 2.8: List of plasmids used in this thesis.**

<i>PLASMID</i>	<i>SOURCE/ REFERENCE</i>
pSV-AR	(Brinkmann <i>et al.</i> , 1989)
Bos- $\beta$ -galactosidase	C. Bevan
pGL3-TAT-GRE-LUC (ARE-luciferase)	(Jenster <i>et al.</i> , 1997)
3 x ERE TATA LUC (ERE-luciferase)	Addgene
pSG5-ER $\alpha$	M. Parker
pSV-AR (C290Y, E355K, S568F, L638M, S663*, Q739*, D840N, D865E, Q868H and L881Q)	M. Alkheilewi
pSG5-Empty	Stratagene
pSG5- ER $\alpha$ HE257G and pSG5-ER $\alpha$ HE464	S. Ali
pGL4.18	Promega
pEGFP-NI-AR	G. Brooke
pRL Renilla	Promega
<i>pcDNA3.1-RFP-ER<math>\alpha</math></i>	R.A. Bryan/ G. Brooke

## 2.9 Gene expression analysis

The relevant cells were plated at approximately 70 % confluence in either 6, 12 or 24 well plates then cultured in hormone-depleted media (Refer: Table 2.3) for the desired time. Following this, cells were treated with the required ligand or drug concentration for either an 8 or 24 hrs.

### **2.9.1 RNA extraction**

After treatment, cells were washed ice cold PBS x2 and then lysed with TRIsure reagent (Bioline). RNA extraction was performed following to the manufacturer's protocol. Glycobule (Ambion) was then added to aid the visualisation of the RNA pellet. After the pellet is formed, the RNA was additionally wash with 75 % Ethanol (EtOH), then pellets were air-dried and re-suspended in 30  $\mu$ L (6 well) or 20  $\mu$ L (12 and 24 well) RNase free. Using the NanoDrop® ND-1000 UV/VIS Spectrophotometer (Nanodrop, LabTech) the RNA concentration was quantified assessed for quality assessed following the manufacturer's protocol.

### **2.9.2 cDNA synthesis**

To synthesise complementary DNA (cDNA), reverse transcription was performed using either the Transcriptor First Strand cDNA Synthesis Kit (Roche) or High Capacity cDNA Reverse Transcription Kit (Applied Biosystems, Thermo Fisher Scientific), following the manufacturer's protocol for each kit. 500 ng of RNA was utilised per cDNA synthesis reaction and the produced cDNA product was diluted 1:4.

### **2.9.3 Real-Time quantitative PCR (qPCR)**

Real-Time quantitative PCR (qPCR) was conducted using 2  $\mu$ L of cDNA with the LightCycler® 480 SYBR Green I Master (Roche) or Fast SYBR™ Green Master Mix (Applied Biosystems), in the reaction conditions were following the manufacturer's quidlines for each kit.

Melt curves were evaluated for each qPCR test was performed using the LightCycler® 480 (Roche) for each reaction. Gene expression was normalised using the *RPL19* ribosomal protein (*L19*) reference gene and analysed using the delta-delta Ct ( $\Delta\Delta C_t$ ) method. Primers used in this thesis were obtained from R. Bryan and G. Brooke or unless otherwise specified (Table 2.9).

**Table 2.9: Sequences of gene expression primers for use with qPCR.** Sequences are displayed in 5' to 3' direction.

<b>GENE</b>	<b>FORWARD</b>	<b>REVERSE</b>	<b>SOURCE</b>
<b>AR</b>	GACGACCAGATGGCTGTCGTCATT	GGGCGAAGTAGAGCATCCT	G. Brooke
<b>ER<math>\alpha</math></b>	GTGTCACCTTGGACA	AGGTTCCCTGTGGCCA	R.A. Bryan
<b>MYC</b>	GGCTCCTGGCAAAGGTCA	CTGCGTAGTTGTGCTGATGT	R.A. Bryan
<b>GREB1</b>	ATGGGAAATTCTTACGC TGGAC	CACTCGGCTACCACCT TCT	R.A. Bryan
<b>NDRG1</b>	CTCCTGCAAGAGTTTG ATGTCC	TCATGCCGATGTCATGGTAGG	R.A. Bryan
<b>TFF1</b>	CTGGATAGTTTGCGGC TGAG	ATGTCAGTGCCAGTAT GGGT	R.A. Bryan
<b>PLC-<math>\beta</math></b>	CGTGGCTTTCCAAGAAGAAG	GCTTCCGATCTGCTGAAAAC	L. Beliokaite
<b>PLC-<math>\delta</math></b>	CTGAGCAACTGAAGGGGAAG	CTCGTCTTCGTCTGACACCA	L. Beliokaite
<b>PLC-<math>\epsilon</math></b>	GCAGCTGCAGTGTGATCATT	AAAAGGTCTTGGCAGCTTGA	L. Beliokaite
<b>PLC-<math>\gamma</math></b>	AGCTGTGGTTCCCATCAAAC	CATGCTGATGGAGAAGACGA	L. Beliokaite
<b>PLC-<math>\eta</math></b>	AGAGATCAAGATGGCGTGCT	CAGATACAGGCAGCGACAAA	L. Beliokaite
<b>PLC-<math>\Delta</math></b>	GTGAAAGGATGCCGTTGTTT	GGCAGTGGAGCAGTGATTTT	L. Beliokaite

## 2.10 Genomic DNA extraction from breast cancer tumours

Tumour tissue ( $\leq 30$  mg) was transferred into a pre-chilled sterile mortar and washed three times with cold PBS before homogenisation. Sample was mixed with liquid nitrogen to keep them frozen, then firmly crushed using a chilled pestle into smaller pieces until a pulp/powder was formed. The sample was transferred into a sterile DNase-free 2ml microcentrifuge tube containing 375 $\mu$ l AGL buffer provided with the appGENE Genomic DNA kit (Appleton Woods). The following steps were applied using the manufacturer's reagents and protocol until final product was eluted with 50  $\mu$ L elution buffer and the eluted DNA stored at -20°C.

To quantify the DNA concentration, a standard curve was constructed using qPCR performed on Roche Human Genomic DNA. Following the manufacturer's instructions, 8 dilutions from the genomic DNA were prepared starting from 20 ng/  $\mu$ l then diluted further (1:2 dilution series). qPCR was conducted using the LightCycler® 480 (Roche) and a melt curve was observed for each reaction. Primers sequence obtained from (Roche) are listed in Table 2.10.

**Table 2.10: List of genomic DNA primers used for the BCa tumours DNA extraction.**

<i>PRIMER</i>	<i>SEQUENCE</i>
Genomic DNA forward	GGCTAGCTGGCCCGATTT
Genomic DNA reverse	GGACACAAGAGGACCTCCATAAA

## **2.11 Protein analysis**

### **2.11.1 Cell collection**

Ice-cold PBS was used to wash cells x2 then were detached via scraping with fresh PBS. Cells were subsequently pelleted for 1 min at (13,000 rpm and 4 °C), after that the supernatant was discarded and cell pellet was snap frozen and kept at -80 °C. If required, cell pellets were re-suspended in Radioimmunoprecipitation buffer (RIPA) combined with Halt Protease Inhibitor (PI) Cocktail (ThermoScientific) and Phenylmethanesulphonylfluoride (PMSF) to a final concentration of 1 µM (Table 2.1) (100 µL of RIPA was utilised per well of a 6 well plate). Sonication was conducted on lysates for 3 cycles on 'high' of 30 secs on and 30 secs off using a Biorupter® Plus (Diagenode). Samples were then pelleted for 10 min at (13,000 rpm and 4 °C) where the supernatant was transferred to a fresh pre-chilled 1.5 mL tube.

### **2.11.2 DC protein assay**

To quantify protein concentration, the Detergent Compatible (DC) Protein assay (Bio-Rad) was conducted using 5 µL of sample against standard concentrations of BSA as a reference concentration, following the manufacturer's guideline. Protein concentrations were measured at absorbance  $\lambda = 650$  nm using the FLUOstar Omega plate reader (BMG Labtech). Samples were diluted to an equal volume of protein per set (10–20 µg/10 µL of sample) with 4 x Laemmli protein sample buffer (Bio-rad) (2.5 µL/10 µL of sample).

### **2.11.3 SDS-PAGE**

Lysates were vortexed and incubated at 95 °C for 5-10 mins before running time. Then samples were immediately transferred to ice and vortexed once cool. 15- 20 µL of lysate was loaded per well of a 10 % polyacrylamide gel, against 5 µL of the Page Ruler Prestained Protein Ladder (Thermo Scientific) unless otherwise specified in results. Sodium dodecyl sulphate polyacrylamide gel electrophoresis (SDS-PAGE) was conducted at 120 V with pre-made running buffer.

### **2.11.4 Immunoblotting**

Proteins were transferred onto a Polyvinylidene difluoride (PVDF) membrane (Immobilion P, Millipore Inc., hydrated in preparation using 100 % Methanol, MeOH) via semi-dry transfer. This was conducted at 15 V and 100 mA for 2 hrs, using semi-dry electro blotting apparatus (Bio-Rad) and pre-made transfer buffer. After that, membranes were incubated with blocking solution for 15 mins, then using the required primary (1<sup>o</sup>) antibody (Ab) membranes were probed (Table 2.11) for 1 hr at (RT or O/N and 4 °C) while gently rocking. Three washes were performed with PBS-T for 5 mins before adding the relevant secondary (2<sup>o</sup>) Ab followed by incubation (Table 2.11) for 1 hr at RT, with gentle rocking. Three washes were then applied again using PBS-T for 5 mins followed by an additional wash with PBS for 5 mins, each were gently rocking. Proteins were subsequently visualised via chemiluminescence using Luminata™



Forte (Millipore) with the Fusion FX imager (Vilber Lourmat).

**Table 2.11: Description of the antibodies and concentrations used for immunoblotting.**

<i>PROTEIN</i>	<i>PRIMARY ANTIBODY</i>	<i>SECONDARY ANTIBODY</i>
<i>Androgen Receptor (AR)</i>	AR (N-20) sc-816 (Santa Cruz, diluted 1:100)	Anti-Rabbit IgG (whole molecule)- Peroxidase (Sigma-Aldrich, diluted 1:2,000)
<i>Oestrogen Receptor alpha (ER<math>\alpha</math>)</i>	ER $\alpha$ HC-20 sc-543 (Santa Cruz diluted 1:200)	Anti-Rabbit IgG (whole molecule)- Peroxidase (Sigma-Aldrich, diluted 1:2,000)
<i>Beta-Actin (<math>\beta</math>-Actin)</i>	Beta Actin Ab8226 (Abcam diluted 1:3,000)	Anti-Rabbit IgG (whole molecule)- Peroxidase (Sigma-Aldrich, diluted 1:2,000)
<i>Beta-Tubulin (<math>\beta</math>-Tubulin)</i>	Beta Tubulin T5168 (Sigma-Aldrich diluted 1:300)	Anti-Mouse IgG (whole molecule)- Peroxidase (Sigma-Aldrich, diluted 1:2,000)
<i>Cleaved PARP</i>	Cleaved PARP Ab9541 (Cell Signalling diluted 1:500 )	Anti-Rabbit IgG (whole molecule)- Peroxidase (Sigma-Aldrich, diluted 1:2,000)

## 2.12 Cell staining and confocal imaging

Cells were seeded at a low confluence (approximately 30 %) on cover-slips in the relevant hormone-depleted media, and incubated for 24 hrs. After that, cells were either transfected with the required plasmid (AR, ER $\alpha$ , ER HE-464, ER HE-257G and AR mutants) and/or treated with the relevant hormones for 2 hrs followed by washing with PBS x3. Fixing

was conducted using 200  $\mu\text{L}$  of 4 % PFA for 15 mins whilst rocking gently at RT. Following that, cells were washed with PBS for 5 mins x3 while shaking then fixed with 200  $\mu\text{L}$  of ice cold 100 % MeOH for 10 mins at  $-20\text{ }^{\circ}\text{C}$ .

Cells were initially incubated with 250  $\mu\text{L}$  of 1 % BSA in PBS-T for 30 mins at RT in preparation for staining, whilst gently rocking. 1<sup>o</sup> Ab incubation was conducted for AR (AR N20, Santa-Cruz diluted 1:200) or ER $\alpha$  (ER $\alpha$  HE20, Santa- Cruz diluted 1:400) in 100  $\mu\text{L}$  1 % BSA PBS-T, for 1 hr at (RT or O/N and  $4\text{ }^{\circ}\text{C}$ ), whilst gently rocking. Cells were washed x3 for 5 mins again before 2<sup>o</sup> Ab incubation was conducted (568- Alexa Fluor conjugated, Invitrogen), in 100  $\mu\text{L}$  of 1 % BSA PBS-T for 1 hr at RT in the dark, whilst gently rocking. Cells were washed an additional x3 for 5 mins then coverslips were fixed onto microscope slides with Fluoroshield Mounting Medium with 4',6-diamidino-2-phenylindole (DAPI, Abcam) and sealed using Fixogum (Marubu). Confocal microscopy was then used to visualise cells.

### **2.13 Single cell tracking by widefield microscopy**

PC3-GFP cells were seeded on 96-well plates (500-1,000 cell/well) for 24 hrs. After that, media was replaced with phenol red-free RPMI (5% SFCS) then cells were incubated post treatment with desired drug concentrations for 72 hrs. Examination was conducted using Widefield microscope with a motorized stage and humidified chamber,  $37\text{ }^{\circ}\text{C}$  in 5 % CO<sub>2</sub> conditions, and images acquired using 10X objective. GFP was excited using blue light (470 nm) via a CoolLED pE excitation system and two-dimensional (2D) time series frames were captured using NIS-Elements AR software (4.13.04 Build 925) every 15 minutes for 24 hrs. Multiple

areas were examined for each treatment well (3 fields minimum) and collected image sequences were pre-processed and analysed by ImageJ software.

## **2.14 WST-1 proliferation assays**

Cells were grown in a 96-well plate with the relevant culture media (Table 2.3), then treated using the required concentration of hormone for 96 hrs. Cellular proliferation was measured using WST-1 Cell Proliferation Reagent (Abcam), following the the manufacturer's guideline. Growth was quantified by measuring the resulting absorbance  $\lambda = 440$  nm on the FLUOstar Omega plate reader (BMG Labtech).

## **2.15 Crystal Violet proliferation assays**

Cells were seeded in 96 well plates in the required media at confluence of approximately 10 %) and incubated at 37 °C for 24 hours prior to treatments. Then medium was refreshed and cells were treated with desired drug concentrations then incubated for 72 hrs. 100  $\mu$ l of 4% PFA was added to each well and incubated at RT for one hour, plates then were washed x3 using PBS and left to dry O/N. Cells then were then incubated for one hour in 50  $\mu$ l of 0.02 % crystal violet stain, followed with x3 washes with distilled H<sub>2</sub>O and left for drying. Lastly, 100  $\mu$ l of 10 % acetic acid was added to all wells and kept for one hour on a rocker. Plates were read using a spectrophotometer microplate reader (FLUOstar Omega, BMG LABTECH, UK) at 490 nm wavelength.

## 2.16 Immunoprecipitation

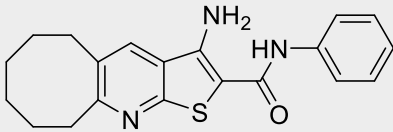
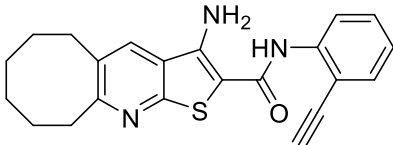
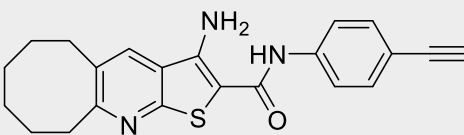
HEK293 cells were seeded at 70% confluence in 10 cm plates in hormone-deprived medium then transfected with plasmids encoding GFP-AR and RFP-ER $\alpha$  using jetPRIME (as described in section 2.4.2). Cells were left for 24 hours then treated for 2 hrs with either vehicle (EtOH), 10 nM Mibolerone and/or 10 nM Estradiol and lysed in IP buffer containing freshly added protease inhibitors. Lysates were centrifuged at 10,000 g for 15 minutes at 4 °C and supernatants transferred to fresh tubes. Protein concentration was obtained using the DC protein assay (as described in section 2.11.2). Lysates were pre-cleared with 50  $\mu$ L of sepharose beads (Sigma-Aldrich, MO, USA, 30 minutes of rotation at 4 °C). After that, the supernatant was transferred to fresh tubes and incubated with anti-GFP antibody (Abcam, Cambridge, UK) for 1hr whilst rotating then 50  $\mu$ L of sepharose beads were added. 1hr post incubation, beads were washed x3 with IP buffer, 2X Protein Loading Buffer added to the beads and samples boiled before protein separation was performed using SDS-PAGE followed by immunoblotting.

## 2.17 Biotin drug pull-down

PC3-GFP cells were seeded at confluency (approximately 70%) in 10 cm plates in full media for 24 hrs and treated with 20  $\mu$ M of the desired drug for 2 hrs at 37 °C (DMSO, DJ0199, DJ0232 and DJ0233) (Table 2.12). After incubation, plates were washed twice with cold PBS and 400  $\mu$ L RIPA (2.5% HALT protease inhibitor was added) then lysate was scraped and transferred to 1.5 mL cold tubes. Cells were broken down using 25G needle (x5 times) and centrifuged (13,000 rpm for 10 min at 4 °C) then supernatant was transferred to fresh tubes. PD10 desalting columns were prepared following the manufacture instructions (PD Spin Trap<sup>TM</sup> G-25) then 300  $\mu$ L of lysate was added from each treatment. Columns were attached to fresh

tubes and centrifuged (800g for 1 min at 4 °C), then 66 uL TBS, 8 uL (1mM Biotin Azide), 4 uL (5mMCuSO<sub>4</sub>), 2 uL (50mM THPTA) and 20 uL (100mM Sodium Absorbate) were added to the collected products/ tube and rotated in the dark (1 hr at RT). During rotation, PD10 columns were washed (x5 times with ddH<sub>2</sub>O) and beads (Pierce Protein A/G Magnetic Beads- Fisher Scientific) 80 uL/ tube were centrifuged for washing (x4 times with ddH<sub>2</sub>O at 1000g). Prepared columns were attached to 1.5 mL tubes following the addition of the samples and 80 uL washed beads then kept rotating for 2 hrs at 4 °C. Beads were washed twice with 500 uL TBS (1500 rpm for 1 min at 4 °C) then an extra wash with cold PBS. 20 uL of trypsin was added to each tube then incubated at 30 °C overnight. To perform Mass Spectrometry, 5 uL of 20% formic acid was added then spectra were generated by collision-induced dissociation of tryptic digests in the linear ion trap of the LTQ Orbitrap Velos instrument.

**Table 2.12: Description of the compounds used for biotin pull- down.**

<i>CODE (MW)</i>	<i>COMPOUND</i>	<i>SPECIFICATIONS</i>
DJ0199 (351.47)		Not biotinylated (-ve control)
DJ0232 (375.49)		Biotinylated
DJ0233 (375.49)		Biotinylated but inactive (-ve control)

## **2.18 Flow Cytometric Measurement of Apoptotic and Necrotic Cells**

PC3-GFP cells were seeded at 70 % confluence in 12 well plates for 48 hrs, treated with the PLC inhibitors (1  $\mu$ M) and cells incubated for a further 24 hrs. The media was collected into 2 ml tubes, the cells washed with 200  $\mu$ L of PBS and collected into respective tubes. The cells were detached with 200  $\mu$ L of trypsin EDTA and were collected using 500  $\mu$ L of media. For apoptosis measurement 150  $\mu$ L of the suspension was moved to new 1.5 ml tubes and spun at 5000 rpm for 2 mins. The supernatant was aspirated, 200  $\mu$ L of Nicoletti buffer added. Necrosis was determined by measuring the number of PI positive cells. The harvested cells were stained with 20  $\mu$ g/ml of PI. For both assays, cells were vortexed and kept on ice until measurement Accuri C6 flow cytometry (BD Biosciences).

## **2.19 Flow cytometric analysis of cell cycle**

PC3-GFP cells were seeded at 70% confluence in 12 well plates for 48 hrs, treated with the PLC inhibitors (1  $\mu$ M) and cells incubated for a further 24 hrs. Media was collected in 2 ml tubes and cells were washed with 500  $\mu$ l of PBS, which then was transferred to the same tube. 100  $\mu$ l of trypsin was added and the cells were incubated for a few minutes to allow cell detachment. 500  $\mu$ l of the collected media and PBS mixture was added to the cells. The cell suspension was transferred back to the 2 ml tube and centrifuged at 5500 rpm for 5 minutes. Media was discarded, and pellets re-suspended in 50  $\mu$ l of PBS. Then cells were fixed with 70% EtOH 500  $\mu$ l added drop-wise and followed with gentle vortex. For analysis, cells were pelleted at 5500 rpm for 5 minutes and PBS was aspirated off then re-suspended in 200  $\mu$ l of PI staining

solution containing RNase A. 10,000 cells per sample were analysed and quantified using Accuri C6 flow cytometry (BD Biosciences).

## **2.20 Assessment of caspase 3/7 activity and viability**

PC3-GFP cells were seeded in 96 well plates at <2,000 cells per well following the manufacturer instructions. After 24 hrs, cells were treated with the desired drugs in different concentrations and 48 hrs post drug treatment Caspase 3/7 activity and viability were assessed using the ApoTox-Glo™ Triplex assay kit. Plates were read using the spectrophotometer microplate reader (FLUOstar Omega, BMG LABTECH, UK) for luminescence and fluorescence at 400 nm wavelength.

## **2.21 Ex vivo culture of human prostate tumours**

This experiment was performed in collaboration with Dr. Damien Leach and Prof. Charlotte Bevan (Imperial Collage London). A tissue from human prostate cancer patient was dissected into smaller pieces sized 1-mm<sup>3</sup> then cultured on a sponge that is pre-soaked with gelatin (Johnson and Johnson) in 24-well plate. Sample was incubated at 37°C for 48 hrs with 500 µL RPMI-1640 with 10% FBS, antibiotic/antimycotic solution, 0.01 mg/mL hydrocortisone and 0.01 mg/mL insulin (Sigma). Harvested sample was then analysed using qPCR for target genes for caspase 3 and PCNA (Centenera *et al.*, 2012).

## **2.22 Statistical analysis**

For each experiment, three independent biological repeats were performed unless otherwise stated. To identify significant differences in values one and two-way ANOVA tests were performed using Prism version 6 (GraphPad Software, San Diego, CA) and expressed as mean value  $\pm$ SE. Adjusted P values following Bonferroni test, less than 0.01 values were considered to be significant.

## **2.23 Image and software analysis**

Three independent biological repeats were performed for each experiment unless otherwise stated. For crystal structures the software PyMol V 2.2 was used to obtain AR protein 3D structures at: <https://pymol.org/2/>. The catalogue of somatic mutations in cancer (COSMIC) database V 89 was used to obtain AR mutation found in breast cancer at: <https://cancer.sanger.ac.uk/cosmic>. The software 4Peaks V1.7.1 was used to obtain AR mutation in BCa comparisons with wild type receptor. To perform heatmap for PCa cell lines, the software plotly V 4.1.0 was used at: <https://plot.ly>. The flow cytometry histograms were obtained using the Accuri C6 V 1.0 software (BD Biosciences).



## CHAPTER 3

# RESULTS I: The Role of the Androgen Receptor in Breast Cancer and its Cross-Talk with Oestrogen Receptor alpha

### 3.1 Introduction

In the UK, breast cancer (BCa) is the cancer with the highest incidence rate amongst women (Cancer Research UK, 2014). Endocrine sensitive BCa subtypes contributes to the majority of the diagnosed cases of the disease where progression is mostly driven by Oestrogen Receptor  $\alpha$  (ER $\alpha$ ), which is dependent upon oestrogens for activation (Chuffa *et al.*, 2017; Gross and Yee, 2002). As previously mentioned, ER $\alpha$  is a member of the ligand-dependent Nuclear Receptor (NR) family which translocate into the nucleus upon the binding of their ligands (Sever and Glass, 2013). 17-  $\beta$ -Oestradiol (E2) is one of the most potent oestrogens as well as the most abundant in circulation (Bean *et al.*, 2014). Another important member of the NR family is the Androgen Receptor (AR), which is activated in response to androgens. Interestingly, androgens are secreted in higher quantities than oestrogens in females (Lehmann-Che *et al.*, 2013). Androstenedione and testosterone, two types of androgens produced in women, are precursors for E2 (Chuffa *et al.*, 2017; Patani and Martin, 2014). The AR appears to have different roles in breast cancer, having oncogenic activity in ER $\alpha$ -negative disease and acting as a tumour suppressor in ER $\alpha$ -positive disease. Therefore, in recent years a significant amount of research has aimed to further our knowledge of the role of AR in BCa (Rahim and O'Regan, 2017).

In ER $\alpha$ -positive BCa, AR appears to be an indicator of positive prognostic outcome, which has been hypothesised to be as a result of AR-ER $\alpha$  cross-talk (Lehmann-Che *et al.*, 2013;

Rahim and O'Regan, 2017). It has been demonstrated that AR and ER $\alpha$  suppress each other's activity, and this cross-talk could explain the inhibitory effect displayed by androgen signalling in ER $\alpha$ -positive BCa (Panet-Raymond *et al.*, 2000). However, in ER $\alpha$ -negative disease it has been suggested that AR can mimic ER $\alpha$  signalling to promote BCa progression in the absence of a functioning ER $\alpha$  (Le Romancer *et al.*, 2011).

A number of mechanisms have been proposed to explain AR-ER $\alpha$  cross-talk. For example, direct interaction between the N-terminus of the AR and the LBD of the ER $\alpha$  blocks the activity of both receptors (Hickey *et al.*, 2012; Panet-Raymond *et al.*, 2000). Also, the AR is able to bind to oestrogen response elements (EREs) and therefore block ER $\alpha$  binding to DNA. This was demonstrated through the transfection of the AR DBD into BC cell lines, which was shown to significantly reduce ER $\alpha$  activity (McNamara *et al.*, 2014). Furthermore, competition for histone modifying cofactors is also likely to have a bearing on receptor activity. For example, Androgen Receptor Associated co-regulator 70 (ARA70) can enhance the activity of both the AR and ER $\alpha$  and the AR may sequester this factor, resulting in a decrease in ER $\alpha$  activity (Lanzino *et al.*, 2005).

### **3.1.1 Chapter Aims**

Investigation of AR signalling in BCa has increased significantly over recent years and several clinical trials are assessing the efficacy of anti-androgens as therapeutics for this disease. There is therefore a need to better characterise the role of AR signalling in BCa:

Aim 1- To characterise the mechanisms of cross-talk between the AR and ER $\alpha$ .

Aim 2 – To identify AR mutations associated with BCa and to investigate if these substitutions affect receptor activity and ligand specificity.

Aim 3 – To investigate if mutations in the AR affect receptor cross-talk with the ER $\alpha$  pathway.

## **3.2 Characterisation of AR-ER $\alpha$ Cross-talk**

### **3.2.1 Androgen signalling inhibits oestrogen induced growth**

It appears that the AR has different roles in BCa development, oncogenic in ER $\alpha$ -negative disease and tumour suppressor in the ER $\alpha$ -positive disease (Hickey *et al.*, 2012). Therefore, an investigation of the AR/ER $\alpha$  cross-talk in the MCF-7 cell line as it provides a useful model because it expresses both receptors. To assess the inhibitory effects of androgen upon MCF7 cells, proliferation assays were performed. Cells were treated with 0.1 nM E2 and increasing concentrations of the synthetic androgen Mibolerone (MIB). E2 significantly increased MCF-7 growth and increasing doses of MIB significantly decreased growth (Figure 3.1a).

To see if the treatment with E2 or MIB altered receptor expression, cells were treated with the ligands for 24 hrs and immunoblotting performed (Figure 3.1b). The immunoblot was repeated 3 times and densitometry analysis performed (Figure 3.1c). The results demonstrated that AR expression levels increases with MIB treatment and remained relatively low in the presence of E2. In contrast, ER $\alpha$  levels decreased in response to E2 and MIB had no effect upon ER $\alpha$  levels.

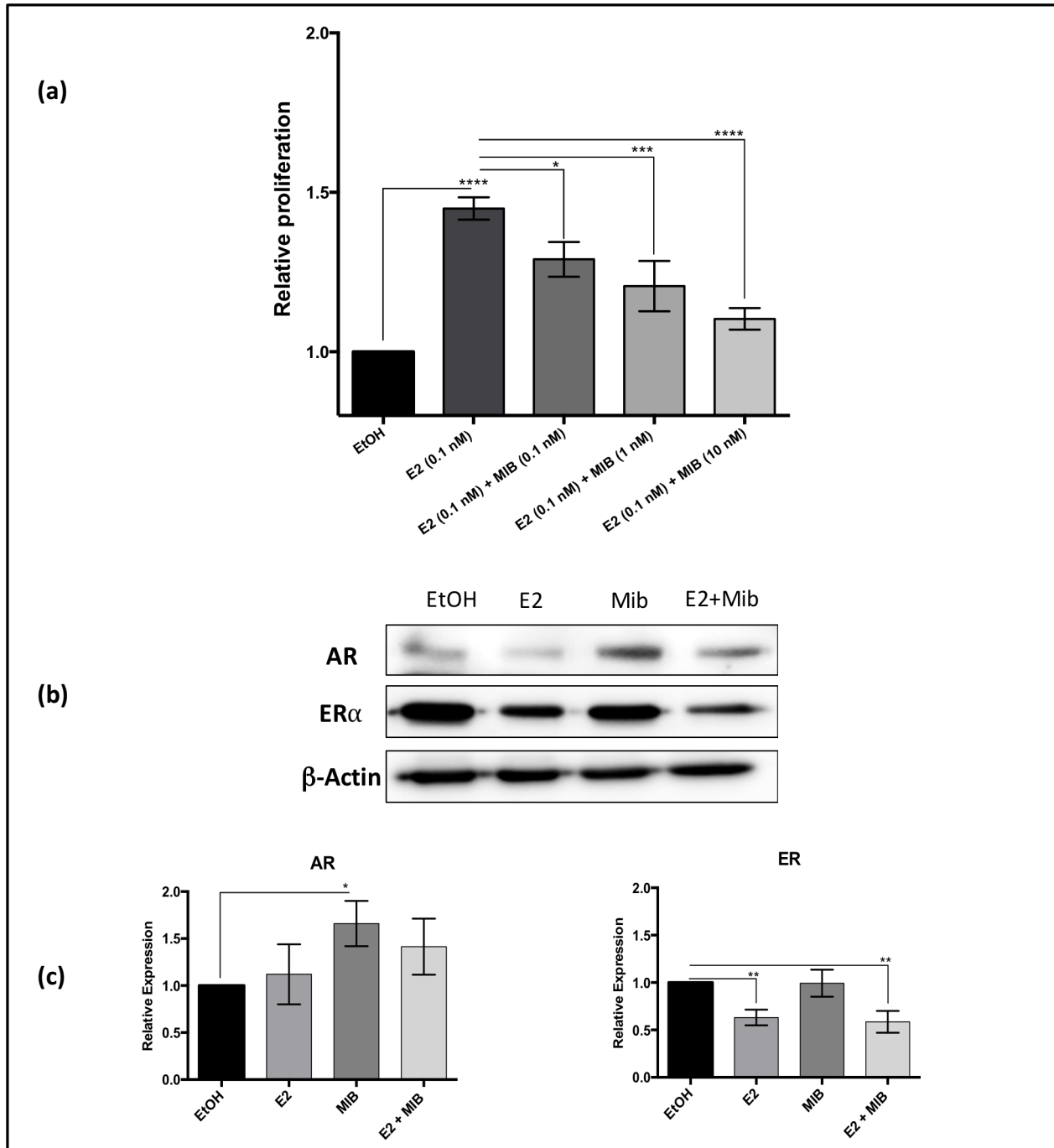


**Figure 3.1: AR signalling inhibits E2-induced proliferation of MCF-7 cells.** MCF-7 were treated with the ligands E2: 17- $\beta$ -oestradiol (0.1 nM) and MIB: mibolerone (0.1 nM, 1.0 nM and 10 nM) for 24 hrs. (a) Relative proliferation of MCF-7 cells. Proliferation assays were done in triplicate. (b) Cells were treated with ligand for 24 hrs, proteins separated using SDS-PAGE and AR and ER $\alpha$  expression analysed using immunoblotting. (c) The immunoblotting was repeated 3 times and densitometry analysis performed using Image J. ANOVA. \*\*\*\*p<0.00001, \*\*\*p<0.0001, \*\*p<0.001, \*p<0.01. Mean  $\pm$  1SE.

### 3.2.2 The interaction between AR and ER $\alpha$ is ligand-independent

Direct interaction between AR and ER $\alpha$  as well as competition for cofactors have been proposed as mechanisms of inhibitory cross-talk between the two receptors (McNamara *et al.*, 2014; Panet-Raymond *et al.*, 2000). To investigate this, plasmids encoding GFP-AR and RFP-ER $\alpha$  were transfected into HEK cells and co-immunoprecipitation was performed using anti-GFP beads. Proteins were visualised using immunoblotting where ER $\alpha$  was found to immunoprecipitate with the AR and this interaction was ligand independent (Figure 3.2).

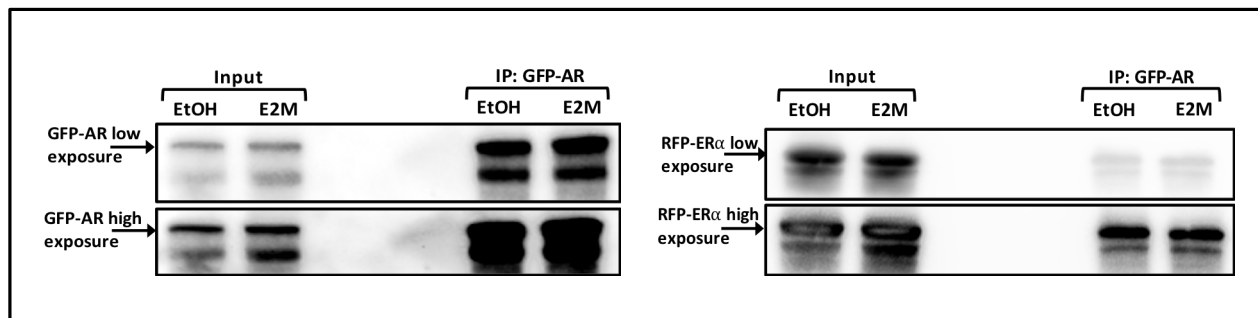


**Figure 3.2: AR-ER $\alpha$  interaction.** HEK cells were transfected with plasmids encoding RFP-ER $\alpha$  and GFP-AR for 48 hrs. Cells treated with EtOH: ethanol, E2: 17- $\beta$ -oestradiol (1.0 nM) and M: mibolerone (1.0 nM) for 2hrs then harvested following co-immunoprecipitation using anti-GFP beads. Immunoblotting was performed to visualise the proteins, using antibodies specific for the AR and ER $\alpha$ .

### **3.2.3 AR and ER $\alpha$ inhibit each others activity in reporter assays**

To further investigate AR-ER $\alpha$  cross-talk, reporter assays were performed (Figure 3.3a). COS-1 cells were transfected with the TAT-GRE-E1B-LUC/ ERE-LUC reporter plasmids, a renilla expression vector and different concentrations of pSV-AR and/or pSG5-ER $\alpha$  plasmids. Cells were left for 24 hrs then treated with 1.0 nM of mibolerone and/or 17- $\beta$ -oestradiol (Figure 3.3b). As expected, AR activity was induced by mibolerone, and this activity was significantly inhibited in response to increasing concentrations of ER $\alpha$ . A similar trend was evident when ER $\alpha$  was constant and AR levels were increased. Immunoblotting analysis was performed to confirm successful transfection and expression of the receptors (Figure 3.3c). Expression levels for AR and ER $\alpha$  receptors increased with the amount of plasmid transfected. Interestingly, increased expression of AR or ER $\alpha$  increased the levels of the other receptor (i.e. when AR expression was increased, ER $\alpha$  levels were also found to increase).

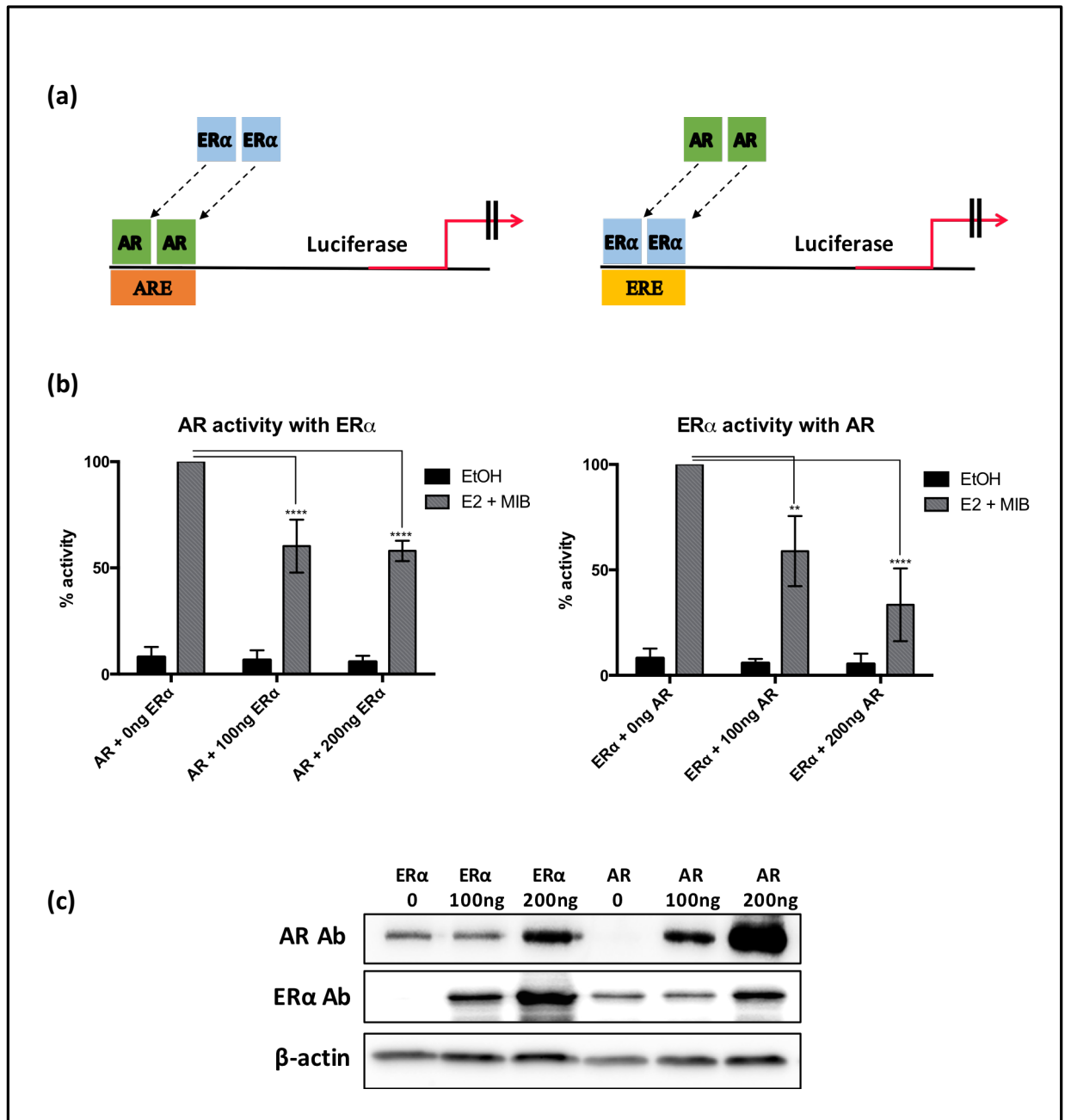


**Figure 3.3: AR and ERα cross-talk inhibits receptor activity.** (a) Schematic representation of the luciferase reporter assays. (b) COS-1 cell lines were transfected with expression plasmids for ERα and/or AR, a luciferase reporter (ERE-LUC or TAT-GRE-E1B-LUC) and a renilla expression vector. Cells were incubated for 24 hours then treated with EtOH: ethanol, E2: 17-β-oestradiol (1.0 nM) and/or MIB: mibolerone (1.0 nM). (c) COS-1 cells were transfected with plasmids encoding ERα and AR for 24 hrs, cells harvested and immunoblotting performed with antibodies specific for ERα and AR. ANOVA \*\*\*\*p<0.00001, \*\*p<0.001. Mean ± 1 SE.

To further investigate the inhibitory effect between the receptors, the effect of the anti-androgen drug Bicalutamide (Bic) was evaluated to what effect AR antagonists have upon receptor crosstalk. AR activity was significantly inhibited in response to 1 and 10 uM Bic (Figure 3.4b). ER $\alpha$  activity was not inhibited by Bic at any of the concentrations tested (Figure 3.4c). In agreement with previous experiments, co-transfection of AR and ER $\alpha$  inhibited receptor activity. When AR activity was assessed, the receptor was inhibited in response to increasing concentration of Bic specially at the 1 and 10 uM treatment. However, this inhibition was witnessed with and without all treatment concentrations with Bic as the reduction in activity was due to the presence of the ER $\alpha$  (Figure 3.4 b and d). On the contrary, the ER $\alpha$  activity was only inhibited when the AR was added but not due to the anti-androgen effect (Figure 3.4 c and e). Bic did not affect receptor cross-talk with ER $\alpha$  activity repressed irrespective of the presence/absence of Bic. To confirm this, we repeated these experiments using another anti-androgen, Enzalutamide (Enza), which has been shown to prevent AR nuclear translocation and co-activator recruitment, and has greater affinity than Bicalutamide (McGhan *et al.*, 2014) (Figures 3.5b). Similar trends were witnessed, Enza significantly reduced AR activity at the concentrations 1 and 10 uM but when the ER $\alpha$  was introduced the inhibition was mainly due to the receptors cross-talk and no significant effects were noticed due to Enza treatments (Figure 3.5 b and d). However, ER $\alpha$  activity was not affected by the drug but the addition of the AR has resulted in reducing receptor activity with all treatment concentrations (Figure 3.5 c and e). Enza inhibits AR activity and no effect upon ER $\alpha$ , as with Bicalutamide, enzalutamide did not affect the cross-talk between AR and ER $\alpha$  etc.



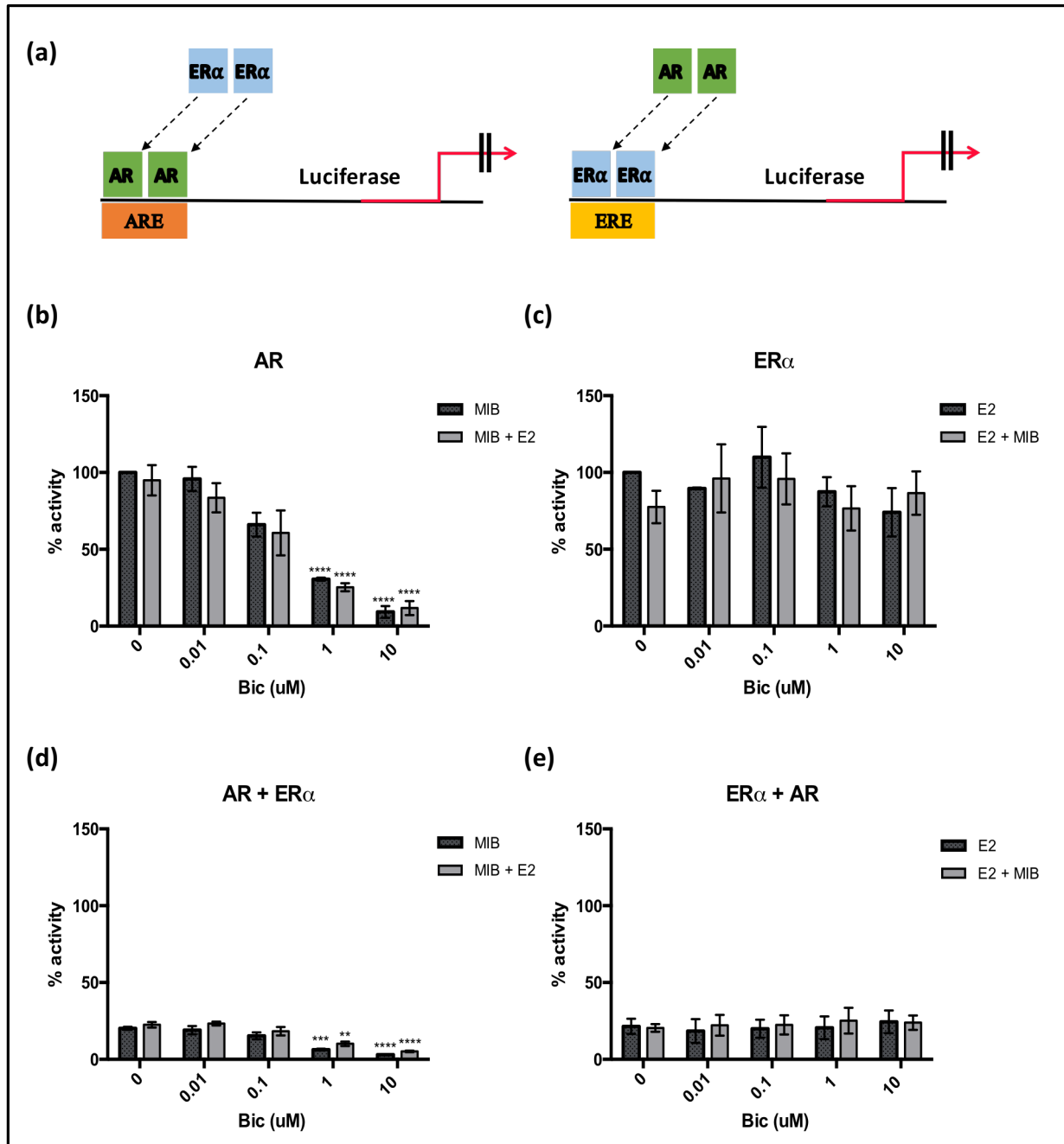


**Figure 3.4: Bicalutamide dose not affect AR and ER $\alpha$  cross-talk.** (a) Schematics representation of the luciferase reporter assays. (b, c, d and e) COS-1 cell lines were transfected with expression plasmids for ER $\alpha$  and/or AR, a luciferase reporter (ERE-LUC or TAT-GRE-E1B-LUC) and a renilla expression vector. Cells were incubated for 24 hours then treated with EtOH: ethanol, Bic: Bicalutamide (0.01 uM, 0.1 uM, 1.0 uM and 10 uM), E2: 17- $\beta$ -oestradiol (1.0 nM) and/or MIB: mibolerone (1.0 nM). ANOVA \*\*\*\*p<0.00001, \*\*\*p<0.0001, \*\*p<0.001. Mean  $\pm$  1SE.

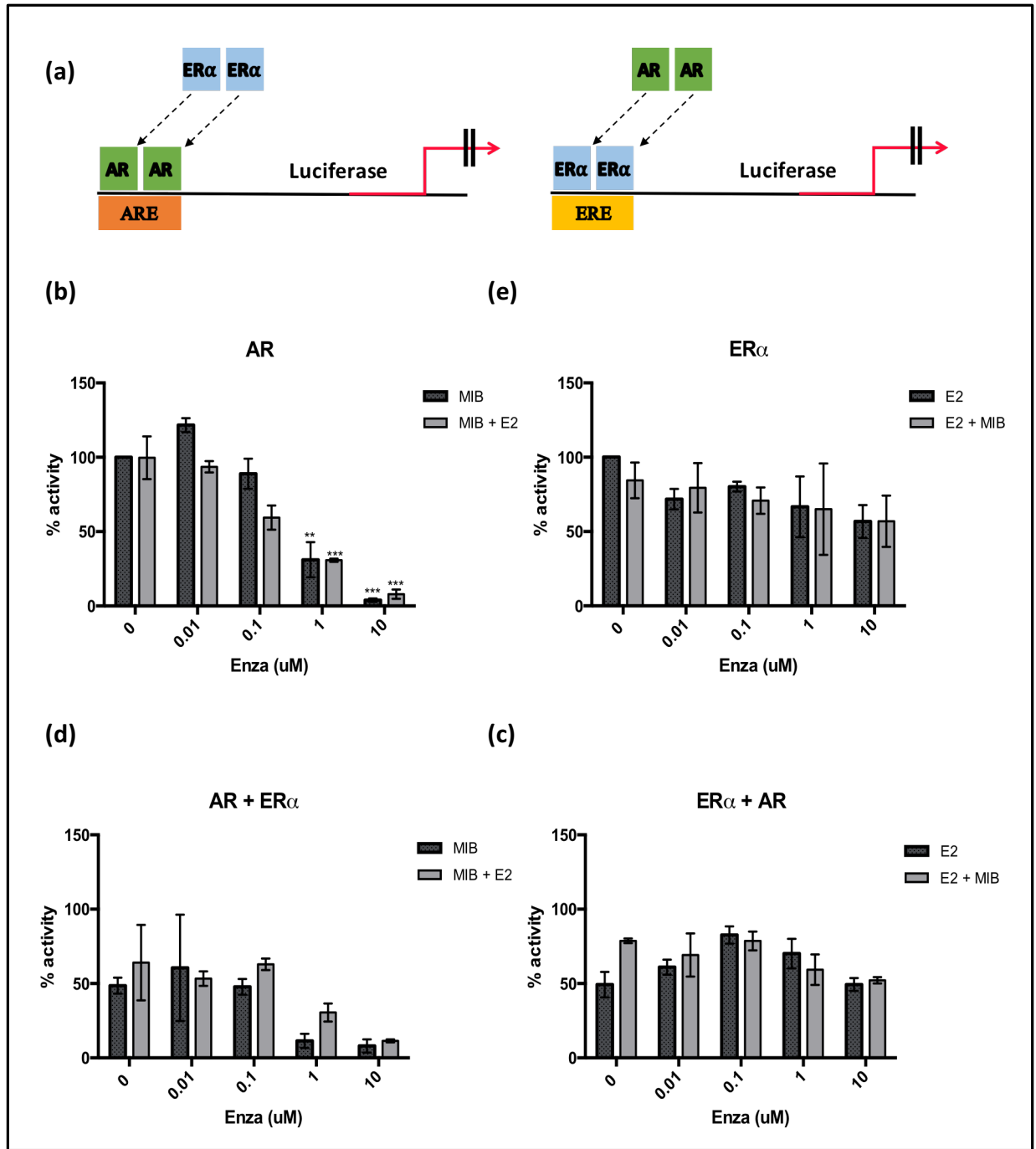
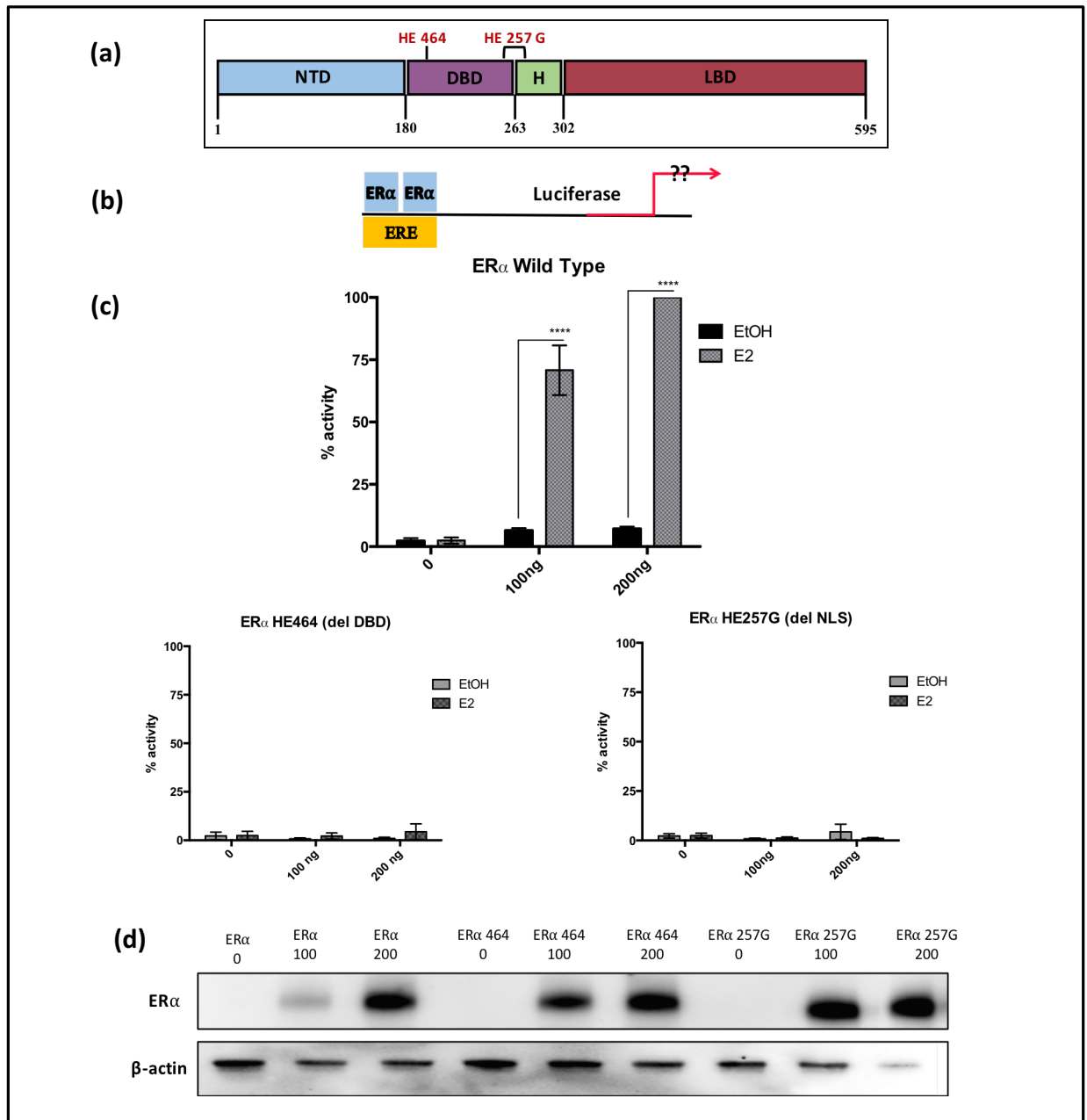


**Figure 3.5: Enzalutamide does not affect AR and ER $\alpha$  cross-talk.** (a) Schematics representation of the luciferase reporter assays. (b, c, d and e) COS-1 cell lines were transfected with expression plasmids for ER $\alpha$  and/or AR, a luciferase reporter (ERE-LUC or TAT-GRE-E1B-LUC) and a renilla expression vector. Cells were incubated for 24 hours then treated with EtOH: ethanol, Enza: Enzalutamide (0.01 uM, 0.1 uM, 1.0 uM and 10 uM), E2: 17- $\beta$ -oestradiol (1.0 nM) and/or MIB: mibolerone (1.0 nM). ANOVA \*\*\*\*p<0.00001, \*\*\*p<0.0001, \*\*p<0.001. Mean  $\pm$  1SE.

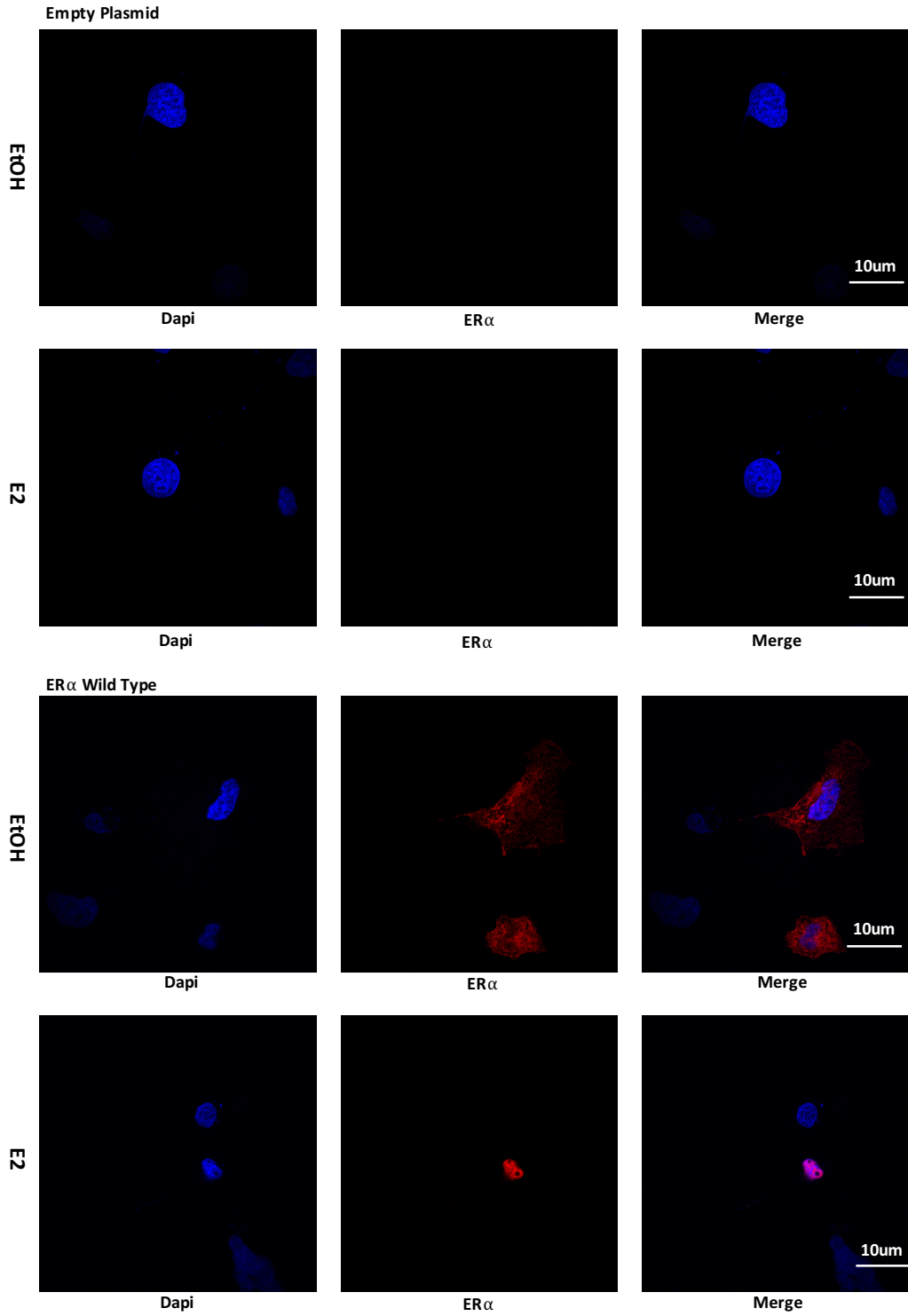
### 3.2.4 Characterisation of AR-ER $\alpha$ cross-talk using ER $\alpha$ mutants

The previous experiments have demonstrated that AR and ER $\alpha$  interact and inhibit each others activity. To further investigate how the mechanism of inhibition, we were kindly gifted 2 ER $\alpha$  variants by Prof. Simak Ali (Imperial College London) (Figure 3.6a): i,  $\Delta$ NLS (ER $\alpha$  HE257G) which has a deletion in the NLS region at amino acids 250-270, and hence is unable to translocate into the nucleus; ii, ER $\alpha$  HE464 has a mutation in the DBD and so is unable to bind to DNA (Lopez-Garcia *et al.*, 2006; Ylikomi *et al.*, 1992). Due to the nature of the mutations, these mutant receptors should be transcriptionally inactive and to confirm this reporter assays were performed (Figure 3.6b). COS-1 cells were transfected with plasmids encoding ER $\alpha$ , ER $\alpha$ -HE464, ER $\alpha$ -HE257G, the ERE- LUC reporter and a renilla expression vector (Figure 3.6c). The ligand-dependent activity of ER $\alpha$  wild-type increased as the amount of plasmid transfected increased, however, the two mutant ER $\alpha$ s were both inactive. To confirm successful transfection and protein expression immunoblotting analysis was performed on the lysates from the transfections. The expression of all receptors was found to increase as the concentration of plasmid transfected increased (Figure 3.6d).

To evaluate the effect of the ER $\alpha$  mutants upon receptor localisation, COS-1 cells were seeded on coverslips and transfected with plasmids encoding ER $\alpha$ , ER $\alpha$ -HE464 and ER $\alpha$ -HE257G. ER $\alpha$  wild-type and the DBD mutant (ER $\alpha$  HE464) were found to be predominantly nuclear in the presence and absence of E2. In contrast, the NLS mutant ER $\alpha$  HE257G, as expected, was found to be nuclear and cytoplasmic and in the presence of E2 appears to form aggregates in the cytosol (Figure 3.7) (Table 3.1).



**Figure 3.6: Mutation of the ERα NLS and DBD inhibits receptor activity.** (a) Image shows four functional domains of the ERα and the gene structure NTD = N- terminal domain. DBD = DNA binding domain. LBD = ligand binding domain highlighting the residues that were mutated. (b) Schematic representation of the luciferase reporter assays. (c) COS-1 cell lines were transfected with expression plasmids for ERα, a luciferase reporter (ERE-LUC) and a renilla expression vector. Cells were incubated for 24 hours then treated with EtOH: ethanol and E2: 17-β-oestradiol (1.0 nM). Proliferation assays done in triplicate. (d) COS-1 cells were transfected with plasmids encoding ERα for 24 hrs, cells harvested and immunoblotting performed with antibodies specific for ERα. ANOVA system. \*\*\*\*p<0.00001. Mean ± 1SE.



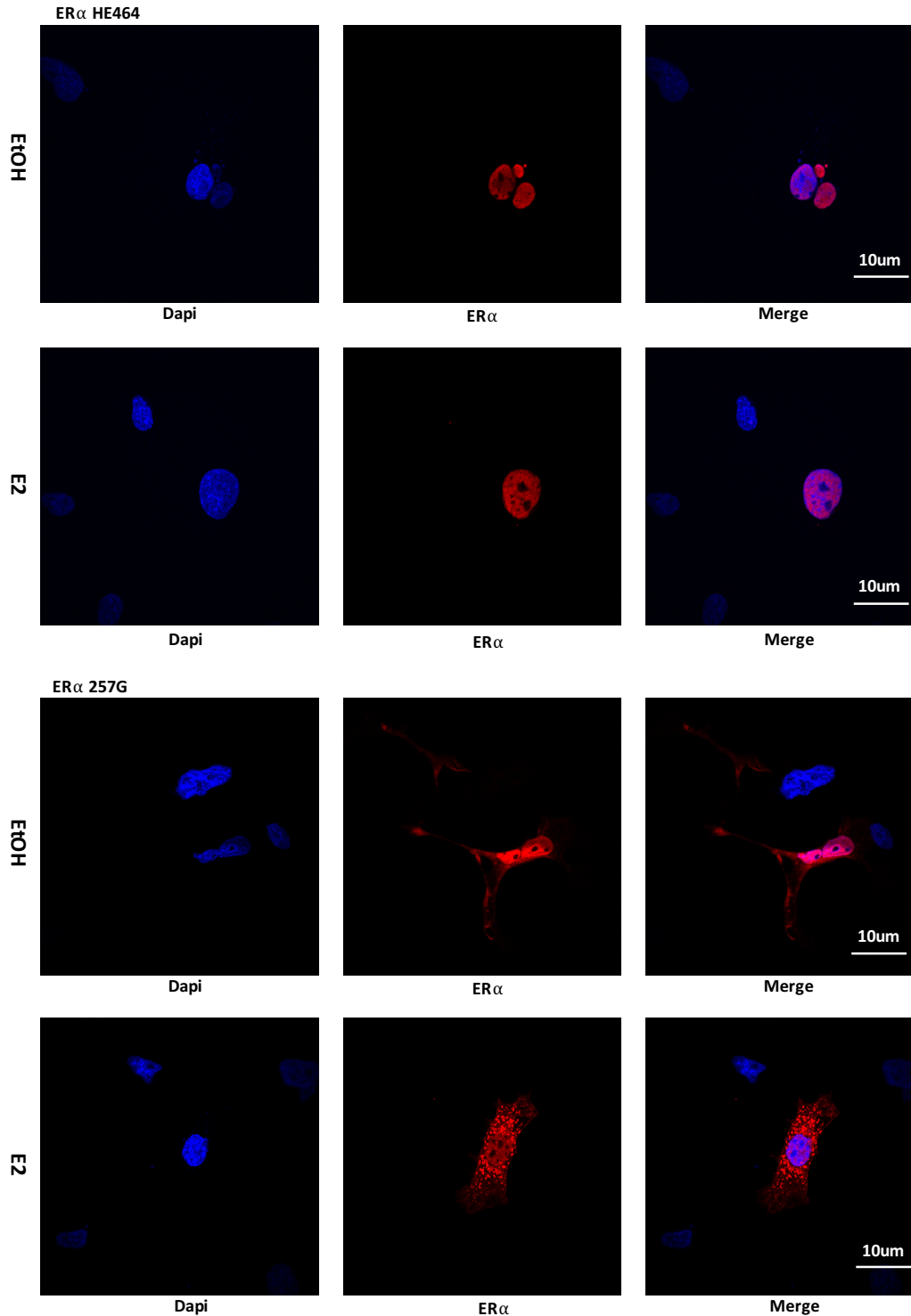


**Figure 3.7: Deletion of the ER $\alpha$  NLS results in cytoplasmic accumulation of the receptor.** COS-1 cells were transfected with plasmids encoding ER $\alpha$  wild type, ER $\alpha$  HE 464 and ER $\alpha$  HE 257G. Cells were fixed with 4 % paraformaldehyde and methanol following 2 hrs of treatment with EtOH (ethanol) or E2 (17- $\beta$ -oestradiol). Confocal microscopy was used to visualise the localisation of the oestrogen receptors (immunofluorescent staining using ALEXA 594 (red)). Nuclear staining = 4',6-diamidino-2-phenylindole (DAPI) in blue.

**Table 3.1: ER $\alpha$  variants cellular localisation upon oestradiol treatment.** Table illustrates if ER $\alpha$  receptors were predominantly nuclear (N), cytoplasmic (C) or both (C + N) after 2 hrs treatment with the oestrogen E2: 17- $\beta$ -oestradiol in COS-1 cell line.

<i>RECEPTOR</i>	<i>EtOH</i>	<i>E2</i>
<b>ER<math>\alpha</math> wild type</b>	C	N
<b>ER<math>\alpha</math> HE464</b>	N	N
<b>ER<math>\alpha</math> 257G</b>	C + N	C + N

To investigate if mutations of ER $\alpha$ , that have altered cellular localisation or DNA binding, affects cross-talk between the AR and ER $\alpha$ , COS-1 cells were transfected with the TAT-GRE-E1B-LUC reporter plasmid, a renilla expression vector, pSVAR and plasmids encoding the wild-type and mutant ER $\alpha$  (Figure 3.8a). As before, wild-type ER $\alpha$  inhibited the transcriptional activity of the AR. Both of the ER $\alpha$  mutants were also found to inhibit AR activity, to a lesser extent, although this was not found to be significant. (Figure 3.8b).

To see if the ER $\alpha$  mutants affected the cellular localisation of the AR, the fluorescent imaging was repeated following co-transfection of pSV-AR (Figure 3.9). AR is predominantly in the cytoplasm in absence of hormone and completely nuclear when treated with MIB. While ER $\alpha$  wild-type and the DBD mutant (ER $\alpha$  HE464) were found to be predominantly nuclear in the presence and absence of E2. The NLS mutant ER $\alpha$  HE257G also was found to be nuclear and cytoplasmic and in the presence of E2 with aggregates formation in the cytosol. The AR was witnessed to not go completely nuclear with the ER $\alpha$  wild type and NLS mutant are treated with ligand. But the AR is completely nuclear with with DBD mutant, this suggested that the AR and all ER $\alpha$  receptors do compete to co-localise (Table 3.2).

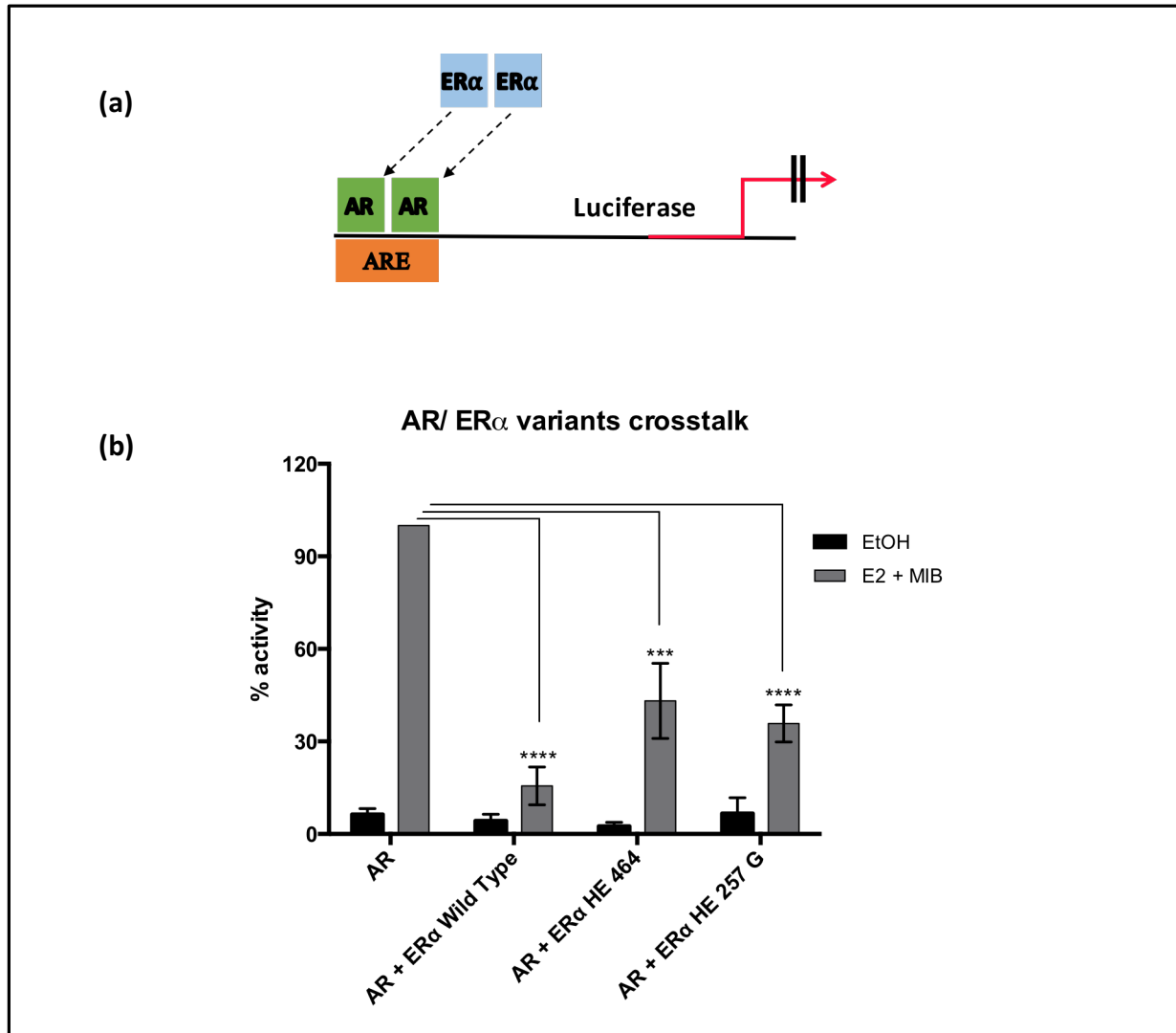
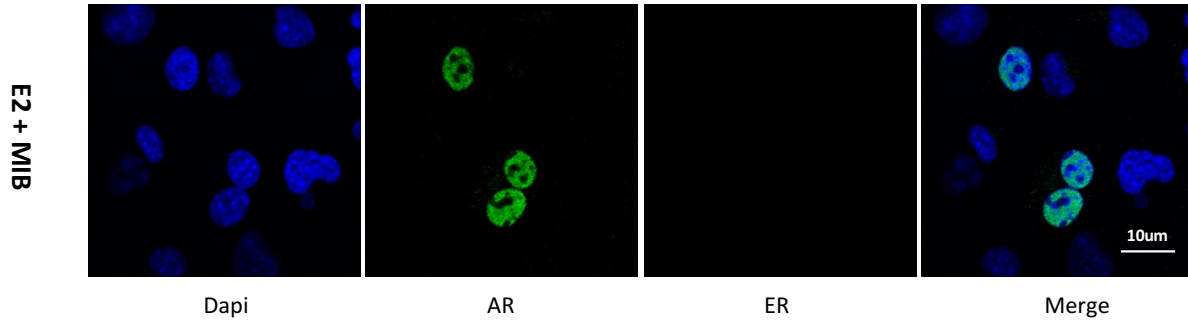
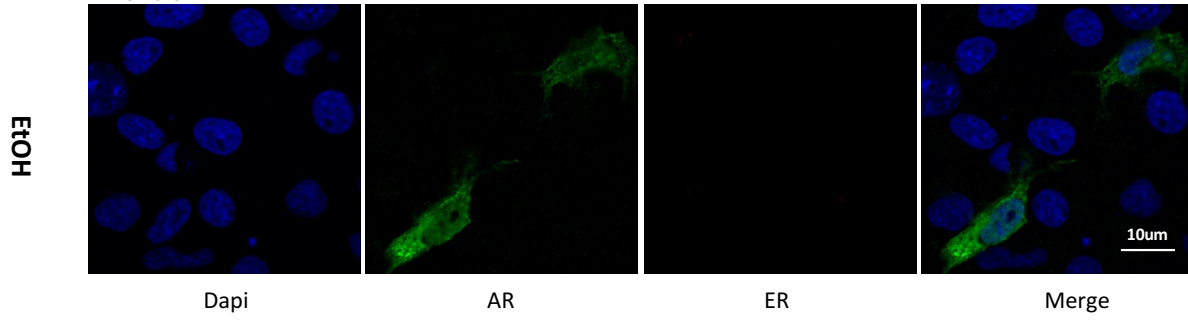


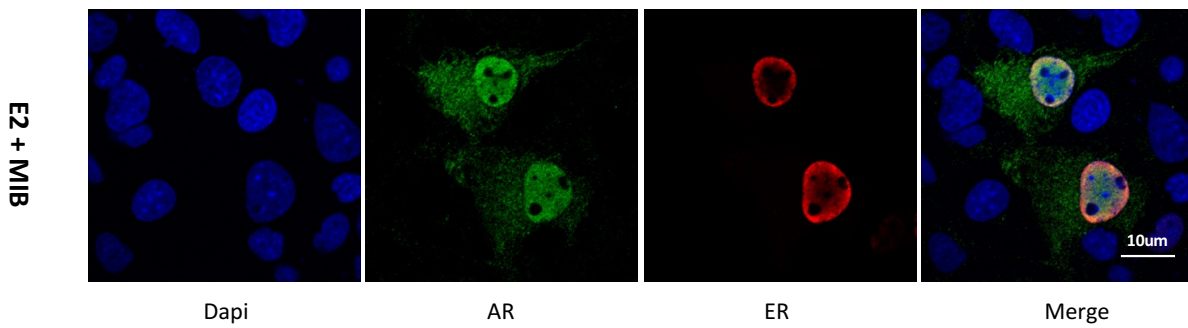
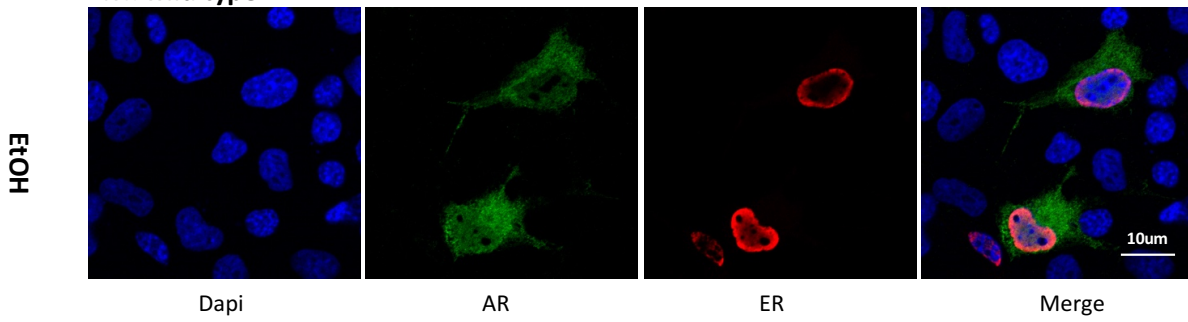
**Figure 3.8: AR/ ERα variants crosstalk measuring AR activity upon ligand binding.** (a) Schematic representation of the luciferase reporter assays. (b) COS-1 cell lines were transfected with expression plasmids for ERα and/or AR, a luciferase reporter (ERE-LUC or TAT-GRE-E1B-LUC) and a renilla expression vector. Cells were incubated for 24 hours then treated with EtOH: ethanol, E2: 17-β-oestradiol (1.0 nM) and/or MIB: mibolerone (1.0 nM). ANOVA system. \*\*\*\*p<0.00001, \*\*\*p<0.0001. Mean ± 1SE.



**Empty plasmid**



**ER $\alpha$  wild type**



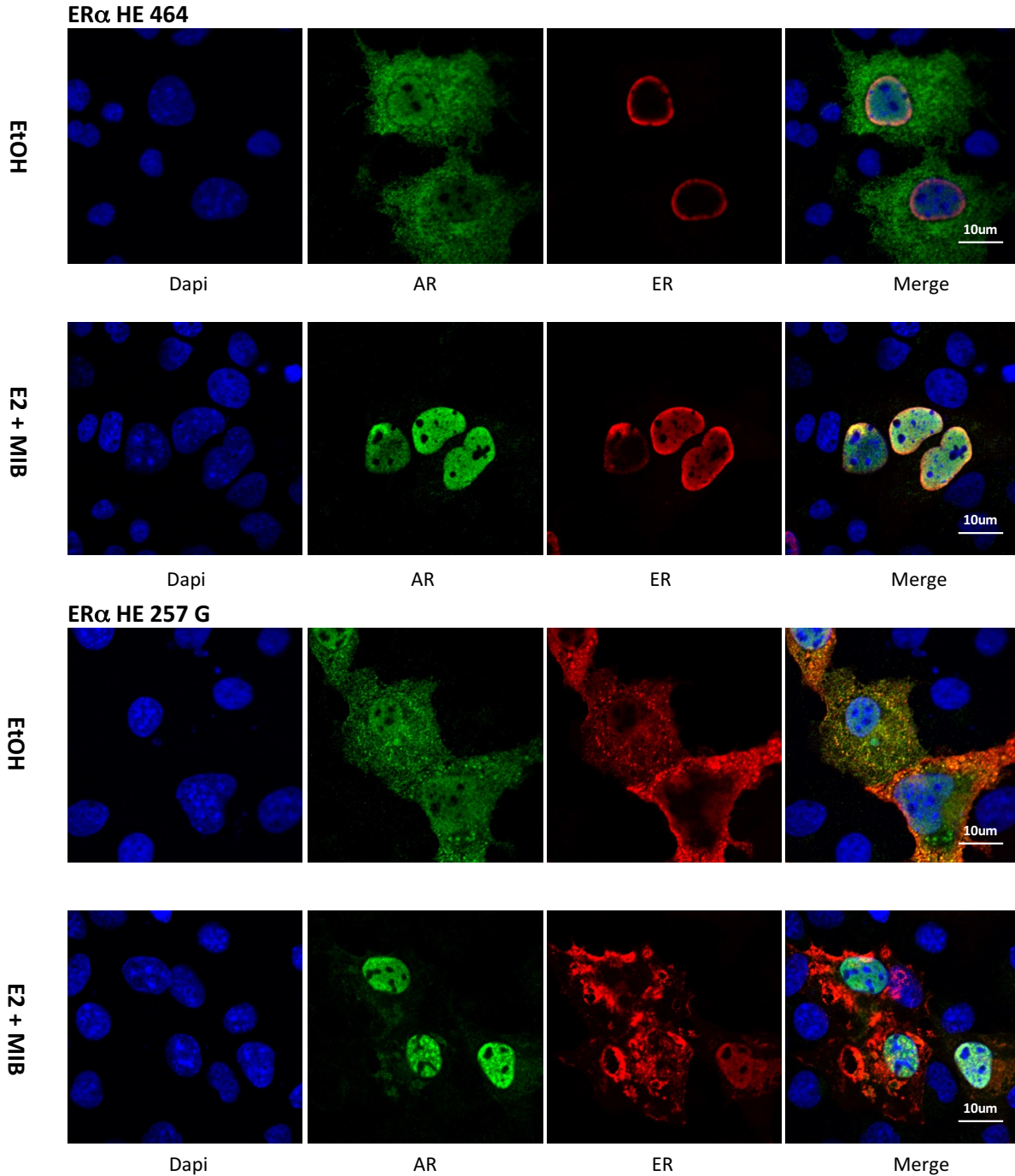


**Figure 3.9: ER $\alpha$  reduces AR nuclear translocation.** COS-1 cells were transfected with plasmids encoding pSV-AR-GFP , ER $\alpha$  wild type, ER $\alpha$  HE 464 and ER $\alpha$  HE 257G. Cells were fixed with 4 % paraformaldehyde and methanol following 2 hrs of treatment with EtOH (ethanol), E2 (17- $\beta$ -oestradiol) or MIB (mibolerone). Confocal microscopy was used to visualise the localisation of androgen receptor-GFP (green) and oestrogen receptors (immunofluorescent staining using ALEXA 594 (red)). Nuclear staining = 4',6-diamidino-2-phenylindole (DAPI) in blue.

**Table 3.2: AR and ER $\alpha$  variants cellular localisation upon androgen and oestradiol treatment.** Table illustrates if AR and ER $\alpha$  receptors were predominantly nuclear (N), cytoplasmic (C) or both (C + N) after 2 hrs treatment with the oestrogen E2: 17- $\beta$ -oestradiol and androgen MIB: mibolerone in COS-1 cell line.

<i>RECEPTOR</i>	<i>EtOH</i>	<i>E2</i>
<b>ER<math>\alpha</math> wild type</b>	C	N
<b>ER<math>\alpha</math> HE464</b>	N	N
<b>ER<math>\alpha</math> 257G</b>	C + N	C + N

### 3.2.5 Investigation of AR-ER $\alpha$ target genes

To investigate if AR/ER $\alpha$  cross-talk inhibits endogenous target gene expression, MCF-7 cells were grown to 70% confluence in hormone-depleted media prior to treatment with 1 nM of E2 and MIB and incubated for a further 24 hrs. After the RNA was harvested, qPCR was performed to investigate the altered expression of ER $\alpha$  target genes *Trefoil Factor 1 (TFF1)* and *Myelocytomatosis Oncogene Cellular Homolog (MYC)*, the AR target gene *N-myc Downstream-Regulated Gene 1 (NDRG1)*, and *Gene Regulated in Breast Cancer 1 (GREB1)* which is regulated by both receptors (Figure 3.10). The ER $\alpha$  target gene *TFF1* was found to be significantly increased in response to E2 and androgen had no effect upon this induction in expression. The other ER $\alpha$  target gene investigated, *MYC*, was not found to be significantly regulated by any of the treatments tested. The AR and ER $\alpha$  target gene, *GREB1*, was significantly regulated in response to E2 treatment only, whereas the AR target (*NDRG1*) was significantly decreased in response to this ligand. In contrast to the reporter assays, receptor cross-talk did not affect the genes investigated here.

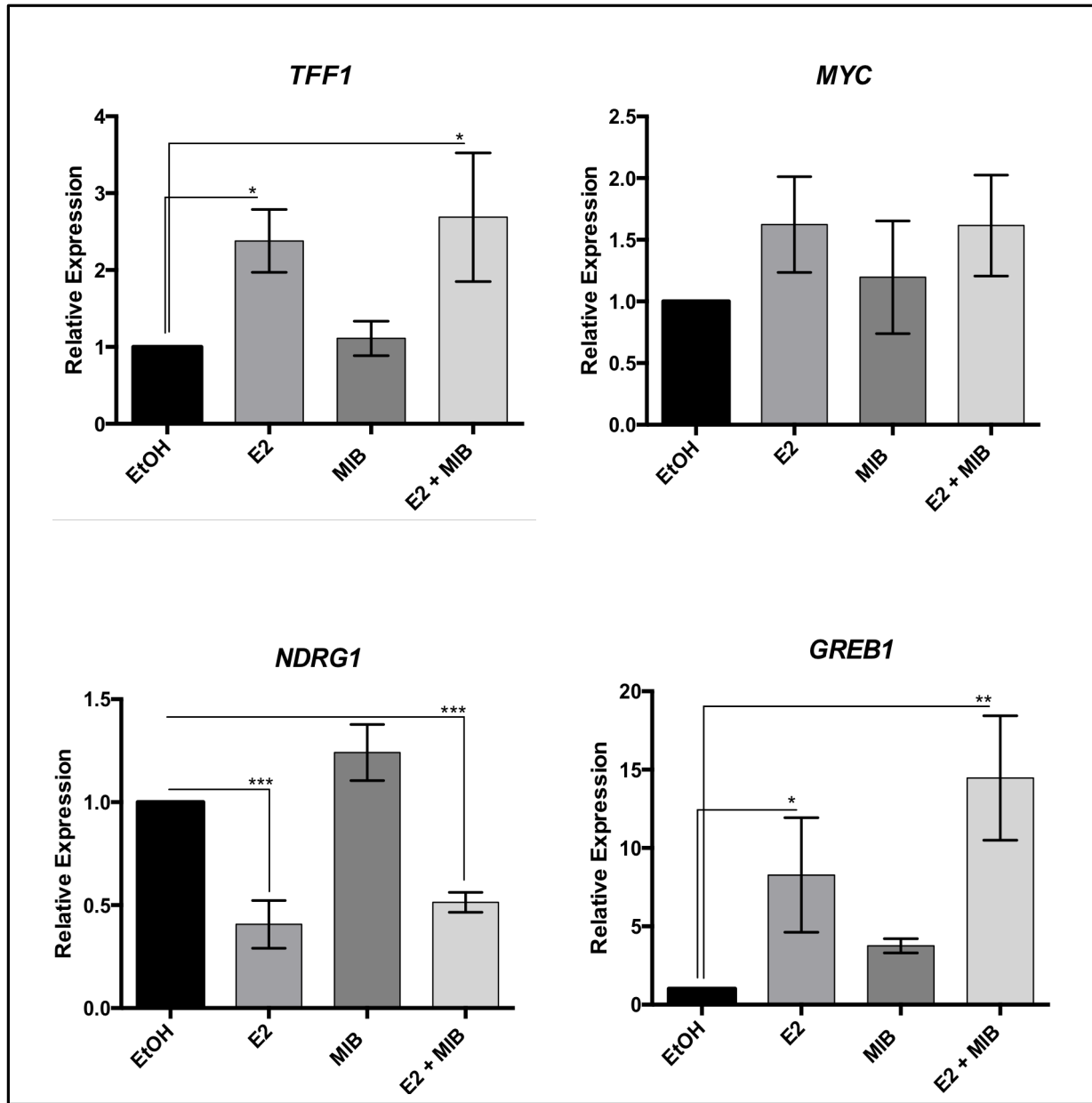


**Figure 3.10: Investigation of the effects of AR-ER $\alpha$  cross-talk on endogenous target genes.** MCF-7 cells were seeded for 24 hrs then treated with the ligands EtOH: ethanol, E2: 17- $\beta$ -oestradiol (1.0 nM) and MIB: mibolerone (1.0 nM) for further 24 hrs. Harvested RNA was reverse transcribed into cDNA and qPCR analysis performed using SYBR green to measure the expression levels of Oestrogen Receptor alpha (ER $\alpha$ ) and Androgen Receptor (AR) in the target genes *TFF1*, *MYC*, *NDRG1* and *GREB1*. ANOVA system. \*\*\*p<0.0001, \*\*p<0.001, \*p<0.01. Mean  $\pm$  1SE.

### **3.2.6 Investigation of target gene expression following siRNA depletion of AR and ER $\alpha$ .**

To further investigate receptor cross-talk, AR and ER $\alpha$  expression was reduced in the MCF-7 cell line using siRNA. qPCR was used to assess the expression of AR and ER $\alpha$  as well as genes known to be AR and/or ER $\alpha$  targets: *Myelocytomatosis Oncogene Cellular Homolog (MYC)*, Transmembrane serine protease 2 *TMPRSS2*, *Gene Regulated in Breast Cancer 1 (GREB1)* and *N-myc Downstream-Regulated Gene 1 (NDRG1)*. AR knock-down affected the ER $\alpha$  at the RNA level and at the protein expressions where 31.9 % reduction was witnessed. Similar trends were demonstrated in AR levels, as the ER $\alpha$  knock-down has reduced the AR RNA expression and protein levels with 62.1 % (Figure 3.11a and b).

*MYC* was found to be up-regulated in response of E2, knock-down of ER $\alpha$  reduced *MYC* expression (Figure 3.12a). Knock-down of AR had no significant effect upon *MYC* expression. *TMPRSS2* (AR target gene) was not found to be androgen-responsive in MCF-7 cells, however, knock-down of ER $\alpha$  resulted in a significant increase in gene expression, independent of treatment (Figure 3.12b). *GREB1* is weakly induced by androgen and more significantly by E2, the androgen induced expression was reversed following knock-down of AR and ER $\alpha$ . The knock-down of AR did not affect the E2-induced expression of *GREB1*, but knock-down of ER $\alpha$  completely inhibited the induction of gene expression (Figure 3.12c). Finally, the AR target gene *NDRG1* was not found to be regulated by the AR or ER $\alpha$  (Figure 3.12d). In summary, the reporter assays demonstrated that AR and ER $\alpha$  cross-talk inhibit each others activity, However, these effects were not replicated when endogenous genes were analysed in MCF-7 cells.

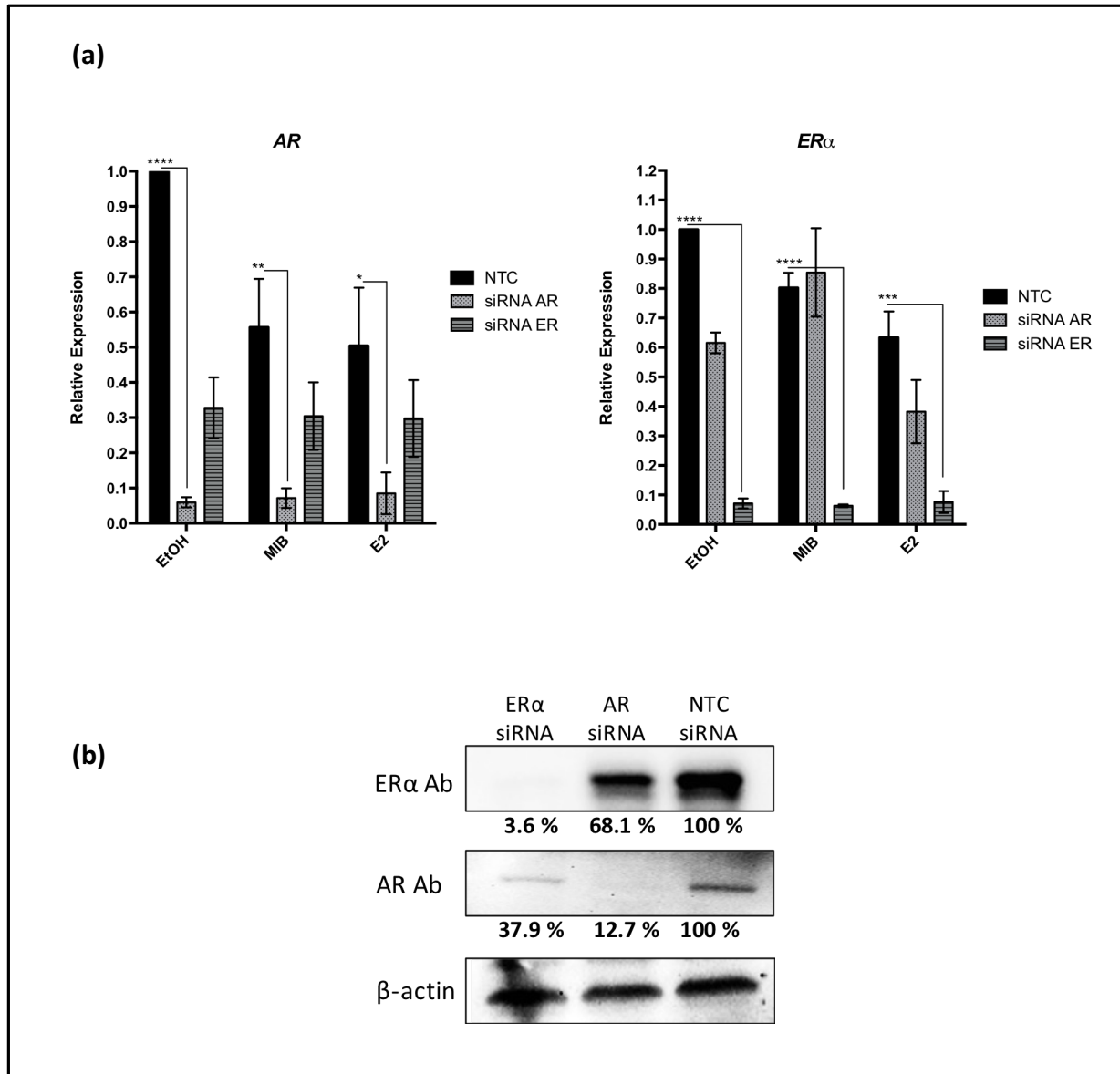


**Figure 3.11: AR and ER $\alpha$  knock-down in MCF-7 cell line.** siRNA transfection in MCF-7 cells was performed for 72 hrs to deplete Androgen Receptor (AR) and Oestrogen Receptor alpha (ER $\alpha$ ) levels alongside Non-Targeting (NTC) siRNA control. **(a)** After transfection, cells were treated with EtOH: ethanol, 1.0 nM E2 (17- $\beta$ -oestradiol or MIB (mibolerone) for 24 hrs. Harvested RNA was reverse transcribed into cDNA and qPCR analysis performed using SYBR green to measure the expression levels of the *AR* and *ER $\alpha$*  genes. **(b)** Immunoblotting analysis to investigate the expression levels of the receptors at the protein level. ANOVA. \*\*\*\* $p < 0.00001$ , \*\*\* $p < 0.0001$ , \*\* $p < 0.001$ , \* $p < 0.01$ . Mean  $\pm$  1SE.

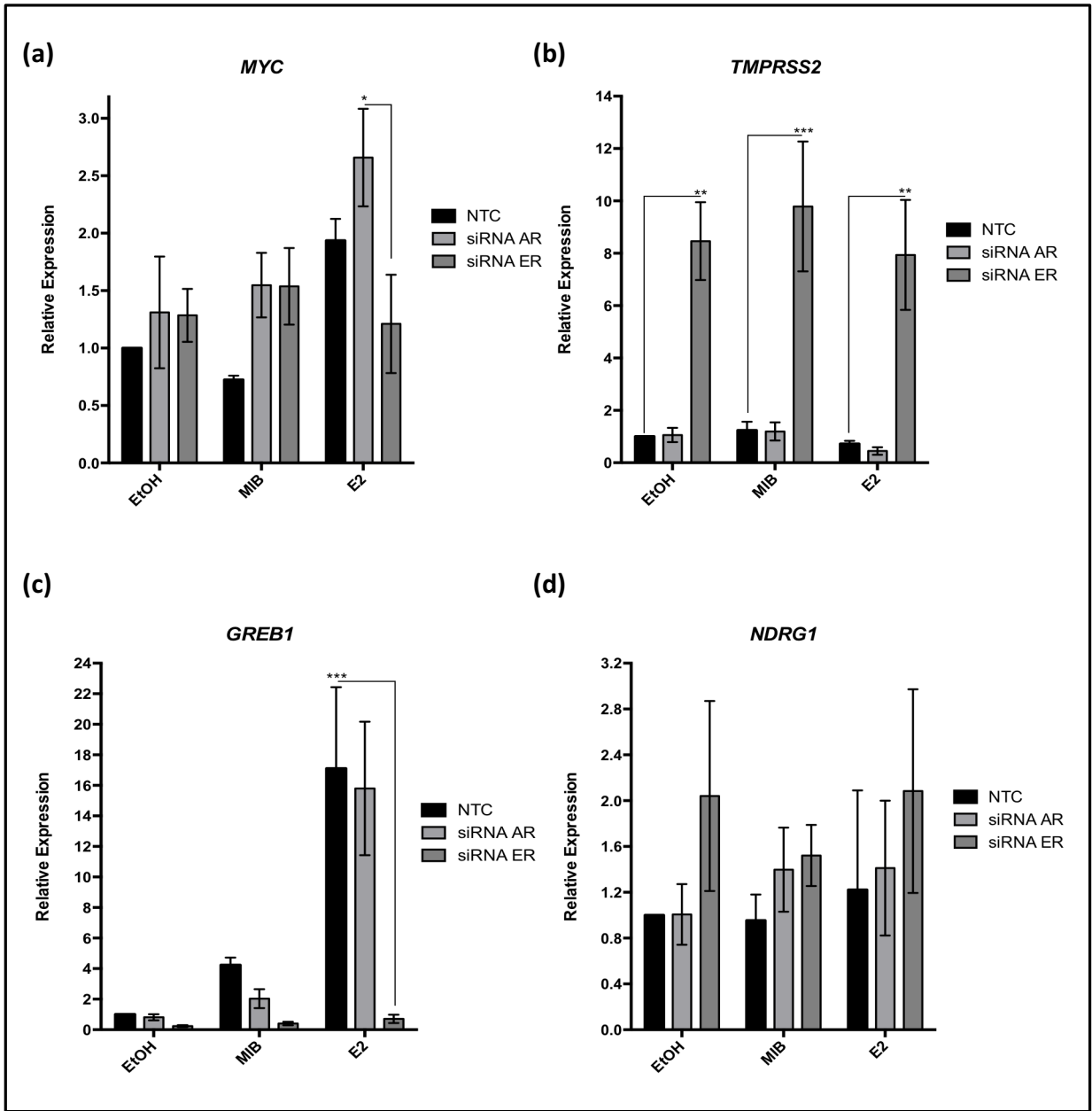


**Figure 3.12: Relative expressions of AR and ER $\alpha$  target genes upon receptors knock-down in MCF-7 cell line.** siRNA transfection in MCF-7 cells was performed for 72 hrs to deplete Androgen Receptor (AR) and Oestrogen Receptor alpha (ER $\alpha$ ) levels alongside Non-Targeting (NT) siRNA control. **(a,b,c and d)** After transfection, cells were treated with EtOH: ethanol, 1.0 nM E2 (17- $\beta$ -oestradiol or MIB (mibolerone) for 24 hrs. Harvested RNA was reverse transcribed into cDNA and qPCR analysis performed using SYBR green to measure the expression levels of the *MYC*, *TMPRSS2*, *GREB* and *NDRG1* genes. Values blotted using ANOVA system. \*\*\*p<0.0001, \*\*p<0.001. Mean  $\pm$  1SE.



### 3.3 Androgen Receptor (AR) Variants in Breast Cancer

#### 3.3.1 Identification of AR mutations in BCa

As previously mentioned, the AR has been found to be highly expressed in breast tissue and appears to be a tumour suppressor in the ER $\alpha$ -positive disease and an oncogene in ER $\alpha$ -negative BCa (Hickey *et al.*, 2012). As a result of selective pressure, therapy resistant BCa tumours can develop mutations in their driver receptors, which subsequently affects proliferation rate and therapeutic response (Alluri *et al.*, 2014). To investigate if AR mutations exist in BCa, the COSMIC cancer mutation database was interrogated and 10 mutations were identified: C290Y, E355K, S568F, L638M, S663\*, Q739\*, D840N, D865E, Q868H and L881Q (Figure 3.13a). BCa patients who had the mutations, S663\*, Q739\* and L881Q, were found to express ER $\alpha$ -positive and PR-positive receptors in their tumours. For patients with L638M and D865E mutations, their tumours have not expressed these two receptors. Further, clinical details for mutations C290Y, E355K, S568F, D840N and Q868H were not available in regard to expressed receptors (Table 3.3).

To investigate the localization of these mutations further, the crystal structures of the AR DBD and LBD were obtained from the Protein Data Bank (Figure 3.13b). The LBD is a pocket formed from 12  $\alpha$ -helices which form a pocket into which the ligand DHT (dihydrotestosterone) fits. Ligand binding promotes the re-localisation of helix 12, creating 2 important protein-protein interaction sites: the co-activator groove and the BF3 region (Estebanez-Perpina *et al.*, 2007 and Brooke *et al.*, 2015). The S568F mutation was found to be on the DBD located on one of the  $\beta$ -sheets, while the mutations D840N, D865E, Q868H and L881Q are located on different helices that form the LBD (Figure 3.13b).

To analyse the effect of these mutations upon AR activity, the substitutions were inserted into the pSVA-AR plasmid using site directed mutagenesis. Plasmids were subsequently sent for sequencing to confirm the successful insertion of the mutant base pair (Figure 3.14).

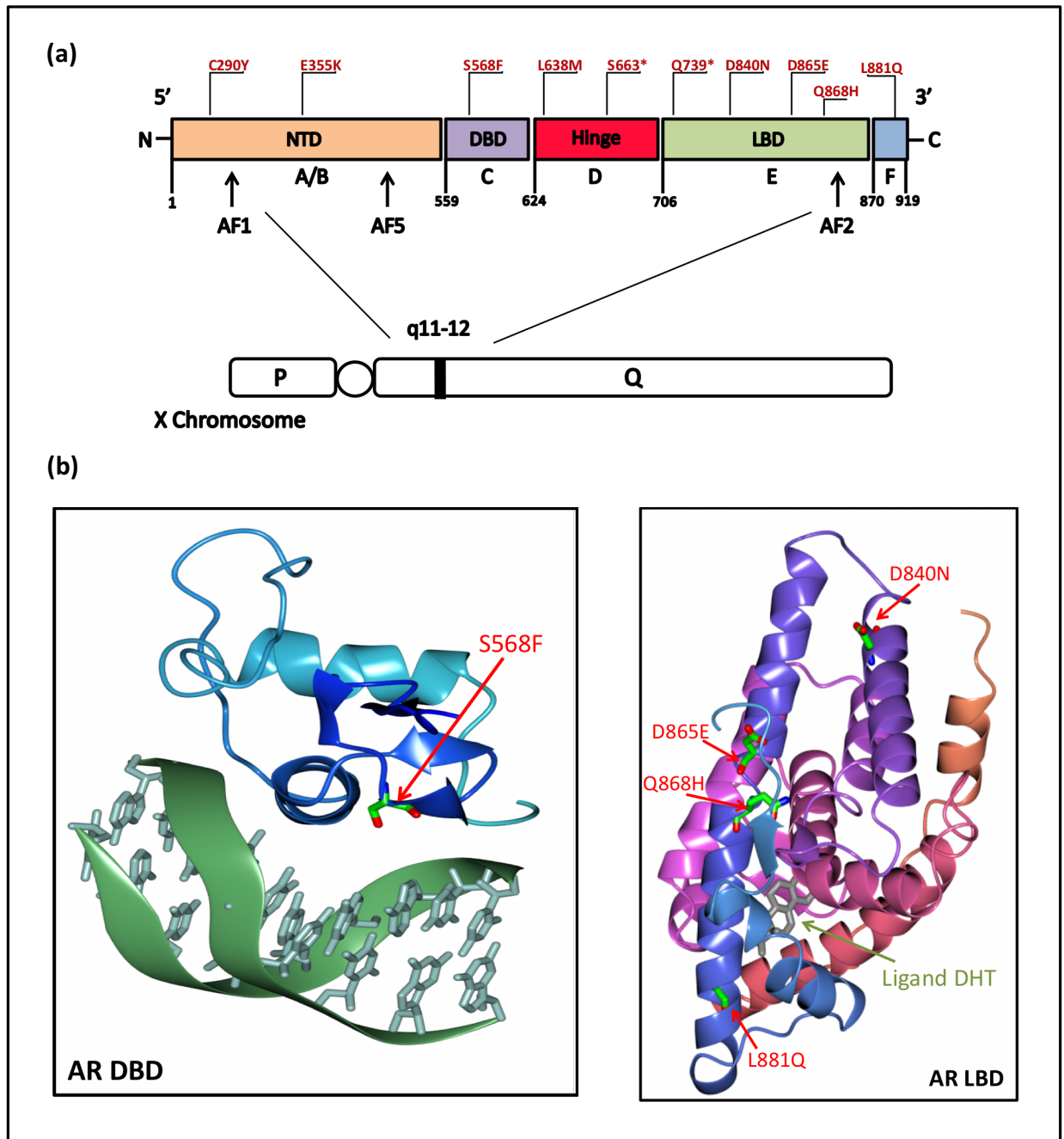


**Figure 3.13: Locations of AR mutations identified in Breast Cancer.** (a) Image shows mutations identified in breast cancer, indicated in red, and their locations on the four functional domains of the AR and the gene structure indicated in chromosome X q11-12. NTD = N- terminal domain, DBD = DNA binding domain, LBD = ligand binding domain and AF = activation function. A-F indicates the different location of the 6 functional domains with amino acids residues numbered. (b) Crystal structures of AR DBD and LBD regions highlighting exact location of mutants ARs in BCa (red) and L-DHT (green). AR structures (PDB:10275) were obtained from PyMOL software ([www.pymol.org](http://www.pymol.org)). AR mutations in BCa were identified in the COSMIC database. (<https://cancer.sanger.ac.uk/cosmic>)

**Table 3.3: AR mutants found in BCa and their expressed receptors.** Mutations were obtained from the COSMIC database.

<i>AR Mutant</i>	<i>ER<math>\alpha</math></i>	<i>PR</i>
<b>C290Y</b>	N/A	N/A
<b>E355K</b>	N/A	N/A
<b>S568F</b>	N/A	N/A
<b>L638M</b>	Negative	Negative
<b>S663*</b>	Positive	Positive
<b>Q739*</b>	Positive	Positive
<b>D840N</b>	N/A	N/A
<b>D865E</b>	Negative	Negative
<b>Q868H</b>	N/A	N/A
<b>L881Q</b>	Positive	Positive

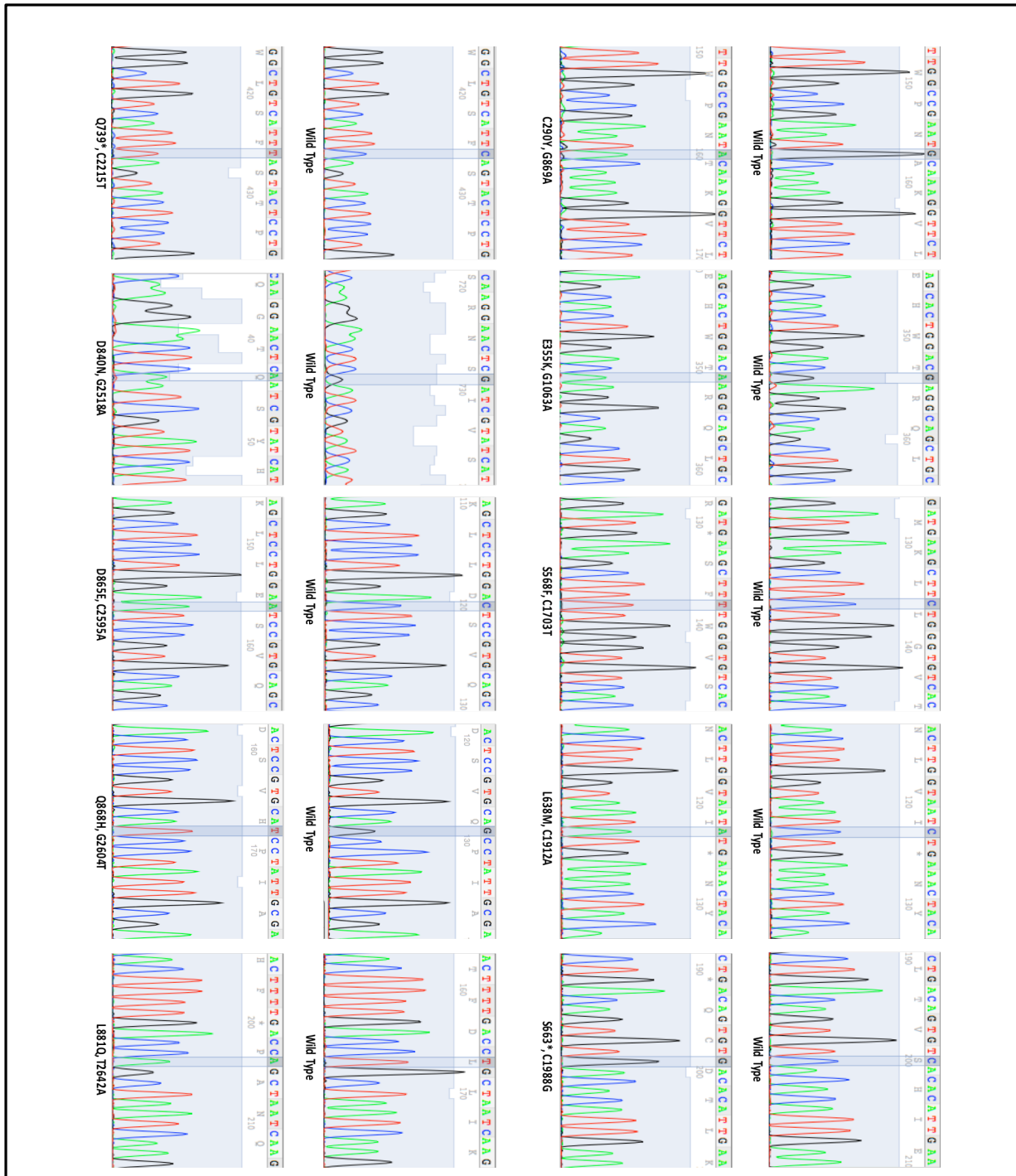


**Figure 3.14: Chromatograms of the wild-type and mutant ARsa.** Chromatograms show the AR mutants: C290Y, E355K, S568F, L638M, S663\*, Q739\*, D840N, D865E, Q868H and L881Q. Changes in single base pair that results in the desired amino acid changes are highlighted. Chromatograms generated using 4Peaks (V1.7.1).

To investigate the protein expression levels of the AR wild-type and mutant receptors, immunoblotting analysis was performed (Figure 3.15). The majority of the mutants had similar expression to wild-type AR except for the mutants L881Q, Q739\* and S663\* which have higher expression levels compared to the wild-type. Also, the truncation mutants were confirmed to be smaller than the wild-type receptor: AR= 110 kDa, S663\*= 79 kDa and Q739\*= 88 kDa.

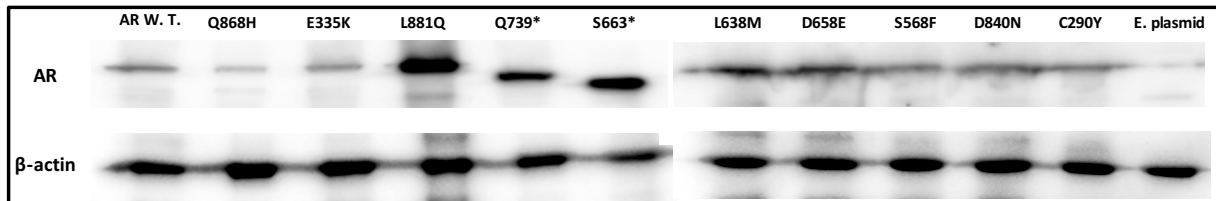


**Figure 3.15: The mutant ARs are successfully expressed in COS-1 cell line.** Immunoblotting analysis of COS-1 cells transfected with AR mutants (C290Y, E355K, S568F, L638M, S663\*, Q739\*, D840N, D865E, Q868H and L881Q), wild type AR and Empty plasmid (E. plasmid).

### **3.3.2 Some of the mutant ARs are constitutively active**

To assess the transcriptional activity of the cloned ARs, plasmids encoding the wild-type and mutant ARs were transfected into COS-1, along with the androgen responsive TAT-LUC reporter plasmid and Renilla expression vector. After 24 hrs cells were treated with different concentrations of MIB (0.0 nM, 0.01 nM and 1.0 nM) (Figure 3.16b). The truncated mutants (S663\* and Q739\*) were active in the presence and absence of androgen treatment. The S663\* mutant was found to have significantly higher activity than wild-type receptor in the absence of ligand and at 0.1 nM MIB, and had similar activity to the wild-type receptor in the presence of 1 nM MIB. In the presence of 1 nM Mibolerone there was no significant difference in the activity of wild-type and mutant receptors, with the exception of D865E which appears to be transcriptionally inactive.

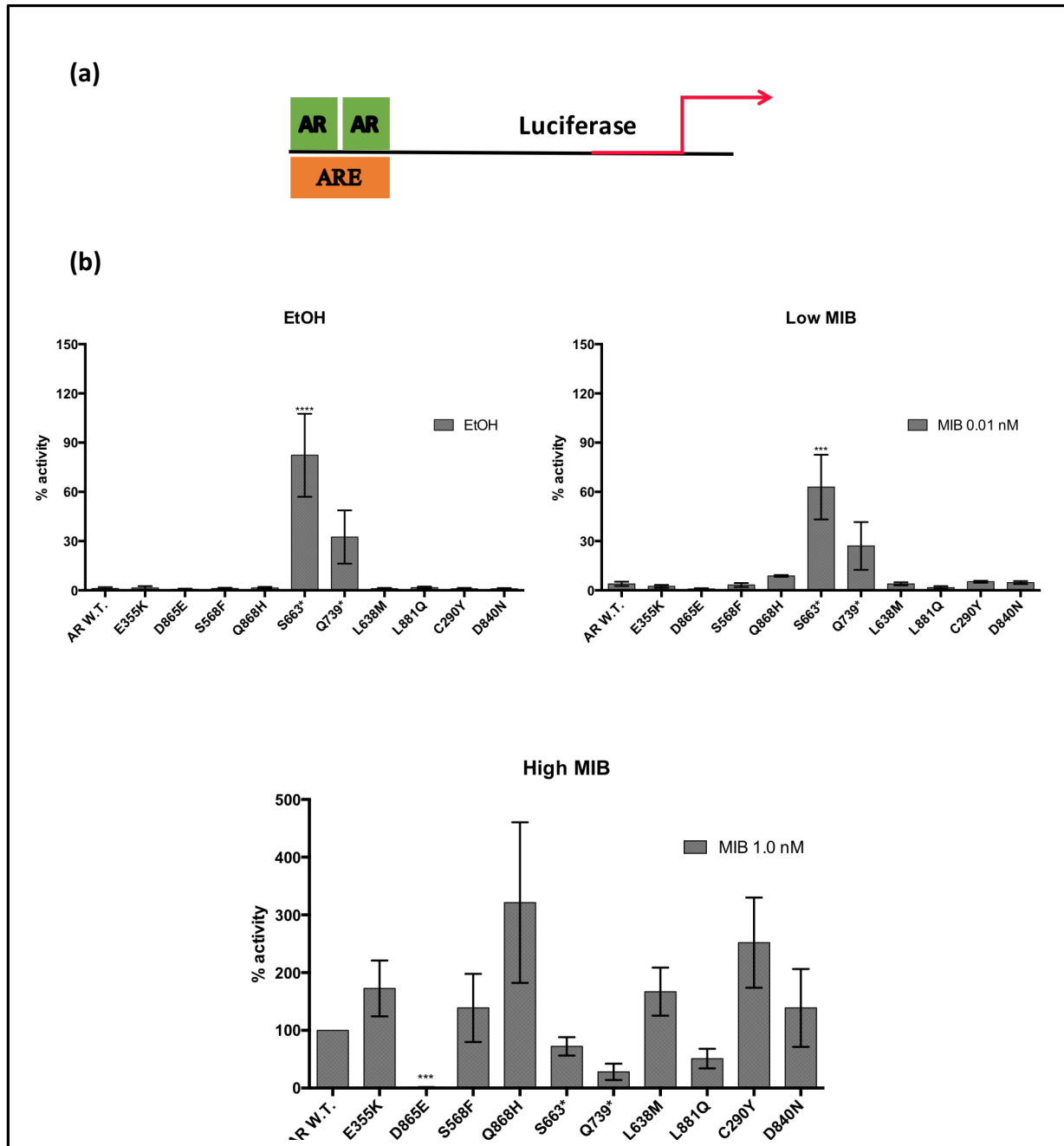
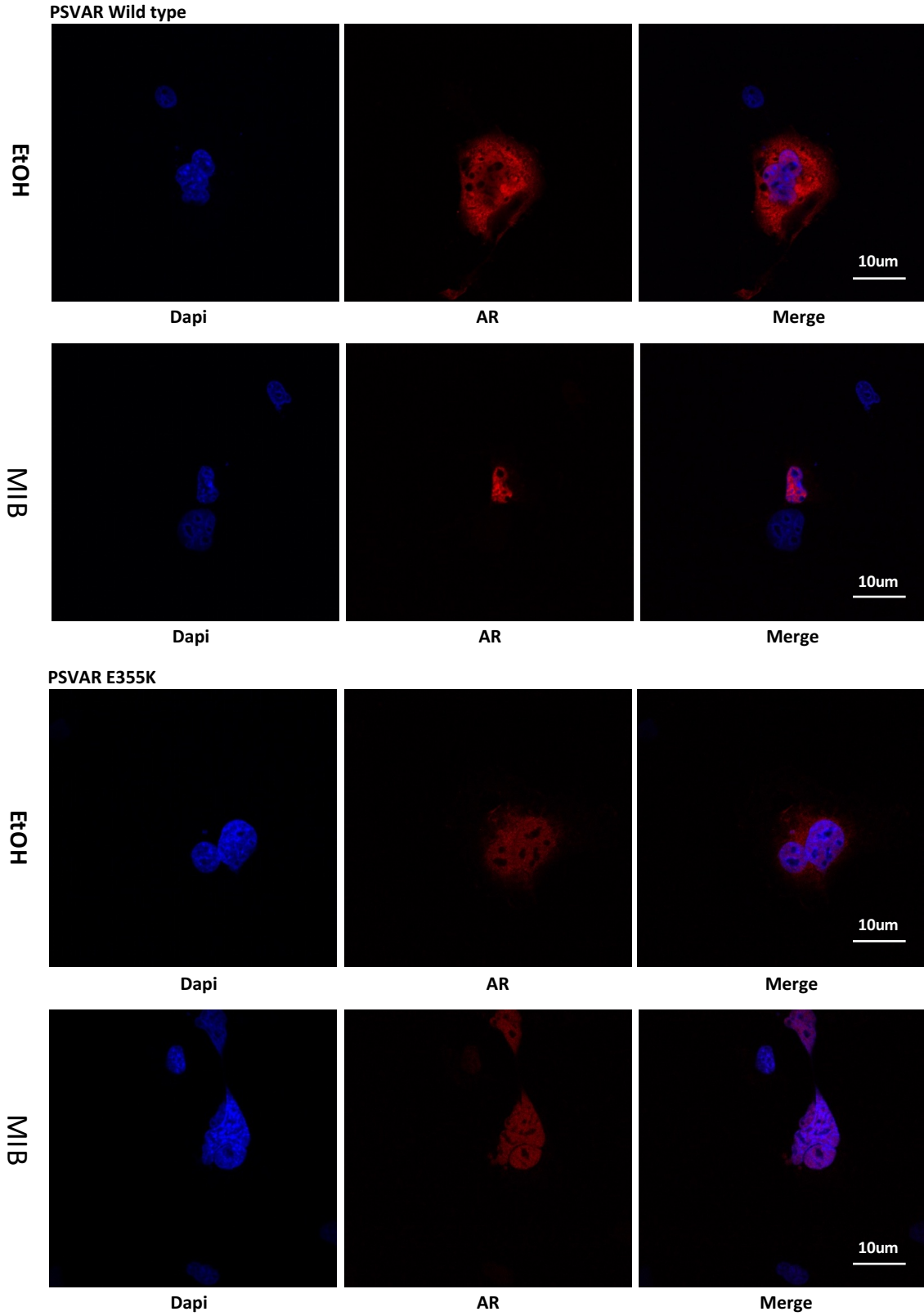


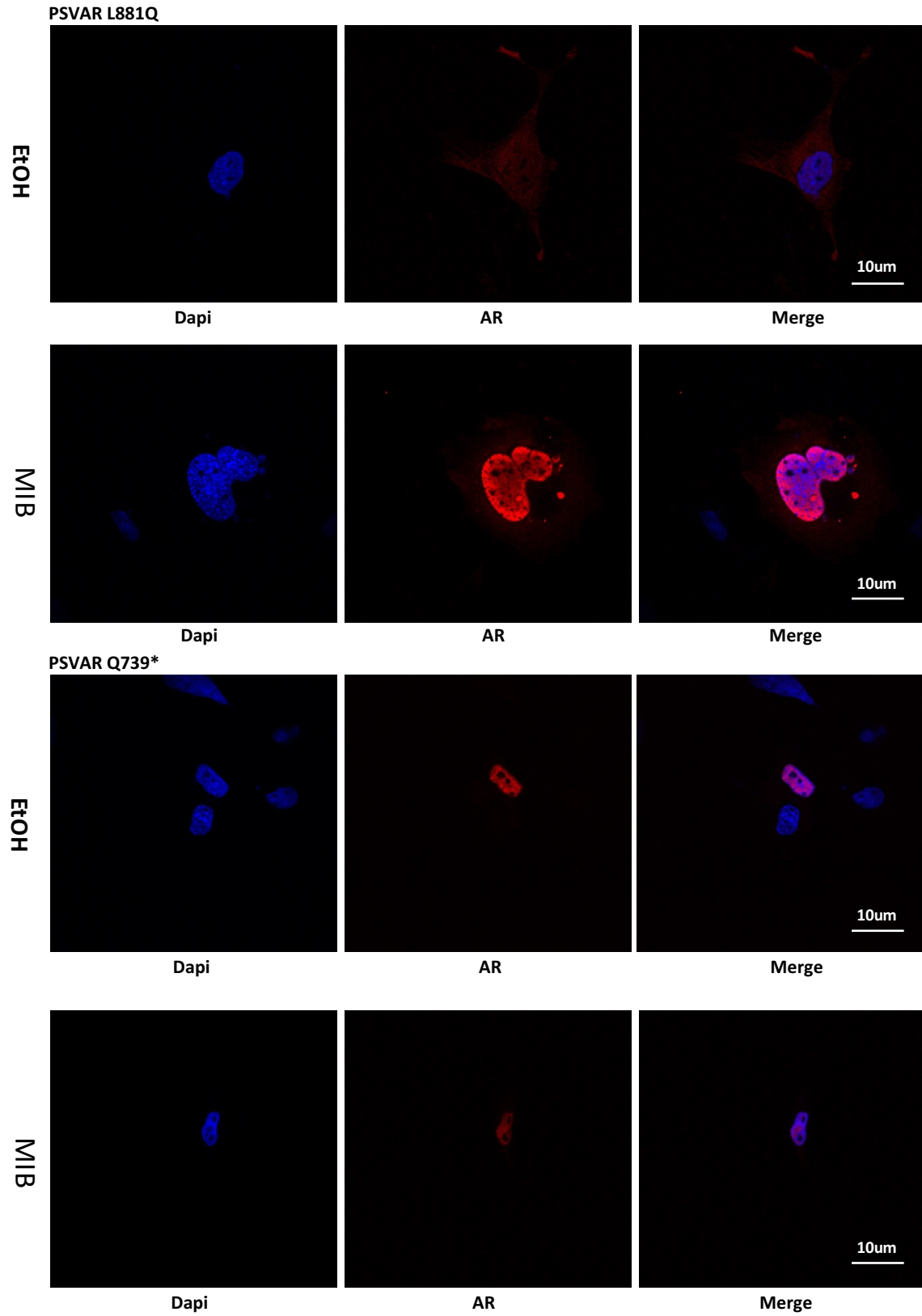
**Figure 3.16: Transcriptional activity of the mutant ARs.** (a) Schematics representation of the reporter assay. (b) COS-1 cells were transfected empty plasmid, pSV-AR wild-type or mutants (C290Y, E355K, S568F, L638M, S663\*, Q739\*, D840N, D865E, Q868H and L881Q), TAT-GRE-E1B-LUC reporter and a renilla expression vector. Cells were treated with EtOH (ethanol) or MIB (miboleron) (0.01 nM or 1.0 nM) to evaluate receptor activity. ANOVA. \*\*\*\* $p < 0.00001$ , \*\*\* $p < 0.0001$ . Mean  $\pm$  1 SE.

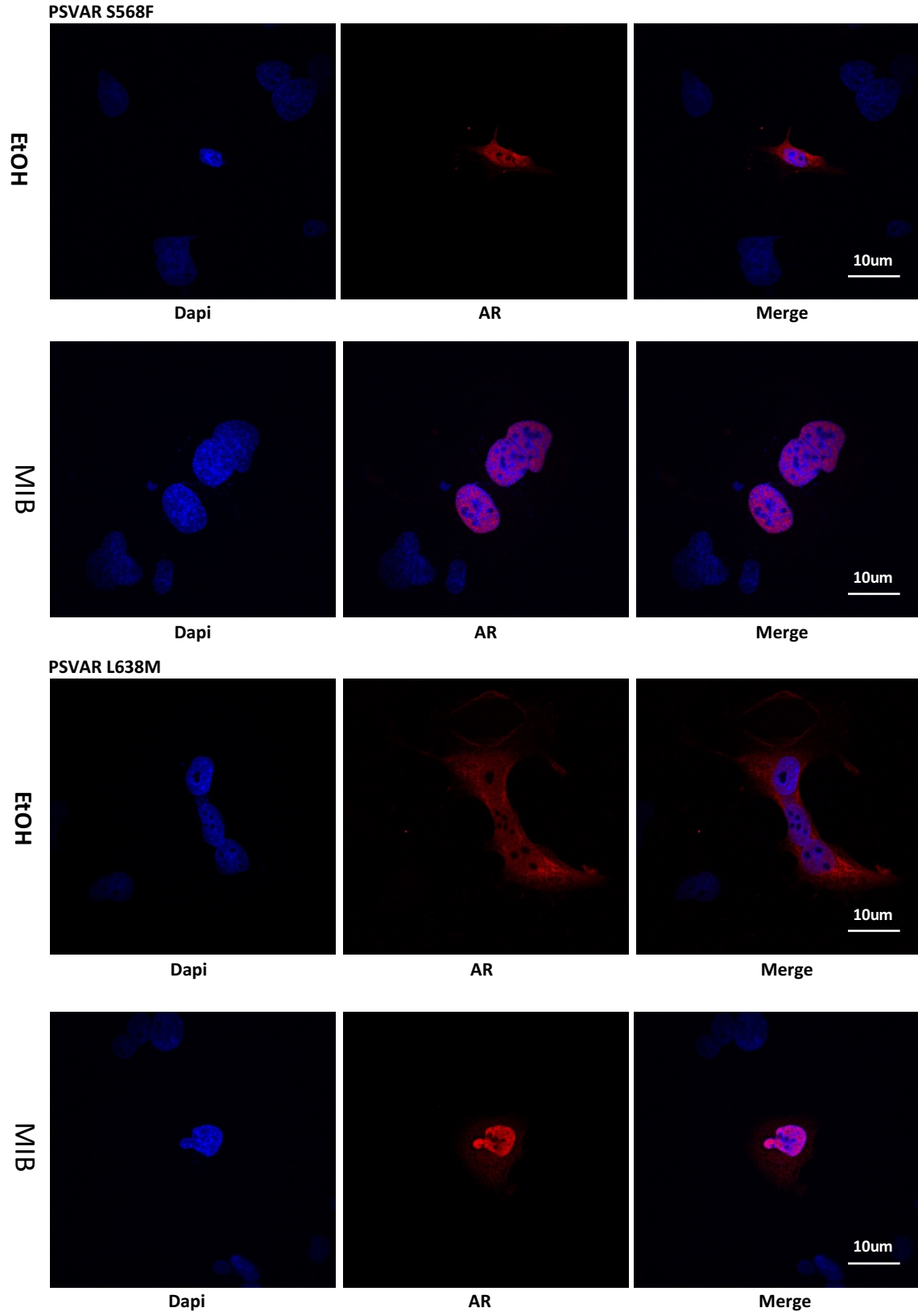


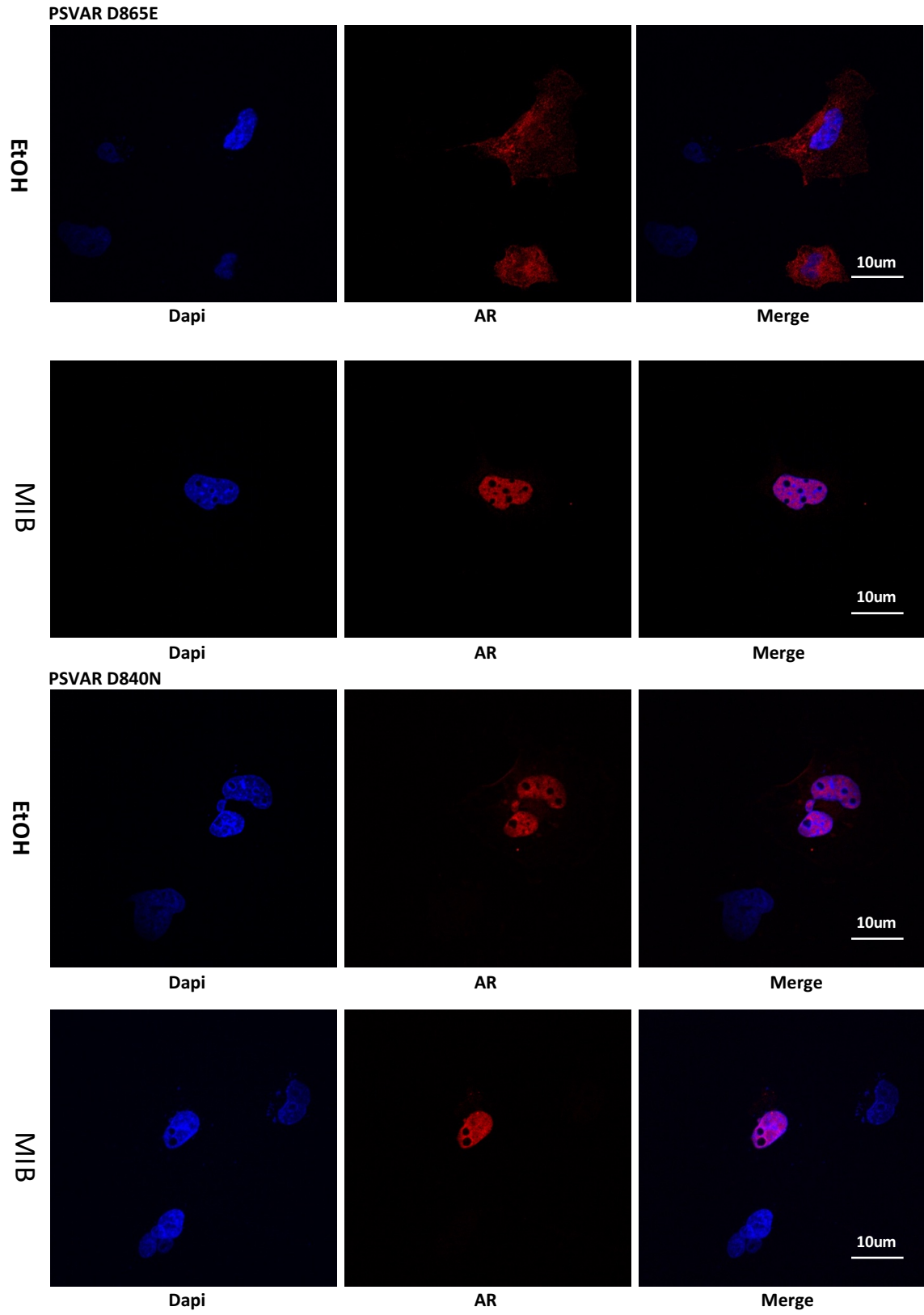
### 3.3.3 Investigation of the cellular localisation of AR mutants identified in BCa

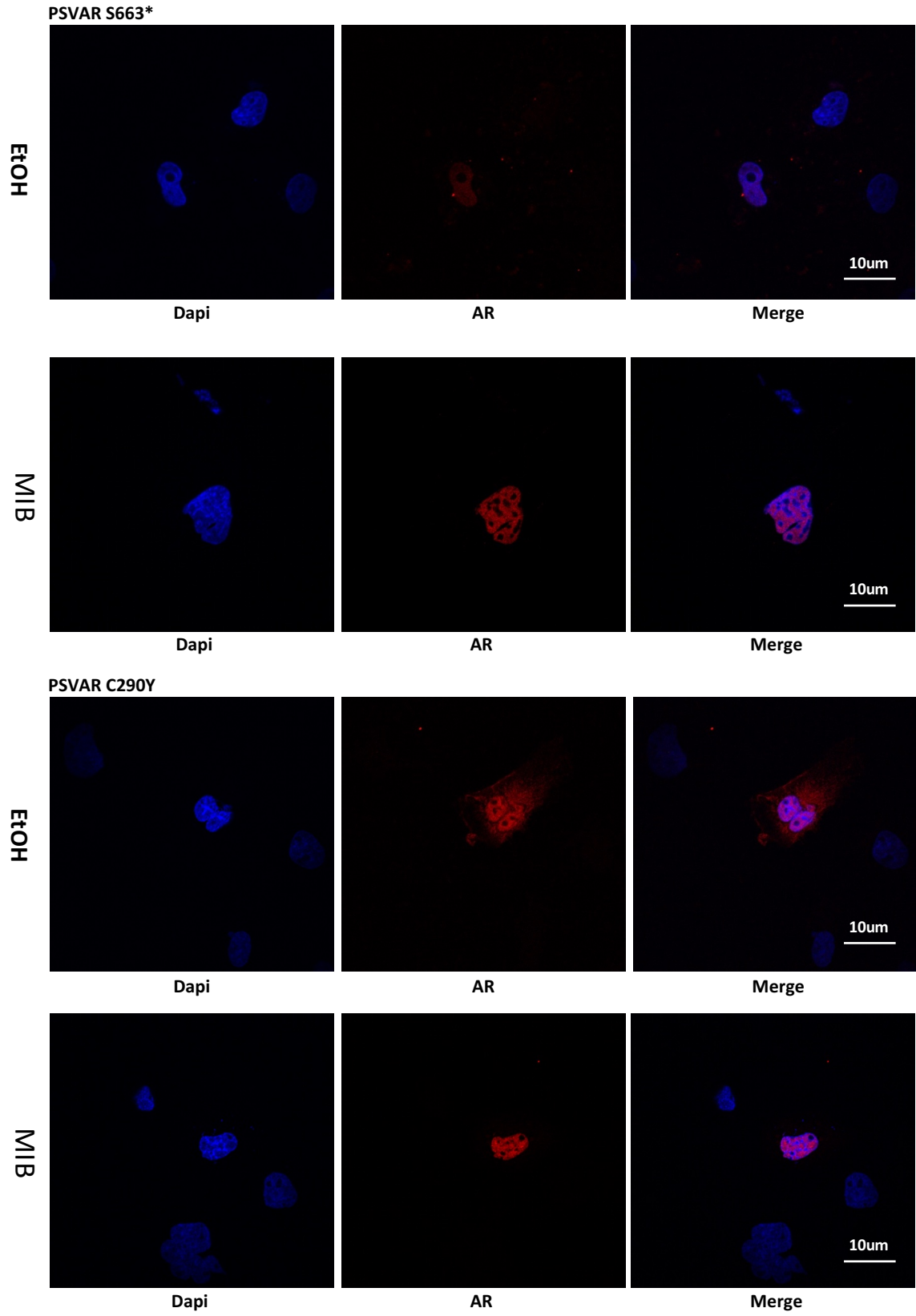
In the absence of androgen, the AR is localised in the cytoplasm and held in an inactive state, however, upon ligand binding the receptor translocates to the nucleus then binds to the DNA to initiate transcription of target genes (Lehmann-Che *et al.*, 2013). To investigate the localisation of the wild-type and mutant receptors, confocal microscopy was performed. COS-1 cells were plated at 30% confluence on cover slips in 24 well plates. Cells were transfected with plasmids encoding pSV-AR and the AR mutants (C290Y, E355K, S568F, L638M, S663\*, Q739\*, D840N, D865F, Q868H and L881Q) using FuGENE HD (Promega) and incubated for 24 hrs before treatment with the ligand MIB for 2 hrs. As expected, in the absence of androgen the wild-type AR is predominantly localized in the cytoplasm and androgen treatment promotes AR nuclear translocation (Figure 3.17). Mutants C290Y, E355K, S568F, L638M, D840N, D865E, Q868H showed similar localisation as wild-type AR with and without androgen treatment. Interestingly, the mutants S663\* and Q739\* were constitutively nuclear in the presence and absence of androgen treatment (Figure 3.17 and Table 3.4).













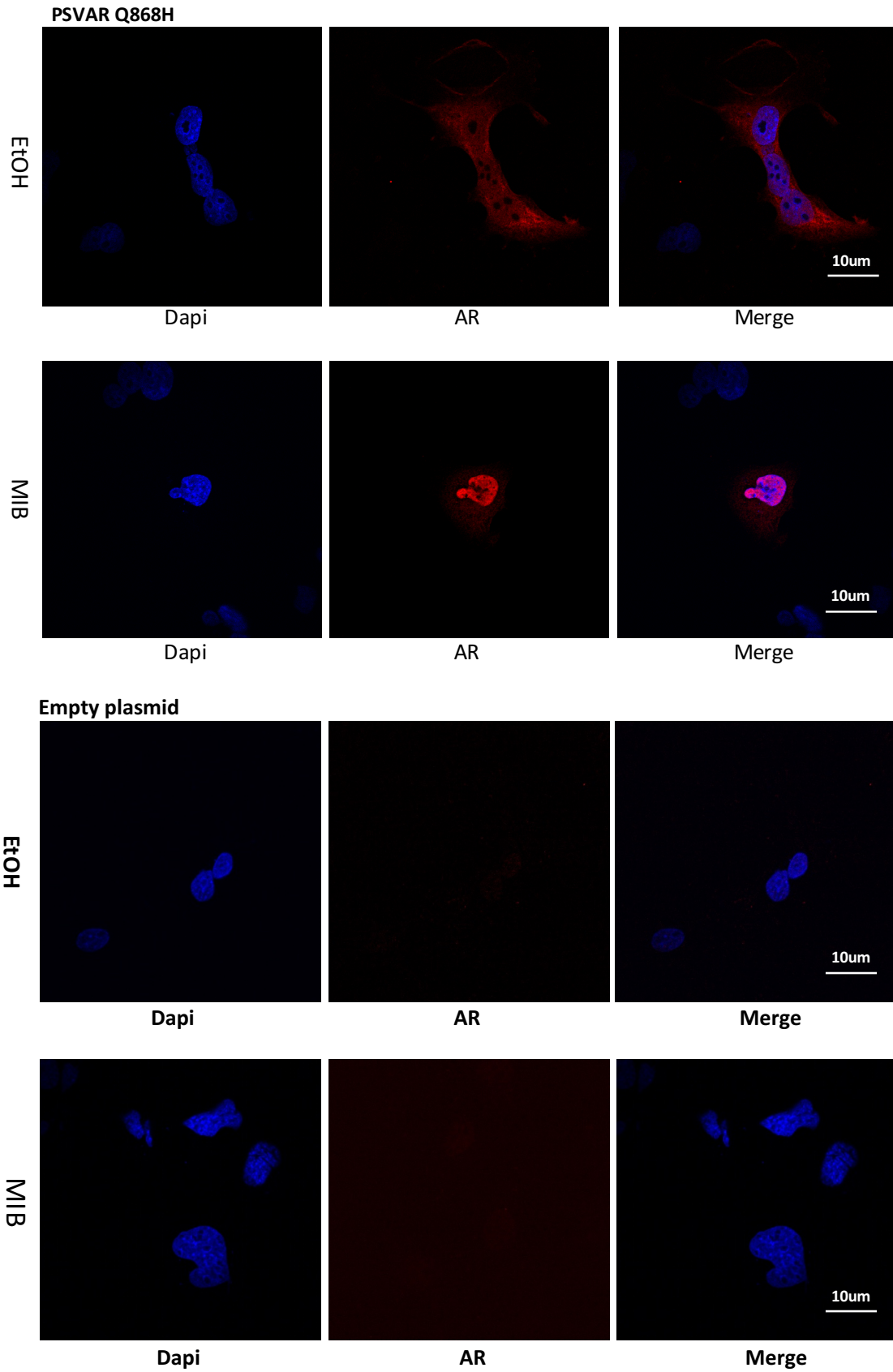


**Figure 3.17: The cellular localisation of wild-type and mutant AR in response to androgen.** COS-1 cells were transfected with plasmids encoding wild-type and mutant AR (C290Y, E355K, S568F, L638M, S663\*, Q739\*, D840N, D865E, Q868H and L881Q). Cells were fixed with 4 % paraformaldehyde and methanol following 2 hrs of treatment with EtOH (ethanol) and MIB (mibolerone). Confocal microscopy was used to visualise the localisation of the ARs (stained using ALEXA 594 (red)). Nuclear staining = 4',6-diamidino-2-phenylindole (DAPI) in blue.

**Table 3.4: AR variants cellular localisation upon androgen treatment.** Table illustrates if ARs were predominantly nuclear (N), cytoplasmic (C) or both (C + N) after 2 hrs treatment with the androgen MIB: mibolerone in COS-1 cell line.

<i>AR Mutant</i>	<i>EtOH</i>	<i>MIB</i>
<b>C290Y</b>	C + N	N
<b>E355K</b>	C + N	N
<b>S568F</b>	C	N
<b>L638M</b>	C	N
<b>S663*</b>	N	N
<b>Q739*</b>	N	N
<b>D840N</b>	N	N
<b>D865E</b>	C	N
<b>Q868H</b>	C	N
<b>L881Q</b>	C	N



### 3.3.4 AR mutants are not activated by alternative hormones or anti-oestrogens

Multiple papers have demonstrated that mutations in the AR reduce receptor's ligand specificity, allowing the receptor to be activated by different hormones and anti-androgens (Eisermann *et al.*, 2013). To investigate if the mutant receptors are activated by alternative physiologically relevant ligands, the transcription assays were repeated in the presence of 17- $\beta$ -oestradiol (E2) and progesterone (P4) hormones. COS-1 cells were transfected for plasmids encoding the wild-type and mutant ARs, the androgen responsive TAT-GRE-E1B-LUC reporter and a renilla expression vector. After 24 hrs, cells were treated with 1.0 nM E2 or 1.0 nM P4 (progesterone) for 24 hrs (Figure 3.18a). Again, the truncated mutants were found to have constitutive activity. The wild-type and mutant receptors were insensitive to E2 and P4. To expand this experiment, the activity of the mutant receptors was investigated in response to the anti-oestrogens Tamoxifen (Tam) and Fulvestrant (Fulv), anti-oestrogens used in the treatment of ER $\alpha$  positive BCa. COS-1 cells were transfected as above and treated with 1.0 nM Tam (tamoxifen) or Fulv (fulvestrant) for further 24 hrs (Figure 3.18b). The truncation mutants were found to have constitutive activity but the anti-oestrogens, E2 and P4 failed to activate any of the receptors. Therefore, the investigation of non-androgenic ligands demonstrates that the AR mutations identified in BCa remain ligand specific.

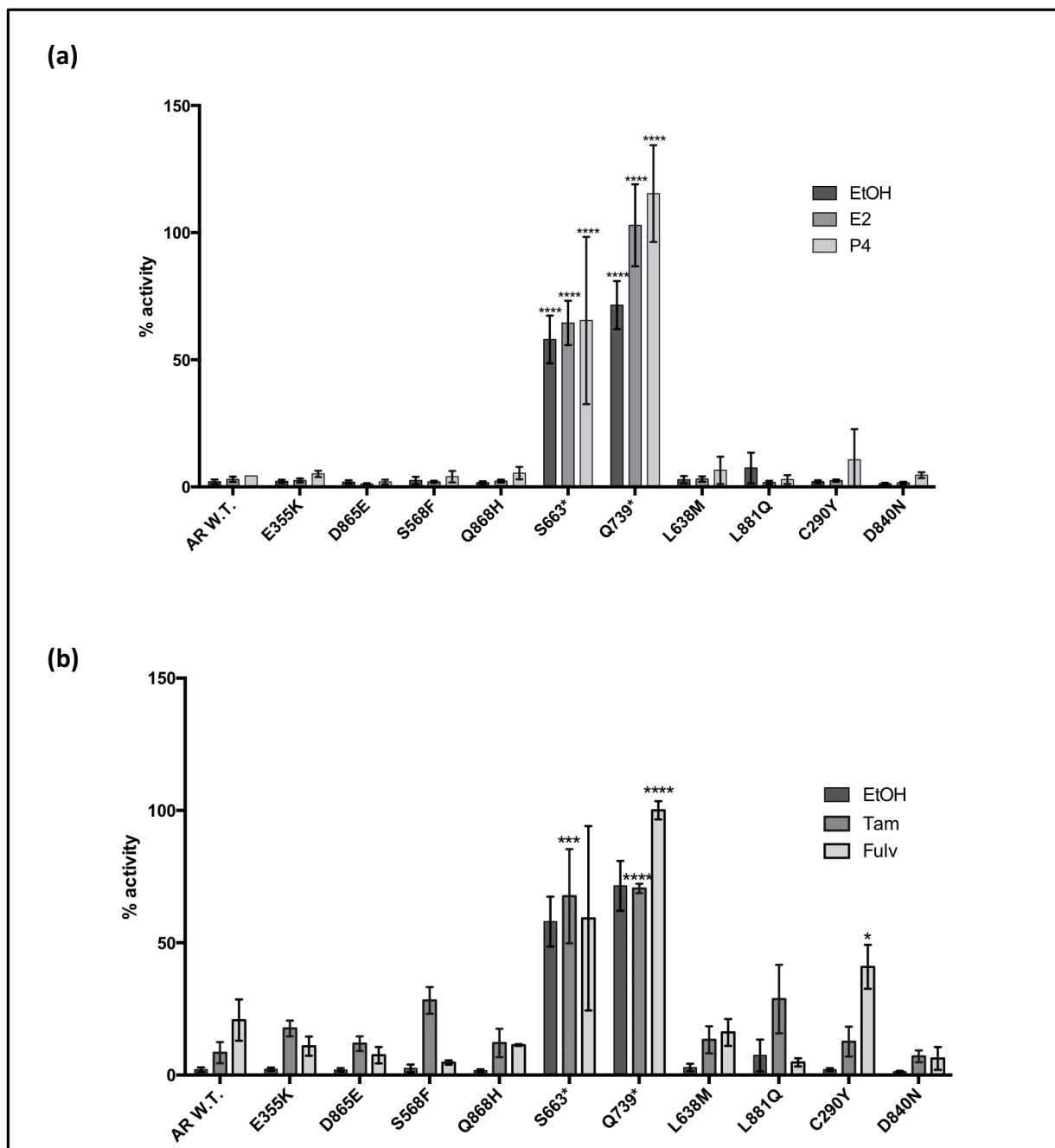


**Figure 3.18: AR variant activity in response to different ligands.** COS-1 cells were transfected with expression plasmid for AR wild-type and mutants (C290Y, E355K, S568F, L638M, S663\*, Q739\*, D840N, D865E, Q868H and L881Q), a luciferase reporter (TAT-GRE-E1B-LUC) and a renilla expression vector. **(a)** Cells were treated with EtOH (ethanol), E2 (17- $\beta$ -oestradiol) (1.0 nM) and P4 (progesterone) (1.0 nM) to evaluate receptor activity. **(b)** Cells were treated with EtOH (ethanol), Tam (tamoxifen) (1.0 nM) and Fulv (fulvestrant) (1.0 nM) to evaluate receptor activity. ANOVA system. \*\*\*\* $p < 0.00001$ , \*\*\* $p < 0.0001$ . Mean  $\pm$  1SE.

### 3.3.5 AR/ ER $\alpha$ cross-talk with AR mutants

To assess if mutations of the AR affect the AR-ER $\alpha$  cross-talk previously investigated, COS-1 cells were transfected with plasmids encoding for wild-type and mutant AR (C290Y, E355K, S568F, L638M, S663\*, Q739\*, D840N, D865E, Q868H and L881Q), ER $\alpha$ , an ERE-LUC reporter and a renilla expression vector (Figure 3.19a). Cells were treated with 1.0 nM E2 and MIB for a further 24 hrs (Figure 3.19b). ER $\alpha$  activity increased in response to ligand treatment. The wild-type and mutant ARs all inhibited ER $\alpha$  activity to a similar extent.

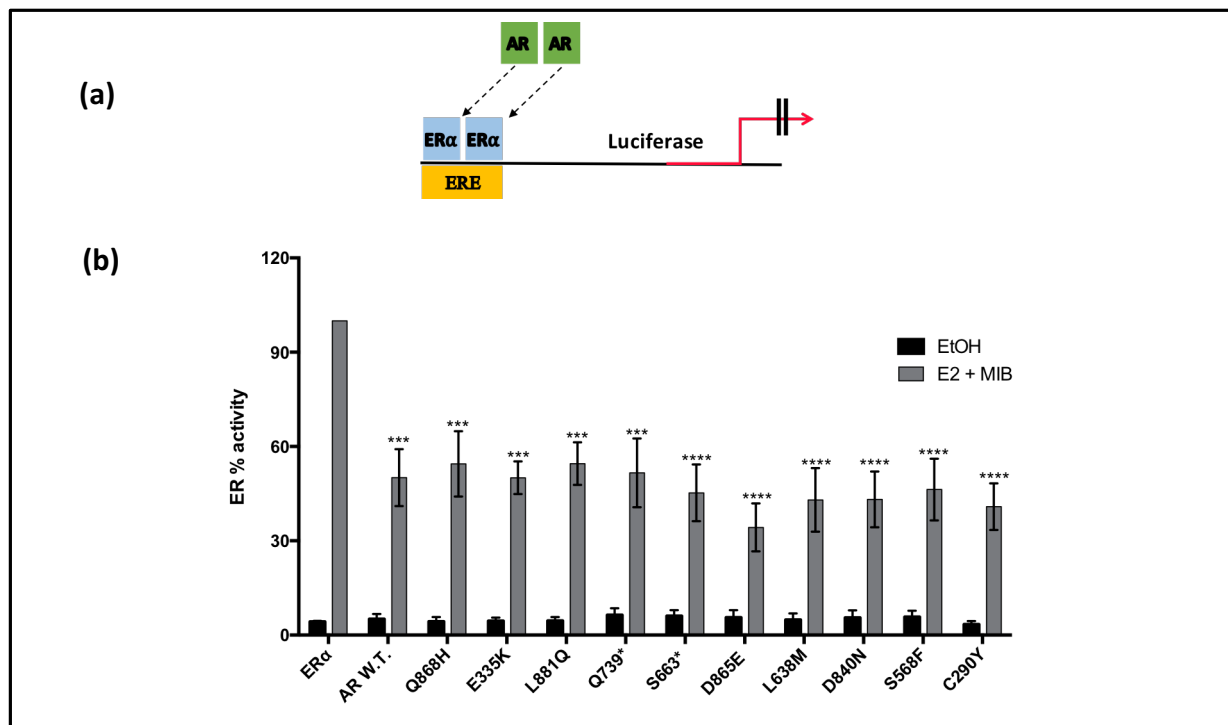


**Figure 3.19: AR mutations in BCa do not affect AR/ ER $\alpha$  cross-talk.** (a) Schematics representation of the reporter assay. (b) COS-1 cells were transfected with expression plasmids for ER $\alpha$ , AR and AR mutants (C290Y, E355K, S568F, L638M, S663\*, Q739\*, D840N, D865E, Q868H and L881Q), a luciferase reporter (ERE-LUC) and a renilla expression vector. Cells were incubated for 24 hrs then treated with EtOH: ethanol E2: 17- $\beta$ -oestradiol (1.0 nM) and MIB: mibolerone (1.0 nM). ANOVA system. \*\*\*\*p < 0.00001, \*\*\*p < 0.0001. Mean  $\pm$  1SE.

### 3.3.6 AR editing in MCF-7 cells using CRISPR/ CAS9

As previously demonstrated, the truncation AR mutants identified in breast cancer were found to be constitutively active. To further characterise the role of these mutations in BCa, CRISPR/CAS9 was used to introduce the AR mutation Q739\* into MCF-7 cells (Figure 3.20a). The ZangLab excel tool (P. Madapura) was used to identify PAM sites near the targeted mutation (Q739\*) and the relevant guide strands were designed (two different target sites). The guide strands were subsequently cloned into the PX459 V2 plasmid and confirmed using sequencing. The corresponding repair strands (Table 2.6) were designed using Benchling (<https://benchling.com>). MCF-7 cells were transfected with the plasmids and repair strands and transfected cells selected for using puromycin. Individual colonies were expanded and more than 40 clones were screened using immunoblotting (example provided in Figure 3.20). Unfortunately, no truncated AR was present in the cells suggesting that the mutation was not inserted. However, the AR was found to be silenced in the majority of lines investigated, suggesting that CRISPR had knocked-out the AR (Figure 3.20).

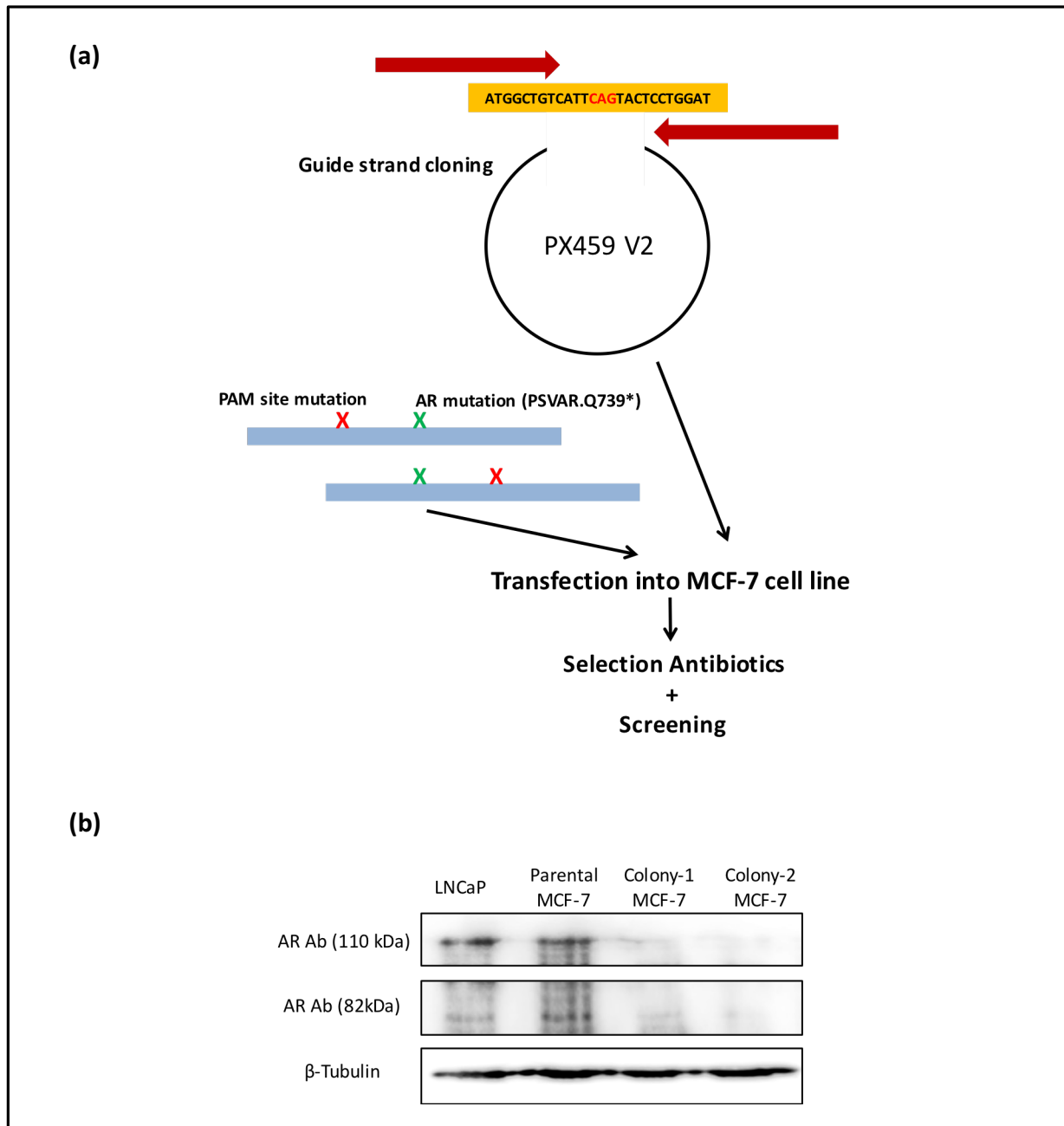


**Figure 3.20: CRISPR/ CAS9 in MCF-7 resulted in AR silencing.** (a) Schematic representation of the cloning steps to introduce the AR mutant Q739\* guide strand into PX459 V2 vector. The repair strand was designed to introduce the Q739\* mutation and to mutate the PAM site. (b) MCF-7 cells were transfected with PX459 V2 739\*\_1 and PX459 V2 739\*\_2 for 24 hrs then treated with puromycin (2 ug/ ml) for a further 48 hrs. Lysates were separated using SDS-PAGE and AR levels visualised using immunoblotting.

### 3.3.7 Genomic DNA was successfully extracted from BCa tissue

To investigate the prevalence of AR mutations in breast cancer, a pilot study was performed to extract genomic DNA from tumour samples from BCa patients, with the aim of sequencing for AR mutations in the future. Tissue was obtained from patients from Colchester General Hospital, genomic DNA extracted and qPCR performed to quantify DNA concentration (Table 3.5). Genomic DNA was successfully isolated from all samples and sufficient quantities were isolated for future sequencing studies.

**Table 3.5: The concentration of genomic DNA extracted from BCa patient tissues.** Table illustrates samples type and genomic DNA concentrations after qPCR performed. N: Normal tissue, T: Tumour tissue (based on the pathological reports included with the samples).

<b>Samples No.</b>	<b>Tissue type</b>	<b>Concentration ng/ul</b>
<b>2224</b>	N	429.3500
	T	1000.9000
<b>2227</b>	N	188.9000
	T	937.7000
<b>2237</b>	N	110.4500
	T	146.3000
<b>2240</b>	N	74.3400
	T	178.3500
<b>2230</b>	N	100.3050
	T	771.0000
<b>2268</b>	N	260.1500
	T	295.9000
<b>2335</b>	N	194.3000
	T	248.6500
<b>2336</b>	N	131.2500
	T	776.5500
<b>2341</b>	N	64.3100
	T	22.1850
<b>2361</b>	N	150.8500
	T	274.1500

## 3.4 Discussion

### 3.4.1 AR and ER $\alpha$ cross-talk in Breast Cancer

It has been demonstrated that the majority of BCa cases are dependent upon ER $\alpha$  for growth and overexpression of the receptor has been shown to increase proliferation (Gross and Yee 2002). However, the AR also appears to be important in BCa and has been found to be the most expressed steroid receptor in normal breast tissue and breast cancer (Robinson *et al.*, 2011). In ER $\alpha$  positive disease, the AR has been shown to be inhibitory to growth and multiple mechanisms have been proposed to explain this cross-talk (Lehmann-Che *et al.*, 2013). In BCa, activation of the AR could therefore be an approach to inhibit ER $\alpha$ -dependent disease, however, in some cases of BCa, such as molecular apocrine, it is proposed that tumour growth is driven by the AR and hence inhibition of receptor activity could be a viable option to block the growth of this sub-type (Alluri *et al.*, 2014).

AR and ER $\alpha$  cross-talk suggests that these receptors inhibit each others activity (Hickey *et al.*, 2012; Panet-Raymond *et al.*, 2000). In agreement with this, the oestrogen-induced proliferation of MCF-7 was inhibited in response to androgen treatment. Further, reporter assays demonstrated that AR and ER $\alpha$  inhibit each-others activity at the transcriptional level. However, this repressive activity was not seen when AR and ER $\alpha$  target genes (*TFF1*, *MYC*, *DRG1*, *GREB1*) were studied in the MCF-7 cell line. To date, the majority of studies have investigated AR and ER $\alpha$  cross-talk using reporter assays. There is therefore little information on which target genes are affected by this cross-talk and this study suggests that not all genes will be affected. Instead the cross-talk is likely to be gene specific and therefore a more global analysis of gene expression (e.g. RNA-Seq) would be informative.

### 3.4.2 Characterisation of the mechanisms of cross-talk between the AR and ER $\alpha$

The mechanisms by which AR and ER $\alpha$  inhibit each others activity includes direct interaction between the N-terminus of the AR and the LBD of the ER $\alpha$  (Panet-Raymond *et al.*, 2000). The fluorescent microscopy demonstrated that the AR and ER $\alpha$  co-localise and the co-immunoprecipitation results indicated that receptors do physically interact. In agreement with Panet-Raymond *et al.* (2000), this interaction was found to be ligand independent. The anti-androgens Bic and Enza did not impact on AR-ER $\alpha$  cross-talk. The use of an anti-androgens therefore does not reduce the inhibitory effect of the AR upon ER $\alpha$ .

Another mechanism that has been proposed to explain AR-ER $\alpha$  cross-talk is direct competition for DNA binding. For example, the AR is able of bind to estrogen response elements (EREs) and therefore block ER $\alpha$  binding to DNA. This was demonstrated through the transfection of the AR DBD into BC cell lines, and resulted in a significant inhibition of ER $\alpha$  activity (McNamara *et al.*, 2014). To investigate this further ER $\alpha$  mutants, that are transcriptionally dead, were utilized in co-expression studies (Figure 3.21). The first, ER $\alpha$  HE 257G, has a deletion of the  $\Delta$ NLS and was used to assess whether the receptors interact in the cytoplasm and block translocation of the other receptor into the nucleus (Ylikomi *et al.*, 1992). The other mutant, ER $\alpha$  HE464, is unable to bind to the DNA and can assess whether the receptors compete for DNA binding. Both receptors were confirmed to be transcriptionally inactive in reporter assays and confocal microscopy confirmed that the  $\Delta$ NLS mutant had reduced nuclear localisation.

Immunofluorescence demonstrated that the delta NLS mutant resulted in partial cytoplasmic retention of AR. This therefore suggests that the receptors interact in the cytoplasm



and can shuttle into the nucleus together. When cells were co-transfected with the DBD mutant, in contrast, the AR and ER $\alpha$  were found to co-localise in the nucleus. The competition for DNA binding and cellular translocation do not appear to be mechanisms by which ER $\alpha$  inhibits AR as both receptors retained their repressive activity upon AR signalling. Also expanding the experimental scale to include another steroid receptor, Progesterone P, could aid the cross-talk mechanism in particular with ER $\alpha$ . This has been demonstrated that P acts on slowing proliferation of the ER $\alpha$  due to changes of the DNA binding sites (Pan *et al.*, 2006). However, only one luciferase reporter was used and a hence more global analysis of the affects of ER $\alpha$  upon AR binding to response elements could be assessed using ChIP-Seq.

### **3.4.3 Regulation of the AR and ER $\alpha$ expressions**

AR-ER $\alpha$  cross-talk has been proposed as a therapeutic strategy for BCa (i.e. activation of AR to inhibit ER $\alpha$ -dependent proliferation) (Yeh *et al.*, 2003). It is therefore essential to understand the different mechanisms that underlie this cross-talk. One finding, that has not been described previously was that the AR and ER $\alpha$  appear to regulate each-others expression. This was demonstrated by the transient transfection experiments, whereby increased expression of one receptor also led to an increase in the levels of the other receptor. Further, in the siRNA experiments, knock-down of one receptor also resulted in a decrease in the expression of the other receptor. How these receptors regulate the expression of the other receptor remains unclear, but this also fits with studies that have demonstrated that AR and ER $\alpha$  expression is highly correlated in BCa (Peters *et al.*, 2009). In summery, competition for cofactors is a plausible mechanism by which ER $\alpha$  represses AR activity and this requires further investigation.

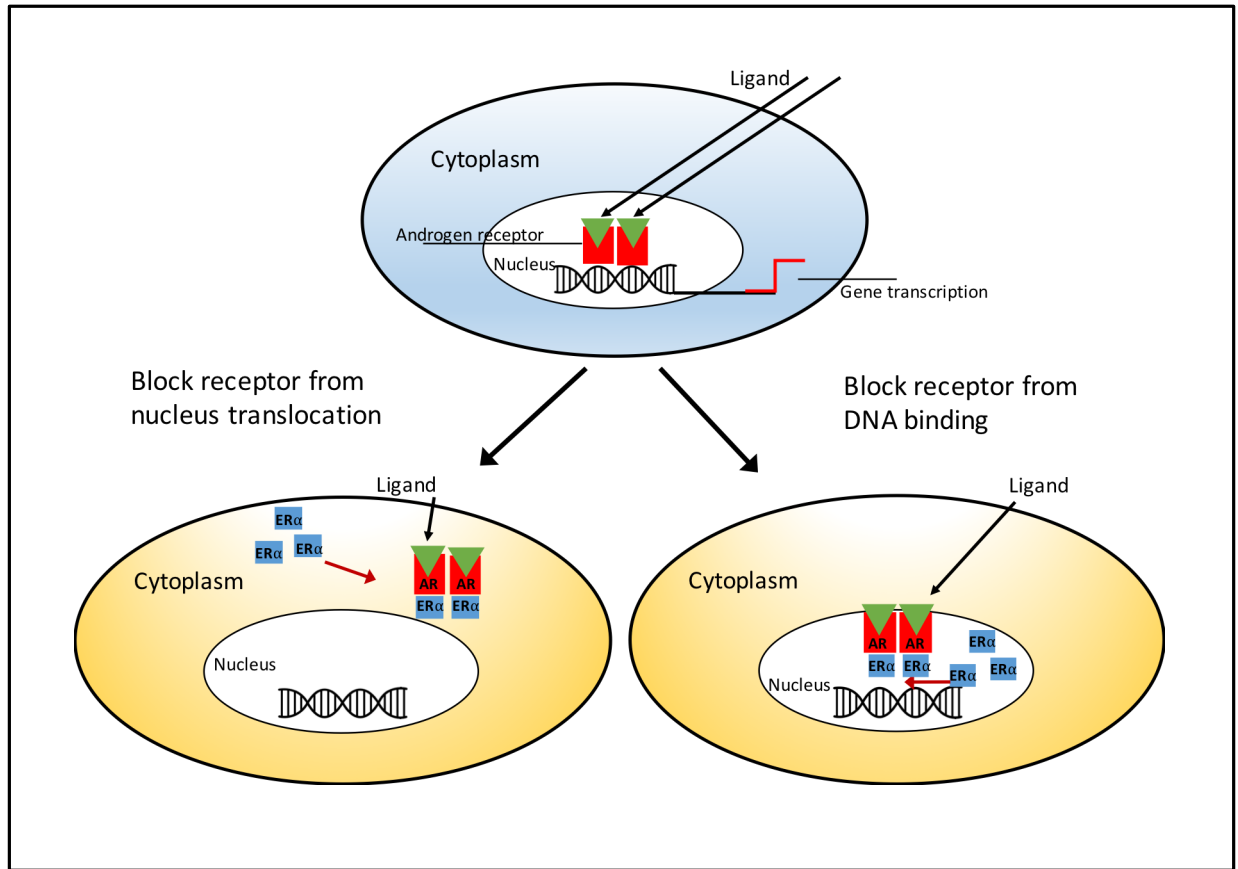


**Figure 3.21: Possible mechanisms of repression present in AR- ER $\alpha$  cross talk.** Schematic representation of normal action of the AR upon ligand binding (blue cell, top). Different mechanisms by the ER $\alpha$  variants could block AR activity (yellow cells, bottom).

### 3.4.4 The potential role of AR mutations in BCa

AR expression has been found to be variable among different BCa subtypes, high in ER $\alpha$ -positive tumours and low in ER $\alpha$ -negative disease. If the AR is not the only receptor (ER $\alpha$ , PR, HER2) expressed, its presence is linked to a better clinical and pathological evaluation (Tsang *et al.*, 2014). However, when the AR is the predominant receptor, such as in molecular apocrine disease, a correlation with higher tumour stage and metastasis is observed (McGhan *et al.*, 2014). Sequencing studies have identified that the AR is mutated in some cases of BCa, these mutations are quite rare as they were found in 1.77 % of patient samples investigated (COSMIC: <https://cancer.sanger.ac.uk/cosmic>). This low prevalence could be due to the fact that much of the sequencing available via databases such as COSMIC, is from early stage tumours. Mutations of the AR may therefore be rare similar to ER $\alpha$  mutations in BCa and AR mutations in PCa in that they are rare in early stages of the disease, but their incidence significantly increase in advanced disease (Brooke and Bevan 2009). Interestingly, the AR mutations identified do not appear to be in specific subtype of BCa since they were found in ER $\alpha$ -positive and negative disease.

AR mutations, associated with BCa, were identified using the COSMIC database and subsequently cloned using site-directed mutagenesis. Some of the mutations were found to affect receptor activity, whereas others appeared to have no effect and may therefore be passenger mutations (Figure 3.22). Two of the identified mutations were S663\* and Q739\* generate truncated receptors due to the presence of the stop codons TGA and TAG respectively. These receptors were found to be nuclear in the presence and absence of androgen and reporter assays demonstrated that these two mutants were constitutively active. This affect is expected as the

mutations result in loss of the LBD region, which holds the receptor in an inactive state in the absence of ligand.

In contrast to the constitutively active receptors, the D865E mutant was transcriptionally dead. The location of this mutation is in the LBD and the substitution may therefore affect ligand binding or co-activator recruitment. Interestingly, this mutation has been associated with complete androgen insensitivity syndrome (CAIS) (Ong *et al.*, 2002). This disease is associated with inactive androgen signalling and in agreement with this, the findings present here demonstrated that this mutation results in a transcriptionally dead AR. Interestingly, confocal microscopy demonstrated that this receptor can translocate to the nucleus and hence it is likely that the mutant receptor can bind ligand and that cofactor recruitment is disrupted. In addition to the truncation mutants, C290Y, E355K and D840N are nuclear in the absence of androgen but do not show enhanced activity. All other mutants, as well as the wild-type receptor, were cytoplasmic in the absence of ligand and translocated into the nucleus after androgen treatment.

In PCa, some AR mutations, especially those in the LBD, lead to loss of ligand specificity resulting in receptors that can be activated by alternative ligands and anti-androgens (Eisermann *et al.*, 2013). Based on the nature and location of the substitution, LBD mutations affect the ligand-induced conformational change of AR, leading to changes in ligand binding specificity, N/C-terminal interactions and interactions with chaperones (Bergerat and Ceraline 2009). Investigation of non-androgenic ligands (e.g. other hormones and anti-oestrogens) demonstrates that the AR mutations identified in BCa remain ligand.

It has been demonstrated, in PCa, that specific AR mutations are selected for in response to anti-androgen treatment (Eisermann *et al.*, 2013). For example, the AR T877A mutation, which can be activated by other hormones and anti-androgens such as hydroxyflutamide, is

selected for when patients are treated with hydroxyflutamide (Taplin *et al.*, 1999). Therefore, it will be interesting to sequence the AR for mutations in more advanced cases of BCa e.g. endocrine resistant disease, to see if mutations have been selected for as a result of the treatment regime. Since anti-androgens are being trialled in breast cancer, it will also be useful to sequence the AR of these patients to see if AR mutations arise during disease progression. In preparation for such studies, DNA isolation from tumour samples was optimised as part of this study.

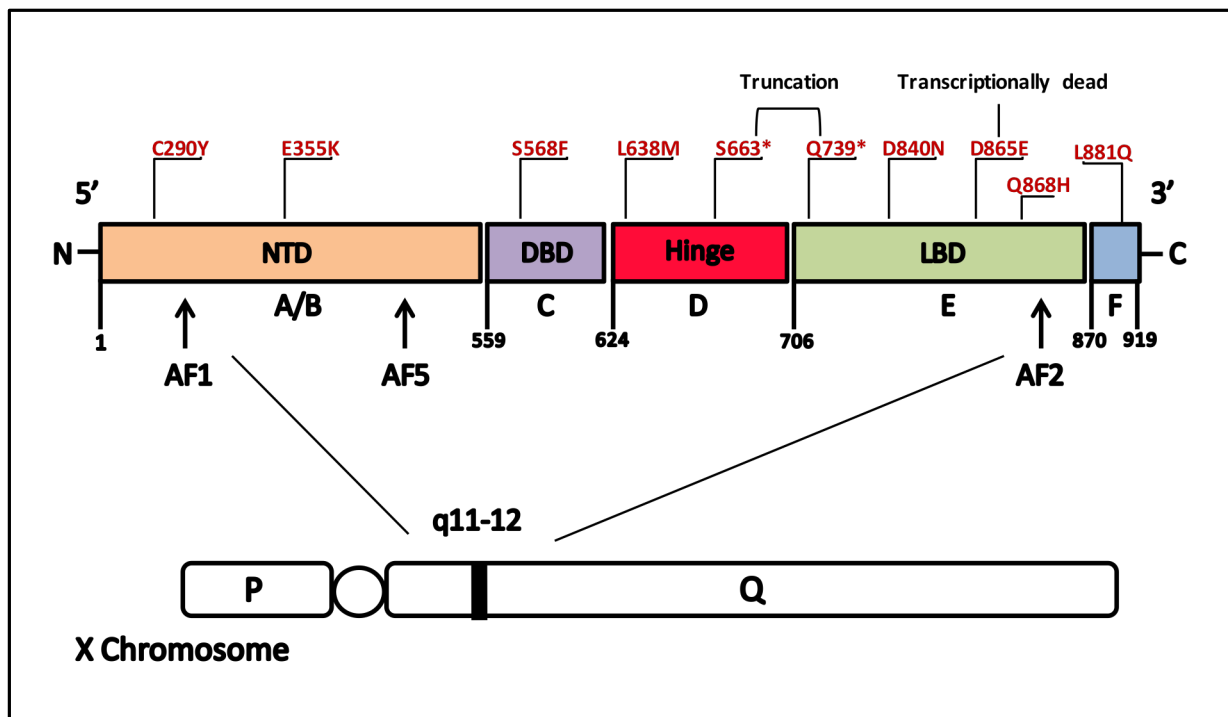


**Figure 3.22: Locations of AR mutations in Breast Cancer.** Image shows mutations identified in breast cancer, indicated in red, and their locations on the four functional domains of the AR and the gene structure indicated in chromosome X q11-12. NTD = N- terminal domain, DBD = DNA binding domain, LBD = ligand binding domain and AF = activation function. A-F indicates the different location of the 6 functional domains with amino acids residues numbers. Mutations S663\* and Q739\* are truncated. Mutation D865E is transcriptionally dead.

### 3.4.5 Investigation of AR mutations in endogenous protein

The experiments that aimed to characterise AR mutations in BCa was limited as the experiments were transient transfections. Part of this study therefore aimed to develop a CRISPR modified line to allow studying of the effect of the truncated constitutively active receptor upon ER $\alpha$  signalling in a more physiologically relevant model. The relevant CRISPR tools were designed and generated. MCF-7 cells were transfected and multiple clones selected. However, instead of generating the truncation mutant, the manipulation resulted in AR knock-out. Although the desired mutation was not inserted, AR knock-out lines have been generated and these will be useful for investigating the effect of AR loss in BCa. In summery, further investigation is needed to sequence patient's samples particularly advanced BCa as there are many limitations in transient based experiments. This includes the smaller cellular systems found in cell lines which are not reflected in real situations within tumour tissues. Also, certain alteration represents specific group of patients e. g. MD-MBA453 has mutated PTEN and PI3K (Vranic *et al.*, 2011).

Investigation of AR-ER $\alpha$  cross-talk also contributes to our understanding of how best to target the AR in BCa. The data presented in This thesis suggests that ER $\alpha$  does not repress AR activity via competition for DNA binding. It is therefore possible that competition for cofactors is the mechanism by which ER $\alpha$  represses AR activity. In addition, this study also investigated the role of AR mutations in BCa. Assessment of receptor transcriptional activity and cellular demonstrated the effect of these substitutions upon receptor function. AR mutations that resulted in a constitutively active and transcriptionally dead receptor were identified. A constitutively active receptor could drive molecular apocrine growth, whereas a transcriptionally dead receptor may not be able to compete with ER $\alpha$  to block growth facilitating E2 induced growth in ER $\alpha$

positive disease. This aids more advanced disease for patients who recieved antiandrogen treatment to see if they have acquired any of the AR mutations invistigated in this study in response to the therapy.

## CHAPTER 4

### Results II: The Effect of thieno[2,3-b]pyridine Derivatives on Prostate Cancer Cell Lines

#### 4.1 Introduction

Prostate cancer (PCa) is the most diagnosed malignancy in men in the UK and 2<sup>nd</sup> most cause of cancer deaths with 25% mortality rate (Cancer Research UK, 2014). The therapeutic management of PCa has become more complex due to the various stage-specific therapeutic options available. Disease management has been complicated further by the lack of randomized clinical trials to compare the efficacy of these therapeutics (Bott *et al.*, 2003; Heidenreich *et al.*, 2010). For non-organ confined disease, hormone therapy is often administered and this is effective in the majority of patients. However, these therapies invariably fail and the tumour relapses within 2 to 3 years, and the disease progresses to the more aggressive CRPC stage, which is associated with poor prognosis and low survival rates (Brooke *et al.*, 2008; Cookson *et al.*, 2013).

A number of mechanisms have been proposed to explain CRPC and these include AR mutations, androgen biosynthesis within the tumour or alterations in co-activators and co-repressors (Mostaghel *et al.*, 2009). Few treatment options exist for CRPC, such as the chemotherapeutic docetaxel, which have been the classical option to treat this stage of the disease (Hotte & Saad 2010). Also the taxane chemotherapy (cabazitaxel), a newly approved drug used for the metastatic CRPC (de Bono *et al.*, 2011). These therapies have limited efficacy and there is therefore a great need for novel therapies for the treatment of CRPC. In PCa the PI3K-Akt-mTOR pathway is often found to be constitutively active due to the loss/inactivation



of the tumour suppressor PTEN. It has therefore been proposed that targeting the PTEN pathway may be a novel targeted approach to treat PCa. Pathways downstream of PTEN, such as Phospholipase C (PLC), therefore represent novel therapeutic targets (Phin *et al.*, 2013).

The Phospholipase C (PLC) family are membrane bound proteins which regulate multiple cellular functions. They play a crucial role in many transmembrane signal transduction pathways, regulating numerous cellular processes (Béziau *et al.*, 2015; Cai *et al.*, 2017). Although their exact role in tumourigenesis is unclear, these enzymes have been shown to modify proliferation, migration and invasion (Lattanzio *et al.*, 2013). In many cancers, an increase in PLC activity and/or expression has been associated with increased metastasis and proliferation in these tumours (Lattanzio *et al.*, 2013). Bertagnolo *et al.*, (2007) found that, in BCa, a poor clinical outcome was linked to increased expression levels of PLC- $\beta$ 2 and it has there been proposed to be a molecular marker indicative of disease severity. In PCa, it has been found that PLC- $\gamma$  is essential in tumour invasion as it has a role in regulating cell motility through the hydrolysis of  $P_2$ , which polymerizes actin in response to growth factors (Lattanzio *et al.*, 2013). Wang *et al.* (2015) investigated 37 PCa patient samples and found increased PLC- $\epsilon$  expression levels, also they demonstrated that the silencing of this isoform in PC3 and LNCaP cells significantly reduced. Therefore, inhibition of PLC could be an effective treatment for PCa (Zhang *et al.*, 2012).

The PLC- $\delta$  has been proposed to be a valid target for the treatment of cancer. To identify novel inhibitors of PLC- $\delta$ , Reynisson *et al.* (2009) performed a virtual high-throughput screen. This screen identified thieno[2,3-*b*]pyridines as novel inhibitors for this enzyme (Reynisson *et al.*, 2009). These compounds were demonstrated to have potent anticancer activity against a variety of breast cancer cell lines, e.g. MDA-MB-231, where they were found to reduce

proliferation, increase G<sub>2</sub>/M arrest and to decrease cell motility (Leung *et al.*, 2016). Similar effects were noticed when the anticancer agents were investigated with stem/progenitor-like cell populations from breast and prostate cancers (Mastelić *et al.*, 2017). Therefore, the thieno[2,3-*b*]pyridine inhibitors have been demonstrated to be promising anti-cancer therapeutic agents and due to the heterogeneity of the molecular alterations in PCa, it appears that targeting common factors downstream of altered signalling pathway could be a more effective strategy in the treatment of CRPC. This chapter will investigate the therapeutic potential of thieno[2,3-*b*]pyridine inhibitors for the treatment of PCa.

#### **4.1.1 Chapter aims**

This chapter investigates the efficacy of thieno[2,3-*b*]pyridine inhibitors as a treatment option for CRPC.

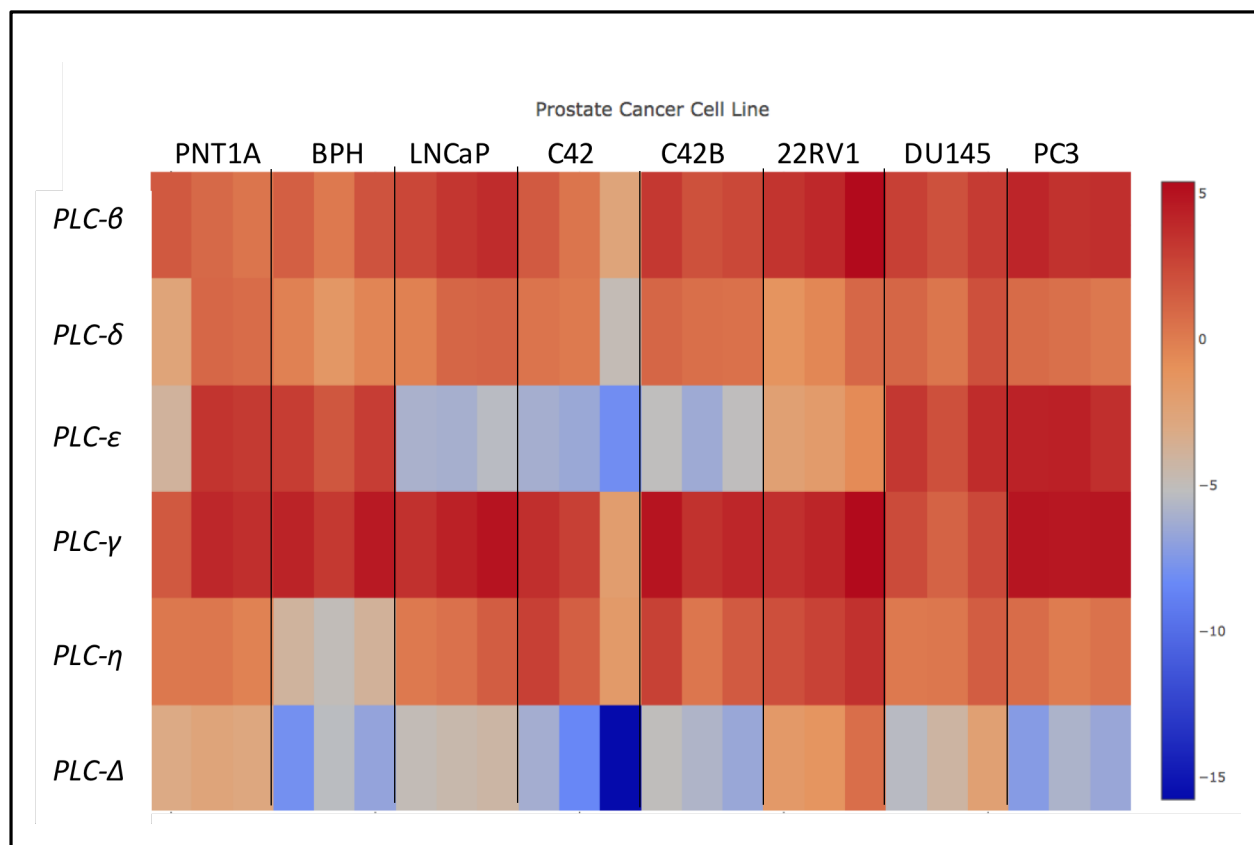
Aim 1 – To investigate the effect of thieno[2,3-*b*]pyridine inhibitors upon the proliferation of a panel of prostate cell lines

Aim 2 – To characterise the effect of thieno[2,3-*b*]pyridine inhibitors upon the cell cycle and mechanism of cell death and to assess the effect of the inhibitors upon cell motility

Aim 3 – To investigate the mechanism of action of the inhibitors and identify which proteins that these inhibitors target

## 4.2 Investigation of the PLC isoforms expression in PCa cell lines

PLCs have been implicated in the development of multiple cancer types, however, there is little information about expression of the different PLC isoforms in PCa. To investigate which PLC isoforms ( $\beta$ ,  $\delta$ ,  $\epsilon$ ,  $\gamma$ ,  $\eta$  and  $\Delta$ ) are expressed in the prostate lines, qPCR was performed on the cell line panel (BPH1, PNT1A, LNCaP, C42, C42B, 22RNV1, DU145 and PC3). A heat map was generated to summarise the expression levels of the different isoforms across the cell lines (Figure 4.1). Generally, the different PLC isoforms were expressed in all cell lines except for PLC $\Delta$ , which was low across all lines. PLC- $\epsilon$  was also low in LNCaP and its derivatives (C42 and C42B). In contrast, PLC- $\gamma$  was highly expressed across the cell lines and the highest levels were evident in PC3.

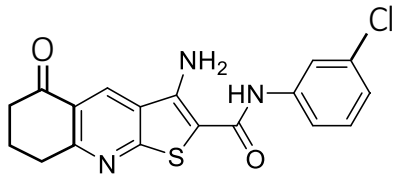
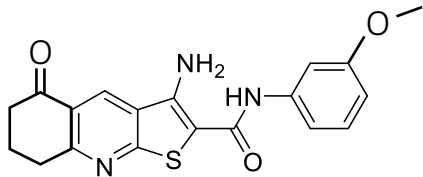
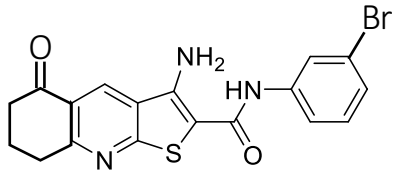


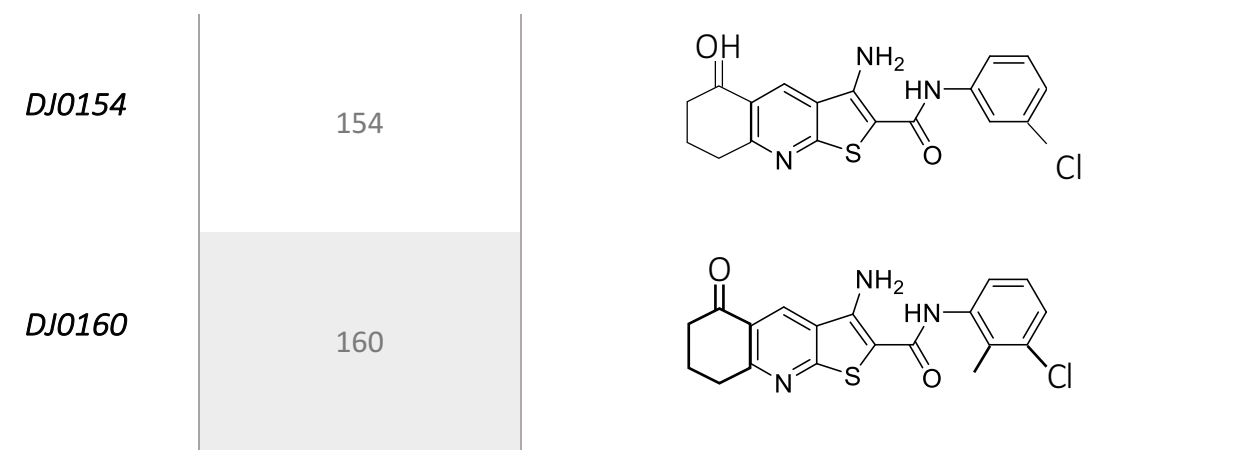
**Figure 4.1: Heat map of PLC isoforms expression levels in PCa cell lines.** RNA was extracted from PNT1A, BPH1, LNCaP, C42, C42B, 22RV1, DU145 and PC3 and reverse transcribed into cDNA. qPCR analysis was performed using SYBR green to measure the expression levels of (*PLC-β*, *PLC-δ*, *PLC-ε*, *PLC-γ*, *PLC-η* and *PLC-Δ*). Experiment was in 3 repeats. Heat map created using (plotly software).

### 4.3 Thieno[2,3-*b*]pyridine inhibit PCa cell lines proliferation and viability

Five anti-cancer thieno[2,3-*b*]pyridine derivatives were developed to target the binding site of the PLC- $\delta$  (Reynisson *et al.*, 2009). These 5 compounds (DJ0097, DJ0144, DJ0145, DJ0154 and DJ0160; Table 4.1) have been previously demonstrated to effectively inhibit the proliferation of the BCa cell line MDA-MB-231 (Leung *et al.*, 2016). To assess this inhibitory effect on PCa, the efficacy of these drugs was assessed in non-cancerous (PNT1A, BPH1) and cancerous (LNCaP, C42, C42B, 22RV1, DU145, PC3) cell lines. Cells were seeded in 96 well plates for 24hrs prior to treatment with the inhibitors at a range of concentrations (0, 0.01, 0.1, 1.0 and 10  $\mu$ M) for 72 hrs and proliferation assessed using crystal violet assays.

**Table 4.1: Description of the thieno[2,3-*b*]pyridine inhibitors used with PCa cell lines.**

<i>CODE</i>	<i>ABBREVIATION</i>	<i>COMPOUND</i>
DJ0097	97	
DJ0144	144	
DJ0145	145	



All of the drugs successfully inhibited the proliferation of all of the cell lines tested, with compounds 160 and 144 the most potent (Figure 4.1). The half maximal inhibitory concentration ( $IC_{50}$ ) was measured for the inhibitors to evaluate the effectiveness of each drug on the cell lines (Table 4.2). All of the drugs have a higher  $IC_{50}$  in BPH1 compared to the cancer cell lines suggesting that these drugs are more specific for tumour cells. However, PNT1A cells were also affected by the drugs as they are more selective when comparing against BPH1, but more normal controls need to be investigated to assess the effect on non-tumorigenic lines.

Drug 160 was the most potent compound across all of the PCa lines tested with  $IC_{50}$  values  $\leq 60$  nM. To further assess the effect of the inhibitors a viability assay was performed. PC3 cells were seeded in 96 well plates for 24hrs prior to treatment with 1.0  $\mu$ M of the compounds, as well as docetaxel (used as a positive control). Viability was assessed using the ApoTox-Glo™ Triplex assay kit. In agreement with the proliferation assays, cell viability was found to be significantly decreased in response to all treatments (Figure 4.3).

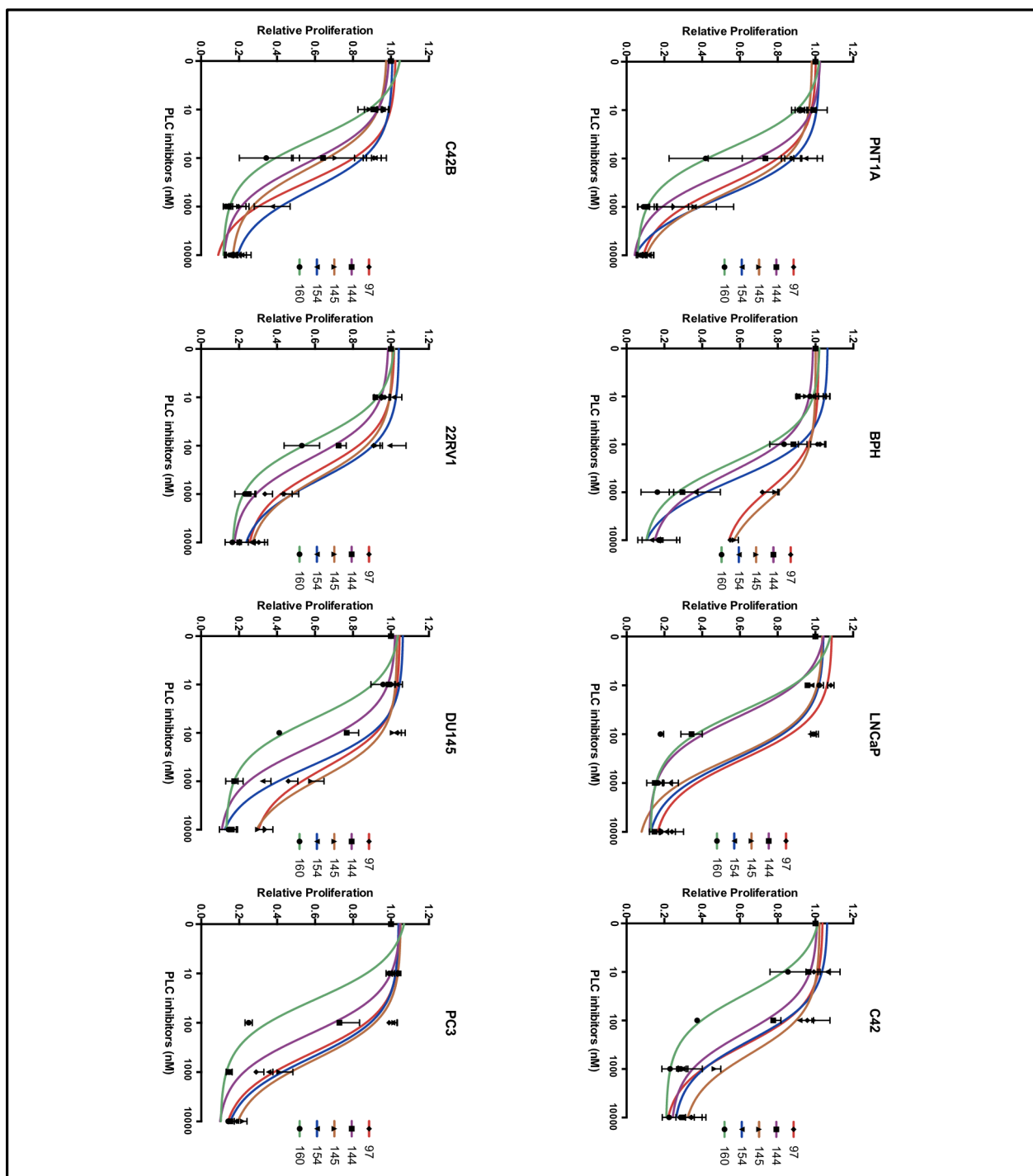


**Figure 4.2: The thieno[2,3-*b*]pyridine compounds inhibit prostate cancer cell lines.** The prostate cancer cell lines (PNT1A, LNCaP, C42, C42B, 22RV1, DU145, PC3) and non-tumorigenic controls PNT1A and BPH1 were seeded 24 hrs prior to treatment with a dose range of the thieno[2,3-*b*]pyridine compounds (97, 144, 145, 154 and 160) (0.01  $\mu$ M, 0.1  $\mu$ M, 1.0  $\mu$ M and 10  $\mu$ M) for 72 hrs. Cells were fixed with 4% paraformaldehyde, stained with 0.02% crystal violet and absorbance measured using a spectrophotometer microplate reader (FLUOstar Omega) at 490 nm. Mean  $\pm$  1SE of 3 independent repeats (6 repeats for each concentration per experiment).

**Table 4.2: The IC<sub>50</sub> values (nM) of the thieno[2,3-*b*]pyridine compounds demonstrate that 160 is the most effective inhibitor.** IC50 values were calculated from the sigmoidal range response curves for the cell lines PNT1A, BPH, LNCaP, C42, C42B, 22RV1, DU145 and PC3 after treatment with the anti-cancer inhibitors (97, 144, 145, 154 and 160). Data is shown as means ± 1 SD.

CELL LINE	IC <sub>50</sub> nM	97	144	145	154	160
<i>PNT1A</i>	Mean	324	238.2	708	902	82.6
	SD	44.3	136.5	140.4	748	35.4
<i>BPH1</i>	Mean	3551.4	442.8	4361.9	806	151.07
	SD	5340.2	275.8	4913.3	523.2	60.3
<i>LNCaP</i>	Mean	481.8	59.4	267.6	451.7	44.9
	SD	123	16.5	177.7	164.3	12.7
<i>C42</i>	Mean	334	187	468	246	29
	SD	6.8	36.7	163.2	74	17.8
<i>C42B</i>	Mean	333	150	230.3	512	54
	SD	24.6	136.5	182.2	305	44
<i>22RV1</i>	Mean	305.5	184.7	499	520.7	100
	SD	54.4	39.6	72.8	125.6	49.3
<i>DU145</i>	Mean	1396	271.4	1959.6	660.4	83.9
	SD	640	52.4	755.5	140.3	16.5
<i>PC3</i>	Mean	572.8	214.1	672.8	723.3	46.5
	SD	128.9	88.6	41.3	99.8	7.3



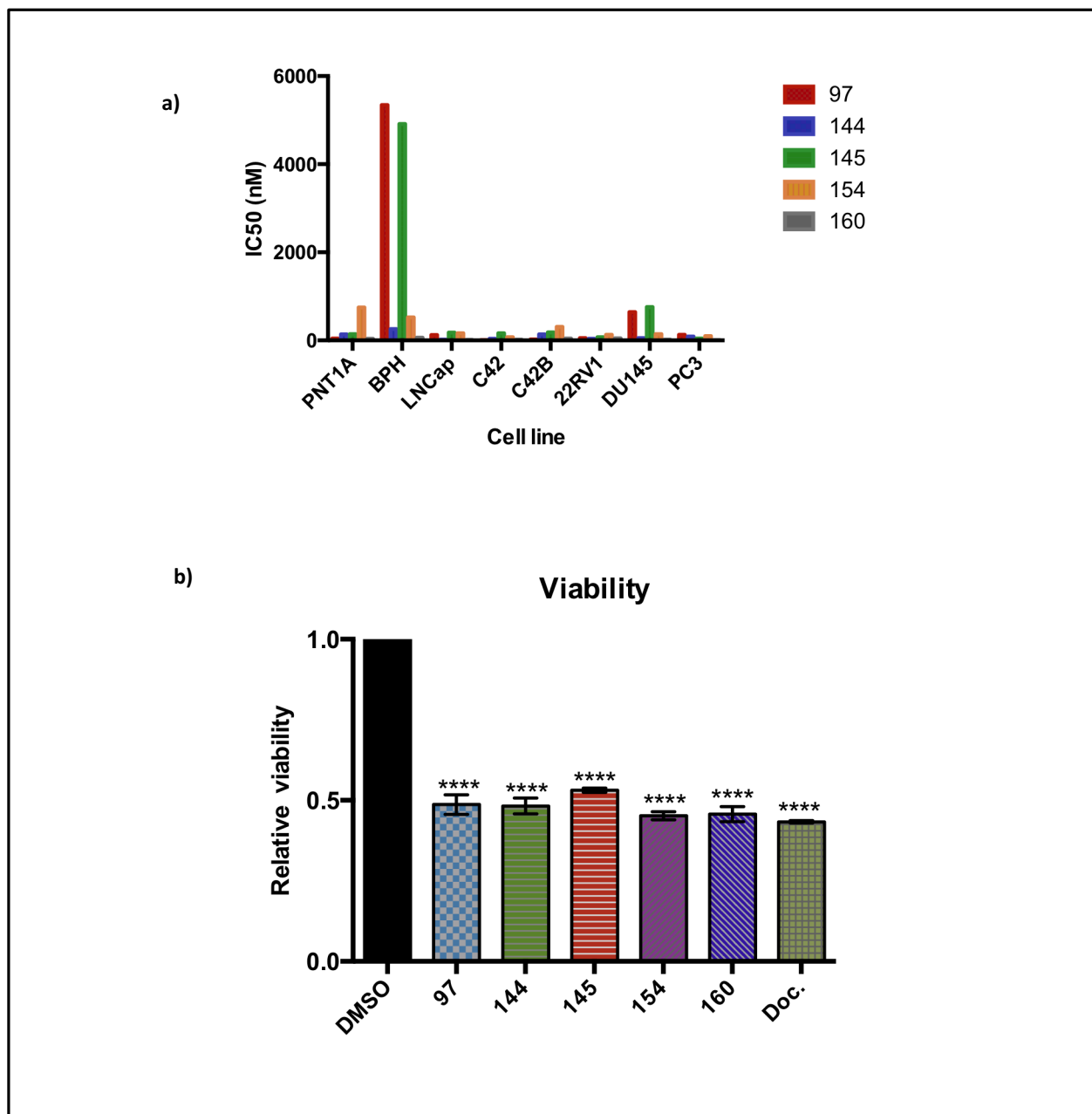


**Figure 4.3: The thieno[2,3-*b*]pyridine compounds IC<sub>50</sub> and cellular viability.** a) IC<sub>50</sub> values were calculated from the sigmoidal range response curves for the cell lines PNT1A, BPH, LNCaP, C42, C42B, 22RV1, DU145 and PC3 after treatment with the anti-cancer inhibitors (97, 144, 145, 154 and 160). b) Cells were seeded at 30% confluence for 24 hrs then treated with 1.0  $\mu$ M of the drugs (97, 144, 145, 154, 160 and Docetaxel) or DMSO for a further 48 hrs. Viability was measured using an ApoTox-Glo™ Triplex assay kit and fluorescence read using a microplate reader (FLUOstar Omega, BMG LABTECH, UK). ANOVA \*\*\*\*p<0.00001. Mean  $\pm$  1SE.

#### **4.4 Thieno[2,3-*b*]pyridine inhibitors induce G2/M arrest in PC3**

The previous experiments demonstrated that the thieno[2,3-*b*]pyridine inhibitors block the proliferation of PCa cell lines. To see if the inhibitors cause cell cycle arrest, PC3 cells were seeded at 30% confluency, incubated for 48 hrs and treated with 1  $\mu$ M of the compounds for different time points (24 hrs, 48 hrs and 72 hrs). DNA was PI stained and DNA content was analysed (10,000 cells per sample were analysed and quantified) using flow cytometry (Accuri, BD Biosciences). Cell with the DMSO treatment, in the absence of inhibitor, PC3 cells were found to be predominantly in G1 phase. Compounds 97, 144, 145, 154 and 160 promoted G2/M arrest at all time points, but most notably after 72hrs treatment. There was also an increase in the number of cells arresting in S-phase with increasing time (Figure 4.4). It therefore appears that the inhibitors block PCa proliferation as a result of cell cycle arrest.

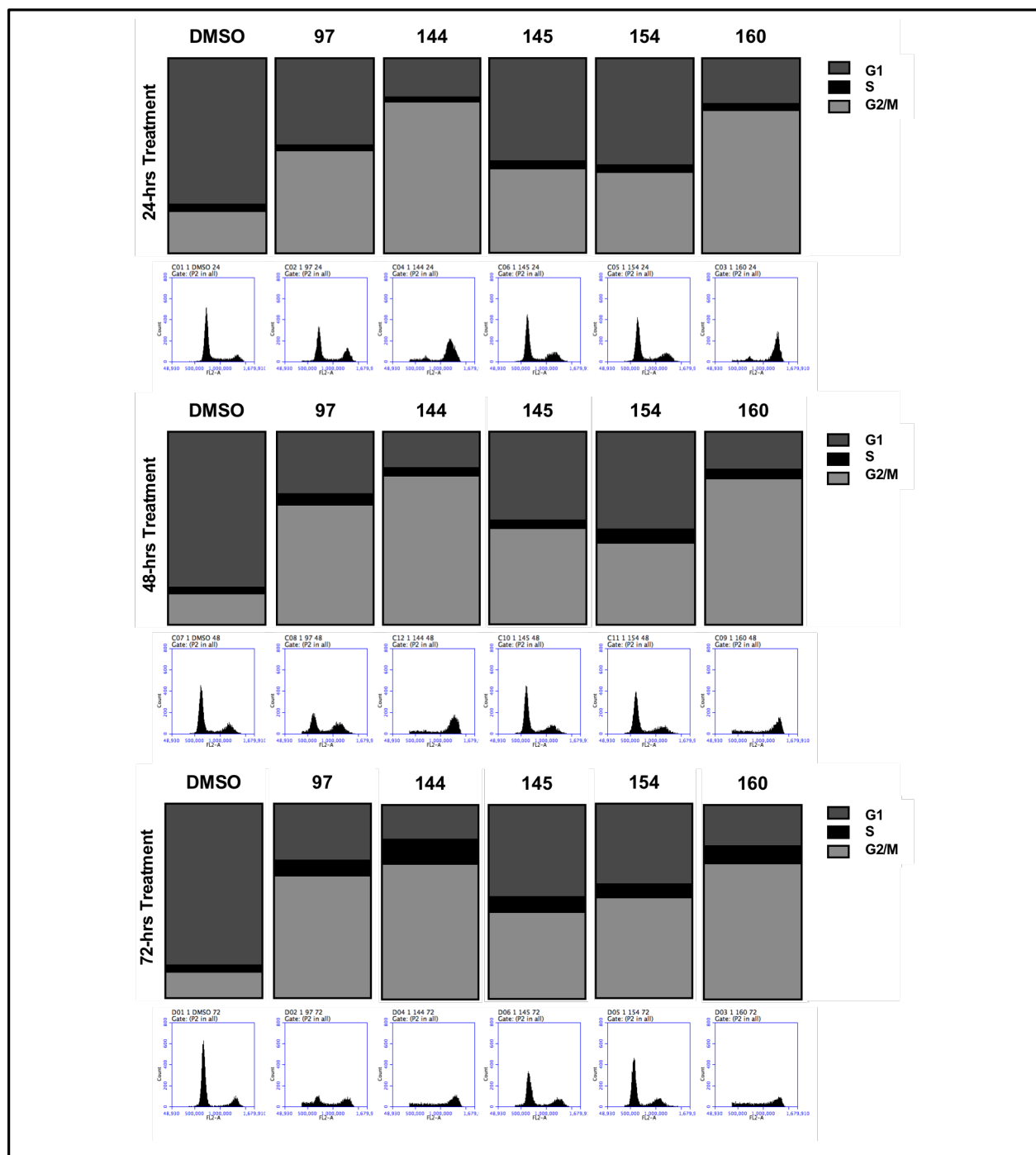


**Figure 4.4:** The thieno[2,3-*b*]pyridine compounds promote cell cycle arrest in PC3 cells. PC3 cells were seeded at 30% confluence for 48 hrs then treated with (1.0  $\mu$ M) of the drugs (97, 144, 145, 154 and 160) or DMSO for different time points (24, 48 and 72 hrs). Cells were PI stained and DNA content measured using flow cytometry. Representative histograms generated using the Accuri C6 software (BD Biosciences). Data was performed for 3 different repeats.

#### 4.5 Thieno[2,3-*b*]pyridine inhibitors promote apoptosis in PC3

The thieno[2,3-*b*]pyridine compounds were found to reduce cell proliferation and to promote cell cycle arrest. To see if the inhibitors also promoted cell death, PC3 cells were seeded at 30 % confluence, incubated for 48 hrs and treated with 1  $\mu$ M of the inhibitors (97, 144, 145, 154 and 160) for different time periods (24 hrs, 48 hrs and 72 hrs). DNA hypodiploidy assays were performed to quantify the % of cells undergoing apoptosis and samples were analysed using an Accuri C6 flow cytometer (BD Biosciences). Result shows apoptosis increases to approximately 5% in the presence of DMSO over the time course. When cells treated with drugs, cells starting at 15% increase in undergoing apoptosis, this was significantly increased in apoptosis for all treatments over time (Figure 4.5a and b). In agreement with this, Leung *et al.*, (2016) indicated that the thieno[2,3-*b*]pyridine inhibitors cause cell cycle arrest in the G<sub>2</sub>/M phase in the MDA-MB-231 BCa cell line.

Multiple mechanisms of cell death, in addition to apoptosis, have been described, including necrosis and necroptosis. To see if the drugs induce cell death via such mechanism cells were also analysed using PI inclusion assays. None of the inhibitors were found to promote necrosis/necroptosis at any of the time points tested (Figure 4.6a and b). It therefore appears that the compounds promote cell death via apoptosis.

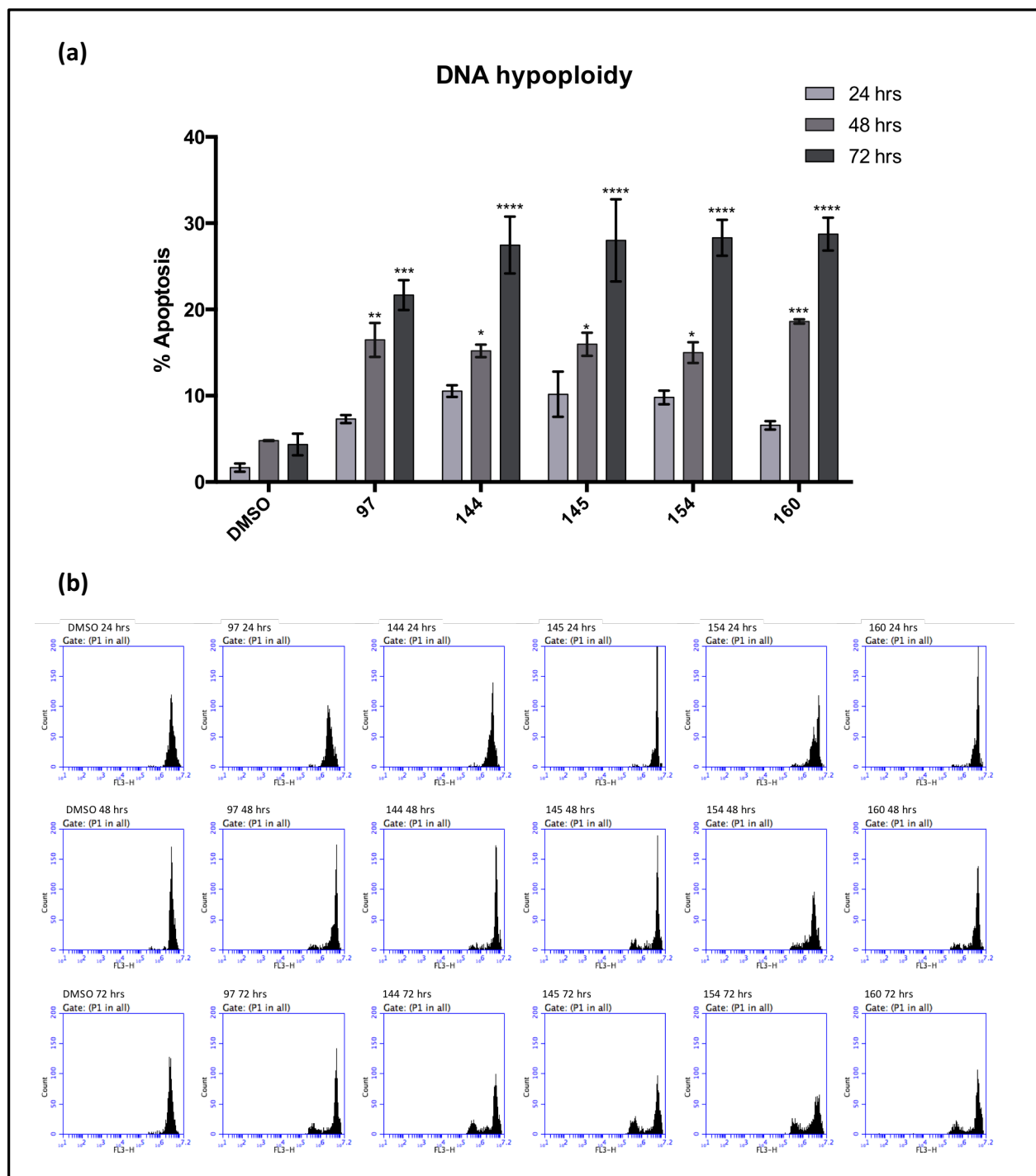


**Figure 4.5: The thieno[2,3-*b*]pyridine compounds promote apoptosis in PC3 cells.** (a) PC3 cells were seeded at 30% confluence and incubated for 48 hrs prior to treatment with 1.0  $\mu$ M of the drugs (97, 144, 145, 154 and 160) or DMSO for different time points (24, 48 and 72 hrs). Cells were harvested and DNA hypodiploidy measured using flow cytometry. (b) Representative histograms generated using the Accuri C6 software (BD Biosciences). ANOVA \*\*\*\* $p < 0.00001$ , \*\*\* $p < 0.0001$ , \*\* $p < 0.001$  and \* $p < 0.01$ . Mean  $\pm$  1SE.

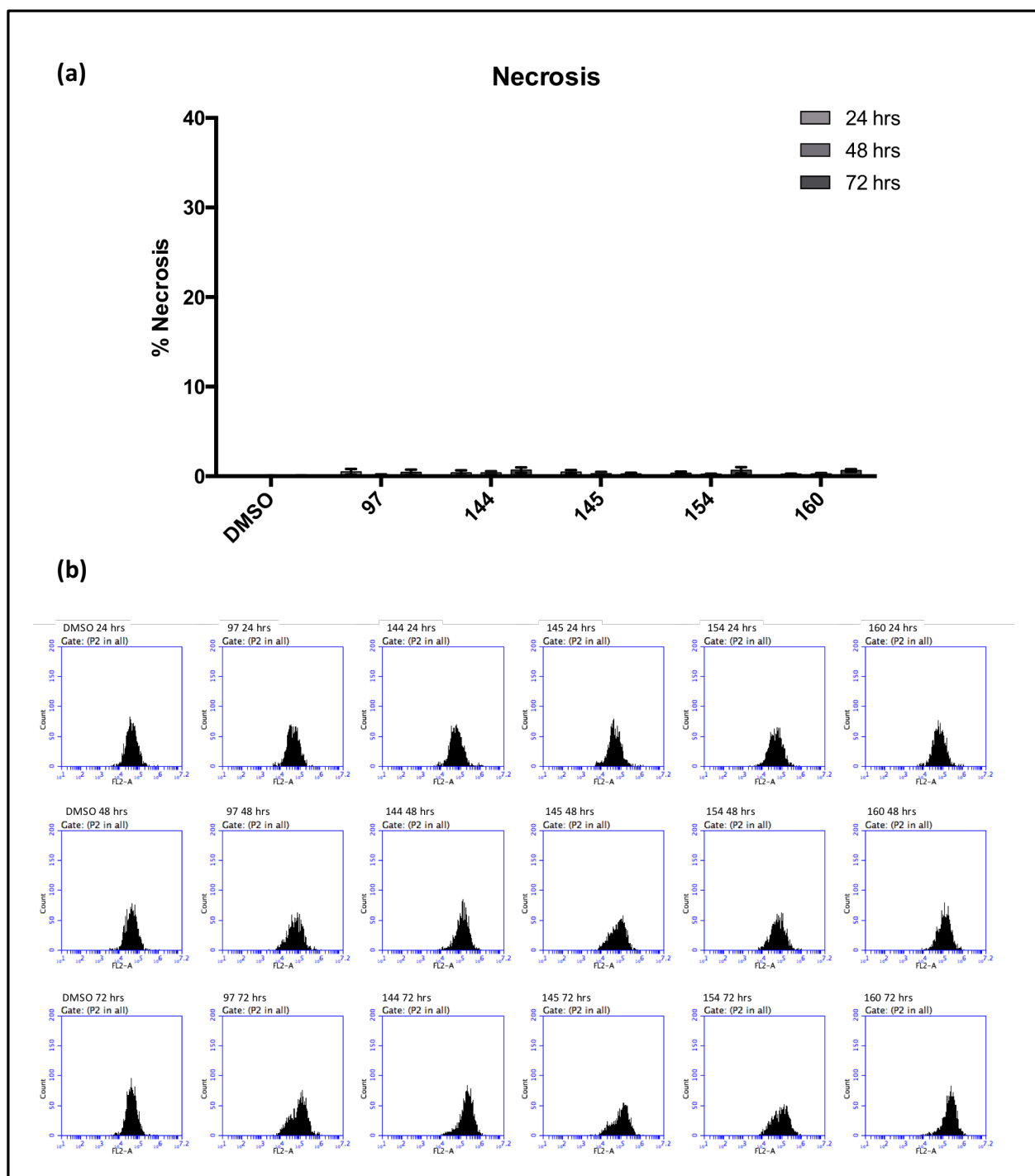


**Figure 4.6: Necrosis analysis of PC3 cells upon the treatment with the thieno[2,3-*b*]pyridine compounds. (a)** PC3 cells were seeded at 30% confluence and incubated for 48 hrs prior to treatment with 1.0  $\mu$ M of the drugs (97, 144, 145, 154 and 160) or DMSO for different time points (24, 48 and 72 hrs). Cells were harvested and PI inclusion assay measured using flow cytometry. **(b)** Representative histograms generated using the Accuri C6 software (BD Biosciences).

#### **4.6 The thieno[2,3-*b*]pyridine inhibitors promote caspase dependant cell death**

The DNA hypodiploidy and PI inclusion assays suggest that cell death is as a result of apoptosis. To confirm that cell death is caspase dependant PC3 cells were seeded in 96 well plates for 24 hrs prior to treatment with (1.0  $\mu$ M) of the inhibitors (97, 144, 145, 154 and 160), and docetaxel as a positive control, for 48 hrs. Post drug treatment, caspase 3/7 activity was assessed using the ApoTox-Glo<sup>TM</sup> Triplex assay kit where luminescence was measured using the spectrophotometer microplate reader (FLUOstar Omega, BMG LABTECH, UK). All of the thieno[2,3-*b*]pyridine compounds significantly increased caspase 3/7 activity approximately 2-fold (Figure 4.7). Docetaxel increased caspase 3/7 activity to the greatest extent (approximately 4 fold).

To further confirm that cell death is a result of apoptosis, cells were treated with the caspase inhibitor  $\pm$  Z-VAD which binds to the catalytic site of caspase proteases and inhibits cascade-dependent apoptosis (Promega). PC3 cells were incubated for 24 hrs, pre- treated with the Z-VAD inhibitor for 25 minutes prior to the addition of the 5 compounds. After 48 hrs, cells were harvested, re-suspended in Nicoletti buffer and DNA hypodiploidy analysed using an Accuri C6 flow cytometer (BD Biosciences). In agreement with the previous experiments, all of the thieno[2,3-*b*]pyridine inhibitors promoted apoptosis. Importantly, Z-VAD significantly reduced the drug induced apoptosis (Figure 4.8a and b) again demonstrating that cell death is as a result of caspase-dependent apoptosis.

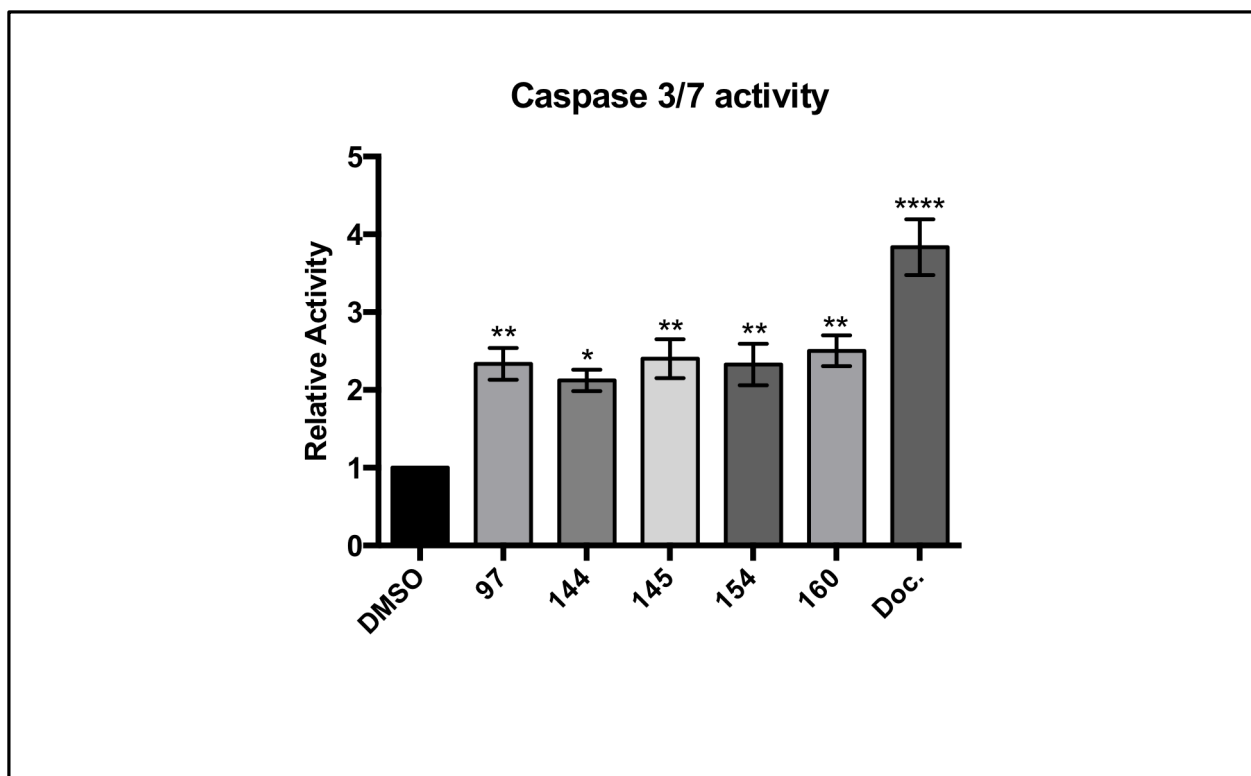


**Figure 4.7: The thieno[2,3-*b*]pyridine compounds promote caspase dependant cell death in PC3.** (a) PC3 cells were seeded at 30% confluence and incubated for 24 hrs prior to treatment with 1.0  $\mu$ M of the drugs (97, 144, 145, 154, 160 and Docetaxel) or DMSO control for 48 hrs. An ApoTox-Glo<sup>TM</sup> Triplex assay kit was used to assess Caspase 3/7 activity and luminescence measured using a microplate reader (FLUOstar Omega, BMG LABTECH, UK). ANOVA \*\*\*\* $p$ <0.00001, \*\* $p$ <0.001, \* $p$ <0.01. Mean  $\pm$  1SE.



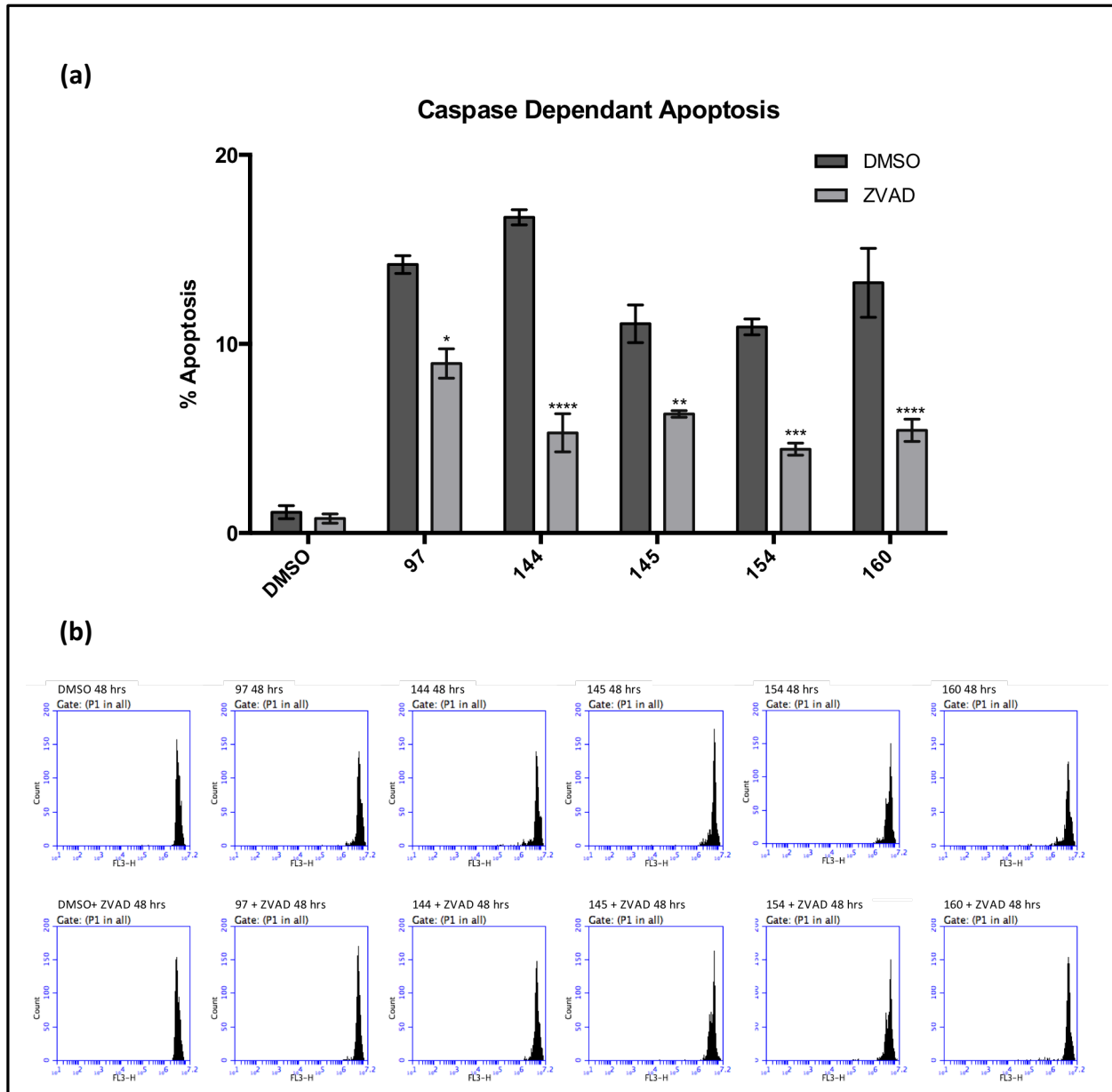


**Figure 4.8: The caspase inhibitor Z-VAD reduces thieno[2,3-*b*]pyridine-induced apoptosis.** (a) PC3 cells were seeded at 30% confluence and incubated for 48 hrs prior to treatment with 1.0  $\mu$ M of the drugs (97, 144, 145, 154 and 160) or DMSO for further 48 hrs. Cells were harvested and DNA hypodiploidy measured using flow cytometry. (b) Representative histograms generated using the Accuri C6 software (BD Biosciences). ANOVA \*\*\*\* $p < 0.00001$ , \*\*\* $p < 0.0001$ , \*\* $p < 0.001$ , \* $p < 0.01$ . Mean  $\pm$  1SE.

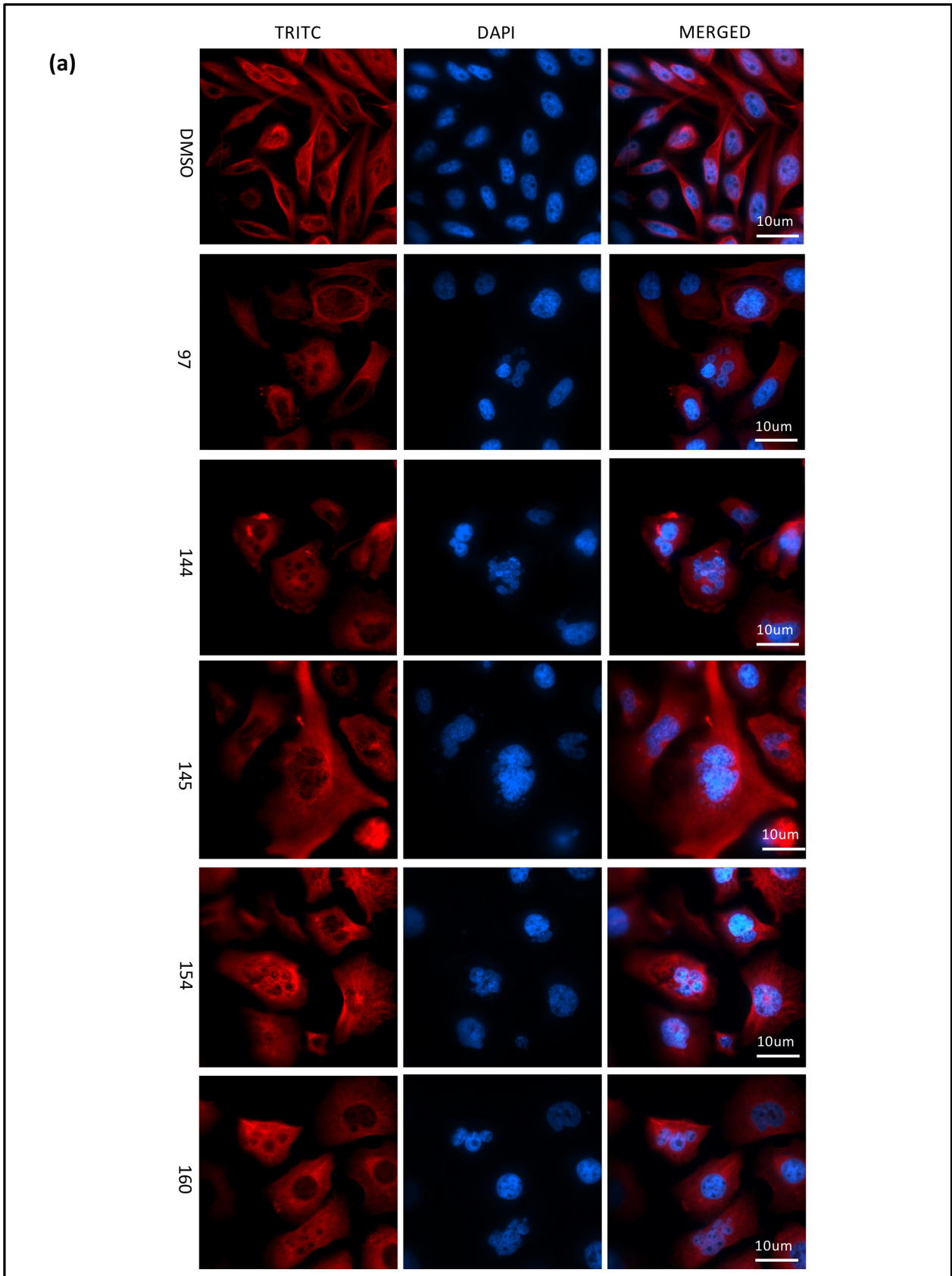
#### **4.7 Thieno[2,3-*b*]pyridine inhibitors increase PC3 cell size and promote multi-nucleation**

The thieno[2,3-*b*]pyridine inhibitors have been previously demonstrated to alter BCa cell morphology and to promote multinucleation, which is likely to explain the anti-proliferative and pro-apoptotic effects described above (Reynisson *et al.*, 2016). To see if this also occurs in PCa lines, PC3 were plated at 30% confluence on cover slips and treated with 1.0  $\mu$ M of the inhibitors 97, 144, 145, 154 and 160 for 24 hrs. Cells were fixed and immunofluorescence performed using anti- $\alpha$ -tubulin. Coverslips were mounted with the nuclear stain DAPI and cells visualised using confocal microscopy. All thieno[2,3-*b*]pyridine compounds appeared to affect cell morphology, with an increase in cell size and multinucleation, in comparison to the control DMSO (Figure 4.9a and b). Furthermore, it also appeared that the inhibitors promoted microtubule depolymerisation. Following treatment with compound 145 for example, tubulin appears to be more diffusely localised than vehicle only treated cells.

To quantify the morphological changes seen (cell size and multinucleation), cover slips were visualised at a lower magnification (x10 objective) and 5 images were examined for each treatment. All inhibitors were found to increase cell size (Figure 4.10a) and significantly increase the percentage of cells with multi-nucleation (Figure 4.10b). Flow-cytometry data demonstrated change in the cell population distribution after treatment with the anti-cancer inhibitors. After treating with DMSO, histograms illustrated most cells were predominantly in G1 phase, however, all inhibitors showed shift in cell population to G<sub>2</sub>/M phase. Also, another cell dot blot was identified at the top of the G<sub>2</sub>/M phase cells and was due to multinuclear cell formation (Figure 4.10 c).

Drugs were found to promote multinucleation, a similar phenotype was identified by

Reynisson *et al.*, (2016) when these inhibitors were tested in BCa cell lines. Furthermore, it has been demonstrated that changes in microtubule assembly inhibits cytokinesis, promoting multinucleation (Bhattachaya and Cabral 2004). These findings therefore also fit with the earlier results that demonstrated that the thieno[2,3-*b*]pyridine inhibitors promote G<sub>2</sub>/M phase arrest. The thieno[2,3-*b*]pyridine derivatives were demonstrated to inhibit PCa proliferation and motility, and to promote caspase-dependant apoptosis. The drugs appear to exert these effects via regulation of the cytoskeleton, which had a subsequent effect upon cell cycle progression and cell morphology. further experiments are required to characterise the inhibitors target(s) and the safety of these inhibitors in additional pre-clinical models.



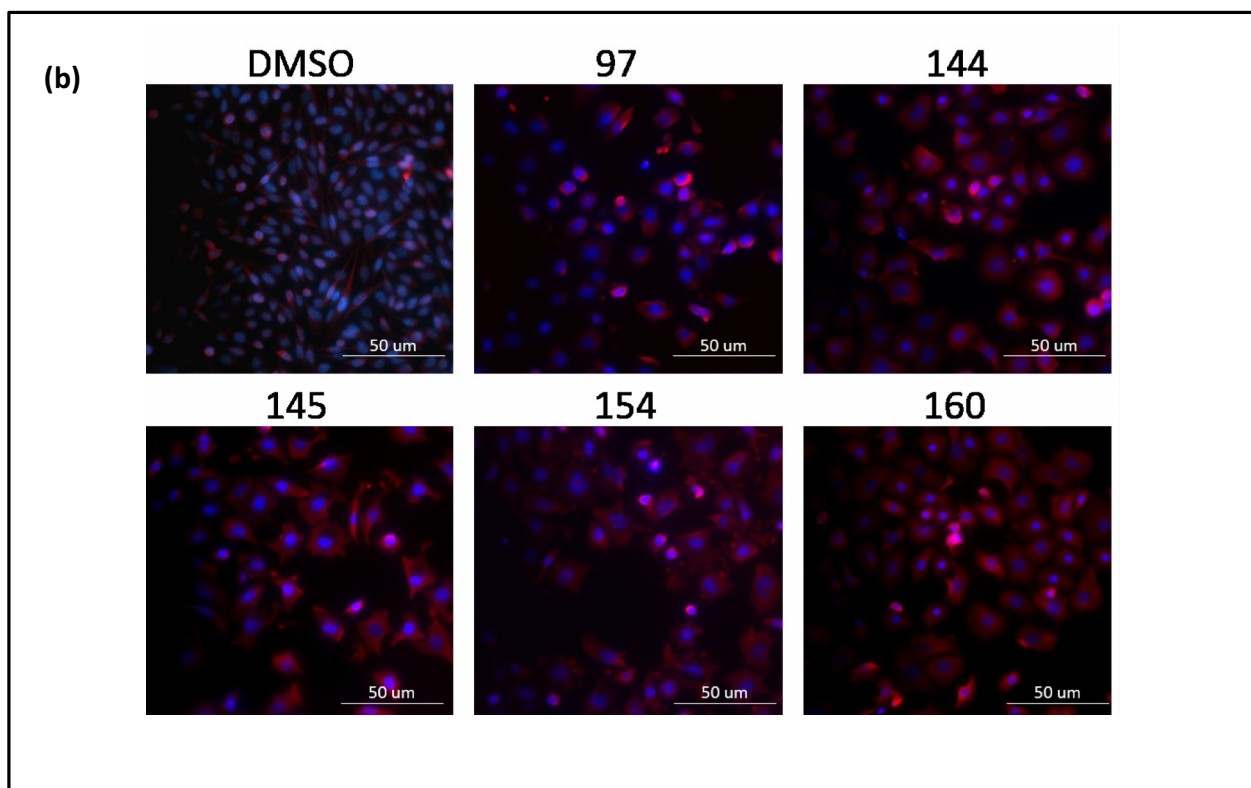


**Figure 4.9: Confocal microscopy analysis for PC3 cell line investigating thieno[2,3-*b*]pyridine inhibitors.** PC3 cells were seeded for 24 hrs on cover slips then treated with (1.0  $\mu$ M) of the drugs (DMSO, 97, 144, 145, 154 and 160) for further 24 hrs. Cells were fixed with 4 % paraformaldehyde and methanol following 1 hr of treatment with primary  $\alpha$ -tubulin and secondary  $\alpha$ -TRITC antibodies. Confocal microscopy was used to visualise the localisation of tubulin (red). Nuclear staining = 4',6-diamidino-2-phenylindole (DAPI) in blue. (a) Cells visualised at x60 objective. (b) Cells were visualised at x10 objective.

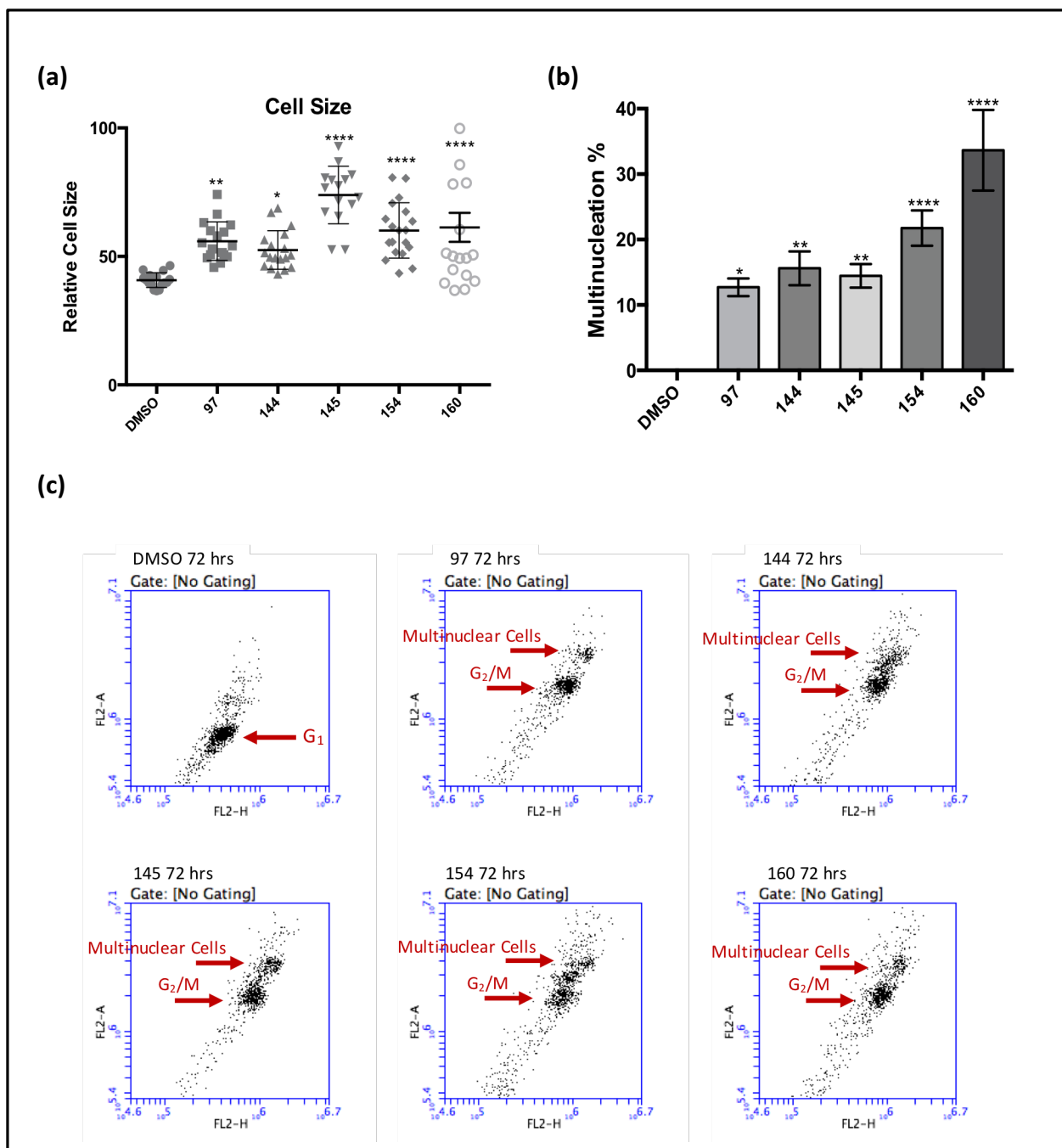


**Figure 4.10: Thieno[2,3-*b*]pyridine inhibitors increase cell size and promote multi-nucleation.** PC3 cells were seeded on cover slips and treated with (1.0  $\mu$ M) of the drugs (97, 144, 145, 154 and 160) or DMSO for 24 hrs. Cells were fixed with 4 % paraformaldehyde and methanol and immunofluorescence performed using an antibody specific for  $\alpha$ -tubulin and a secondary  $\alpha$ -TRITC antibody. Confocal microscopy was used at x10 objective and 5 images were taken for each treatment to quantify (a) cell size and (b) multi-nucleation. (c) Flow cytometry dot blots representing highlighting cells in G<sub>1</sub> or G<sub>2</sub>/M and multinuclear cells. Dot blots generated using Accuri C6, BD Biosciences software. ANOVA \*\*\*\*p<0.00001, \*\*p<0.001, \*p<0.01. Mean  $\pm$  1SE.

#### 4.8 Thieno[2,3-*b*]pyridine inhibitors reduce PC3 motility

PLC enzymes have been demonstrated to be important in regulating numerous cell processes, including cell migration and invasion (Béziau *et al.*, 2015; Cai *et al.*, 2017; Lattanzio *et al.*, 2013). To investigate which of the compounds can inhibit cell motility, PC3-GFP cells (cells stable transfected GFP) were seeded at 10% confluence in 96 well-plates for 24 hrs then treated with a sub-toxic concentration (0.1  $\mu\text{M}$ ) of the inhibitors for 48 hrs. Cell motility was quantified using a Nikon Eclipse T7 wide-field microscope for 24 hrs using time-lapse photography single cell tracking. The speed of the cells in untreated cells was found to be approximately 0.2  $\mu\text{m}/\text{min}$  and this was reduced to approximately 0.1 $\mu\text{m}/\text{min}$  following treatment with the inhibitors (Figure 4.11a). The cell tracking videos were further analysed using TrackMate (Image J) (Tinevez *et al.*, 2017). The images generated provides a summary of the cell tracking data and demonstrates that the inhibitors reduced cell motility (Figure 4.11b). Inhibitors affect cytoskeleton dynamics and therefore reduce cell motility. Time-lapse photography was performed using sub-lethal concentrations of the compounds. PC3 cell motility was significantly decreased in response to all of the compounds. Investigation of the effect of these compounds in *in vivo* models of PCa metastasis should be used to further characterise the effects of these compounds.

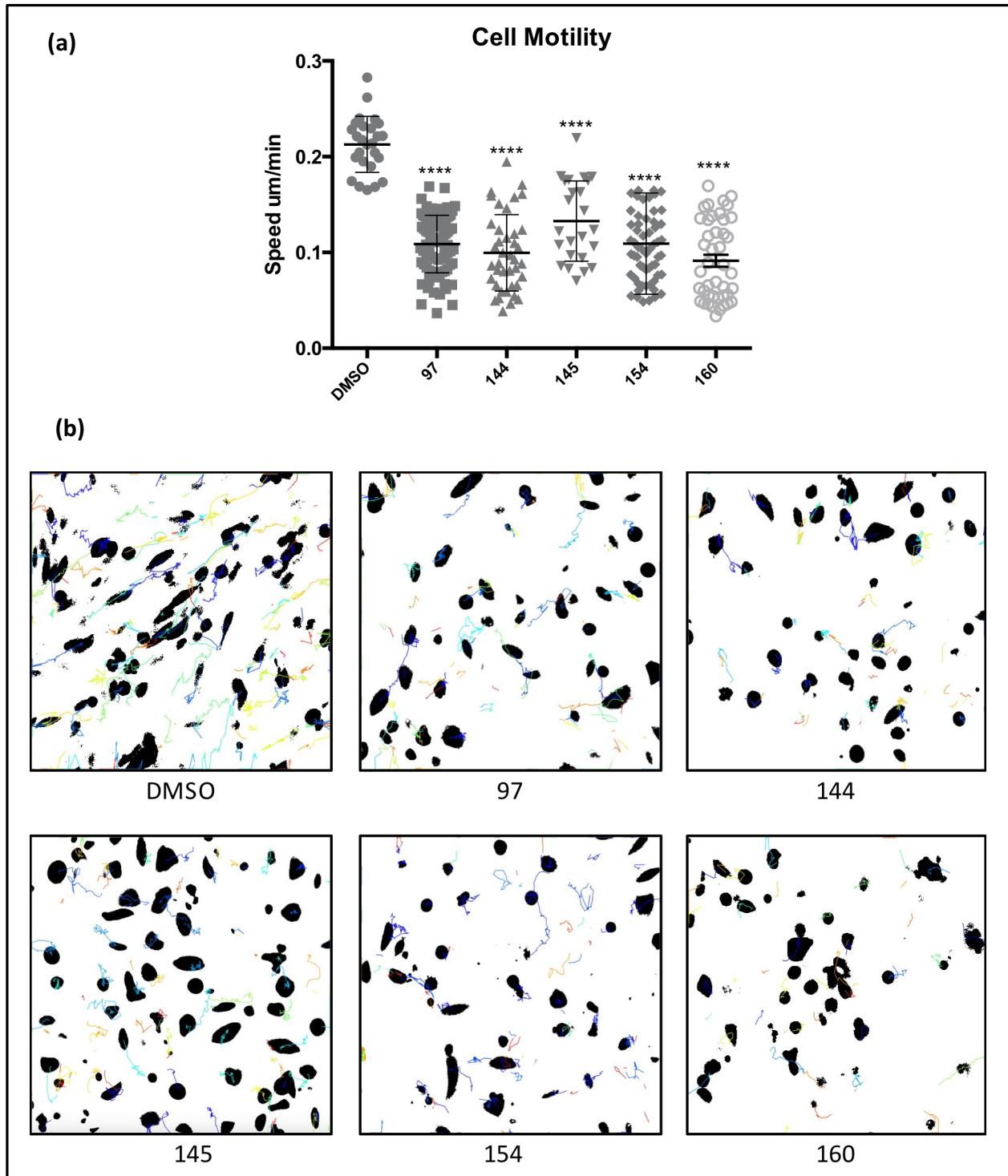


**Figure 4.11: The thieno[2,3-*b*]pyridine inhibitors reduce cell motility.** (a) PC3-GFP cells were incubated for 24 hrs prior to treatment with 0.1  $\mu$ M of the drugs (97, 144, 145, 154 and 160) or DMSO for 48 hrs. Images for all treatment and control were acquired every 15 min for 24 hrs, mean of cell speed ( $\mu$ m/frame) calculated from time-laps sequences. (b) Images show tracks of PC3-GFP cells after treatment with the Thieno[2,3-*b*]pyridine inhibitors, images were acquired using TrackMate (Image J) . ANOVA \*\*\*\* $p < 0.00001$ . Mean  $\pm$  1SE.



#### **4.9 The thieno[2,3-*b*]pyridine 160 inhibits human prostate tumours**

After characterising the inhibitory effect of the thieno[2,3-*b*]pyridine derivatives in PCa cell lines, the effect of the compounds was investigated in a more physiologically relevant model, namely human derived prostate cancer explants (Centenera *et al.*, 2012). This experiment was done in collaboration with Dr. Damien Leach and Prof. Charlotte Bevan (Imperial Collage London). Compound 160 was selected to be tested in this model system due to its high potency in the majority of cell line experiments performed. Prostate tissue from PCa patients was dissected and seeded on a collagen sponge in 24 well-plates. The explants were treated with compound 160 (100 nM) or the antiandrogen Enzalutamide (Enza), and incubated at 37°C for 48 hrs. The tumours were lysed, RNA harvested and qPCR performed to investigate the expression of the caspase 3 and PCNA. Results demonstrated inhibition in proliferation in 4 tissues when treated with compound 160, while Enza reduced cell growth in 3 samples.

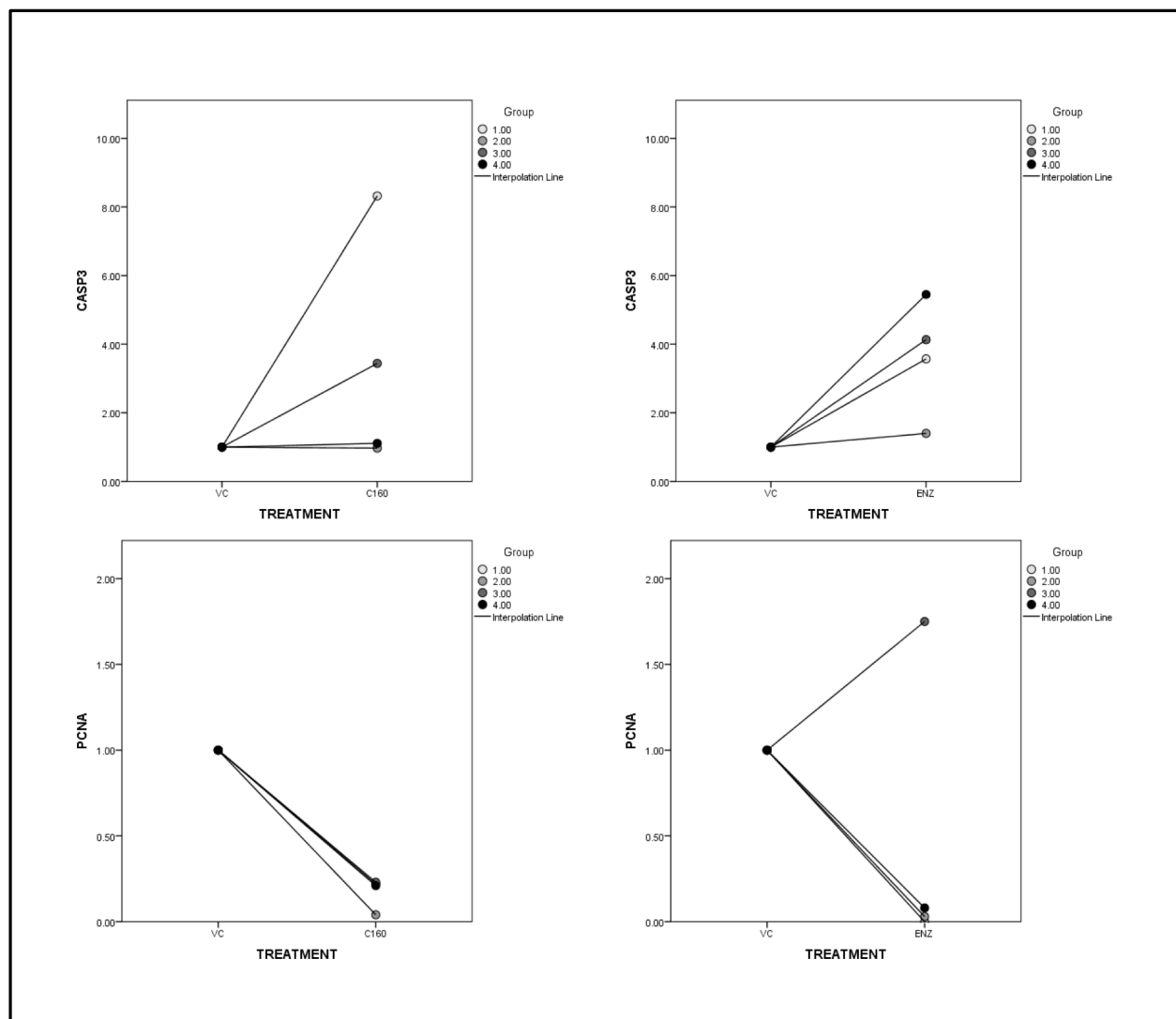


**Figure 4.12: The thieno[2,3-*b*]pyridine 160 anti-cancer inhibit activity in cultured human prostate tumours.** Tumour dissected into 1-mm<sup>3</sup> pieces then treated with the drugs (160 and Enza) and incubated for 48 hrs. Harvested RNA was reverse transcribed into cDNA and qPCR analysis performed using SYBR green to measure the expression levels of caspase 3 and PCNA. VC: Vehicle control and Enza: Enzalutamide.

#### **4.10 Investigation of the thieno[2,3-*b*]pyridine inhibitors bind to PLC- $\delta$**

The thieno[2,3-*b*]pyridine derivatives were designed to bind to PLC- $\delta$ , however no investigations beyond the computational level have been performed to confirm their specificity. To investigate this, drug-biotin pull-down experiments were performed. To facilitate this, additional compounds were synthesised by Drs Reynisson and van Rensburg and Prof Barker (University of Auckland). These drugs were designed with similar specifications as the thieno[2,3-*b*]pyridine compounds previously used, but were modified specifically for this experiment (Table 2.12). PC3-GFP cells were incubated for 24 hrs then treated with 20  $\mu$ M of the drug (DMSO, DJ0199 (-ve control), DJ0232 (biotinylated) and DJ0233 (inactive)) for 24 hrs. Lysed cells were sent for Mass Spectrometry (Dr Metodi Metodiev) (LTQ Orbitrap Velos) and obtained data analysed in Table 4.3. Proteins that were only pulled-down by the active compound were considered as positive hits. It therefore appears that these compounds do not bind to PLCs as expected and instead may mediate their effects via binding to multiple proteins, many of which are involved in the cytoskeletal organisation. Proteins identified by quantitative mass spectrometry illustrated potential target(s) of the anti-cancer compounds, but surprisingly none of these were PLC family members. However, the targets identified do fit with the phenotype observed, being important in e.g. regulating apoptosis, the p53/TP53 tumour suppressor and DNA damage repair. Furthermore, other proteins were found to be involved in cytoskeletal organization, actin dynamics and cell cycle progression all linked to cause similar damages to cells when manipulated.

**Table 4.3: Biotin pull-down analysis of the thieno[2,3-*b*]pyridine compounds.** Data analysis for the top hit proteins after Mass Spectrometry performed for thieno[2,3-*b*]pyridine derivatives. PC3-GFP treated with 20  $\mu$ M of the drugs (DJ0199, DJ0232 and DJ0233) and DMSO for 24 hrs. Biotin pull-down was performed, summery of pulled-down proteins and their function obtained from UniPort and The Human Protien Atlas.

<i>No.</i>	<i>Protein (Gene)</i>	<i>Molecular Function</i>	<i>Cellular Localisation</i>
1	Translational activator GCN1 (GCN1L1)	Mediated reprogramming of amino acid biosynthetic gene expression to alleviate nutrient depletion.	Ribosomes
2	Ras GTPase-activating-like protein (IQGAP1)	Plays a crucial role in regulating the dynamics and assembly of the actin cytoskeleton.	Nucleus and plasma membrane
3	E3 ubiquitin-protein ligase HUWE1 (HUWE1)	Regulates apoptosis by catalysing the polyubiquitination and degradation of MCL1. Also ubiquitinates the p53/TP53 tumour suppressor.	Cytoplasm
4	E3 ubiquitin-protein ligase UBR4 (UBR4)	Involved in membrane morphogenesis and cytoskeletal organization.	Membrane structures involved in actin motility
5	Eukaryotic translation initiation factor 5A; Eukaryotic translation initiation factor 5A-1; Eukaryotic translation initiation factor 5A-2 (EIF5A)	Involved in actin dynamics and cell cycle progression, functions as a regulator of p53/TP53 and p53/TP53-dependent apoptosis. Also regulates TNF-alpha-mediated apoptosis. Mediates effects of polyamines on neuronal process extension and survival. May play an important role in brain development and function, and in skeletal muscle stem cell differentiation.	Nucleus
6	26S proteasome non-ATPase regulatory subunit 12 (PSMD1)	Proteasome participates in numerous cellular processes, including cell cycle progression, apoptosis, or DNA damage repair.	Cytosol and nucleus
7	Abl interactor 1 (ABI1)	Role in the regulation of EGF-induced Erk pathway activation. Involved in cytoskeletal reorganization and EGFR signalling.	Nucleus
8	RNA-binding protein (FUS)	DNA/RNA-binding protein that plays a role in various cellular processes such as transcription regulation, RNA splicing, RNA transport, DNA repair and damage response.	Nucleus

## 4.11 Discussion

PCa can be effectively managed when diagnosed in the early stages of the disease. Once the tumour has spread from the prostate capsule, the disease is often treated with hormone therapy (Mostaghel *et al.*, 2009). This therapy is initially successful in the majority of patients, however it has been demonstrated that these therapies invariably fail within 2-3 years and the tumours progress to the CRPC stage (Cookson *et al.*, 2013). Many mechanisms have been proposed to explain CRPC, including AR mutations or overexpression or activation of the AR by alternative signalling pathways (Brooke *et al.*, 2008). There are few treatment options for CRPC and hence there is a great need for novel therapeutics for this stage of the disease.

### 4.11.1 Thieno[2,3-*b*]pyridine derivatives potently inhibit PCa cell line proliferation

Reynisson *et al.*, (2009) proposed PLCs as potential targets for the treatment of cancer due to their essential role in many transduction pathways and regulation of numerous cell processes. The thieno[2,3-*b*]pyridine derivatives were developed following a computational screen to identify novel inhibitors of PLC- $\delta$  (Reynisson *et al.*, 2009). These compounds have been investigated in BCa cell lines and were found to potently reduce proliferation, promote G<sub>2</sub>/M cell cycle arrest and to decrease cell motility (Leung *et al.*, 2016). To investigate if these inhibitors are effective in PCa, the efficacy of the inhibitors (97, 144, 145, 154 and 160) was investigated in a PCa cell line panel and cultured human prostate tumours. Growth assays demonstrated that all of the inhibitors inhibit proliferation. Compounds 144 and 160 were found to be the most potent inhibitors in reducing cellular proliferation. This result fits with Reynisson

*et al.*, (2016) findings, as they investigated these inhibitors against the BCa cell lines (MCF-7, T47D, MDA-MB-231 and MDA-MB-468) and drugs 144 and 160 were the most effect in these lines.

The IC<sub>50</sub> values suggest that the compounds may show some specificity for cancer cells, as this was witnessed in BCa (Reynisson *et al.*, 2016). The drugs appeared to have some selectivity for cancer cells, as BPH1 was inhibited less than the cancer cell lines. However, PNT1A (SV40 immortalised normal prostate) had similar sensitivity to the cancer cell lines. The selectivity of these compounds therefore needs to be investigated further with other control lines. Importantly, these compounds have been tested in mouse models and were found to be well tolerated (Leung *et al.*, 2016). Although all of the inhibitors share a similar core structure there were differences in potency. For example, compounds 145 and 154 were found to be less potent than the other compounds tested. The difference in potency between compounds is not clearly understood, however, differences in the side chain bound to the benzene ring could be affecting their binding to target sites.

The testing of the inhibitors in the cell lines models demonstrated that these compounds have the potential to be novel therapeutics for the treatment of PCa. To test these compounds in a more physiologically relevant model, the effect of compound 160 was investigated in human PCa explants. In agreement with the cell line data, compound 160 increased the expression of a pro-apoptotic marker (caspase 3) and decreased a mitotic marker (PCNA) in the explant model. This effect was compared to Enzalutamide, an antiandrogen which is used clinically for the treatment of PCa. In the 4 tissues examined, compound 160 was able to reduce the proliferation of all samples whereas Enzalutamide inhibited the growth of 3 tissues. Compound 160 therefore appears to have similar, if not better, efficacy to Enzalutamide.

#### **4.11.2 Thieno[2,3-*b*]pyridine derivatives promote caspase-dependant apoptosis in PC3**

As previously described, the exact mechanism of cell death is dependent upon many factors. Two pathways are of particular relevance in the treatment of cancer, namely programmed cell death (apoptosis) and necrosis (Ricci and Zong 2006; Ouyang *et al.*, 2012). It was therefore of interest to characterise the mechanism of cell death induced by the thieno[2,3-*b*]pyridine inhibitors. The DNA hypoploidy assay indicated that PC3 cells undergo apoptosis in response to treatment with the inhibitors and the percentage of cell death increased over the time course. Furthermore, PI inclusion assays demonstrated that necrosis/necroptosis was not induced. Activation of caspases, as a result of a protease cascade, is an indication of apoptotic pathway activation and caspase 3/7 activity is often used as a measure of apoptosis (Degterev *et al.*, 2003). To confirm that the thieno[2,3-*b*]pyridine inhibitors promote cell death via activation of caspases, caspase 3/7 activity was assessed. As expected, caspase 3/7 activity was found to be enhanced in response to the compounds. The caspase inhibitor Z-VAD was included in the flow cytometry analysis to further confirm that the thieno[2,3-*b*]pyridine inhibitors promote cell death via caspase activation. This drug binds to the catalytic site of caspase proteases and inhibits cascade-dependent apoptosis. As expected, the inhibitor reduced the level of apoptosis induced by the thieno[2,3-*b*]pyridine compounds. This result confirms that cell death in PC3 is via apoptosis. Leung *et al.*, (2016) indicated that the thieno[2,3-*b*]pyridine inhibitors cause cell cycle arrest in the G<sub>2</sub>/M phase in the MDA-MB-231 BCa cell line. In agreement with this, analysis of the cell cycle demonstrated that PC3 cells also undergo a G<sub>2</sub>/M phase arrest in response to the inhibitors.

### 4.11.3 Anti-cancer drugs affect on cell morphology impact PC3 cell motility

As previously described, the thieno[2,3-*b*]pyridine derivatives were developed to target PLC- $\delta$  (Reynisson *et al.*, 2009), however the phenotype observed suggested that the inhibitors could be targeting PLC- $\gamma$  due to its role in microtubule and spindle fibre formation, and its importance in PCa (Castedo *et al.*, 2004; Lattanzio *et al.*, 2013). Little is known about PLC expression in PCa and hence the expression of all isoforms was measured using qPCR. The majority of the different PLC isoforms were expressed in the PCa cell lines, however the isoform with the highest expression in most cell lines was PLC- $\gamma$ . This result correlates with a previous study, which demonstrated that this isoform is highly expressed in PCa (Lattanzio *et al.*, 2013).

To confirm what target the inhibitors bind to, the inhibitors were biotinylated and drug-protein complexes were pulled-down. The proteins were subsequently identified by quantitative mass spectrometry, the pull-down identified potential target(s) of the anti-cancer compounds, but surprisingly none of these were PLC family members. However, the targets identified do fit with the phenotype observed, being important in e.g. regulating apoptosis, the p53/TP53 tumour suppressor and DNA damage repair. Also, other proteins were found to be involved in cytoskeletal organization, actin dynamics and cell cycle progression.

The flow cytometry analysis investigating the effect of the inhibitors upon cell cycle suggested that the drugs may promote multinucleation. A similar phenotype was identified by Reynisson *et al.*, (2016) when these inhibitors were tested in BCa cell lines. Immunofluorescence imaging identified morphological changes, increased cell size and multinucleation, in the PC3 cell line following treatment with all 5 compounds. Interestingly, it also appeared that the compounds may be affecting microtubule dynamics. Microtubule integrity is crucial in mitotic



spindle formation and is important for normal cell division (Kimura *et al.*, 2013). It has been demonstrated that changes in microtubule assembly inhibits cytokinesis, promoting multinucleation (Bhattachaeaya and Cabral 2004). Therefore, disruption of this process is likely to result in G<sub>2</sub>/M arrest and multinucleation. These findings therefore also fit with the earlier results that demonstrated that the thieno[2,3-*b*]pyridine inhibitors promote G<sub>2</sub>/M phase arrest.

Metastatic spread is a significant issue in the management of cancer. The identification of inhibitors that can block cell motility is therefore of interest. Since the inhibitors appeared to affect cytoskeleton dynamics, these compounds were tested to investigate if they could reduce cell motility. Time-lapse photography was therefore performed using sub-lethal concentrations of the compounds. PC3 cell motility was significantly decreased in response to all of the compounds. Investigation of the effect of these compounds in *in vivo* models of PCa metastasis should be used to further investigate the effects of these compounds (Havens *et al.*, 2008).

In conclusion, the thieno[2,3-*b*]pyridine derivatives were demonstrated to inhibit PCa proliferation and motility, and to promote caspase-dependant apoptosis. The drugs appear to exert these effects via regulation of the cytoskeleton, which had a subsequent effect upon cell cycle progression and cell morphology. The drugs appear to be potent and are effective at low concentrations, in the nanomolar range. The drugs also showed some specificity for cancer cells compared to the non-tumorigenic control BPH1 and were demonstrated to be effective in patient samples. Despite that the majority of the experiments done on these compounds were investigated in a PCa cell line panel and cultured human prostate tumours, the preliminary data is encouraging. However, more experiments are needed to encounter variations between cell lines and patient's tissues such as: different origins of cells for certain cell lines and variety in metastasis intensity. Finally, inhibitors target(s) and the safety of these inhibitors must be further

investigated in additional pre-clinical models for drug toxicity and effect on macro systems environments.

## CHAPTER 5

### CONCLUSION

#### 5.1 The role of the Androgen Receptor in Breast Cancer

The role of the AR in BCa has received increased interest in recent years and a number of clinical trials have been completed/ongoing to investigate if AR targeting could be an effective treatment option for the disease (Chia *et al.*, 2015). Importantly, the role of the AR in BCa has been demonstrated to be subtype dependant (Yeh *et al.*, 2003). In AR and ER $\alpha$ -positive disease, androgens were previously trialled as a treatment options. However, this therapeutic strategy fell out of favour due to the high risk of oestrogens aromatization and the virilising patterns witnessed in patients (Boni *et al.*, 2014; Cops *et al.*, 2008). More recently, AR targeting has focused on the inhibition of AR in molecular apocrine disease. For example, a clinical trial was conducted in 26 AR-positive ER/PR-negative BCa patients, targeting AR with the antagonist Bicalutamide (BIC). Following 24 weeks of the treatment, the clinical benefit rate (CBR) was 19% and the median progression free survival (PFS) was 12 weeks. This finding has established a potential therapeutic strategy, and supports further development of AR-targetting therapeutic strategies for this subtype of the disease.

Enzalutamide (Enza) is an antiandrogen that has recently been introduced clinically for the treatment of advanced PCa and has been shown to have greater survival rates compared to the previously used chemotherapies e. g. Docetaxel. Enza binds to the AR LBD leading to an inhibition in nuclear translocation and cofactor recruitment (Tran *et al.*, 2009). Enza was clinically investigated in advanced AR-positive BCa and was demonstrated to have a greater efficacy in tumour inhibition than BIC (Siemens *et al.*, 2018). Enza was also well tolerated in

patients and the study reported 29% CBR at 24 weeks with 14.7 median PFS, hence further analysis of the drug in AR-positive BCa is on-going (Rampurwala *et al.*, 2016).

Currently, multiple agents are under investigation for AR-positive BCa. TAK-700 is nonsteroidal drug that acts as a selective inhibitor and it has been found to be effective in CRPC (Fizazi *et al.*, 2015). A phase 2 study with this inhibitor is undergoing clinical trials in TNBC (NCT01990209). Further, VT-474 is another drug in ongoing trials that is a second-generation CYP17 inhibitor (important in androgen synthesis) and is being investigated in multiple subtypes of male and female BCa (NCT02580448). Additionally, combinations of AR antagonists with other therapeutic agents have been demonstrated to have additive effects. Administration of BIC with an inhibitor for PI3K, commonly mutated in AR-positive TNBC, showed convincing results in preclinical studies which has led to the initiation of clinical trials to assess this regime (Lehmann *et al.*, 2014). The PI3K inhibitor Taselisib in combination with Enza is also currently in an ongoing study in advanced TNBC patients (NCT02457910).

Several selective AR modulators (SARMs), which have tissue and transcriptome specificity, also appear to have activity in TNBC. C1-4AS-1, for example, is a SARM that inhibits the proliferation of TNBC in preclinical models. This drug binds to the LBD similar to DHT, but regulates different genes resulting S phase arrest and cell death (Ahram *et al.*, 2018; Moore *et al.*, 2012).

A number of trials are also investigating AR targetting as treatment options even for ER-positive disease. RAD140 is a nonsteroidal SARM that behaves as an AR agonist. This compound has been demonstrated to have anti-tumour effects *in vivo* in AR/ER-positive BCa models (Yu *et al.*, 2017). This novel drug was found potent with and without the administration

with other agent inhibitors such as palbociclib. Enobosarm is another SARM that is undergoing clinical trials in both ER-positive (NCT02463032) and TNBC (NCT02368691) BCa, where preliminary data indicated promising effects in stabilising the disease. Further, Cyp17A1 has been targeted in clinical trials by abiraterone acetate to inhibit androgen and oestrogen signalling in ER-positive BCa (Narayanan and Dalton, 2016). However, no significant clinical activity was demonstrated, which was attributed to increased levels of progesterone in the serum of patients.

Characterisation of AR-ER $\alpha$  cross-talk also contributes to our understanding of how best to target the AR in BCa (e.g. activate or inhibit). It has been demonstrated that the sequence homology of the ARE is less restricted than ERE resulting in the AR being more able than ER $\alpha$  to bind to response elements other than AREs (Jia *et al.*, 2008). Peters *et al.*, (2009) demonstrated that the AR DBD domain is essential for the inhibition of ER $\alpha$  activity, presumably via competition for DNA binding. However, the data presented suggests that ER $\alpha$  does not repress AR activity via competition for DNA binding. This was demonstrated via the use of an ER $\alpha$  mutant that is unable to bind DNA due to a mutation in one of the zinc fingers. This mutant was still able to repress AR activity suggesting that competition for DNA binding is not a mechanism of repression. Equally, a mutation in the NLS of ER $\alpha$ , which blocks nuclear localisation, was also able to repress AR activity. There is therefore little information on which target genes are affected by this cross-talk and this study suggests that not all genes will be affected. Instead the cross-talk is likely to be gene specific and therefore a more global analysis of gene expression (e.g. RNA-Seq) would be informative.

Investigation of AR-ER $\alpha$  cross-talk also contributes to our understanding of how best to target the AR in BCa. The data presented in This thesis suggests that ER $\alpha$  does not repress AR

activity via competition for DNA binding. It is therefore possible that competition for cofactors is the mechanism by which ER $\alpha$  represses AR activity. In addition, this study also investigated the role of AR mutations in BCa. Assessment of receptor transcriptional activity and cellular inhibition demonstrated the effect of these substitutions upon receptor function. AR mutations that resulted in a constitutively active and transcriptionally dead receptor were identified. A constitutively active receptor could drive molecular apocrine growth, whereas a transcriptionally dead receptor may not be able to compete with ER $\alpha$  to block growth facilitating E2 induced growth in ER $\alpha$  positive disease. This aids more advanced disease for patients who recieved antiandrogen treatment to see if they have acquired any of the AR mutations invistigated in this study in response to the therapy.

In addition to receptor cross-talk, this study also investigated the role of AR mutations in BCa. Assessment of receptor transcriptional activity and cellular inhibition demonstrated the effect of these substitutions upon receptor function. AR mutations that resulted in a constitutively active and transcriptionally dead receptor were identified. A constitutively active receptor could drive molecular apocrine growth, whereas a transcriptionally dead receptor may not be able to compete with ER $\alpha$  to block growth facilitating E2 induced growth in ER $\alpha$  positive disease. It is therefore important to further chatacterise the importance of AR mutations in BCa. Also inistigating more advanced disease and patients that have recieved antiandrogen treatment to see if they have acquired AR mutations in response to the therapy.

## **5.2 The development of novel targeted therapies for the treatment of prostate cancer**

There are few therapeutic options for therapy resistant PCa. Docetaxel and Cabazitaxel are chemotherapies which are given to patients with hormone refractory disease and these aim to prolong survival rates (Oudard *et al.*, 2017). Administration of the new generation of hormonal therapies, Enzalutamide and Abiraterone, has been found to provide improved survival rates in metastatic CRPC (Ohlmann *et al.*, 2017). However, resistance to these therapies, de novo and acquired, is also associated with these antagonists (Pal *et al.*, 2018; Watson *et al.*, 2015). An ongoing clinical trial combining Enza with Metformin aims to target the AR along with a mechanisms of therapy resistance (autophagy mechanisms) (NCT02339168). Metformin is a clinical drug used for the type 2 diabetes mellitus patients and has been demonstrated to have effects against tumour cells such as induction of apoptosis, autophagy and cell cycle arrest (Zi *et al.*, 2018). Preliminary efficacy data from the trial reported that the combination is well tolerated and recommended continuation of the study.

In this thesis, thieno[2,3-*b*]pyridine derivatives were investigated as novel therapeutics for PCa. These were demonstrated to successfully inhibit PCa proliferation and motility and to induce apoptosis. These compounds were potent at low concentrations and found to effect cell cycle progression and cell morphology, possibly as a result of regulation of the cytoskeleton. The anti-cancer derivatives cause G2 arrest and multinucleation, it is therefore hypothesized that the inhibitors promote their effects via deregulation of the cytoskeleton, which subsequently affects cell division, resulting in multinucleation, which leads to apoptosis. The specificity of the drugs for cancer cells remains to be clarified, as although the drugs had lower IC<sub>50</sub> concentrations compared to cancer cells, the IC<sub>50</sub> concentrations of drugs in PNT1A was similar to the

tumorigenic lines. It is therefore possible that the compounds could have significant side effects *in vivo* and this will need to be assessed using *in vivo* models prior to progression to clinical trials.

The anti-cancer drugs appear to exert their effects via regulation of the cytoskeleton, which had a subsequent effect upon cell cycle progression and cell morphology. The drugs appear to be potent and are effective at low concentrations, in the nanomolar range. The drugs also showed some specificity for cancer cells compared to the non-tumorigenic control BPH1 and were demonstrated to be effective in patient samples. Although the compounds were originally designed to target PLC, this does not appear to be the case. The drug pull-down assay identified multiple potential targets, and characterisation of these targets will confirm which protein is the target. This is important to allow for further optimisation of the compounds. The inhibitors could be novel therapeutics for the treatment of PCa and CRPC, however more research is required, in particular to assess its safety and efficacy *in vivo*



### 5.3 Future work

In the BCa project, further investigation of AR-ER $\alpha$  cross-talk with other steroid receptors would be interesting. For example, the PR has an important role in some BCas subtypes and there is little knowledge of the cross-talk between these steroid receptors. Further, the development of endogenous systems to evaluate the effect of AR mutations will be useful. It would therefore be good to make fresh attempts to generate the CRISPR modified lines. More AR mutations have been identified in BCa, since the conclusion of this study. It will therefore be useful to repeat the studies presented here to investigate if these substitutions have a bearing upon receptor activity. Additionally, sequencing of BCa patient samples, particularly advanced stages of the disease, will be informative in determining the incidence and importance of AR mutations in BCa.

In the PCa project, investigation of the efficacy and safety of the thieno[2,3-*b*]pyridine inhibitors in pre-clinical animal models is essential. Further, the target(s) of these molecules need to be validated. Based on the results obtained from the experiments, the molecules can be further refined to increase specificity and potency. These experiments would then provide the necessary data to support progression to clinical trials.

## References

- Aaron, L., Franco, O. E. and Hayward, S. W. (2016) Review of Prostate Anatomy and Embryology and the Etiology of Benign Prostatic Hyperplasia. *Urol Clin North Am*, **43**, 279-88.
- Abate-Shen, C. and Shen, M. M. (2000) Molecular genetics of prostate cancer. *Genes Dev*, **14**, 2410-34.
- Abrahamsson, P. A. (1999) Neuroendocrine cells in tumour growth of the prostate. *Endocr Relat Cancer*, **6**, 503-19.
- Africander, D. J., Storbeck, K. H. and Haggood, J. P. (2014) A comparative study of the androgenic properties of progesterone and the progestins, medroxyprogesterone acetate (MPA) and norethisterone acetate (NET-A). *J Steroid Biochem Mol Biol*, **143**, 404-15.
- Ahram, M., Mustafa, E., Abu Hammad, S., Alhudhud, M., Bawadi, R., Tahtamouni, L., Khatib, F. and Zihlif, M. (2018) The cellular and molecular effects of the androgen receptor agonist, CI-4AS-1, on breast cancer cells. *Endocr Res*, **43**, 203-214.
- Ali, S. and Coombes, R. C. (2002) Endocrine-responsive breast cancer and strategies for combating resistance. *Nat Rev Cancer*, **2**, 101-12.
- Alluri, P. G., Speers, C. and Chinnaiyan, A. M. (2014) Estrogen receptor mutations and their role in breast cancer progression. *Breast Cancer Res*, **16**, 494.
- Andriole, G., Bruchofsky, N., Chung, L. W., Matsumoto, A. M., Rittmaster, R., Roehrborn, C., Russell, D. and Tindall, D. (2004) Dihydrotestosterone and the prostate: the scientific rationale for 5alpha-reductase inhibitors in the treatment of benign prostatic hyperplasia. *J Urol*, **172**, 1399-403.
- Anestis, A., Karamouzis, M. V., Dalagiorgou, G. and Papavassiliou, A. G. (2015) Is androgen receptor targeting an emerging treatment strategy for triple negative breast cancer? *Cancer Treat Rev*, **41**, 547-53.
- Arai, S., Jonas, O., Whitman, M. A., Corey, E., Balk, S. P. and Chen, S. (2018) Tyrosine Kinase Inhibitors Increase MCL1 Degradation and in Combination with BCLXL/BCL2 Inhibitors Drive Prostate Cancer Apoptosis. *Clin Cancer Res*, **24**, 5458-5470.
- Auffenberg, G. B., Helfand, B. T. and McVary, K. T. (2009) Established medical therapy for benign prostatic hyperplasia. *Urol Clin North Am*, **36**, 443-59, v-vi.
- Ayala, A. G. and Ro, J. Y. (2007) Prostatic intraepithelial neoplasia: recent advances. *Arch Pathol Lab Med*, **131**, 1257-66.
- Bain, D. L., Heneghan, A. F., Connaghan-Jones, K. D. and Miura, M. T. (2007) Nuclear receptor structure: implications for function. *Annu Rev Physiol*, **69**, 201-20.
- Bean, L. A., Ianov, L. and Foster, T. C. (2014) Estrogen receptors, the hippocampus, and memory. *Neuroscientist*, **20**, 534-45.
- Ben-Baruch, N. E., Bose, R., Kavuri, S. M., Ma, C. X. and Ellis, M. J. (2015) HER2-Mutated Breast Cancer Responds to Treatment With Single-Agent Neratinib, a Second-Generation HER2/EGFR Tyrosine Kinase Inhibitor. *J Natl Compr Canc Netw*, **13**, 1061-4.

- Berger, A. P., Deibl, M., Strasak, A., Bektic, J., Pelzer, A. E., Klocker, H., Steiner, H., Fritsche, G., Bartsch, G. and Horninger, W. (2007) Large-scale study of clinical impact of PSA velocity: long-term PSA kinetics as method of differentiating men with from those without prostate cancer. *Urology*, **69**, 134-8.
- Bergerat, J. P. and Céraline, J. (2009) Pleiotropic functional properties of androgen receptor mutants in prostate cancer. *Hum Mutat*, **30**, 145-57.
- Bertagnolo, V., Benedusi, M., Brugnoli, F., Lanuti, P., Marchisio, M., Querzoli, P. and Capitani, S. (2007) Phospholipase C-beta 2 promotes mitosis and migration of human breast cancer-derived cells. *Carcinogenesis*, **28**, 1638-45.
- Bhattacharya, R. and Cabral, F. (2004a) A ubiquitous beta-tubulin disrupts microtubule assembly and inhibits cell proliferation. *Mol Biol Cell*, **15**, 3123-31.
- Bhattacharya, R. and Cabral, F. (2004b) A ubiquitous beta-tubulin disrupts microtubule assembly and inhibits cell proliferation. *Mol Biol Cell*, **15**, 3123-31.
- Bitting, R. L. and Armstrong, A. J. (2013) Targeting the PI3K/Akt/mTOR pathway in castration-resistant prostate cancer. *Endocr Relat Cancer*, **20**, R83-99.
- Bockhorn, M., Jain, R. K. and Munn, L. L. (2007) Active versus passive mechanisms in metastasis: do cancer cells crawl into vessels, or are they pushed? *Lancet Oncol*, **8**, 444-8.
- Bonekamp, D., Jacobs, M. A., El-Khouli, R., Stoianovici, D. and Macura, K. J. (2011) Advancements in MR imaging of the prostate: from diagnosis to interventions. *Radiographics*, **31**, 677-703.
- Boni, C., Pagano, M., Panebianco, M., Bologna, A., Sierra, N. M., Gnoni, R., Formisano, D. and Bisagni, G. (2014) Therapeutic activity of testosterone in metastatic breast cancer. *Anticancer Res*, **34**, 1287-90.
- Bostwick, D. G., Burke, H. B., Djakiew, D., Euling, S., Ho, S. M., Landolph, J., Morrison, H., Sonawane, B., Shifflett, T., Waters, D. J. and Timms, B. (2004) Human prostate cancer risk factors. *Cancer*, **101**, 2371-490.
- Bott, S. R., Birtle, A. J., Taylor, C. J. and Kirby, R. S. (2003) Prostate cancer management: (1) an update on localised disease. *Postgrad Med J*, **79**, 575-80.
- Brinkmann, A. O., Faber, P. W., van Rooij, H. C., Kuiper, G. G., Ris, C., Klaassen, P., van der Korput, J. A., Voorhorst, M. M., van Laar, J. H. and Mulder, E. (1989) The human androgen receptor: domain structure, genomic organization and regulation of expression. *J Steroid Biochem*, **34**, 307-10.
- Brooke, G. N. and Bevan, C. L. (2009) The role of androgen receptor mutations in prostate cancer progression. *Curr Genomics*, **10**, 18-25.
- Brooke, G. N., Gamble, S. C., Hough, M. A., Begum, S., Dart, D. A., Odontiadis, M., Powell, S. M., Fioretti, F. M., Bryan, R. A., Waxman, J., Wait, R. and Bevan, C. L. (2015) Antiandrogens act as selective androgen receptor modulators at the proteome level in prostate cancer cells. *Mol Cell Proteomics*, **14**, 1201-16.
- Brooke, G. N., Parker, M. G. and Bevan, C. L. (2008) Mechanisms of androgen receptor activation in advanced prostate cancer: differential co-activator recruitment and gene expression. *Oncogene*, **27**, 2941-50.
- Bushman, W. (2009) Etiology, epidemiology, and natural history of benign prostatic hyperplasia. *Urol Clin North Am*, **36**, 403-15, v.

- Béziau, D. M., Toussaint, F., Blanchette, A., Dayeh, N. R., Charbel, C., Tardif, J. C., Dupuis, J. and Ledoux, J. (2015) Expression of phosphoinositide-specific phospholipase C isoforms in native endothelial cells. *PLoS One*, **10**, e0123769.
- Cai, S., Sun, P. H., Resaul, J., Shi, L., Jiang, A., Satherley, L. K., Davies, E. L., Ruge, F., Douglas-Jones, A., Jiang, W. G. and Ye, L. (2017) Expression of phospholipase C isozymes in human breast cancer and their clinical significance. *Oncol Rep*, **37**, 1707-1715.
- Cardillo, M. R. and Ippoliti, F. (2006) IL-6, IL-10 and HSP-90 expression in tissue microarrays from human prostate cancer assessed by computer-assisted image analysis. *Anticancer Res*, **26**, 3409-16.
- Carroll, J. S., Meyer, C. A., Song, J., Li, W., Geistlinger, T. R., Eeckhoutte, J., Brodsky, A. S., Keeton, E. K., Fertuck, K. C., Hall, G. F., Wang, Q., Bekiranov, S., Sementchenko, V., Fox, E. A., Silver, P. A., Gingeras, T. R., Liu, X. S. and Brown, M. (2006) Genome-wide analysis of estrogen receptor binding sites. *Nat Genet*, **38**, 1289-97.
- Castedo, M., Perfettini, J. L., Roumier, T., Andreau, K., Medema, R. and Kroemer, G. (2004) Cell death by mitotic catastrophe: a molecular definition. *Oncogene*, **23**, 2825-37.
- Centenera, M. M., Gillis, J. L., Hanson, A. R., Jindal, S., Taylor, R. A., Risbridger, G. P., Sutherland, P. D., Scher, H. I., Raj, G. V., Knudsen, K. E., Yeadon, T., Tilley, W. D., Butler, L. M. and BioResource, A. P. C. (2012) Evidence for efficacy of new Hsp90 inhibitors revealed by ex vivo culture of human prostate tumors. *Clin Cancer Res*, **18**, 3562-70.
- Cesaretti, J. A., Stone, N. N., Skouteris, V. M., Park, J. L. and Stock, R. G. (2007) Brachytherapy for the treatment of prostate cancer. *Cancer J*, **13**, 302-12.
- Chaitanya, G. V., Steven, A. J. and Babu, P. P. (2010) PARP-1 cleavage fragments: signatures of cell-death proteases in neurodegeneration. *Cell Commun Signal*, **8**, 31.
- Chan, S. C., Li, Y. and Dehm, S. M. (2012) Androgen receptor splice variants activate androgen receptor target genes and support aberrant prostate cancer cell growth independent of canonical androgen receptor nuclear localization signal. *J Biol Chem*, **287**, 19736-49.
- Chia, K., O'Brien, M., Brown, M. and Lim, E. (2015) Targeting the androgen receptor in breast cancer. *Curr Oncol Rep*, **17**, 4.
- Chuffa, L. G., Lupi-Júnior, L. A., Costa, A. B., Amorim, J. P. and Seiva, F. R. (2017) The role of sex hormones and steroid receptors on female reproductive cancers. *Steroids*, **118**, 93-108.
- Claessens, F. and Tilley, W. (2014) Androgen signalling and steroid receptor crosstalk in endocrine cancers. *Endocr Relat Cancer*, **21**, E3-5.
- Cookson, M. S., Roth, B. J., Dahm, P., Engstrom, C., Freedland, S. J., Hussain, M., Lin, D. W., Lowrance, W. T., Murad, M. H., Oh, W. K., Penson, D. F. and Kibel, A. S. (2013) Castration-resistant prostate cancer: AUA Guideline. *J Urol*, **190**, 429-38.
- Cops, E. J., Bianco-Miotto, T., Moore, N. L., Clarke, C. L., Birrell, S. N., Butler, L. M. and Tilley, W. D. (2008) Antiproliferative actions of the synthetic androgen, mibolerone, in breast cancer cells are mediated by both androgen and progesterone receptors. *J Steroid Biochem Mol Biol*, **110**, 236-43.
- Coutinho, I., Day, T. K., Tilley, W. D. and Selth, L. A. (2016) Androgen receptor signaling in castration-resistant prostate cancer: a lesson in persistence. *Endocr Relat Cancer*, **23**, T179-T197.

- Crumbaker, M., Khoja, L. and Joshua, A. M. (2017) AR Signaling and the PI3K Pathway in Prostate Cancer. *Cancers (Basel)*, **9**.
- Culig, Z., Hobisch, A., Cronauer, M. V., Radmayr, C., Trapman, J., Hittmair, A., Bartsch, G. and Klocker, H. (1994) Androgen receptor activation in prostatic tumor cell lines by insulin-like growth factor-I, keratinocyte growth factor, and epidermal growth factor. *Cancer Res*, **54**, 5474-8.
- Damber, J. E. (2005) Endocrine therapy for prostate cancer. *Acta Oncol*, **44**, 605-9.
- de Bono, J. S., Logothetis, C. J., Molina, A., Fizazi, K., North, S., Chu, L., Chi, K. N., Jones, R. J., Goodman, O. B., Saad, F., Staffurth, J. N., Mainwaring, P., Harland, S., Flaig, T. W., Hutson, T. E., Cheng, T., Patterson, H., Hainsworth, J. D., Ryan, C. J., Sternberg, C. N., Ellard, S. L., Fléchon, A., Saleh, M., Scholz, M., Efstathiou, E., Zivi, A., Bianchini, D., Loriot, Y., Chieffo, N., Kheoh, T., Haqq, C. M., Scher, H. I. and Investigators, C.-A.-. (2011) Abiraterone and increased survival in metastatic prostate cancer. *N Engl J Med*, **364**, 1995-2005.
- Degterev, A., Boyce, M. and Yuan, J. (2003) A decade of caspases. *Oncogene*, **22**, 8543-67.
- Djulgovic, M., Beyth, R. J., Neuberger, M. M., Stoffs, T. L., Vieweg, J., Djulgovic, B. and Dahm, P. (2010) Screening for prostate cancer: systematic review and meta-analysis of randomised controlled trials. *BMJ*, **341**, c4543.
- Domes, T., Lo, K. C., Grober, E. D., Mullen, J. B., Mazzulli, T. and Jarvi, K. (2012) The incidence and effect of bacteriospermia and elevated seminal leukocytes on semen parameters. *Fertil Steril*, **97**, 1050-5.
- Donjacour, A. A. and Cunha, G. R. (1988) The effect of androgen deprivation on branching morphogenesis in the mouse prostate. *Dev Biol*, **128**, 1-14.
- Edwards, D. P. and Boonyaratanakornkit, V. (2003) Rapid extranuclear signaling by the estrogen receptor (ER): MNAR couples ER and Src to the MAP kinase signaling pathway. *Mol Interv*, **3**, 12-5.
- Eiserich, J. P., Hristova, M., Cross, C. E., Jones, A. D., Freeman, B. A., Halliwell, B. and van der Vliet, A. (1998) Formation of nitric oxide-derived inflammatory oxidants by myeloperoxidase in neutrophils. *Nature*, **391**, 393-7.
- Eisermann, K., Wang, D., Jing, Y., Pascal, L. E. and Wang, Z. (2013) Androgen receptor gene mutation, rearrangement, polymorphism. *Transl Androl Urol*, **2**, 137-147.
- Elmore, S. (2007) Apoptosis: a review of programmed cell death. *Toxicol Pathol*, **35**, 495-516.
- Estébanez-Perpiñá, E., Arnold, L. A., Arnold, A. A., Nguyen, P., Rodrigues, E. D., Mar, E., Bateman, R., Pallai, P., Shokat, K. M., Baxter, J. D., Guy, R. K., Webb, P. and Fletterick, R. J. (2007) A surface on the androgen receptor that allosterically regulates coactivator binding. *Proc Natl Acad Sci U S A*, **104**, 16074-9.
- Ewing, C. M., Ray, A. M., Lange, E. M., Zuhlke, K. A., Robbins, C. M., Tembe, W. D., Wiley, K. E., Isaacs, S. D., Johng, D., Wang, Y., Bizon, C., Yan, G., Gielzak, M., Partin, A. W., Shanmugam, V., Izatt, T., Sinari, S., Craig, D. W., Zheng, S. L., Walsh, P. C., Montie, J. E., Xu, J., Carpten, J. D., Isaacs, W. B. and Cooney, K. A. (2012) Germline mutations in HOXB13 and prostate-cancer risk. *N Engl J Med*, **366**, 141-9.
- Ferlay, J., Shin, H. R., Bray, F., Forman, D., Mathers, C. and Parkin, D. M. (2010) Estimates of worldwide burden of cancer in 2008: GLOBOCAN 2008. *Int J Cancer*, **127**, 2893-917.

- Ferlay, J., Soerjomataram, I., Dikshit, R., Eser, S., Mathers, C., Rebelo, M., Parkin, D. M., Forman, D. and Bray, F. (2015) Cancer incidence and mortality worldwide: sources, methods and major patterns in GLOBOCAN 2012. *Int J Cancer*, **136**, E359-86.
- Fioretti, F. M., Sita-Lumsden, A., Bevan, C. L. and Brooke, G. N. (2014) Revising the role of the androgen receptor in breast cancer. *J Mol Endocrinol*, **52**, R257-65.
- Fizazi, K., Jones, R., Oudard, S., Efstathiou, E., Saad, F., de Wit, R., De Bono, J., Cruz, F. M., Fountzilas, G., Ulys, A., Carcano, F., Agarwal, N., Agus, D., Bellmunt, J., Petrylak, D. P., Lee, S. Y., Webb, I. J., Tejura, B., Borgstein, N. and Dreicer, R. (2015) Phase III, randomized, double-blind, multicenter trial comparing orteronel (TAK-700) plus prednisone with placebo plus prednisone in patients with metastatic castration-resistant prostate cancer that has progressed during or after docetaxel-based therapy: ELM-PC 5. *J Clin Oncol*, **33**, 723-31.
- Fulda, S. and Debatin, K. M. (2006) Extrinsic versus intrinsic apoptosis pathways in anticancer chemotherapy. *Oncogene*, **25**, 4798-811.
- Gaddipati, J. P., McLeod, D. G., Heidenberg, H. B., Sesterhenn, I. A., Finger, M. J., Moul, J. W. and Srivastava, S. (1994) Frequent detection of codon 877 mutation in the androgen receptor gene in advanced prostate cancers. *Cancer Res*, **54**, 2861-4.
- Gardner, W. A. (1982) Histologic grading of prostate cancer: a retrospective and prospective overview. *Prostate*, **3**, 555-61.
- Garg, R., Benedetti, L. G., Abera, M. B., Wang, H., Abba, M. and Kazanietz, M. G. (2014) Protein kinase C and cancer: what we know and what we do not. *Oncogene*, **33**, 5225-37.
- Geddes, D. T. (2007) Inside the lactating breast: the latest anatomy research. *J Midwifery Womens Health*, **52**, 556-63.
- Giovannelli, P., Di Donato, M., Galasso, G., Di Zazzo, E., Bilancio, A. and Migliaccio, A. (2018) The Androgen Receptor in Breast Cancer. *Front Endocrinol (Lausanne)*, **9**, 492.
- Goa, K. L. and Spencer, C. M. (1998) Bicalutamide in advanced prostate cancer. A review. *Drugs Aging*, **12**, 401-22.
- Gross, J. M. and Yee, D. (2002) How does the estrogen receptor work? *Breast Cancer Res*, **4**, 62-4.
- Gucalp, A., Tolaney, S., Isakoff, S. J., Ingle, J. N., Liu, M. C., Carey, L. A., Blackwell, K., Rugo, H., Nabell, L., Forero, A., Stearns, V., Doane, A. S., Danso, M., Moynahan, M. E., Momen, L. F., Gonzalez, J. M., Akhtar, A., Giri, D. D., Patil, S., Feigin, K. N., Hudis, C. A., Traina, T. A. and 011), T. B. C. R. C. T. (2013) Phase II trial of bicalutamide in patients with androgen receptor-positive, estrogen receptor-negative metastatic Breast Cancer. *Clin Cancer Res*, **19**, 5505-12.
- Hanahan, D. and Weinberg, R. A. (2000) The hallmarks of cancer. *Cell*, **100**, 57-70.
- Hanahan, D. and Weinberg, R. A. (2011) Hallmarks of cancer: the next generation. *Cell*, **144**, 646-74.
- Hassiotou, F. and Geddes, D. (2013) Anatomy of the human mammary gland: Current status of knowledge. *Clin Anat*, **26**, 29-48.

- Havens, A. M., Pedersen, E. A., Shiozawa, Y., Ying, C., Jung, Y., Sun, Y., Neeley, C., Wang, J., Mehra, R., Keller, E. T., McCauley, L. K., Loberg, R. D., Pienta, K. J. and Taichman, R. S. (2008) An in vivo mouse model for human prostate cancer metastasis. *Neoplasia*, **10**, 371-80.
- Heemers, H. V. and Tindall, D. J. (2007) Androgen receptor (AR) coregulators: a diversity of functions converging on and regulating the AR transcriptional complex. *Endocr Rev*, **28**, 778-808.
- Heidenreich, A., Bellmunt, J., Bolla, M., Joniau, S., Mason, M., Matveev, V., Mottet, N., Schmid, H. P., van der Kwast, T., Wiegel, T., Zattoni, F. and Urology, E. A. o. (2011) EAU guidelines on prostate cancer. Part 1: screening, diagnosis, and treatment of clinically localised disease. *Eur Urol*, **59**, 61-71.
- Hengartner, M. O. (2000) The biochemistry of apoptosis. *Nature*, **407**, 770-6.
- Hickey, T. E., Robinson, J. L., Carroll, J. S. and Tilley, W. D. (2012) Minireview: The androgen receptor in breast tissues: growth inhibitor, tumor suppressor, oncogene? *Mol Endocrinol*, **26**, 1252-67.
- Hotte, S. J. and Saad, F. (2010) Current management of castrate-resistant prostate cancer. *Curr Oncol*, **17 Suppl 2**, S72-9.
- Humphrey, P. A. (2004) Gleason grading and prognostic factors in carcinoma of the prostate. *Mod Pathol*, **17**, 292-306.
- Héquet, D., Bricou, A., Delpech, Y. and Barranger, E. (2011) Surgical management modifications following systematic additional shaving of cavity margins in breast-conservation treatment. *Ann Surg Oncol*, **18**, 114-8.
- Inman, J. L., Robertson, C., Mott, J. D. and Bissell, M. J. (2015) Mammary gland development: cell fate specification, stem cells and the microenvironment. *Development*, **142**, 1028-42.
- Isbarn, H., Boccon-Gibod, L., Carroll, P. R., Montorsi, F., Schulman, C., Smith, M. R., Sternberg, C. N. and Studer, U. E. (2009) Androgen deprivation therapy for the treatment of prostate cancer: consider both benefits and risks. *Eur Urol*, **55**, 62-75.
- Javed, A. and Lteif, A. (2013) Development of the human breast. *Semin Plast Surg*, **27**, 5-12.
- Jia, L., Berman, B. P., Jariwala, U., Yan, X., Cogan, J. P., Walters, A., Chen, T., Buchanan, G., Frenkel, B. and Coetzee, G. A. (2008) Genomic androgen receptor-occupied regions with different functions, defined by histone acetylation, coregulators and transcriptional capacity. *PLoS One*, **3**, e3645.
- Jordan, V. C. and Brodie, A. M. (2007) Development and evolution of therapies targeted to the estrogen receptor for the treatment and prevention of breast cancer. *Steroids*, **72**, 7-25.
- Kadamur, G. and Ross, E. M. (2013) Mammalian phospholipase C. *Annu Rev Physiol*, **75**, 127-54.
- Karantanos, T., Corn, P. G. and Thompson, T. C. (2013) Prostate cancer progression after androgen deprivation therapy: mechanisms of castrate resistance and novel therapeutic approaches. *Oncogene*, **32**, 5501-11.
- Kellokumpu-Lehtinen, P., Santti, R. and Pelliniemi, L. J. (1980) Correlation of early cytodifferentiation of the human fetal prostate and Leydig cells. *Anat Rec*, **196**, 263-73.

- Kelly, C. M., Juurlink, D. N., Gomes, T., Duong-Hua, M., Pritchard, K. I., Austin, P. C. and Paszat, L. F. (2010) Selective serotonin reuptake inhibitors and breast cancer mortality in women receiving tamoxifen: a population based cohort study. *BMJ*, **340**, c693.
- Kimura, M., Yoshioka, T., Saio, M., Banno, Y., Nagaoka, H. and Okano, Y. (2013) Mitotic catastrophe and cell death induced by depletion of centrosomal proteins. *Cell Death Dis*, **4**, e603.
- Korpál, M., Korn, J. M., Gao, X., Rakiec, D. P., Ruddy, D. A., Doshi, S., Yuan, J., Kovats, S. G., Kim, S., Cooke, V. G., Monahan, J. E., Stegmeier, F., Roberts, T. M., Sellers, W. R., Zhou, W. and Zhu, P. (2013) An F876L mutation in androgen receptor confers genetic and phenotypic resistance to MDV3100 (enzalutamide). *Cancer Discov*, **3**, 1030-43.
- Labrie, F., Luu-The, V., Labrie, C., Bélanger, A., Simard, J., Lin, S. X. and Pelletier, G. (2003) Endocrine and intracrine sources of androgens in women: inhibition of breast cancer and other roles of androgens and their precursor dehydroepiandrosterone. *Endocr Rev*, **24**, 152-82.
- Lanzino, M., De Amicis, F., McPhaul, M. J., Marsico, S., Panno, M. L. and Andò, S. (2005a) Endogenous coactivator ARA70 interacts with estrogen receptor alpha (ERalpha) and modulates the functional ERalpha/androgen receptor interplay in MCF-7 cells. *J Biol Chem*, **280**, 20421-30.
- Lanzino, M., De Amicis, F., McPhaul, M. J., Marsico, S., Panno, M. L. and Andò, S. (2005b) Endogenous coactivator ARA70 interacts with estrogen receptor alpha (ERalpha) and modulates the functional ERalpha/androgen receptor interplay in MCF-7 cells. *J Biol Chem*, **280**, 20421-30.
- Lattanzio, R., Piantelli, M. and Falasca, M. (2013) Role of phospholipase C in cell invasion and metastasis. *Adv Biol Regul*, **53**, 309-18.
- Le Romancer, M., Poulard, C., Cohen, P., Sentis, S., Renoir, J. M. and Corbo, L. (2011) Cracking the estrogen receptor's posttranslational code in breast tumors. *Endocr Rev*, **32**, 597-622.
- Lee, T. J., Kim, E. J., Kim, S., Jung, E. M., Park, J. W., Jeong, S. H., Park, S. E., Yoo, Y. H. and Kwon, T. K. (2006) Caspase-dependent and caspase-independent apoptosis induced by evodiamine in human leukemic U937 cells. *Mol Cancer Ther*, **5**, 2398-407.
- Lehmann, B. D., Bauer, J. A., Chen, X., Sanders, M. E., Chakravarthy, A. B., Shyr, Y. and Pietenpol, J. A. (2011) Identification of human triple-negative breast cancer subtypes and preclinical models for selection of targeted therapies. *J Clin Invest*, **121**, 2750-67.
- Lehmann, B. D., Bauer, J. A., Schafer, J. M., Pendleton, C. S., Tang, L., Johnson, K. C., Chen, X., Balko, J. M., Gómez, H., Arteaga, C. L., Mills, G. B., Sanders, M. E. and Pietenpol, J. A. (2014) PIK3CA mutations in androgen receptor-positive triple negative breast cancer confer sensitivity to the combination of PI3K and androgen receptor inhibitors. *Breast Cancer Res*, **16**, 406.
- Lehmann-Che, J., Hamy, A. S., Porcher, R., Barritault, M., Bouhidel, F., Habuella, H., Leman-Detours, S., de Roquancourt, A., Cahen-Doidy, L., Bourstyn, E., de Cremoux, P., de Bazelaire, C., Albitet, M., Giacchetti, S., Cuvier, C., Janin, A., Espié, M., de Thé, H. and Bertheau, P. (2013) Molecular apocrine breast cancers are aggressive estrogen receptor negative tumors overexpressing either HER2 or GCDFP15. *Breast Cancer Res*, **15**, R37.
- Lemaine, V. and Simmons, P. S. (2013) The adolescent female: Breast and reproductive embryology and anatomy. *Clin Anat*, **26**, 22-8.



- Leung, E., Pilkington, L. I., van Rensburg, M., Jeon, C. Y., Song, M., Arabshahi, H. J., De Zoysa, G. H., Sarojini, V., Denny, W. A., Reynisson, J. and Barker, D. (2016) Synthesis and cytotoxicity of thieno[2,3-b]quinoline-2-carboxamide and cycloalkyl[b]thieno[3,2-e]pyridine-2-carboxamide derivatives. *Bioorg Med Chem*, **24**, 1142-54.
- Lipovka, Y. and Konhilas, J. P. (2016) The complex nature of oestrogen signalling in breast cancer: enemy or ally? *Biosci Rep*, **36**.
- Lipski, B. A., Garcia, R. L. and Brawer, M. K. (1996) Prostatic intraepithelial neoplasia: significance and management. *Semin Urol Oncol*, **14**, 149-55.
- Lito, P., Rosen, N. and Solit, D. B. (2013) Tumor adaptation and resistance to RAF inhibitors. *Nat Med*, **19**, 1401-9.
- Lombardi, S., Honeth, G., Ginestier, C., Shinomiya, I., Marlow, R., Buchupalli, B., Gazinska, P., Brown, J., Catchpole, S., Liu, S., Barkan, A., Wicha, M., Purushotham, A., Burchell, J., Pinder, S. and Dontu, G. (2014) Growth hormone is secreted by normal breast epithelium upon progesterone stimulation and increases proliferation of stem/progenitor cells. *Stem Cell Reports*, **2**, 780-93.
- Lopez-Garcia, J., Periyasamy, M., Thomas, R. S., Christian, M., Leao, M., Jat, P., Kindle, K. B., Heery, D. M., Parker, M. G., Buluwela, L., Kamalati, T. and Ali, S. (2006) ZNF366 is an estrogen receptor corepressor that acts through CtBP and histone deacetylases. *Nucleic Acids Res*, **34**, 6126-36.
- Lund, L., Svolgaard, N. and Poulsen, M. H. (2014) Prostate cancer: a review of active surveillance. *Res Rep Urol*, **6**, 107-12.
- Macias, H. and Hinck, L. (2012) Mammary gland development. *Wiley Interdiscip Rev Dev Biol*, **1**, 533-57.
- Mapelli, P. and Picchio, M. (2015) Initial prostate cancer diagnosis and disease staging--the role of choline-PET-CT. *Nat Rev Urol*, **12**, 510-8.
- Marker, P. C., Donjacour, A. A., Dahiya, R. and Cunha, G. R. (2003) Hormonal, cellular, and molecular control of prostatic development. *Dev Biol*, **253**, 165-74.
- Markozannes, G., Tzoulaki, I., Karli, D., Evangelou, E., Ntzani, E., Gunter, M. J., Norat, T., Ioannidis, J. P. and Tsilidis, K. K. (2016) Diet, body size, physical activity and risk of prostate cancer: An umbrella review of the evidence. *Eur J Cancer*, **69**, 61-69.
- Mastelić, A., Čikeš Čulić, V., Režić Mužinić, N., Vuica-Ross, M., Barker, D., Leung, E. Y., Reynisson, J. and Markotić, A. (2017) Glycophenotype of breast and prostate cancer stem cells treated with thieno[2,3-. *Drug Des Devel Ther*, **11**, 759-769.
- Mayeur, G. L., Kung, W. J., Martinez, A., Izumiya, C., Chen, D. J. and Kung, H. J. (2005) Ku is a novel transcriptional recycling coactivator of the androgen receptor in prostate cancer cells. *J Biol Chem*, **280**, 10827-33.
- McGhan, L. J., McCullough, A. E., Protheroe, C. A., Dueck, A. C., Lee, J. J., Nunez-Nateras, R., Castle, E. P., Gray, R. J., Wasif, N., Goetz, M. P., Hawse, J. R., Henry, T. J., Barrett, M. T., Cunliffe, H. E. and Pockaj, B. A. (2014a) Androgen receptor-positive triple negative breast cancer: a unique breast cancer subtype. *Ann Surg Oncol*, **21**, 361-7.
- McGhan, L. J., McCullough, A. E., Protheroe, C. A., Dueck, A. C., Lee, J. J., Nunez-Nateras, R., Castle, E. P., Gray, R. J., Wasif, N., Goetz, M. P., Hawse, J. R., Henry, T. J., Barrett, M. T., Cunliffe, H. E. and Pockaj, B. A.

- (2014b) Androgen receptor-positive triple negative breast cancer: a unique breast cancer subtype. *Ann Surg Oncol*, **21**, 361-7.
- McNamara, K. M., Moore, N. L., Hickey, T. E., Sasano, H. and Tilley, W. D. (2014) Complexities of androgen receptor signalling in breast cancer. *Endocr Relat Cancer*, **21**, T161-81.
- Meyer, M. R., Haas, E., Prossnitz, E. R. and Barton, M. (2009) Non-genomic regulation of vascular cell function and growth by estrogen. *Mol Cell Endocrinol*, **308**, 9-16.
- Mohammed, H., Russell, I. A., Stark, R., Rueda, O. M., Hickey, T. E., Tarulli, G. A., Serandour, A. A., Birrell, S. N., Bruna, A., Saadi, A., Menon, S., Hadfield, J., Pugh, M., Raj, G. V., Brown, G. D., D'Santos, C., Robinson, J. L., Silva, G., Launchbury, R., Perou, C. M., Stingl, J., Caldas, C., Tilley, W. D. and Carroll, J. S. (2015) Progesterone receptor modulates ER $\alpha$  action in breast cancer. *Nature*, **523**, 313-7.
- Moore, N. L., Buchanan, G., Harris, J. M., Selth, L. A., Bianco-Miotto, T., Hanson, A. R., Birrell, S. N., Butler, L. M., Hickey, T. E. and Tilley, W. D. (2012a) An androgen receptor mutation in the MDA-MB-453 cell line model of molecular apocrine breast cancer compromises receptor activity. *Endocr Relat Cancer*, **19**, 599-613.
- Moore, N. L., Buchanan, G., Harris, J. M., Selth, L. A., Bianco-Miotto, T., Hanson, A. R., Birrell, S. N., Butler, L. M., Hickey, T. E. and Tilley, W. D. (2012b) An androgen receptor mutation in the MDA-MB-453 cell line model of molecular apocrine breast cancer compromises receptor activity. *Endocr Relat Cancer*, **19**, 599-613.
- Mostaghel, E. A., Montgomery, B. and Nelson, P. S. (2009) Castration-resistant prostate cancer: targeting androgen metabolic pathways in recurrent disease. *Urol Oncol*, **27**, 251-7.
- Naji, L., Randhawa, H., Sohani, Z., Dennis, B., Lautenbach, D., Kavanagh, O., Bawor, M., Banfield, L. and Profetto, J. (2018) Digital Rectal Examination for Prostate Cancer Screening in Primary Care: A Systematic Review and Meta-Analysis. *Ann Fam Med*, **16**, 149-154.
- Nakamura, Y. (2017) [Regulation and physiological functions of phospholipase C]. *Seikagaku*, **89**, 189-98.
- Nakamura, Y. and Fukami, K. (2009) Roles of phospholipase C isozymes in organogenesis and embryonic development. *Physiology (Bethesda)*, **24**, 332-41.
- Narayanan, R., Ahn, S., Cheney, M. D., Yepuru, M., Miller, D. D., Steiner, M. S. and Dalton, J. T. (2014) Selective androgen receptor modulators (SARMs) negatively regulate triple-negative breast cancer growth and epithelial:mesenchymal stem cell signaling. *PLoS One*, **9**, e103202.
- Narayanan, R. and Dalton, J. T. (2016) Androgen Receptor: A Complex Therapeutic Target for Breast Cancer. *Cancers (Basel)*, **8**.
- Ni, M., Chen, Y., Fei, T., Li, D., Lim, E., Liu, X. S. and Brown, M. (2013) Amplitude modulation of androgen signaling by c-MYC. *Genes Dev*, **27**, 734-48.
- Niklas, C., Saar, M., Berg, B., Steiner, K., Janssen, M., Siemer, S., Stöckle, M. and Ohlmann, C. H. (2016) da Vinci and Open Radical Prostatectomy: Comparison of Clinical Outcomes and Analysis of Insurance Costs. *Urol Int*, **96**, 287-94.
- Ohlmann, C. H., Jäschke, M., Jaehnig, P., Krege, S., Gschwend, J., Rexer, H. and Stöckle, M. (2017) Abiraterone acetate plus LHRH therapy versus abiraterone acetate while sparing LHRH therapy in patients with

- progressive, metastatic and chemotherapy-naïve, castration-resistant prostate cancer (SPARE): study protocol for a randomized controlled trial. *Trials*, **18**, 457.
- Ong, Y. C., Kolatkar, P. R. and Yong, E. L. (2002) Androgen receptor mutations causing human androgen insensitivity syndromes show a key role of residue M807 in Helix 8-Helix 10 interactions and in receptor ligand-binding domain stability. *Mol Hum Reprod*, **8**, 101-8.
- Oudard, S., Fizazi, K., Sengeløv, L., Daugaard, G., Saad, F., Hansen, S., Hjalml-Eriksson, M., Jassem, J., Thiery-Vuillemin, A., Caffo, O., Castellano, D., Mainwaring, P. N., Bernard, J., Shen, L., Chadjaa, M. and Sartor, O. (2017) Cabazitaxel Versus Docetaxel As First-Line Therapy for Patients With Metastatic Castration-Resistant Prostate Cancer: A Randomized Phase III Trial-FIRSTANA. *J Clin Oncol*, **35**, 3189-3197.
- Pal, S. K., Patel, J., He, M., Foulk, B., Kraft, K., Smirnov, D. A., Twardowski, P., Kortylewski, M., Bhargava, V. and Jones, J. O. (2018) Identification of mechanisms of resistance to treatment with abiraterone acetate or enzalutamide in patients with castration-resistant prostate cancer (CRPC). *Cancer*, **124**, 1216-1224.
- Pan, H., Deng, Y. and Pollard, J. W. (2006) Progesterone blocks estrogen-induced DNA synthesis through the inhibition of replication licensing. *Proc Natl Acad Sci U S A*, **103**, 14021-6.
- Panet-Raymond, V., Gottlieb, B., Beitel, L. K., Pinsky, L. and Trifiro, M. A. (2000) Interactions between androgen and estrogen receptors and the effects on their transactivational properties. *Mol Cell Endocrinol*, **167**, 139-50.
- Park, J. B., Lee, C. S., Jang, J. H., Ghim, J., Kim, Y. J., You, S., Hwang, D., Suh, P. G. and Ryu, S. H. (2012) Phospholipase signalling networks in cancer. *Nat Rev Cancer*, **12**, 782-92.
- Patani, N. and Martin, L. A. (2014) Understanding response and resistance to oestrogen deprivation in ER-positive breast cancer. *Mol Cell Endocrinol*, **382**, 683-694.
- Peters, A. A., Buchanan, G., Ricciardelli, C., Bianco-Miotto, T., Centenera, M. M., Harris, J. M., Jindal, S., Segara, D., Jia, L., Moore, N. L., Henshall, S. M., Birrell, S. N., Coetzee, G. A., Sutherland, R. L., Butler, L. M. and Tilley, W. D. (2009) Androgen receptor inhibits estrogen receptor-alpha activity and is prognostic in breast cancer. *Cancer Res*, **69**, 6131-40.
- Phin, S., Moore, M. W. and Cotter, P. D. (2013) Genomic Rearrangements of PTEN in Prostate Cancer. *Front Oncol*, **3**, 240.
- Prat, A., Pineda, E., Adamo, B., Galván, P., Fernández, A., Gaba, L., Díez, M., Viladot, M., Arance, A. and Muñoz, M. (2015) Clinical implications of the intrinsic molecular subtypes of breast cancer. *Breast*, **24 Suppl 2**, S26-35.
- Rahim, B. and O'Regan, R. (2017) AR Signaling in Breast Cancer. *Cancers (Basel)*, **9**.
- Rampurwala, M., Wisinski, K. B. and O'Regan, R. (2016) Role of the androgen receptor in triple-negative breast cancer. *Clin Adv Hematol Oncol*, **14**, 186-93.
- Rebecchi, M. J. and Pentylala, S. N. (2000) Structure, function, and control of phosphoinositide-specific phospholipase C. *Physiol Rev*, **80**, 1291-335.
- Reynisson, J., Court, W., O'Neill, C., Day, J., Patterson, L., McDonald, E., Workman, P., Katan, M. and Eccles, S. A. (2009) The identification of novel PLC-gamma inhibitors using virtual high throughput screening. *Bioorg Med Chem*, **17**, 3169-76.

- Reynisson, J., Jaiswal, J. K., Barker, D., D'mello, S. A., Denny, W. A., Baguley, B. C. and Leung, E. Y. (2016) Evidence that phospholipase C is involved in the antitumour action of NSC768313, a new thieno[2,3-b]pyridine derivative. *Cancer Cell Int*, **16**, 18.
- Rezaei, R., Wu, Z., Hou, Y., Bazer, F. W. and Wu, G. (2016) Amino acids and mammary gland development: nutritional implications for milk production and neonatal growth. *J Anim Sci Biotechnol*, **7**, 20.
- Ricci, M. S. and Zong, W. X. (2006) Chemotherapeutic approaches for targeting cell death pathways. *Oncologist*, **11**, 342-57.
- Robinson, J. L., Macarthur, S., Ross-Innes, C. S., Tilley, W. D., Neal, D. E., Mills, I. G. and Carroll, J. S. (2011) Androgen receptor driven transcription in molecular apocrine breast cancer is mediated by FoxA1. *EMBO J*, **30**, 3019-27.
- Robinson-Rechavi, M., Escriba Garcia, H. and Laudet, V. (2003) The nuclear receptor superfamily. *J Cell Sci*, **116**, 585-6.
- Sadeghi, M., Enferadi, M. and Shirazi, A. (2010) External and internal radiation therapy: past and future directions. *J Cancer Res Ther*, **6**, 239-48.
- Schaeffer, E. M., Marchionni, L., Huang, Z., Simons, B., Blackman, A., Yu, W., Parmigiani, G. and Berman, D. M. (2008) Androgen-induced programs for prostate epithelial growth and invasion arise in embryogenesis and are reactivated in cancer. *Oncogene*, **27**, 7180-91.
- Scher, H. I., Fizazi, K., Saad, F., Taplin, M. E., Sternberg, C. N., Miller, K., de Wit, R., Mulders, P., Chi, K. N., Shore, N. D., Armstrong, A. J., Flaig, T. W., Fléchon, A., Mainwaring, P., Fleming, M., Hainsworth, J. D., Hirmand, M., Selby, B., Seely, L., de Bono, J. S. and Investigators, A. (2012) Increased survival with enzalutamide in prostate cancer after chemotherapy. *N Engl J Med*, **367**, 1187-97.
- Schröder, F. H., Hugosson, J., Roobol, M. J., Tammela, T. L., Zappa, M., Nelen, V., Kwiatkowski, M., Lujan, M., Määttä, L., Lilja, H., Denis, L. J., Recker, F., Paez, A., Bangma, C. H., Carlsson, S., Puliti, D., Villers, A., Rebillard, X., Hakama, M., Stenman, U. H., Kujala, P., Taari, K., Aus, G., Huber, A., van der Kwast, T. H., van Schaik, R. H., de Koning, H. J., Moss, S. M., Auvinen, A. and Investigators, E. (2014) Screening and prostate cancer mortality: results of the European Randomised Study of Screening for Prostate Cancer (ERSPC) at 13 years of follow-up. *Lancet*, **384**, 2027-35.
- Schwartzberg, L. S., Yardley, D. A., Elias, A. D., Patel, M., LoRusso, P., Burris, H. A., Gucalp, A., Peterson, A. C., Blaney, M. E., Steinberg, J. L., Gibbons, J. A. and Traina, T. A. (2017) A Phase I/Ib Study of Enzalutamide Alone and in Combination with Endocrine Therapies in Women with Advanced Breast Cancer. *Clin Cancer Res*, **23**, 4046-4054.
- Serra, V., Scaltriti, M., Prudkin, L., Eichhorn, P. J., Ibrahim, Y. H., Chandarlapaty, S., Markman, B., Rodriguez, O., Guzman, M., Rodriguez, S., Gili, M., Russillo, M., Parra, J. L., Singh, S., Arribas, J., Rosen, N. and Baselga, J. (2011) PI3K inhibition results in enhanced HER signaling and acquired ERK dependency in HER2-overexpressing breast cancer. *Oncogene*, **30**, 2547-57.
- Sever, R. and Brugge, J. S. (2015) Signal transduction in cancer. *Cold Spring Harb Perspect Med*, **5**.
- Sever, R. and Glass, C. K. (2013) Signaling by nuclear receptors. *Cold Spring Harb Perspect Biol*, **5**, a016709.
- Siemens, D. R., Klotz, L., Heidenreich, A., Chowdhury, S., Villers, A., Baron, B., van Os, S., Hasabou, N., Wang, F., Lin, P. and Shore, N. D. (2018) Efficacy and Safety of Enzalutamide vs Bicalutamide in Younger and

- Older Patients with Metastatic Castration Resistant Prostate Cancer in the TERRAIN Trial. *J Urol*, **199**, 147-154.
- Sinn, H. P. and Kreipe, H. (2013) A Brief Overview of the WHO Classification of Breast Tumors, 4th Edition, Focusing on Issues and Updates from the 3rd Edition. *Breast Care (Basel)*, **8**, 149-54.
- Skowronek, J., Piorunek, T., Kanikowski, M., Chichel, A. and Bieleńda, G. (2013) Definitive high-dose-rate endobronchial brachytherapy of bronchial stump for lung cancer after surgery. *Brachytherapy*, **12**, 560-6.
- Smittenaar, C. R., Petersen, K. A., Stewart, K. and Moitt, N. (2016) Cancer incidence and mortality projections in the UK until 2035. *Br J Cancer*, **115**, 1147-1155.
- Souzaki, M., Kubo, M., Kai, M., Kameda, C., Tanaka, H., Taguchi, T., Tanaka, M., Onishi, H. and Katano, M. (2011) Hedgehog signaling pathway mediates the progression of non-invasive breast cancer to invasive breast cancer. *Cancer Sci*, **102**, 373-81.
- Strief, D. M. (2007) An overview of prostate cancer: diagnosis and treatment. *Urol Nurs*, **27**, 475-9; quiz 480.
- Taplin, M. E., Bubley, G. J., Ko, Y. J., Small, E. J., Upton, M., Rajeshkumar, B. and Balk, S. P. (1999) Selection for androgen receptor mutations in prostate cancers treated with androgen antagonist. *Cancer Res*, **59**, 2511-5.
- Tilstra, S. and McNeil, M. (2017) New Developments in Breast Cancer Screening and Treatment. *J Womens Health (Larchmt)*, **26**, 5-8.
- Timms, B. G. and Hofkamp, L. E. (2011) Prostate development and growth in benign prostatic hyperplasia. *Differentiation*, **82**, 173-83.
- Tinevez, J. Y., Perry, N., Schindelin, J., Hoopes, G. M., Reynolds, G. D., Laplantine, E., Bednarek, S. Y., Shorte, S. L. and Eliceiri, K. W. (2017) TrackMate: An open and extensible platform for single-particle tracking. *Methods*, **115**, 80-90.
- Tocchini-Valentini, G. D., Rochel, N., Escriva, H., Germain, P., Peluso-Iltis, C., Paris, M., Sanglier-Cianferani, S., Van Dorselaer, A., Moras, D. and Laudet, V. (2009) Structural and functional insights into the ligand-binding domain of a nonduplicated retinoid X nuclear receptor from the invertebrate chordate amphioxus. *J Biol Chem*, **284**, 1938-48.
- Toivanen, R. and Shen, M. M. (2017) Prostate organogenesis: tissue induction, hormonal regulation and cell type specification. *Development*, **144**, 1382-1398.
- Tomasetti, C., Li, L. and Vogelstein, B. (2017) Stem cell divisions, somatic mutations, cancer etiology, and cancer prevention. *Science*, **355**, 1330-1334.
- Tomasetti, C. and Vogelstein, B. (2015) Cancer etiology. Variation in cancer risk among tissues can be explained by the number of stem cell divisions. *Science*, **347**, 78-81.
- Touma, N. J. and Nickel, J. C. (2011) Prostatitis and chronic pelvic pain syndrome in men. *Med Clin North Am*, **95**, 75-86.
- Traina, T. A., Miller, K., Yardley, D. A., Eakle, J., Schwartzberg, L. S., O'Shaughnessy, J., Gradishar, W., Schmid, P., Winer, E., Kelly, C., Nanda, R., Gucalp, A., Awada, A., Garcia-Estevez, L., Trudeau, M. E., Steinberg, J., Uppal, H., Tudor, I. C., Peterson, A. and Cortes, J. (2018) Enzalutamide for the Treatment of Androgen Receptor-Expressing Triple-Negative Breast Cancer. *J Clin Oncol*, **36**, 884-890.

- Tran, C., Ouk, S., Clegg, N. J., Chen, Y., Watson, P. A., Arora, V., Wongvipat, J., Smith-Jones, P. M., Yoo, D., Kwon, A., Wasielewska, T., Welsbie, D., Chen, C. D., Higano, C. S., Beer, T. M., Hung, D. T., Scher, H. I., Jung, M. E. and Sawyers, C. L. (2009) Development of a second-generation antiandrogen for treatment of advanced prostate cancer. *Science*, **324**, 787-90.
- Tsang, J. Y., Ni, Y. B., Chan, S. K., Shao, M. M., Law, B. K., Tan, P. H. and Tse, G. M. (2014) Androgen receptor expression shows distinctive significance in ER positive and negative breast cancers. *Ann Surg Oncol*, **21**, 2218-28.
- Ukimura, O., Troncoso, P., Ramirez, E. I. and Babaian, R. J. (1998) Prostate cancer staging: correlation between ultrasound determined tumor contact length and pathologically confirmed extraprostatic extension. *J Urol*, **159**, 1251-9.
- Verze, P., Cai, T. and Lorenzetti, S. (2016) The role of the prostate in male fertility, health and disease. *Nat Rev Urol*, **13**, 379-86.
- Viedma-Rodríguez, R., Baiza-Gutman, L., Salamanca-Gómez, F., Diaz-Zaragoza, M., Martínez-Hernández, G., Ruiz Esparza-Garrido, R., Velázquez-Flores, M. A. and Arenas-Aranda, D. (2014) Mechanisms associated with resistance to tamoxifen in estrogen receptor-positive breast cancer (review). *Oncol Rep*, **32**, 3-15.
- Vontela, N., Koduri, V., Schwartzberg, L. S. and Vidal, G. A. (2017) Selective Androgen Receptor Modulator in a Patient With Hormone-Positive Metastatic Breast Cancer. *J Natl Compr Canc Netw*, **15**, 284-287.
- Vorobiof, D. A. (2016) Recent advances in the medical treatment of breast cancer. *F1000Res*, **5**, 2786.
- Vranic, S., Gatalica, Z. and Wang, Z. Y. (2011) Update on the molecular profile of the MDA-MB-453 cell line as a model for apocrine breast carcinoma studies. *Oncol Lett*, **2**, 1131-1137.
- Wang, Y., Hayward, S., Cao, M., Thayer, K. and Cunha, G. (2001) Cell differentiation lineage in the prostate. *Differentiation*, **68**, 270-9.
- Watson, P. A., Arora, V. K. and Sawyers, C. L. (2015) Emerging mechanisms of resistance to androgen receptor inhibitors in prostate cancer. *Nat Rev Cancer*, **15**, 701-11.
- Weidner, W., Wagenlehner, F. M., Marconi, M., Pilatz, A., Pantke, K. H. and Diemer, T. (2008) Acute bacterial prostatitis and chronic prostatitis/chronic pelvic pain syndrome: andrological implications. *Andrologia*, **40**, 105-12.
- Weiss, S. J., Lampert, M. B. and Test, S. T. (1983) Long-lived oxidants generated by human neutrophils: characterization and bioactivity. *Science*, **222**, 625-8.
- Williams, M. M., Lee, L., Hicks, D. J., Joly, M. M., Elion, D., Rahman, B., McKernan, C., Sanchez, V., Balko, J. M., Stricker, T., Estrada, M. V. and Cook, R. S. (2017) Key Survival Factor, Mcl-1, Correlates with Sensitivity to Combined Bcl-2/Bcl-xL Blockade. *Mol Cancer Res*, **15**, 259-268.
- Wu, J. D., Haugk, K., Woodke, L., Nelson, P., Coleman, I. and Plymate, S. R. (2006) Interaction of IGF signaling and the androgen receptor in prostate cancer progression. *J Cell Biochem*, **99**, 392-401.
- Yang, X., Wang, H. and Jiao, B. (2017) Mammary gland stem cells and their application in breast cancer. *Oncotarget*, **8**, 10675-10691.

- Yeh, S., Hu, Y. C., Wang, P. H., Xie, C., Xu, Q., Tsai, M. Y., Dong, Z., Wang, R. S., Lee, T. H. and Chang, C. (2003) Abnormal mammary gland development and growth retardation in female mice and MCF7 breast cancer cells lacking androgen receptor. *J Exp Med*, **198**, 1899-908.
- Ylikomi, T., Bocquel, M. T., Berry, M., Gronemeyer, H. and Chambon, P. (1992) Cooperation of proto-signals for nuclear accumulation of estrogen and progesterone receptors. *EMBO J*, **11**, 3681-94.
- Yu, Z., He, S., Wang, D., Patel, H. K., Miller, C. P., Brown, J. L., Hattersley, G. and Saeh, J. C. (2017) Selective Androgen Receptor Modulator RAD140 Inhibits the Growth of Androgen/Estrogen Receptor-Positive Breast Cancer Models with a Distinct Mechanism of Action. *Clin Cancer Res*, **23**, 7608-7620.
- Zhang, W., Haines, B. B., Efferson, C., Zhu, J., Ware, C., Kunii, K., Tamman, J., Angagaw, M., Hinton, M. C., Keilhack, H., Paweletz, C. P., Zhang, T., Winter, C., Sathyanarayanan, S., Cheng, J., Zawel, L., Fawell, S., Gilliland, G. and Majumder, P. K. (2012) Evidence of mTOR Activation by an AKT-Independent Mechanism Provides Support for the Combined Treatment of PTEN-Deficient Prostate Tumors with mTOR and AKT Inhibitors. *Transl Oncol*, **5**, 422-9.
- Zi, F., Zi, H., Li, Y., He, J., Shi, Q. and Cai, Z. (2018) Metformin and cancer: An existing drug for cancer prevention and therapy. *Oncol Lett*, **15**, 683-690.